

https://dspace.org/

# The influence of imidazolium-based ionic liquids on the spontaneous combustion characteristic of hydrothermal hydrochars and hydrochar/coal blends

**Matsobane, Ethel Tsholofelo**

**2024**

https://hdl.handle.net/10539/37367

Downloaded from a DSpace repository. https://dspace.org/




# The influence of imidazolium-based ionic liquids on the spontaneous combustion characteristic of hydrothermal hydrochars and hydrochar/coal blends.

Prepared by:

**Ethel Tsholofelo Matsobane (888743)**

Masters dissertation submitted to:

The School of Chemical and Metallurgical Engineering, Faculty of Engineering and the Built Environment, University of the Witwatersrand, Johannesburg, South Africa, in fulfilment of the requirements for the degree of Master of Science in Engineering.

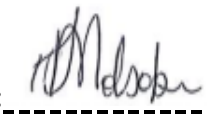
Supervisor and Co-Supervisor:

**Prof. Samson O. Bada and Prof. Bekir Genc**

February 2023

**DECLARATION**

I declare that this dissertation is my own unaided work unless otherwise stated and acknowledged. It is being submitted for the degree of Master of Science in Engineering to the University of the Witwatersrand, Johannesburg. It has not been submitted before for any degree or examination to any other university

**Signed:**  **on this 24th day of October Year 2022**

**ABSTRACT**

Spontaneous combustion is a major problem facing South African coal mines. It is caused by the build-up of heat during oxidation, which eventually leads to the temperature of the coal reaching the point of ignition. The adverse effects of spontaneous combustion, such as the release of large toxic gases into the environment and the loss of valuable materials, called for a solution to the problem and for further new fuels to be explored. Biomass, hydrochar and hydrochar/coal blends have been proposed as alternative energy sources to coal to reduce greenhouse gas emissions. However, given that the new fuels are derived from biomass, which is highly reactive, there is a need to investigate their susceptibility to spontaneous combustion and preventative measures thereof.

This study assessed the factors that contribute to the spontaneous combustion of 100% coal discard, 100% biomass, 100% hydrochar, 25% hydrochar + 75% discard coal, 50% hydrochar + 50% discard coal and 75% hydrochar + 25% discard coal through their characteristics. The thermogravimetric analysis (TGA) and the Wits-Ehac apparatus were used to predict the spontaneous combustion susceptibility of the fuels. Those that were found to be highly susceptible to spontaneous combustion from the six were treated with three imidazolium-based ionic liquids, 1-butyl-3-methyl-imidazolium hydrogen sulphate [$Bmim^+HSO_4^-$] (IL-A), 1-ethyl-3-methyl-imidazolium hydrogen sulphate [$Emim^+HSO_4^-$] (IL-B) and 1-Butyl-3-methyl-imidazolium acetate [$Bmim^+OAc^-$] (IL-C), to inhibit their spontaneous combustion characteristic.

The physicochemical analysis results for the samples revealed an increase in the energy characteristic of the hydrochar produced from 100% biomass. In addition, the 100% discard coal was found to have low energy characteristics, however, the quality improved when it was blended with 100% hydrochar at different ratios. 100% biomass was found to have the highest moisture content, volatile matter and oxygen content at 8.01%, 60.52% and 37.67%, respectively. Additionally, the sample was also found to have the lowest ash content, fixed carbon, and total carbon at 2.92%, 19.54% and 44.60%, respectively. As a result, 100% biomass is highly susceptible to spontaneous combustion compared to other fuels. The Fourier Transform Infrared Spectroscopy (FTIR) analysis results revealed that all samples had a transmittance of the C=O stretch, which is known to promote spontaneous combustion. The fingerprint region of the FTIR spectra of the samples showed that the 100% discard coal had the highest mineral content, which tends to inhibit spontaneous combustion. Whereas 100%

biomass had the lowest mineral content in comparison to other fuels, making it more susceptible to spontaneous combustion.

The TGA results showed that 100% biomass is highly reactive with a $TG_{spc}$ index of 0.1457 %/ ˚C.min, while 100% discard coal was found to be non-reactive with a $TG_{spc}$ index of 0.0135 %/ ˚C.min. The remaining fuels were classified as low reactive given that their $TG_{spc}$ index was between 0.02 and 0.03 %/ ˚C.min. A significant correlation was seen between the TGA susceptibility data and the physiochemical properties of the samples. The Wits-Ehac results showed that the 100% biomass had the lowest spontaneous combustion susceptibility index of 3.49, while the 50% hydrochar/50% discard coal blend was found to have the highest spontaneous combustion susceptibility index of 4.79. The remaining fuel was classified as medium risk as their Wits-Ehac values ranged from 3 to 5. No correlation was found between the TGA and Wits-Ehac spontaneous combustion results, as the Wits-Ehac results showed some inconsistencies, especially for samples derived from 100% biomass. In addition, the Wits-Ehac results were inconsistent with the characterisation results from the samples.

The three imidazolium-based ionic liquids were used to treat 100% biomass to inhibit its spontaneous combustion characteristic, as it was the only sample that was highly susceptible to spontaneous combustion. The TGA results from the treated biomass showed that 1-butyl-3-methyl-imidazolium hydrogen sulfate [$Bmim^+HSO_4^-$] (IL-A) and 1-ethyl-3-methyl-imidazolium hydrogen sulfate [$Emim^+HSO_4^-$] (IL-B) reduced the $TG_{spc}$ index of 100% biomass from 0.1457 %/ ˚C.min to 0.0839 and 0.0576 %/ ˚C.min, respectively at a lower heating rate. The two imidazolium-based ionic liquids were found to be inefficient in inhibiting the spontaneous combustion of 100% biomass, as the samples were still classified as highly reactive after treatment. 1-Butyl-3-methyl-imidazolium acetate [$Bmim^+OAc^-$] (IL-C) showed the best inhibitory effects given that the $TG_{spc}$ index of 100% was reduced to 0.0207 %/ ˚C.min, and the sample was classified as low reactive after treatment. The results of the physicochemical analysis showed that after IL-C treatment, the physicochemical properties, textural properties and microstructure of the 100% biomass improved significantly.

**ACKNOWLEDGEMENTS**

All Glory be to God, who carried me through this challenging journey. I am extremely grateful to my main supervisor Prof. Samson Bada (School of Chemical and Metallurgical Engineering, University of the Witwatersrand) for his guidance, patience, motivation and expertise, and for trusting me even when I doubted myself. I feel privileged to have worked with him. This journey would have been almost impossible without him. I would also like to express my deepest gratitude to my co-supervisor, Prof. Bekir Genc (School of Mining Engineering, University of the Witwatersrand) and Dr. Moshood Onifade for their expertise, resources, support and invaluable contribution to this research. Many thanks to Dr. Jibril Abdulsalam, who was readily available to assist and advise whenever I needed guidance.

I am especially grateful to the Department of Science and Innovation/National Research Foundation (grant number: 86421) for the financial support I received to complete my studies and the Clean Coal Technology group for their support and encouragement in this journey. Lastly, I would like to thank my father, aunt, uncle and grandmother for their unconditional love, continued support and prayers. This study is dedicated to my unborn child, who gave me a purpose to achieve my dreams and revived my passion again just as I was about to give up. I will forever be grateful to God for this blessing.

## Table of Contents

DECLARATION ..... i

ABSTRACT ..... ii

ACKNOWLEDGEMENTS ..... iv

LIST OF FIGURES ..... viii

LIST OF TABLES ..... xii

LIST OF UNITS, ABBREVIATIONS AND ACRONYMS ..... xiii

CHAPTER 1: INTRODUCTION ..... 1

1.1 Background of the Study ..... 1

1.2 Problem Statement ..... 2

1.3 Aims and Objectives ..... 3

1.4 Research Questions ..... 3

1.5 Hypothesis ..... 3

1.6 Layout of the Dissertation ..... 4

CHAPTER 2: LITERATURE REVIEW ..... 5

2.1 Introduction to Spontaneous Combustion ..... 5

2.2 Spontaneous Combustion Mechanisms ..... 6

2.3 Spontaneous Combustion of Coal ..... 9

2.3.1 Factors affecting the spontaneous combustion of coal ..... 9

2.3.2 Techniques used to predict the spontaneous combustion of coal ..... 18

2.3.3 Inhibition of spontaneous coal combustion ..... 28

2.4. Spontaneous Combustion of Biomass ..... 36

2.4.1 Factors affecting the spontaneous combustion characteristic of biomass ..... 38

2.4.2 The prediction of the spontaneous combustion liability of biomass ..... 41

2.4.3 Inhibition of spontaneous combustion of biomass ..... 42

2.5 Hydrochar Production ..... 44

2.6 Spontaneous Combustion of Hydrochar ..... 45

2.7 Summary ..... 46

CHAPTER 3: RESEARCH METHODOLOGY .....47
3.1 Material Preparation .....48
3.2 Hydrochar Production .....49
3.3 Sample Characterisation .....50
3.3.1 Proximate analysis .....50
3.3.2 Ultimate analysis .....50
3.3.3 Calorific value .....51
3.3.4 Fourier Transforms Infrared Spectroscopy Analysis .....51
3.4 Spontaneous Combustion Tests .....52
3.4.1 Thermogravimetry analysis .....52
3.4.2 Wits-Ehac test .....53
3.5 The Treatment of the Samples with Ionic Liquids .....55
3.6 Summary .....56
CHAPTER 4: RESULTS AND DISCUSSION .....57
4.1 Characterisation of Raw Biomass, Discard Coal, Hydrochar and Hydrochar/Coal Blends .....57
4.1.1 Proximate analysis, ultimate analysis and calorific value .....57
4.1.2 Fourier transform infrared spectroscopy .....59
4.2 Spontaneous Combustion Tests .....61
4.2.1 Thermogravimetric analysis .....61
4.2.2 Spontaneous combustion liability of the samples from the Wits-Ehac index .....68
4.2.3 A comparison between the thermogravimetric analysis spontaneous combustion results and the Wits-Ehac index .....71
4.3 Spontaneous Combustion Liability of Samples Treated with Imidazolium-based Ionic Liquids .....73
4.4 Post-Treatment Characterisation .....81
4.4.1 Proximate analysis, ultimate analysis and calorific value .....81
4.4.2 Fourier transform infrared spectroscopy of treated samples .....82
4.4.3 Fourier transform infrared spectroscopy of imidazolium-based ionic liquids (used and unused) .....84

4.4.4 Surface morphology and pore structure of 100% biomass untreated and treated samples ..... 86
4.5 Summary ..... 89
CHAPTER 5: CONCLUSION AND RECOMMENDATIONS ..... 90
5.1 Conclusion ..... 90
5.2 Recommendations ..... 91
References ..... 93
APPENDIX A ..... 121
APPENDIX B ..... 128
APPENDIX C ..... 132
APPENDIX D ..... 139
APPENDIX E ..... 146
APPENDIX F ..... 147

**LIST OF FIGURES**

Figure 2.1: A thermogram generated by differential thermal analysis, extracted from Gouws & Wade (1989) ..... 19
Figure 2.2: The results of the isothermal oven test, extracted from Beamish *et al*. (2001)..... 23
Figure 2.3: Expected results of the XPT method extracted from Mohalik *et al*. (2016) ..... 24
Figure 2.4: Thermogravimetric analysis and differential thermogravimetric analysis curves, extracted from Mohalik *et al*. (2016) ..... 27
Figure 2.5: Self-heating of biomass extracted from Meijer and Gast (2004) ..... 38
Figure 2.6: An overview of hydrothermal carbonisation of biomass adapted from Mazumber (2019) ..... 45
Figure 3.1: Site for Searsia lancea samples collection ..... 48
Figure 3.2: Berghof stirring system axis and stainless-steel reactor vessel ..... 49
Figure 3.3: Flowsheet for the hydrothermal carbonisation of the Searsia lancea ..... **Error! Bookmark not defined.**
Figure 3.4: Characterisation of the samples before and after treatment with imidazolium-based ionic liquids ..... 52
Figure 3.5: An outline of the spontaneous combustion tests ..... 52
Figure 3.6: A schematic diagram of the Wits-Ehac apparatus (Wade *et al*., 1987) ..... 54
Figure 3.7: A typical differential thermal analysis thermogram profile (Wade *et al*., 1987; Gouws & Eroglu, 1993) ..... 55
Figure 3.8: Sample treatment with imidazolium-based ionic liquids ..... 56
Figure 4.1: The FTIR spectra of six samples (H: Hydrochar, DC: Discard coal) ..... 60
Figure 4.2: Derivative weight versus time profile showing the intersection method and points used for gradient calculations (DTG: differential thermogravimetric) ..... 63
Figure 4.3: The derivative profile and slopes obtained for 100% discard coal (DTG: differential thermogravimetric) ..... 64
Figure 4.4: Heating rates applied vs the slopes of the derivative curve for 100% discard coal ..... 66
Figure 4.5: Wits-Ehac differential thermal analysis thermograms for six samples. H: Hydrochar, DC: Discard coal ..... 69
Figure 4.6: Wits-Ehac differential thermal analysis thermogram for a repeated 100% biomass test with a Wits-Ehac index of 3.53 ..... 72
Figure 4.7: The derivative profile of 100% biomass that was treated with 10% IL-A (DTG: differential thermogravimetric) ..... 74

Figure 4.8: The derivative profile of 100% biomass treated with 20% IL-A (DTG: differential thermogravimetric) ..... 74
Figure 4.9: The derivative profile of 100% biomass that was treated with 30% IL-A (DTG: differential thermogravimetric) ..... 75
Figure 4.10: The derivative profile of 100% biomass treated with 40% IL-A (DTG: differential thermogravimetric) ..... 75
Figure 4.11: The derivative profile of 100% biomass treated with 50% IL-A (DTG: differential thermogravimetric) ..... 76
Figure 4.12: Relationship between imidazolium-based ionic liquids concentration and $TGspc$ index at (i) lower heating rates (4, 8, 12, 16 ℃/min), (ii) middle heating rates (4, 8, 12, 16, 20 ℃/min) and (iii) higher heating rates (4, 8, 12, 16, 20, 24 ℃/min) ..... 80
Figure 4.13: Fourier Transform Infrared spectra of treated and untreated 100% biomass (tb: treated 100% biomass) ..... 83
Figure 4.14: Fourier Transform Infrared spectra of IL-A before and after it was used to treat 100% biomass ..... 84
Figure 4.15: Fourier Transform Infrared spectra of IL-B before and after it was used to treat 100% biomass ..... 85
Figure 4.16: Fourier Transform Infrared spectra of IL-C before and after it was used to treat 100% biomass ..... 86
Figure 4.17: Microscopic appearance of biomass samples (tb: treated 100% biomass) ..... 87
Figure 4.18: Pore diameter distribution of treated and untreated 100% biomass samples, generated by the Density Functional Theory model (tb; treated 100% biomass) ..... 89
Figure A1.1: The derivative profile of 100% biomass ..... 121
Figure A1.2: The derivative profile of 100% hydrochar ..... 122
Figure A1.3: The derivative profile of 25% hydrochar + 75% discard coal ..... 122
Figure A1.4: The derivative profile of 50% hydrochar + 50% discard coal ..... 123
Figure A1.5:The derivative profile of 75% hydrochar + 25% discard coal ..... 123
Figure A3.1: Heating rates applied vs the slopes of the derivative curve for 100% biomass 125
Figure A3.2: Heating rates applied vs the slopes of the derivative curve for 100% hydrochar ..... 125
Figure A3.3: Heating rates applied vs the slopes of the derivative curve for 25% hydrochar + 75% discard coal ..... 126

Figure A3.4: Heating rates applied vs the slopes of the derivative curve for 50% hydrochar + 50% discard coal ..... 126
Figure A3.5: Heating rates applied vs the slopes of the derivative curve for 75% hydrochar + 25% discard coal ..... 127
Figure B2.1: Heating rates applied vs the slopes of the derivative curve for 100% biomass treated with 10% IL-A ..... 129
Figure B2.2: Heating rates applied vs the slopes of the derivative curve for 100% biomass treated with 20% IL-A ..... 129
Figure B2.3: Heating rates applied vs the slopes of the derivative curve for 100% biomass treated with 30% IL-A ..... 130
Figure B2.4: Heating rates applied vs the slopes of the derivative curve for 100% biomass treated with 40% IL-A ..... 130
Figure B2.5: Heating rates applied vs the slopes of the derivative curve for 100% biomass treated with 50% IL-A ..... 131
Figure C1.1: The derivative profile of 100% biomass treated with 10% IL-B..... 132
Figure C1.2: The derivative profile of 100% biomass treated with 20% IL-B..... 132
Figure C3.1: Heating rates applied vs the slopes of the derivative curve for biomass treated with 10% IL-B ..... 136
Figure C3.2: Heating rates applied vs the slopes of the derivative curve for biomass treated with 20% IL-B ..... 136
Figure C3.3: Heating rates applied vs the slopes of the derivative curve for biomass treated with 30% IL-B ..... 137
Figure C3.4: Heating rates applied vs the slopes of the derivative curve for biomass treated with 40% IL-B ..... 137
Figure C3.5: Heating rates applied vs the slopes of the derivative curve for biomass treated with 50% IL-B ..... 138
Figure D1.1: The derivative profile of 100% biomass that was treated with 10% IL-C ..... 139
Figure D1.2: The derivative profile of 100% biomass that was treated with 20% IL-C ..... 139
Figure D1.3: The derivative profile of 100% biomass that was treated with 30% IL-C ..... 140
Figure D1.4: The derivative profile of 100% biomass that was treated with 40% IL-C ..... 140
Figure D1.5: The derivative profile of 100% biomass that was treated with 50% IL-C ..... 141
Figure D3.1: Heating rates applied vs the slopes of the derivative curve for biomass treated with 10% IL-C ..... 143

Figure D3.2: Heating rates applied vs the slopes of the derivative curve for biomass treated with 20% IL-C .....143
Figure D3.3:Heating rates applied vs the slopes of the derivative curve for biomass treated with 30% IL-C .....144
Figure D3.4: Heating rates applied vs the slopes of the derivative curve for biomass treated with 40% IL-C .....144
Figure D3.5: Heating rates applied vs the slopes of the derivative curve for biomass treated with 40% IL-C .....145
Figure F1.1: Repeatability test of 100% discard coal at a heating rate of 4 ℃/min .....147

**LIST OF TABLES**

Table 4.1: Physicochemical analysis of biomass, discard coal, hydrochar and hydrochar/coal blends ..... 57
Table 4.2: The specific temperatures and differential thermogravimetric values used for calculating the slopes of the derivative profile of 100% discard coal at different heating rates ..... 65
Table 4.3: Calculated slopes for all samples at different heating rates ..... 67
Table 4.4: $TGspc$ and regression of fuels in descending order at the lower, middle and higher heating rates. ..... 67
Table 4.5: Classification of spontaneous combustion susceptibility based on $TGspc$ index values abducted from Manic *et al*. (2021) ..... 68
Table 4.6: A summary of crossing-point temperature, Stage II slope and the Wits-Ehac slope for six samples in Wits-Ehac index descending order ..... 70
Table 4.7: Classification of the spontaneous combustion potential ..... 70
Table 4.8: Comparison of the thermogravimetric analysis and the Wits-Ehac index spontaneous combustion tests data arranged in descending order for each test ..... 71
Table 4.9: Slopes obtained for every heating rate applied to the IL-treated 100% biomass samples ..... 77
Table 4.10: The $TGspc$ indices obtained at different sets of heating rates for 100% biomass treated samples. ..... 79
Table 4.11: Physicochemical analysis of 100% biomass and three biomass samples treated with IL-A, IL-B and IL-C. ..... 81
Table 4.12: Pore structure parameters of 100% biomass treated and untreated samples ..... 88
Table A2.1: The specific temperatures and differential thermogravimetric analysis values used for calculating the slopes of the sample's derivative profile at different heating rates (H; Hydrochar, DC: Discard coal) ..... 124
Table B1.1: The specific temperatures and differential thermogravimetric analysis values used for calculating the slopes of the derivative profile of the samples treated with IL-A ..... 128
Table C2.1: The specific temperatures and differential thermogravimetric analysis values used for calculating the slopes of the derivative profile of the samples treated with IL-B ..... 135
Table D2.1: The specific temperatures and differential thermogravimetric analysis values used for calculating the slopes of the derivative profile of the samples treated with IL-C ..... 142
Table E1.1: The pore diameter distribution data ..... 146

**LIST OF UNITS, ABBREVIATIONS AND ACRONYMS**

℃ – degrees Celcius

$\Delta H$ – energy

kg – kilogram

mg – milligrams

MJ – megajoule

ml – millilitre

nm – namometer

g – gram

μm – micrometre

J/kmol – joule per kilomole

BET – Brunauer-Emmett-Telle

C – carbon element

CAFS – Compressed Air Foam System

CO – carbon monoxide

$CO_2$ – carbon dioxide

DSC – Differential scanning calorimetry

DTA – Differential thermal analysis

DTG – Differential thermogravimetric analysis

FTIR – Fourier Transform Infrared Spectroscopy

H – hydrogen element

$H_2O$ – water

HTC – hydrothermal carbonisation

O – oxygen element

$O_2$ – oxygen

SOM – soluble organic matter

TGA – thermogravimetric analysis

XTP – crossing-point temperature

IL – Imidazolium-based ionic liquid

S/L – solid:liquid ratio

# CHAPTER 1: INTRODUCTION

## 1.1 Background of the Study

Coal is used extensively as a global primary energy resource presently (Cui *et al*., 2018). It is one of the most abundant fossil fuels, available at a lower cost than other fossil fuels from different international suppliers (Zaman *et al*., 2018). The main industries that rely on coal as a primary energy source include electricity power plants, cement production, and ferroalloys aluminium and steel manufacturing (IEA, 2018b; WEC, 2018). As of 2019, coal accounts for 37% of global electricity supply and is predicted to account for 26% of the global electricity generation by 2040 (IEA, 2018b). Currently, coal use is at a record level worldwide, and credit is owed to the fact that it is relatively easier to mine, process and transport than natural gas and oil (Melikoglu, 2018).

Coal is used more for electricity generation than other fossil fuels, but there is a public outcry to reduce its utilisation due to its greenhouse gas emission. An estimated 15 billion tonnes of carbon dioxide ($CO_2$) per annum are produced conventionally by generating electricity from coal-fired plants, and this is a major contributor to global warming (World Nuclear Association, 2020). Additionally, other pollutants that are produced and emitted include nitrous oxide ($NO_x$), sulphur dioxide ($SO_2$) and particulate matters (IEA, 2017). These pollutants are produced from the combustion of coal. Coal comprises a complex chemical lattice of carbon, hydrogen, and a collection of major/minor elements such as aluminium, nitrogen, silica, nickel, lead, arsenic and mercury (Franco & Diaz, 2009). Natural gas has also been considered an alternative source for power generation due to its relatively reduced greenhouse gas emissions per kWh of electricity generated (Oboirien *et al*., 2018). However, an attempt to substitute coal with natural gas has failed, given that natural gas is more expensive than coal (Melikoglu, 2018). Solar and wind energy are other clean and renewable energy sources that are a potential alternative source for electricity generation. Nonetheless, they are deemed intermittent since they both depend on weather conditions, and the storage of solar energy is expensive (Williams, 2013; Slabbert, 2017).

An increase in both the human population and electricity demand implies that there must be an advancement in clean coal technology to reduce emissions and inhibit climate change. In addition, it also implies exploring new potential energy sources for a clean electricity generation to reduce coal dominance. Biomass is by far the most available renewable energy source; it accounted for 50% of all renewable energy sources consumed in 2017 (IEA, 2018a).

With the availability of different and suitable combustion technologies, it can be co-fired with fossil fuel (coal) by modifying it through a hydrothermal process and blending it with coal to produce a new fuel (hydrochar/biocoal) (Setepu *et al.*, 2021). Coal must continue to play its role as the largest share of energy resources in the South African total energy mix. With over 2 billion tonnes of discard coal of various grades available in the country, hydrochar and coal blends suitable for application in existing coal power plants can be produced as new fuels meeting the regulated emission standard.

With the production of these new fuels (hydrochar and hydrochar/coal blends), comprising biomass, which is highly reactive, there is a need to understand the mechanism responsible for its susceptibility to spontaneous combustion to prevent explosion during transportation and storage. This will provide reliable data on the oxidation of these fuels and the measures necessary to mitigate this tragedy.

Limited studies have been reported using the Wits-Ehac index, along with thermogravimetric analysis (TGA), to measure the spontaneous combustion liability of coal and coal shale (Onifade, 2018; Onifade & Genc, 2019; Onifade *et al.*, 2020). A recent investigation has also utilised the Wits-Ehac index approach to determine the spontaneous combustion liability of different coals used for producing activated carbon (Abdulsalam *et al.*, 2020). Nevertheless, the Wits-Ehac index has never been used in determining the combustion liability of hydrochar and hydrochar/coal blends; therefore, this study sought to use this invention and compare the data with the calculated index from the TGA. Furthermore, this study sought to treat these new fuels with different ionic liquids to delay the oxidation and susceptibility of the products to spontaneous combustion.

### 1.2 Problem Statement

An increasingly prevalent concern pertinent to the hazards and lethal disasters caused by spontaneous combustion motivated this study. It has led to an outcry for extensive research to be conducted to find a viable, efficient and economically friendly method of inhibiting the spontaneous combustion of coal, biomass, hydrochar and hydrochar/coal blend using imidazolium-based ionic liquids. The findings of this study will contribute towards paving a way for other researchers, in line with the prevention of spontaneous combustion and the advancement of clean coal technology leading to the global dominance of coal for sustainable power and energy generation.

### 1.3 Aims and Objectives

This study aimed to determine the spontaneous combustion liability and to investigate the influence of imidazolium-based ionic liquids on the spontaneous combustion characteristics of coal, biomass and hydrochar/coal blends. The specific objectives of this study were:

I. To conduct physicochemical tests (calorific value, ultimate analysis, total sulphur and proximate analysis) of the raw *Searsia lancea* (biomass), coal, hydrochar and hydrochar/coal blends.
II. To produce hydrochar by hydrothermal carbonisation using *Searsia lancea* (biomass) as feedstock at known optimal set parameters.
III. To conduct spontaneous combustion tests on the untreated samples and predict their spontaneous combustion susceptibility using the Wits-Ehac Index and $TG_{spc}$ index.
IV. To pretreat the samples with three different imidazolium-based ionic liquids.
V. To conduct spontaneous combustion liability tests on the treated samples (coal, biomass, hydrochar and hydrochar/coal blends) before and after imidazolium-based ionic liquid pretreatment.

### 1.4 Research Questions

I. How do the imidazolium-based ionic liquids affect the intrinsic properties of coal, biomass, hydrochar and hydrochar/coal blend?
II. How do imidazolium-based ionic liquids affect the spontaneous combustion liability of coal, biomass and hydrochar/coal blend?
III. Which imidazolium-based ionic liquids show the best inhibiting effect on the spontaneous combustion characteristic of the samples?
IV. Which concentration of ionic liquid had the best inhibiting effect?
V. How does the rate of heating affect the spontaneous combustion characteristics of the samples?

### 1.5 Hypothesis

Three imidazolium-based ionic liquids inhibit the spontaneous combustion characteristic of coal. Therefore, it will be unlikely for the reagents not to suppress the spontaneous combustion liability of biomass, hydrochar and hydrochar/coal blends.

### 1.6 Layout of the Dissertation

The dissertation is structured as follows.

I. Chapter one introduces the background of the study, problem statement, aims and objectives, research questions and hypothesis.

II. Chapter two presents a detailed literature review of the study. It introduces spontaneous combustion and its mechanisms, the factors affecting the spontaneous combustion of coal and biomass, the techniques used to predict the occurrence of spontaneous combustion, and a survey on inhibitory measures previously applied to coal and biomass to prevent low-temperature oxidation.

III. Chapter three provides the research methodology followed to achieve the aims and objectives of this study. The chapter is divided into five sections: sample preparation; sample characterisation; hydrochar production; spontaneous combustion tests; and the treatment of the samples with three imidazolium-based ionic liquids.

IV. Chapter four presents the discussion of the results of the experimental studies as outlined in Chapter three. The results from the characterisation of biomass, coal, hydrochar and hydrochar/coal blends were discussed first, followed by the discussion of the spontaneous combustion test of the untreated and treated sample, and lastly, the characterisation results showing reduced spontaneous combustion liability.

V. Chapter five summarises the main findings and conclusions of the study, and the recommendations for future work are also included in the chapter.

## CHAPTER 2: LITERATURE REVIEW

This chapter presents a thorough literature review of the history and the inhibition of spontaneous combustion of coal, biomass, hydrothermal hydrochar and hydrochar/coal blends. The review explores different techniques previously investigated by academics, industries and various research institutes regarding the inhibition of the spontaneous combustion characteristic of the materials. Major factors that contribute to the cause of the event were also considered in the review. However, a special focus of the chapter is on imidazolium-based ionic liquids since this study sought to investigate their influence on the spontaneous combustion characteristic of hydrothermal hydrochar and hydrochar/coal blends. Research developments in line with the application of imidazolium-based ionic liquids in the coal industry, as well as different techniques used to predict and evaluate the risk of spontaneous combustion, are also discussed.

### 2.1 Introduction to Spontaneous Combustion

Many disasters can arise from coal mines. Spontaneous combustion is one of these major disasters that can restrain satisfactory yield and efficiency in the coal mining industry. The occurrence of spontaneous combustion in coal mines and the attempt to understand the phenomena dates to the early twentieth century (Guney, 1968; Phillips *et al*., 2011; Sloss, 2015). It occurs when a material is exposed to oxygen at ambient temperature for a long period during mining activities such as extraction, storage, stockpiling and transportation (Govender, 2015). The interaction between the material and oxygen results in an oxidation reaction, which generates heat within the material and causes its temperature to increase without any external heat source (Nelson & Chen, 2007). The material, therefore, self-heats and reaches a point of ignition as the heat accumulates due to a lack of sufficient heat dissipation by convection and conduction. As a result, there is an exponential net temperature increase within the material (Onifade, 2018). This process is more prominent in coal with an extremely low thermal conductivity as it tends to accumulate heat more than coal with excellent thermal conductivity (Zhang, 2004; Mohalik *et al*., 2006).

According to Mohalik *et al*. (2016), the following conditions are required for coal to undergo low-temperature oxidation without any source of heat.

I. The coal must react with oxygen.
II. The reaction must be exothermic and accompanied by heat generation.
III. The rate of heat generation must be greater than the rate of heat dissipation by radiation,

conduction and convection.

Spontaneous combustion is a known phenomenon in the coal industry, but it is not limited to coal since it can also occur in other materials (Phillips *et al*., 2011). However, the development of the coal industry is also restricted by this phenomenon, given that its occurrence presents a major safety issue in mines (Beamish & Blazak, 2005; Singh *et al*., 2007; Xue *et al*., 2010; Song & Kuenzer, 2014; Beamish *et al*., 2021). Additionally, the oxidation of coal leads to the deterioration in the molecular structure, elemental composition and other coal properties, thereby influencing its technological application (Cimadevilla *et al*., 2005; Mastalerz *et al*., 2009; Zhang *et al*., 2013). Significant environmental problems, such as the emission of greenhouse gases and the release of hazardous trace elements, may result due to the occurrence of low-temperature oxidation, known as spontaneous combustion (Pone *et al*., 2007; Zhao *et al*., 2008; Carras *et al*., 2009). This phenomenon in coal mines can also result in mortality of workers, gas and dust explosions, property destruction, loss of energy resources, methane leaking and a potential economic downturn (Bo-tao *et al*., 2009; Wang, 2012). In addition, restoring damage from spontaneous combustion may require significant financial incentives, which may lead to a mine shutdown (Zhang *et al*., 2018).

### 2.2 Spontaneous Combustion Mechanisms

The initial stages of coal oxidation concerning the weathering phenomena are one of the earliest investigations carried out by Parr and Wheeler (1908). The authors demonstrated this phenomenon by placing a coal sample in a sealed jar and storing it for ten months. The compressibility of the produced gas and the partial pressure of the gases released in a jar were measured to quantify the combustibility of the gases produced and the effect of volatile matter released. The study reported a loss of calorific value due to weathering, and the author concluded that the sample's low-temperature aerial oxidation was responsible for the change observed. The effects of spontaneous combustion on the volatile matter release and oxygen adsorption were quantified by measuring the combustibility and the partial pressure of the gases generated during the reaction. Regarding the spontaneous combustion liability of coal, some studies focused on the mechanisms involved in understanding oxygen consumption and identifying the products formed during the oxidation reaction (Wang *et al*., 2002; Yuan & Smith, 2011; Zhang *et al*., 2015b). These studies revealed the major pathways involved in the low-temperature oxidation of coal. Generally, the process of low-temperature oxidation of coal has been referred to as a complicated process. However, Yang *et al*. (2017) reported that

spontaneous combustion occurs because of several complex chemical reactions and a combination of several physical phenomena such as mass transfer, heat transfer, phase change and turbulent flow.

Coal can undergo several oxidation reactions depending on the factors involved in the process. Although the reaction processes may be different, they all have an exothermic characteristic that leads to the self-heating of the coal sample. To explain the mechanism of the self-heating phenomena, the chemical reactions and the factors involved during the reaction must be known. According to the literature, three exothermic reactions are possible in limiting coal oxidation at low temperatures. The initial reaction is due to the oxidation of coal by direct contact with oxygen, followed by the oxidation of pyrite in the coal matrix, and the water molecule's adsorption by the coal surface (Wang *et al*., 2003). The biochemical reaction of bacteria on the coal surface is another possible heat-producing reaction, but it is mostly ignored by researchers due to its insignificant heat contribution.

Three key factors required for these reactions to take place are the concentration of oxygen and the presence of pyrite and water. The following equations show the three heat-releasing reactions in detail (Avila, 2012).

**Coal oxidation**

$$Oxygen + Dried\ coal \longrightarrow Heat \quad (2.1)$$

**Pyrite oxidation**

$$Water + Oxygen + High\ pyrite\ content\ in\ coal \longrightarrow Heat \quad (2.2)$$

**Water absorption/desorption**

$$Water + Oxygen + High\ active\ coal\ surface \longrightarrow Heat \quad (2.3)$$

Schmal (1989), Rosema *et al*. (2001) and Stracher & Taylor (2004) reported from their investigations that when spontaneous combustion takes place, oxygen is adsorbed through a physical process, which, in turn, is converted into a chemical chain reaction. This process leads to the production of carbon monoxide and carbon dioxide gases and the oxidation of the pyrite content in the coal. The findings from these authors suggested that the oxidation reaction is exothermic and that it can be represented by Equation 2.4

$$Coal + Oxygen \rightarrow Oxygen + Heat \rightarrow Gas\ products \quad (2.4)$$

According to Mohalik *et al*. (2009. Pg 271), the process of coal oxidation may consist of three steps:

I. Physical adsorption.
II. Chemisorption, whereby oxygen-coal complexes are formed.
III. The chemical reaction, where some unstable oxygen-coal complexes are broken down and gases such as carbon monoxide, carbon dioxide and water are released.

These processes may be summarised according to Equation 2.5 (Sinha & Singh, 2005; Mohalik *et al*., 2009).

$$Coal + O_2 \rightarrow CO_2 + \Delta H \uparrow \quad (2.5)$$

However, the reaction represented by Equation 2.5 may take place in several steps. Therefore, Equation 2.6 represents the total oxidation of coal (Schmal, 1989; Sinha & Singh, 2005).

$$C_{110}H_{74}O_{11} + 113O_2 \rightarrow 100CO_2 + 37H_2O + 4.2 \times 10^8 J/kmol\ O_2 \quad (2.6)$$

The chemisorption of oxygen on the surface of coal may be represented as (Schmal, 1989; Sinha & Singh, 2005):

$$C_{110}H_{74}O_{11} + 17.5O_2 \rightarrow C_{110}H_{74}O_{46} + 2.5 \times 10^8 J/kmol\ O_2 \quad (2.7)$$

If coal contains catalytic components such as pyrite, the exothermic reactions can be represented by Equations 2.8 and 2.9 (Schmal, 1989; Sinha & Singh, 2005).

$$2FeS_2 + 7O_2 + 2H_2O \rightarrow 2H_2SO_4 + 2FeSO_4 + 0.37 \times 10^8 J/kmol\ O_2 \quad (2.8)$$

$$4FeS_2 + 15O_2 + 2H_2O \rightarrow 2H_2SO_4 + 2Fe_2(SO_4)_2 + 0.56 \times 10^8 J/kmol\ O_2 \quad (2.9)$$

Besides carbon, coal also contains other organic components such as hydrogen, oxygen, nitrogen and sulphur. The presence of these components in coal may initiate other side reactions. Therefore, Kim (1993) reported that the oxidation of coal by oxygen can be better represented by Equation 2.10.

$$CH_{1.18}N_{0.15}O_{0.35}S_{0.005} + 1.125O_2 + 4.15N_2 \rightarrow CO_2 + 0.58H_2O + 0.005SO_2 + 4.15N_2 + Heat \quad (2.10)$$

Other theories have been used to explain the spontaneous combustion mechanism. According to the free radical theory of coal spontaneous combustion, a lot of alkyl free radicals are generated by coal as it oxidises. Thereafter, peroxide radicals are formed when oxygen further

reacts with the alkyl radicals generated. Since heat is generated during the reactions, hydroperoxide is formed due to peroxide radicals reacting further. The hydroperoxide decomposes according to different structures, releasing gases such as carbon monoxide and carbon dioxide (Li, 1996; Wang *et al*., 2003). The release of these gases indicates the number of active sites in coal and the degree to which the free radical chain reaction can take place.

## 2.3 Spontaneous Combustion of Coal

### 2.3.1 Factors affecting the spontaneous combustion of coal

The low-temperature oxidation of coal takes place as soon as the coal seam is exposed to oxygen after extraction. The oxidation reaction is a complex process that occurs in different pathways, and numerous steps are involved depending on the coal's physicochemical characteristics. However, given that heat accumulation is crucial for several exothermic reactions, the oxidation of coal also depends on the particle size of the coal and the stockpile of coal (Singh & Demirbilek, 1987). In the case of coal and stockpile sizes being a factor, various parameters also play a significant part in promoting heat accumulation. These parameters include the storage period, the speed of wind in contact with coal, compaction degree, the height of the deposit and the lateral angle of the stockpiles (Fierro *et al*., 1999). The combination of these parameters promotes the occurrence of the oxidation of coal during processing and transportation.

Singh & Demirbilek (1987) and Wang *et al*. (2003) reported on numerous factors responsible for the spontaneous combustion of coal. The authors identified the temperature of the surroundings and the oxygen concentration as the most important factors. The presence of water, particle surface area, coal rank, pore structure, maceral groups, sand particular matter, pyrite content and metamorphic degree are other important factors that affect the extent of the oxidation reaction (Liang & Wang, 2003; Zhang *et al*., 2016). Additionally, two constants account for the physical and chemical factors that influence the kinetics of this reaction: the activation energy and the pre-exponential factor A (Arisoy & Beamish, 2015). The intrinsic reactivity and the reaction rate are also strongly affected by these factors. The following section provides a detailed description of each of the factors mentioned.

#### *2.3.1.1 Temperature*

Studies on the self-heating of coal done by Carpenter & Giddings (1964), Jimenez *et al*. (1999)

and Nugroho *et al*. (2000) reported temperature as the most significant factor affecting the reaction rate during spontaneous combustion. The relationship between the temperature and the rate of reaction during the self-heating of coal can be described using the Arrhenius equation (Nugroho *et al*., 2000). Temperature does not only affect the rate of reaction but also has an impact on secondary reactions. Those reactions include the diffusion rate of oxygen through the coal, the diffusion and desorption of the formed products from the coal surface, and the adsorption of oxygen and water (Carpenter & Giddings, 1964; Jimenez *et al*., 1999).

The temperature profile within the coal pile can be established through the changes that occur within the coal pile and the surroundings. On a chemical level, the temperature profile is affected by the exothermic reaction since it results in heat release, and it is also affected by the vapours adsorbed onto the coal's surface on a physical level (Bhattacharyya, 1971; Krajciova *et al*., 2004). One of the factors that are found in the surroundings but impact the temperature of the coal bed is solar radiation (Krajciova *et al*., 2004). However, there is not much extensive research done on solar radiation, although it has been reported that it depends on the season, it is still considered a relevant factor (Krajciova *et al*., 2004).

To understand the mechanism of spontaneous combustion, Lu & Hu (2007) discovered that as the temperature of the coal bed rises, the coal's active functional groups become activated and react with oxygen, leading to spontaneous combustion. In a thermal study of the spontaneous combustion behaviour of partially oxidised coal, Deng *et al*. (2016) investigated the effect of temperature on the oxidation characteristics of fresh and oxidised coal. The authors reported that the oxidation characteristics of oxidised coal increased rapidly with temperature compared to fresh coal.

Wang *et al*. (2019) investigated the effect of temperature on the spontaneous combustion of coal before oxidisation and found that when the coal bed's temperature increases, its susceptibility to spontaneous combustion increases. It was further reported that low-temperature oxidation could occur if the coal bed becomes oxidised at a temperature above 130 ℃. Li *et al.* (2021) found that as the temperature increases from 70 to 350 ℃, the porosity of the coal gangue also increases, causing thermal degradation, potentially leading to the coal gangue's spontaneous combustion. Shi *et al.* (2021) reported that temperature is a dominant factor that affects the spontaneous combustion of coal significantly in the initial stage of coal oxidation. The authors further reported that heat insulation could help to inhibit the propagation of coal's spontaneous combustion.

#### *2.3.1.2 The moisture content in coal and the atmosphere*

Naturally, coal is a highly hygroscopic material, likely absorbing moisture from the atmosphere (Avila, 2012). The moisture content of a freshly mined coal sample depends on the maturity reached by the coal as it was formed geologically (Van Krevelen, 1993). The energy required to evaporate moisture from the coal's surface depends on its molecular structure. Moisture molecules in coal can be arranged in three ways: loosely bound, tightly bound or free (Chen, 1994). The presence of moisture in coal has two implications. Firstly, moisture can promote the oxidation of coal by behaving as a catalyst leading to the corresponding heat release (Hao *et al*., 2014). Secondly, high moisture content can achieve inhibition by obstructing the pores on the coal surface and the free active sites. This allows for coal oxidation by oxygen, reduces the temperature of the coal and retards the spontaneous combustion of coal (Saffari *et al*., 2019).

A temperature-rise and oxidation of coal from 30 to 110 ℃ was simulated by Zheng *et al*. (2014). The authors found that the formation of peroxyl complex was promoted by high moisture content, while high moisture content showed an inhibitory effect on coal oxidation at a high-temperature stage. Studies by Tang & Xue (2017) and Zhai *et al*. (2019) showed that after bituminous coal was immersed in water, the porosity and the specific surface area of the coal increased. As a result, an increase in the functional group's activity was also realised, leading to the coal's spontaneous combustion. Zhong *et al*. (2019) reported that coal samples immersed in the water had a higher spontaneous combustion liability than raw coal. Wang *et al*. (2020b) found that coal with a moisture content of 10.11% had a high spontaneous combustion liability.

As coal is exposed to the atmosphere, water adsorption and desorption occurs between the atmosphere and coal, and this process ceases as an environmental equilibrium is established. The water desorption process is an exothermic reaction; about 44.4 kJ/mol of heat is released into the atmosphere (Mahajan & Walker, 1971). The moisture absorption process is directly affected by other factors, such as the coal's surface area and porosity. These factors also depend on the rank of the coal (Mohalik *et al*., 2016).

According to Mahajan & Walker (1971), should the moisture absorption process result in the absorption of the evolved heat instead of heat release, a chain of oxidation reactions may occur

due to an increase in coal bed temperature. For this reason, relative air humidity is considered one of the most important factors affecting the coal oxidation process (Bhattacharyya, 1971). The effect of atmospheric moisture content on the propensity of coal to undergo spontaneous combustion was investigated by Smith & Glasser (2005). The results showed that the atmospheric moisture content plays a catalytic role by accelerating the oxidation rate of coal. In a study by Miura (2016), three brown coal samples were exposed to saturated air at 38 ℃. The coals absorbed moisture rapidly, and the coal's temperature increased from 40 to 43 ℃ within one minute, heating the surroundings and promoting the self-heating of coal. Ma *et al*. (2017) investigated the relationship between coal's spontaneous combustion and air humidity levels and reported that the concentration of gases released during the coal oxidation reaction increases as the air humidity increases.

#### *2.3.1.3 The concentration of oxygen on the coal surface*

Several researchers have reported oxygen concentration as one of the major causes of the self-heating of coal (Marinov, 1977; Hull *et al*., 1997). On the coal's surface, there is a directly proportional relationship between the oxygen partial pressure and the rate at which coal oxidises (Van der Plaats *et al*., 1984). This is because the active sites of coal reduce during oxygen adsorption leading to a state of saturation. At this state, the ignition point temperature shifts to a much higher value (Medek & Weishauptova, 1999).

Secondary reactions, such as the oxidation of pyrite and the adsorption of water molecules, can also be affected by the concentration of oxygen, which may, in turn, induce the low-temperature oxidation of coal (Qi *et al*., 2010). Therefore, the concentration of the oxygen absorbed by coal has been used as a factor to predict coal's susceptibility to undergo spontaneous combustion (Parr & Kressman, 1911). This factor is used to predict the self-heating characteristic of different types of coal (Qi *et al*., 2010). In an investigation conducted by Wen *et al*. (2017), the oxygen concentration was found to have a very intricate and complex effect on the coal's spontaneous combustion characteristic index (Wen *et al*., 2017). Huangfu *et al*. (2018) discovered that increasing oxygen concentration and heating rate stimulates coal oxidation. It was further reported that as the oxygen concentration increase, the self-ignition temperature decreases by 10.1% to 19.4%. The effect of oxygen concentration on the spontaneous combustion characteristic of neutral and acidic coal was investigated (Li *et al*., 2020b). The results showed that when the oxygen concentration decreased, the thermogrametric and different scanning calorimetry analysis (TG-DSC) shifted to a region of

high temperature, leading to a decreased heat release rate.

#### *2.3.1.4 Coal particle size*

The influence of coal particle size on the spontaneous combustion characteristic of coal was investigated by Carpenter & Sergeant (1966), Akgun & Arisoy (1994) and Mathews *et al*. (1997). These authors used pulverised coal of – 75 μm, and their findings show that the smaller the particle size, the higher the external surface leading to an increased rate of oxygen consumption (Carpenter & Sergeant, 1966). Another investigation by Kucuk *et al.* (2003) reported that the combination of small particle size and high external surface area is not as significant as high internal surface area, given that an increase in the surface area directly impacts the self-oxidation reaction. Saleh & Nugroho (20l3) also found that as the particle sizes decrease, the spontaneous combustion propensity of coal increases. Rifella *et al*. (2019) likewise reported that larger coal particles are less susceptible to spontaneous combustion than smaller coal particles. Li *et al*. (2020a) observed that as the coal particle size increases, the ignition delay time also increases, and that is why larger particles are less susceptible to spontaneous combustion.

An investigation was conducted by Ejlali *et al.* (2009) to investigate the relationship between different coal particle sizes and their spontaneous combustion liability. The oxidation and heat transfer rates were higher in smaller coal particles. It was further reported that the oxidation rate of the small particles stops increasing when the critical diameter of the particle is reached. At critical diameter, oxygen diffuses through the particle easily since there is no mass transfer resistance at that point. However, according to the authors, other factors, such as the permeability of the particles and the surrounding conditions, should not be neglected when investigating the effect of particle sizes on the self-heating characteristic of coal since they also play a major role. In conclusion, it was reported that smaller particle sizes are highly susceptible to spontaneous combustion compared to bigger particle sizes.

#### *2.3.1.5 The internal surface area and porosity of the coal*

The coal’s surface area is one of the factors that affect the progress of its self-oxidation reaction (Carpenter & Sergeant, 1966). In enhancing the oxidation reaction through the surface area of the coal, Van Krevelen (1993) found that the coal's internal porosity structure provides the main contributing factor, especially when the diameter is less than 2 nm. It has been reported that low-rank coals, such as brown coal, are highly prone to spontaneous combustion because

this type of coal is not tightly packed, or carbon-dense and it has a high surface area. Unlike other types of coal, brown coal tends to have high volatile matter and moisture content, contributing to the progress of the oxidation reaction (Avila, 2012).

Xu *et al*. (2013) reported that anthracitic coal, which reflects a high degree of metamorphism, is less prone to spontaneous combustion than lignite coal, which reflects a low degree of metamorphism. Coal with a low degree of metamorphism has high porosity, implying a high internal surface area, and a high number of active sites that are available to absorb moisture and react with oxygen (Wang *et al*., 2003). According to Moroeng (2015), the high oxidation rate of coal results in an increased rate of coal weathering, which releases high energy since it is an exothermic reaction, thus promoting coal's spontaneous combustion.

#### *2.3.1.6 Coal mineral composition*

The mineral contents found in coal can have two effects on its spontaneous combustion. Some minerals have been proven to behave like catalysts during the oxidation reaction (Herman *et al*., 1984; Sunjanti & Zhang, 1999). The presence of minerals, such as calcium carbonate ($CaCO_3$), sodium acetate ($NaAc$), copper (II) acetate ($Cu(Ac)_2$) and potassium acetate ($KAc$), during the oxidation reaction of coal may result in the release of heat. Although, the concentration of these minerals in coal is usually small (ranging from 1 to 5%), depending on the nature of the coal (Avila, 2012). The occurrence of organic and inorganic trace elements in coal mineral matter significantly impacts its spontaneous combustion liability, the environment and the economy (Mardon & Hower, 2004; Wagner & Hlatshwayo, 2005).

The presence of higher concentrations of minerals in coal, such as pyrite, carbonates (dolomite, calcite and siderite), illite, kaolinite, quartz, oxides (hematite and magnetite), muscovite and kaolinite, are advantageous as they tend to behave like inhibitors during the oxidation reaction (Beamish & Hamilton, 2005). They achieve inhibition by behaving as a heat sink and obstructing the active sites of coal (Beamish & Arisoy, 2008). Onifade (2018) reported that coal and coal shales with high mineral content are less susceptible to spontaneous combustion. The total concentration of the mineral is usually taken as the remains of coal after it burns out, which is the ash content. It has been reported that when the concentration of the minerals is higher than 10 wt%, its ability to act as an inhibitor becomes independent of the mineral's chemical composition (Beamish & Arisoy, 2008).

Wagner & Hlatshwayo (2005) reported that coal's sulphur content could vary between 0.4%

and 1.29%. In another investigation, Robert (2008) reported that it can vary between 1.74% and 1.56% and from 5.4% to 15.1% for some Southern African coal (Olivella *et al*., 2002). An excess amount of sulphur in coal accelerates its propensity to undergo spontaneous combustion (Deng *et al*., 2015a). Zheng *et al*. (2021) investigated the effect of organic sulphur on coal's spontaneous combustion and found that the added organic sulphur compound inhibits the coal's oxidation reaction and free-radicals production. Wang *et al*. (2021b) investigated the effect of a different type of sulphur, pyritic, on the low-temperature oxidation of coal. It was found that when pyritic sulphur content is greater than 3%, the spontaneous combustion of coal is accelerated, and their result was similar to that of Beamish & Beamish (2012). Sunjanti & Zhang (1999) reported that calcium carbonate could also promote coal's spontaneous combustion, given that the high content of carbonates absorbs heat, causing the temperature of coal to increase.

#### *2.3.1.7 Maceral group in coal*

Maceral composition, also referred to as coal's organic content, is made up of carbon structures formed by the carbonisation of plant material. The most known groups of macerals found in coal are vitrinite, liptinite and inertinite (Van Krevelen, 1993). The composition and structure of the three maceral groups vary widely, influencing their combustion liability (Moroeng, 2015). Unlike northern hemisphere coals, Southern African coal found in the main Karoo Basin is rich in inertinite ranging from 20% to 80%, and variable proportions of vitrinite (Falcon, 1986). Vitrinite macerals are made up of woody plant tissue containing lignin, cellulose and a fraction of hemicellulose (O'Keefe *et al*., 2013; Moereng *et al*., 2019). On the other hand, inertinites originate through multiple pathways, but the most common formation pathway is through the aerial oxidation of plant tissues such as parenchymatous and xylem (Falcon & Snyman, 1986; ICCP, 2001). Southern African coal has a very low concentration of the liptinite group, which is formed from waxy plant material (Onifade, 2018).

Generally, maceral groups (vitrinite, inertinite and liptinite) found in coal are susceptible to spontaneous combustion and weathering due to changes in environmental conditions such as temperature and humidity (Onifade, 2018). Amongst the three maceral groups, vitrinite has the highest spontaneous combustion liability compared to inertinite and liptinite macerals (Falcon, 1986; Beamish & Blazak, 2005; Ivanova & Zaitseva, 2006). Avila (2012) found that as the vitrinite reflectance increases, the spontaneous combustion liability of coal also increases. However, Misra & Singh (1994) stated that if inertinite is very abundant in coal, it might

propagate the spontaneous combustion of that coal due to its high porosity and high gas absorption affinity.

In terms of petrography and spontaneous combustion liability of South African coal shales, Onifade (2018) found that coal shales with high inertinite macerals are more susceptible to spontaneous combustion. However, Mohalik *et al*. (2017) found that there was no correlation between the maceral groups present in coal and its spontaneous combustion susceptibility. Saffari *et al*. (2020) investigated the effect of maceral content on the tendency of coal to undergo spontaneous combustion. The authors reported that coal samples with high vitrinite and liptinite and low inertinite are more susceptible to spontaneous combustion.

#### *2.3.1.8 Coal rank*

The coal rank, also known as coal maturity, is used in the industry to predict the spontaneous combustion characteristic of coal (Moroeng, 2015). Coal of different ranks is formed when carbonaceous materials are metamorphosed at different degrees of coalification (Suarez-Ruiz & Crelling, 2007). The reflection of light, particularly that of the maceral contained in the coal, gives the measurement of the coal rank, matrix crystal structure and maturity (British Standard Institute, 1995b). The porous structure of a low-rank coal such as peat or brown coal captures most of the light directed to them; therefore, they are low-rank coals with high porosity and structural isotropy (Deng *et al*, 2014).

Coke and anthracites are regarded as high-rank coals since they have a high reflectance value due to the organised aromatic carbon structure in the coal matrix and a highly developed anisotropy (Avila, 2012). Given that coal reactivity and the crystal structure of the coal matrix have a directly proportional relationship, high-rank coals are less reactive than low-rank coals (Arisoy & Beamish, 2015). Deng *et al*. (2014) reported that high-rank coal has a slower rate of oxidation reaction when using $CO$ and $C_2H_4$ initial gas concentration to determine the spontaneous combustion liability of different ranks of coals. A study conducted by Zhang *et al*. (2020) also revealed that the production of $CO$ and $CO_2$, as well as the oxygen absorption rate, were high for low-rank coal and lower for high-rank coal. Wang *et al*. (2021a) reported the same trend when investigating the spontaneous combustion of different ranks of coal using a comprehensive index evaluation.

#### *2.3.1.9 Coal density*

The density of a coal sample is one of the most important parameters in the mining industry regarding spontaneous combustion. It has been said to indicate the rate of the oxidation

reaction, the distribution of moisture content in the coal, the volatile matter content, ash content and the fixed carbon (British Standard Institute, 1995a). However, little research links coal density to its spontaneous combustion characteristic (Avila, 2010). It has been reported that the rate of coal weight loss during low-temperature oxidation is directly proportional to the amount of volatile matter emitted during the reaction (Marinov, 1977). However, the findings of these studies are not reliable enough to conclude the relationship between coal density and spontaneous combustion.

#### *2.3.1.10 The chemical composition of coal*

Coal samples cannot be differentiated by their ranks and their macerals compositions only but by their chemical compositions as well. The susceptibility of the coal to self-oxidation and other reactions can be understood from the coal's chemical composition. One important factor playing a major role in the spontaneous combustion of coal is its change in aliphatic hydrocarbons, which is caused by the oxidation reaction (Zhang *et al*., 2016). Measuring the change in the coal's aliphatic hydrocarbons during low-temperature oxidation gives the reaction kinetics of the methyl and methylene groups in the coal matrix. Several techniques are usually used to analyse the chemical composition of the coal samples. Those techniques include gas chromatography, mass spectroscopy, Fourier Transform Infrared Spectroscopy (FTIR), ultimate analysis and proximate analysis (Iglesias *et al*., 1998). The results from these analyses can be used to predict the rate of the oxidation reaction and the postulated mechanism and identify the chemical reactions involved (Wang *et al*., 2003).

#### *2.3.1.11 Presence of soluble organic matter in coal*

According to modern chemistry, coal is made up of various substances. The micro-molecules in coal are embedded in a macromolecular network, which forms when some structural unions that are similar but not mutually identical bridge with each other (Lopez *et al*., 1998; Krzesinska, 2002; Marzec, 2002). Approximately 1 to 30% of micro-molecules in coal can be leached out by solution (Zeng & Xie, 2004; Sun & Duan, 2011). Although soluble organic matter (SOM) found in coal affects its spontaneous combustion characteristic and the inhibitory effect of coal, relevant in-depth research still needs to be done to prove this. Only a few researchers have reported on the effect of SOMs on the coal structure, and their findings have proved that the coal pores and fracture structure are shaped by the contents of the SOMs (Yang *et al*., 2017). Additionally, the spontaneous combustion characteristic of coal is said to be affected by the active side chains and free radicals.

Yang *et al.* (2017) conducted some experiments to investigate the effect of the SOM composition on the structure of coal. They extracted SOMs from coal samples before and after low-temperature oxidation at different metamorphic degrees. SOMs accelerated the oxidation reaction of coal by releasing heat, given that they contain an increased number of side chains and active functional groups that can generate and break free radicals (Yang *et al*., 2017). However, when the SOMs are extracted, the coal pores increase, allowing for inhibitors to easily penetrate the coal to inhibit the low-temperature oxidation of the coals' functional groups. Additionally, the absence of SOMs reduces the severity of the low-temperature oxidation of coal by allowing water to cover the tiny cracks on the coal's surface.

### 2.3.2 Techniques used to predict the spontaneous combustion of coal

Generally, methods commonly used to predict the spontaneous combustion liability of different materials are based on thermal analysis (Nelson & Chen, 2007). Predicting the spontaneous combustion liability of coal is imperative as it is one of the most important safety measures in the mining environment (Rath, 2012). The results from the prediction also inform the decision to be made about the coal seam incubation period. Various methods that have been adopted by several researchers to measure the susceptibility of coal to undergo spontaneous combustion are described in detail below.

#### *2.3.2.1. Differential thermal analysis*

Several researchers have used differential thermal analysis (DTA) to measure the spontaneous combustion liability of coal samples (Whitehead & Breger, 1950; Mohalik *et al*., 2009). Several studies recommend this technique for predicting spontaneous combustion instead of characterising coal samples. Additionally, DTA may be used for quantitative and qualitative analysis (Mohalik *et al*., 2016). To predict the spontaneous combustion liability, a coal sample is subjected to a constant rate of heating while measuring the difference in the temperature change of the coal sample and that of the inert material. The temperature difference between the two materials shows how the coal sample evolved as it was heated.

The results obtained from the test are usually plotted on a thermogram, as shown in Figure 2.1, with three reaction stages. The first stage (I) shows the release of moisture from the coal sample. The second stage (II) involves the start of an exothermic oxidation reaction, while the third stage (III) reveals the burnout of the coal. For a coal sample with a low spontaneous

combustion liability, the slope of the second stage is expected to be low (Gouws & Wade, 1989). The point where the thermogram crosses the zero-base line gives the crossing point temperature, which is the point where the temperature of the coal is equal to that of the inert material.

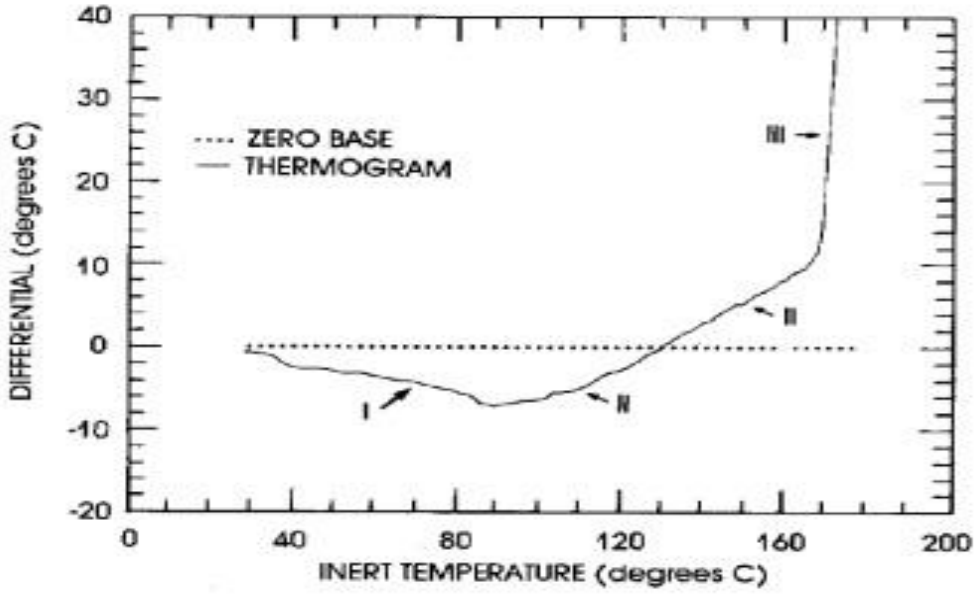



*Figure 2.1: A thermogram generated by differential thermal analysis, extracted from Gouws & Wade (1989)*

Kim & Chaiken (1990) studied the spontaneous combustion liability of coal, carbonaceous shale and roof coal using a differential thermal analyser. The equipment evaluated the temperature change of the samples within the shortest period. The extent of the spontaneous combustion of the samples was evaluated based on the depletion of $O_2$, as well as the release of $CO_2$ and $CO$. The authors concluded that the high amount of gases released could be associated with the high spontaneous combustion liability of coal. Using DTA, Pis *et al*. (1996) investigated the spontaneous combustion liability of six types of coal, from bituminous coal to semi-anthracite. The authors reported that as the rank of the coal increases, both the self-heating and temperature reached after combustion increase; lower-rank coal has the least ignition temperature and is more susceptible to spontaneous combustion. There is no rule of thumb when selecting parameters in the application of DTA (Mohalik *et al*., 2009). Therefore, reproducing the results from one sample tested twice under the same conditions is difficult.

#### *2.3.2.2. Differential scanning calorimetry*

Differential scanning calorimetry (DSC) is used to measure the propensity of coal and its

response to spontaneous combustion by heating a coal sample and an inert sample under identical conditions over a certain period (Garcia *et al*., 1999; Sahu *et al*., 2004; Mohalik *et al*., 2009). Unlike the DTA, which measures the difference in temperature between the inert and coal, DSC measures the difference between the amount of energy required to raise the temperature of the coal sample and that needed to raise the temperature of the inert material. The difference is plotted as a function of temperature change (William, 1986). The chemical and physical transformation during the oxidation reaction causes the difference in energy required for both materials (Mohalik *et al*., 2016).

Raymond (2015) used DSC to investigate the inhibition effect on the spontaneous combustion of coal using inorganic phosphates and sulfonate salts. The result showed that the reagents used successfully inhibited spontaneous combustion by making coal thermally stable. Tang (2017b) used the same method to investigate the inhibitory effect of phosphorus flame retardants and reported that at a temperature range of 50 to 150 ℃, there was an increase in the activation energy of coal after treatment, indicating a lower ignition temperature and reduction in combustion rate. Tsai *et al*. (2017) compared the results from the DSC and TGA to determine the inhibition mechanisms of five types of inhibitors, reporting a similar spontaneous combustion index. A study by Mohalik *et al*. (2009) was conducted using DSC to measure the spontaneous combustion of coal proved no uniformity in the laboratory parameters when using this technique.

#### *2.3.2.3. X-ray diffractometer*

The X-ray diffractometer (XRD) technique can also be used to predict the spontaneous combustion liability of coal, specifically by analysing and quantifying the minerals contained in the sample (Kelemen *et al*., 1990; Gong *et al*., 1998; Kok, 2008). To confirm the viability of this method, the results are usually compared to those obtained using other thermal analyses, as well as petrographic analysis. Given that coal contains iron, the catalytic reaction of the mineral (iron) and oxygen also takes place in coal during the low-temperature oxidation reaction (Mohalik *et al*., 2016). Because of this catalytic reaction, the iron minerals, such as pyrite, tend to be altered as coal undergoes low-temperature oxidation. Their alterations are based on their mineralogy and the form of sulphur present in coal (Ribeiro *et al*., 2016).

Deng *et al*. (2015a) investigated coal samples with different pyrite contents in a laboratory and found that spontaneous combustion liability of coal increased when the pyrite content was

between 5 and 7%. From the XRD analysis, Zhang *et al*. (2015a) observed that $Fe_2O_3$ and C form a compound, which results in weathering of the coal surface walls, increases the exposure of coal to oxygen. The same authors concluded that pyrite promotes the spontaneous combustion of coal. Wang *et al*. (2020a) reported that the oxidation of coal with seven types of oxygen-containing groups is accelerated by pyrite content between 2-4 mass% under oxidising conditions.

#### *2.3.2.4. The Frank-Kamenetskii method*

This technique is based on a mathematical model derived from the Frank-Kamenetskii theory for self-heating material (Frank-Kamenetskii, 1940). The model was derived by applying mass and energy balance around coal. The differential Equation (2.11) computes the energy balance around coal.

$$\rho \cdot Cp \cdot \frac{\partial T}{\partial t} = \lambda \frac{\partial^2 T}{\partial x^2} + \dot{q}' \quad (2.11)$$

Where: $\rho$ = density of coal

$Cp$ = heat capacity

$\lambda$ = thermal conductivity

$\dot{q}'$ = heat that is generated during the reaction

The temperature profile of the material is shown by Equation 2.12, which represents a stationary solution of Equation 2.11.

$$\lambda \frac{\partial^2 T}{\partial x^2} = -\dot{q}' \quad (2.12)$$

Frank-Kamenetskii found a stationary solution when balancing Equation 2.12 and expressed it as Equation 2.13.

$$\dot{q}' = -\Delta H_{Rx} \cdot \rho \cdot A \cdot e^{-E/RT} \quad (2.13)$$

Where: $\Delta H_{Rx}$ = heat of the reaction

$A \cdot e^{-E/RT}$ = the relationship between the reaction and temperature

Assuming that L is the size of a slab of coal, Frank-Kamenetskii applied border conditions to a slab of coal and defined parameter $\delta$ according to Equation 2.14) (Frank-Kamenetskii, 1940).

$$\delta = \left(\frac{\Delta H_{Rx} \cdot \rho \cdot A}{\lambda} \cdot \frac{E \cdot L^2}{R \cdot T_0^2} e\right)^{-E/R \cdot T_0^2} \quad (2.14)$$

$T_0$ represents the ambient temperature. The parameter $\delta$ does not have dimensions. As per Equation 2.14, the parameter is the ratio of the heat generated during the reaction to the heat diffusivity (Avila, 2012). The self-ignition temperature of different materials, such as coal and waste, can be predicted using the Frank-Kamenetskii parameter (Gray *et al*., 1984; Jones & Vais, 1991; Jones, 1999).

#### *2.3.2.5. Isothermal oven/reactor testing*

This technique involves heating the coal sample at a constant temperature in an oven. For this method, the most important measurement is the time taken for the coal sample to undergo a thermal runaway reaction. If there is no thermal runaway within the pre-set time, then the oven temperature is increased. Yuan & Smith (2012) used an isothermal oven to investigate the effect of ventilation on the spontaneous heating of coal, and the results demonstrated that the thermal runaway of coal could be reached at lower temperatures with sufficient ventilation. Chen *et al*. (2015) compared the isothermal oven method to a metal basket heating method to predict the spontaneous ignition temperature. The authors reported the ignition temperature of coal to be 120 ℃ for a ventilated isothermal oven and 100 ℃ for a metal basket. In a test conducted by Yin & Song (2019), the data obtained from the isothermal oven experiment was used to validate a model for spontaneous combustion prediction at a high-temperature stage instead of low-temperature oxidation. Figure 2.2 shows the type of graphical results expected from an isothermal oven spontaneous combustion test.

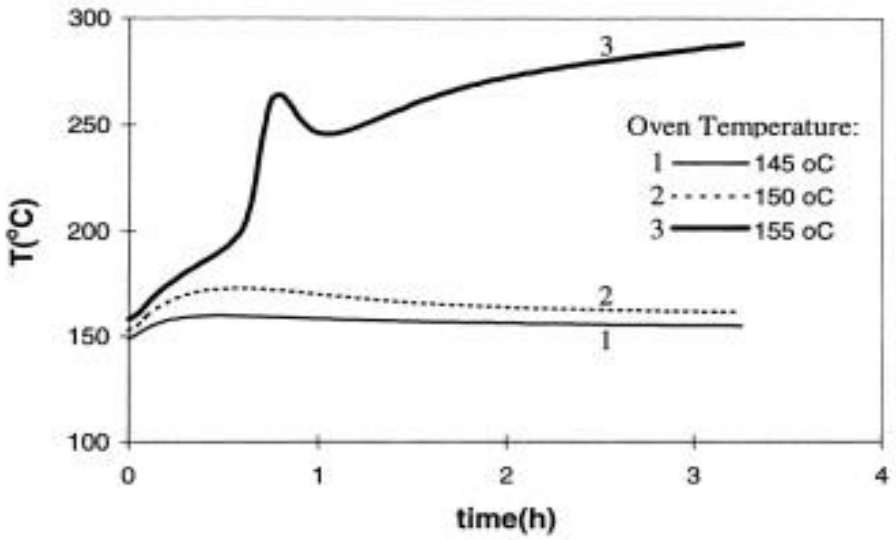



*Figure 2.2: The results of the isothermal oven test, extracted from Beamish et al. (2001)*

Although the isothermal oven test method shares the same theoretical base as the Frank-Kamenetskii method, it was developed independently. It is not as popular as other thermal analysis methods since there has not been much work reported in line with its application. Some technical issues may be encountered when this method is used to determine the self-heating characteristic of coal. Another problem with using this method is that the design of isothermal reactors is not feasible, hence the difference between the results reported on this method by various researchers (Beamish *et al*., 2001).

#### *2.3.2.6. Crossing-point temperature*

The crossing-point temperature (XPT) is used by most researchers in determining the spontaneous combustion liability index of coal samples by measuring their ignition temperatures (Humphreys, 1979; Gouws, 1987). It is one of the most popular techniques applied in countries such as India, South Africa, Turkey and Poland to measure the susceptibility of different types of coal to spontaneous combustion. Experimentally, a coal sample is heated so that it undergoes low-temperature oxidation until its ignition temperature is reached. A study showed a relationship between the XPT and some coal parameters, such as the coal's volatile matter, moisture and oxygen content (Nandy *et al*., 1972). It was reported that coal with a high volatile matter, moisture and oxygen content has a low XPT. Generally, a low XPT is expected for coal samples that are highly susceptible to spontaneous combustion, while a higher XPT is expected for samples that are less likely to undergo spontaneous combustion. Figure 2.3 show a graphical representation of results that can be expected when

using the XPT method on coal.

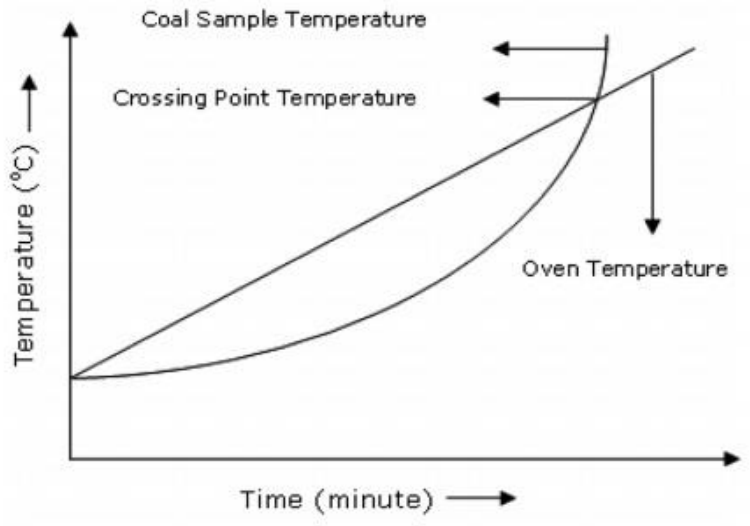



*Figure 2.3: Expected results of the XPT method extracted from Mohalik et al. (2016)*

In the first design of the XPT that was developed by Nubling & Wanner (1915), coal was heated at a constant rate in an oil bath as the flowing oxygen accessed the coal bed. Following this design, other researchers proposed to modify the experimental setup of the first design, while others proposed to alter the experimental conditions given that they impact the XPT (Banerjee, 2000). In the application of this method, the best experimental conditions were found to be a heating rate of $0.5\,℃\,\mathrm{min}^{-1}$ with a flowrate of $80\,\mathrm{ml\,min}^{-1}$ of oxygen on 20 g of coal submerged in a glycerine bath (Bagchi, 1965; Bagchi, 1973).

Given that the heating ramp of this method does not allow for a stationary temperature profile across the sample containers, the XPT tends to be overestimated on some occasions (Mohalik *et al*., 2016). Humphreys (1979) deemed this method inefficient because of some modifications to the method and the fact that its application does not account for the inherent properties of coal. On the contrary, Barve & Mahadevan (1994) reported that XPT affects coal's ash and moisture content. The authors represented the relationship of the factors using Equation 2.15.

$$XPT = 168.8 - 10.3M + 0.2A - 0.06MA + 0.01A^2 \quad (2.15)$$

Where: $XPT$ = crossing-point temperature

$M$ = moisture content

$A$ = ash content

#### *2.3.2.7. Adiabatic calorimetric method*

This approach was first explored in 1914 by Winmill. It is prominently used for simulating the self-heating behaviour of coal in countries such as South Africa, New Zealand, the United States of America and the United Kingdom (Cliff *et al*., 1996). However, the test was referred to as $R_{/v}$ in New Zealand (Beamish *et al*., 2000; Beamish *et al*., 2001). The equipment used for this method operates in the incubation mode and the rising temperature mode. In the incubation mode, coal is heated from a known temperature in a calorimeter under ambient conditions. When the sample reaches the predetermined temperature, oxygen is passed through the sample at a controlled rate. The rise in temperature above the predetermined temperature results from the low-temperature oxidation that takes place exothermically during the process.

The specific parameters that can be determined through the incubation mode in predicting the self-heating characteristics of coal are the kinetic constants, the minimum self-heating temperature, the initial heating rate and the total temperature rise (Kuchta *et al*., 1980; Singh, 1984; Smith & Lazzara, 1987). Ren *et al*. (1999) investigated the effects of coal ageing, particle size, moisture content and initial temperature on spontaneous combustion. They found that smaller particles are highly prone to spontaneous combustion and their propensities were ranked according to their initial heating rate and total temperature rise.

The rising temperature mode is described in detail by Shonhardt (1984). For this mode, a coal sample is placed in an oven to minimise heat dissipation. Then a linear rate of heating is applied to it. Also, there is an oxygen supply to the oven. The deviation of the response temperature of the coal sample from linearity is associated with the chemical and physical properties of that coal (Gouws *et al*., 1991). The temperature rising mode functions like the XPT and the DTA method. To investigate whether this method is viable, Moxon and Richardson (1985) and Ren *et al.* (1999) studied the relationship between the inherent properties of coal and the method. Other factors, such as the time taken to run a single test, the equipment design, the amount and particle size of the sample required for the test and the oxygen flow rate, were considered to determine the method's viability.

In a study conducted by Gouws *et al.* (1991) to establish the propensity of coal to undergo spontaneous combustion using an adiabatic apparatus, the spontaneous combustion index was derived from the DTA. Also, the adiabatic calorimeter was used to obtain the XPT. The information was, therefore, used to define the Wits-Ehac index according to Equation 2.16.

$$Wits - Ehac\ Index = (Stage\ \ II\ slope/\ XPT) * 500 \qquad (2.16)$$

The Wits-Ehac index represents the spontaneous combustion liability of coal, and, based on Equation 2.16, the index is calculated with the assumption that coal is more likely to undergo spontaneous combustion at stage Ⅱ. Therefore, it is expected to have a steep slope and a low XPT compared to coal less prone to spontaneous combustion. In the Wits-Ehac experiments, the temperature of the inert material is used as a reference to compare the temperature response of coal relative to it. At stage Ⅱ, an exothermic reaction takes place, and the temperature of the coal sample is higher than that of the inert material due to the coal sample heating faster.

When the Wits-Ehac index value is less than 3, the risk of spontaneous combustion is low. When the value of the index is 3-5, the risk of coal self-heating is medium, and when the index had a value above 5, the coal sample is highly prone to spontaneous combustion (Onifade, 2018). In South Africa, some researchers have used this method to study the spontaneous combustion of different types of coal, and they did not encounter any problems when using the technique (Genc & Cook, 2015; Genc *et al*., 2018). Thus, this technique was used in this study to predict the spontaneous combustion liability of discard coal, biomass, hydrochar and hydrochar/coal blends.

With a laboratory-scale testing apparatus, Uludag (2007) studied the spontaneous combustibility of South African coal by DTA, XPT and the Wits-Ehac index. In the study, the inherent properties of the coal were determined, and a relationship between the DTA results and the inherent moisture of the coal was established. It was also reported that coal samples with high moisture content had a high Wits-Ehac index, implying high spontaneous combustion liability. Uludag (2007) also reported the same trend for coal samples with high carbon content.

#### *2.3.2.8. Thermogravimetric analysis*

This technique has been explored by several researchers to analyse the spontaneous combustion liability of coal (Avila *et al*.,2014; Vaan Graan & Blunt, 2016; Onifade *et al*., 2020; Manic *et al*., 2021). Avila (2012) reported this technique as a valuable tool for analysing coal properties at low temperatures, and it is viable for assessing the reactivity of coal at different temperatures. This technique measures the relationship between the rate of coal mass loss against temperature changes. According to previous studies, there is a relationship between the rate of mass loss of coal and its spontaneous combustion liability (Marinov, 1977; Nishimoto *et al*., 1986; Kidena *et al*., 2003). The results are usually plotted on a TGA curve and a DTG curve, which is plotted based on the difference between the inert sample curve and the coal sample curve (Onifade *et al*., 2020). Figure 2.4 shows an example of the TGA and DTG curves on the same thermogram.

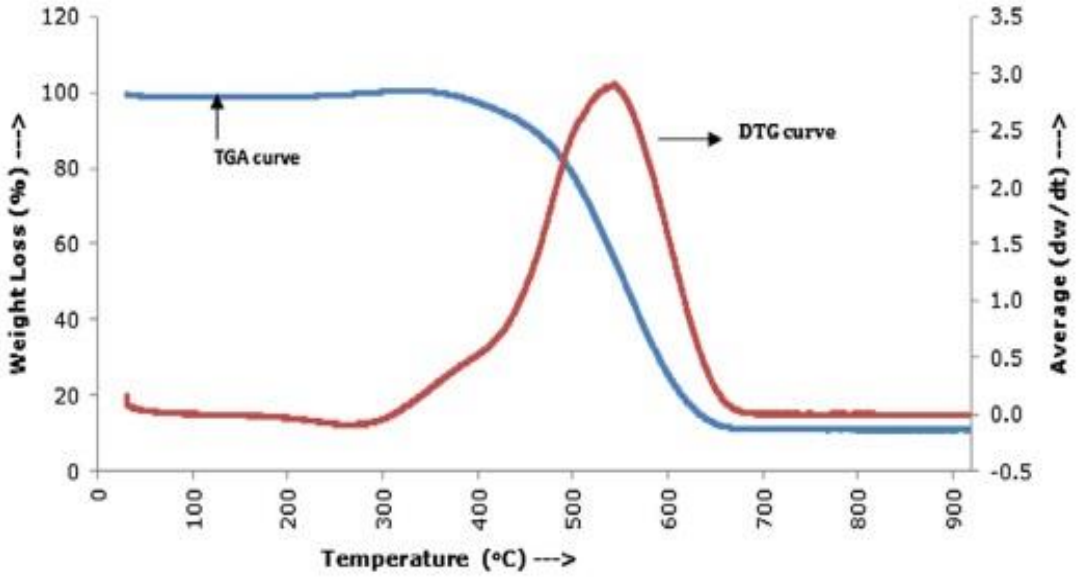



*Figure 2.4: Thermogravimetric analysis and differential thermogravimetric analysis curves, extracted from Mohalik et al. (2016)*

The mining industries use this technique to analyse the reactivity of coal under different atmospheric conditions and to acquire parameters such as the activation energy, reaction order and pre-exponential factors (Vamvuka *et al*., 2003; Kizgut & Yilmaz, 2004; Sima-Ella *et al*., 2005). Unlike other thermal analysis methods, TGA produces excellent results that are accurate and repeatable on a laboratory scale. TGA equipment can also characterise fuels by determining properties such as volatile matter, fixed carbon, inherent moisture and ash content (Elder, 1983; Serageldin & Pan, 1984).

Several studies have been carried out utilising this technique to determine the spontaneous combustion liability of coal. It was used by Choudhury *et al.* (2007) when investigating the effect of the mean reflectance and macerals on the spontaneous combustion characteristic of coal. The study's results showed a good correlation between the TGA parameters and the combination of the total reactive macerals and the coal rank (Choudhury *et al*., 2007). Du *et al*. (2020) investigated the effectiveness of an inhibitor liquid on spontaneous combustion using TGA. The authors reported that the inhibitor liquid had the strongest inhibitory effect between the temperature range of 0 - 200 ℃. The heat release and coal oxidation were also delayed after using the inhibitor liquid. Junkovic *et al*. (2020) used the same technique at five different heating rates under an air atmosphere on coal. The authors reported that the Kolubara coal had the highest reactivity based on the ignition of the coal at the lowest temperature region and the

maximum mass loss rate of the sample. Onifade *et al*. (2020) investigated the spontaneous combustion of coal and coal shales using the Wits-Ehac and TGA indices; the results from both methods were similar. Shen & Zheng (2021) used TGA to predict the spontaneous combustion liability of major coal seams. The authors observed that when fine coal particles are heated, their mineral content increases, but their carbon content decreases, resulting in the inhibition of coal oxidation.

Over the years, it was found that the accuracy of the data acquired using the TGA improved because of the technological advancement of the equipment. Additionally, a significant improvement in the temperature control of the equipment has led to it being one of the best methods for measuring the spontaneous combustion liability of fuels at low temperatures (Avila, 2012).

### 2.3.3 Inhibition of spontaneous coal combustion

Several coal mines have experienced spontaneous combustion over the years, but the frequency differs in every country. For instance, a coal mine fire claimed the lives of 12 people because of spontaneous combustion in 2012 in Longshan Town, China. Another incident occurred whereby coal combusted spontaneously and caused an explosion in a closed fire zone leading to the deaths of 36 people in 2013 at Babao coal mine, Tongua city, China (Li *et al*., 2017). Between 2001 and 2013, 800 people were killed by fire caused by the occurrence of spontaneous combustion (Jiang *et al*., 2013). Spontaneous combustion also occurs frequently in South Africa, thus introducing major challenges in the mining sector (Genc *et al*., 2018). The occurrence of these incidents has called for scientific, experimental and theoretical research by institutions globally to prevent and control spontaneous combustion.

The prevention and control of spontaneous combustion can be achieved by combining various techniques. However, inhibitors have been the centre of attention when it comes to the prevention of spontaneous combustion. According to Rath (2012), inhibitors functions in the following ways:

I. They form a heat-insulating layer around the treated coal by forming a protective surface that coats the macropores and the micropores on the material.
II. They accelerate the rate of heat removal from local hotspots by increasing the thermal conductivity of the treated coal with the layer formed around it.
III. During the process of coal oxidation, the layer formed by the inhibitor consumes

heat generated before coal reaches its critical temperature.

IV. In a case where the layer formed by the inhibitors is gaseous, heat can also be removed because the layer tends to act as a diluent.

V. The inhibitors enhance the chain-breaking reaction, which eventually retard the oxidation reaction.

Several types of inhibitors have been studied and applied to retard the low-temperature oxidation of fuel materials with a fair amount of success, especially on coal. Generally, an inhibitor plays two roles in preventing spontaneous combustion. It prevents the interaction of oxygen with active functional groups in coal and the absorption of water (Dou *et al*., 2014). Inhibitors could be in gaseous, solid and liquid phases, and they are physical or chemical.

Their categorisation is based upon their interaction with the material in question. Some inhibitors prevent spontaneous combustion by altering the structure of coal through chemical reactions, while others retard the process by forming a physical barrier between the coal surface and oxygen. The advantages of inhibitors include a broader scope of application, low pollution, they are easy to use, and they are one of the most used technologies for fire prevention and extinguishment in coal mines (Deng *et al*., 2015b; Chen *et al*., 2016; Wang *et al*., 2016). To select an excellent inhibitor, it is important to study its inhibitory mechanisms. The following sections discuss the advantages, shortcomings and applications of physical and chemical inhibitors.

#### *2.3.3.1 Physical inhibitors*

When an inhibitor achieves retardation of spontaneous combustion by isolating coal from oxygen without interfering with the humidity of the surroundings, it is called a physical inhibitor (Wang, 2011; Wang *et al*., 2012c). Some physical inhibitors are made of inorganic salts, which achieve inhibition of spontaneous combustion by covering the coal particle with a water film, thereby decreasing the temperature of the surrounding (Qi *et al*., 2016). These inhibitors successfully prevent contact between oxygen and the coal surface (Zhou *et al*., 2006). However, they have not received as much attention as chemical inhibitors in the coal mining industry. Examples of physical inhibitors include three-phase foam, water glass, gels, ammonium salts, $Ca(OH)_2$, and $Na_2CO_3$ (Zeng, 2010). Water-absorbing salts such as also function in the same way as chemical inhibitors (Beamish *et al*., 2012; Rath, 2012). Water-absorbing salts are the most commonly used physical inhibitors worldwide because they are environmentally friendly, economically viable and have an excellent moisture effect. However,

water-absorbing salts are said to have a non-ideal inhibitory effect. This is because most research studies on these salts are based on physical properties, with little knowledge of their inhibitory mechanism (Wang *et al*., 2014)

Other physical inhibitors that have been explored to control and mitigate the effect of spontaneous combustion include infusing gelatine, mud grouting and resistance spraying agents (Michalski, 2004; Qin *et al.,* 2005; Fu-bao *et al.,* 2007; Tian *et al.,* 2010. Injecting inert gases such as nitrogen and carbon dioxide into the fire areas is one of the major methods used to physically control, prevent and extinguish spontaneous fires in underground coal mines. It is believed that injecting large amounts of inert gases into the finite spaces of the coal mines could decrease the oxygen concentration, hence inhibiting the occurrence of spontaneous combustion of coal (Gurdal *et al*., 2015).

Jiang *et al.* (1991) investigated the relationship between injected nitrogen gas in the goafs and the oxygen concentration after injection. This led to predicting the spontaneous combustion in the goafs by simulating the reaction using a tunnel model and 2-t coal samples. The oxygen concentration decreased by five per cent after injecting nitrogen gas. Other inert media investigated and injected into the goafs include foams, fly ash, yellow mud, gels, and normal mud. When in contact with coal, the inert material covers the coal mass to decrease the rate of coal oxidation to control and inhibit the spontaneous combustion of coal. Another approach was utilised by the Goodson Association Company in America by substituting the conventional inhibitory methods with a thermo-cell made of foam to backfill the oxygen barriers into the goafs to control fires caused by spontaneous combustion (Colaizzi, 2004). These materials exhibited satisfactory inhibitory and extinguishing effects. However, the materials were expensive.

Given that spontaneous combustion is a common disaster in China, Zhou *et al*. (2006) reported that the large fires in the Baijigou coal mine in China could be extinguished successfully by using inert gases such as nitrogen and carbon dioxide, three-phase foam, water in a liquid state, and non-combustible materials such as fly ash and yellow mud. Using mechanically foaming surfactants, polymer solutions and cross-linking agents, Zhang & Qin (2014) combined the advantages of gels and foams to prepare stable gel foam materials. The materials exhibited the characteristics of both the gel and foam, and the resulting material exhibited excellent plugging performance and an exceptional inhibiting characteristic.

Lu & Qin (2015a; 2015b) developed an inorganic curing foam with favourable mechanical properties to control spontaneous combustion and back-fill cracks in the goafs. Foam is one of the materials that has attracted substantial research focus for the inhibition of coal spontaneous combustion (Xue *et al*., 2020; Zhang *et al*., 2020; Tang *et al*., 2021). Nonetheless, they were deemed unstable since they wrap gases in liquids. Moreover, foam materials are not suitable for extinguishing and controlling fires underground because they have a limited life span, and their isolation potency is supposedly lost if they break. The most common disadvantage of these inhibitors is that they are difficult to spray over the coal stockpile and inhibitors percolate underground, thus causing the underground mining machines to corrode. Additionally, applying ammonium salts, $Ca(OH)_2$, and $Na_2CO_3$ produce toxic gases (Qi *et al*., 2016).

Since physical inhibitors cannot alter the chemical composition of coal, it was concluded that these inhibitors are not viable for totally removing the risk of spontaneous combustion. Moreover, they are effective for a short period due to their interaction with water and air, which affects their efficiency (Sunjanti & Zhang, 2000; Watanable & Zhang, 2001; Slovak & Taraba, 2012). Because of these shortcomings, more research has explored other types of inhibitors.

#### *2.3.3.2 Chemical inhibitors*

If an inhibitor retards spontaneous combustion by introducing a halt to the chain of reactions during the oxidation of coal and reacting with the active groups through surface interactions with coal, then it is a chemical inhibitor (Qi *et al*., 2016; Xi *et al*., 2020). The efficiency of some physical inhibitors may be improved by converting them into chemical inhibitors using additives and antioxidants (Yu *et al*., 2010; Beamish *et al*., 2012). According to the literature, the most common type of inhibitor that has proved to work effectively is the chemical inhibitor. It is widely used to prevent and extinguish fires caused by spontaneous combustion in coal mines (Dong & Drysdale, 1997; Sunjanti & Zhang, 1999). When in contact with coal, the chemical inhibitor hinders the formation of active groups and retards the free radical reactions by reacting with the active functional groups in coal.

Generally, there are three types of chemical inhibitors: chloride, ammonium and alkalies (Zeng, 2010). To inhibit spontaneous combustion, the chloride-based chemical inhibitors such as $MgCl_2$, $CaCl_2$ and $NaCl$ absorb moisture from coal by evaporative cooling in the presence of an antioxidant (Peng *et al*., 2016). The ammonium-based chemical inhibitors such asutilise thermal degradation to achieve a decreased coal surface temperature, while the oxygen concentration around the coal is lowered by inert gases released. Lastly, alkali-based inhibitors

such as $Ca(OH)_2$ function on a mechanism that focuses on reducing the rate of coal oxidation. However, the three types of chemical inhibitors are inefficient when applied to pulverised coal.

More investigations have been carried out to find an effective chemical inhibitor to inhibit the spontaneous combustion of coal. Dou *et al*. (2014) investigated the effectiveness of the combination of catechin and poly(ethylene glycol) on the inhibition of the spontaneous combustion of coal. The authors reported that an additive consisting of a combination of catechin and poly(ethylene glycol) was successful in retarding the oxidation of coal. Additionally, the surface of the coal samples was monitored during oxidation, and it was revealed that the additives suppressed coal oxidation by favouring the formation of ether bonds. An antioxidant (chemical inhibitor) that is commonly used in the rubber and petroleum industries was also utilised to inhibit the spontaneous combustion of coal by Shui-jun *et al*. (2012). The use of antioxidants was also proposed by Li *et al.* (2017) to terminate the chain reactions resulting from the free radical theory of the coal spontaneous combustion mechanism. Since the effectiveness of the antioxidants was based on the concentration of the gas produced before and after the inhibition, the antioxidants were found to exhibit a good inhibitory effect. It was reported by Jiao *et al*. (2012) that the critical temperature of coal oxidation can be improved by sodium silicate, gel, antioxidant and calcium chloride acting as inhibitors.

Other researchers also investigated the effect of antioxidant inhibitors on coal spontaneous combustion. For example, Yang & Yu (1999) compared the inhibitory effect of different concentrations of anti-agers and inorganic salts on the spontaneous combustion of coal. The authors discovered that the anti-agers showed a satisfactory performance compared to inorganic salts. On the other hand, Yu *et al*. (2011) investigated the effect of antioxidant A, ammonia-free gel and magnesium chloride on the low-temperature oxidation of coal by studying the amount of $CO$ produced during oxidation. It was reported that as the dispersion degree of antioxidant A in water increased, the inhibition effect also increased.

The effect of poly(ethylene glycol) on the low-temperature oxidation of coal with different metamorphism degrees was investigated by Wang *et al*. (2014) using infrared spectroscopy. It was found that the inhibitor could prevent further oxidation of the coal surface functional groups formed during coal oxidation and inhibit spontaneous combustion ultimately. The inhibitive effect of the complex inhibitors of acrylic acid and ascorbic acid on different types of coal was studied by Ma *et al.* (2016). The complex inhibitors successfully stopped heat accumulation and prevented free-radical chain reactions. Li *et al*. (2016) used a rubber anti-

ager known as diphenylamine to inhibit the spontaneous combustion of coal. The result proved that the low-temperature oxidation of coal could be inhibited by the rubber anti-ager. Based on the above-mentioned studies, it was concluded that antioxidants have a satisfactory inhibitory effect on coal spontaneous combustion. Although, the studies only focused on investigating the inhibitory effects of the antioxidants and neglected their mechanism.

The disadvantages of using foams as a physical inhibitor led to the investigation conducted by Tang (2017a) on the use of zinc foams made up of foaming agents, water, zinc acetate, hydroxyethylcellulose and ethanolamine to curb coal's spontaneous combustion effectively and continuously. The result from this study confirmed that the ultrafine zinc oxides from the foam disperse uniformly over the coal surface and decreases the functional groups significantly, leading to effective inhibition of the low-temperature oxidation of coal. In addition, the extinguishing attribute of the foam is due to its potential to isolate oxygen leading to the smothering effect, which inhibits the low-temperature oxidation reaction and, ultimately, the spontaneous combustion of coal (Tang, 2017a).

Using a temperature-programmed oxidation device, the inhibiting mechanism of foam inhibitors in treating coal was investigated with an FTIR spectrophotometer Cao (2013). The author reported that the foam inhibitors successfully reduced the susceptibility of coal to spontaneous combustion (Cao, 2013). While a handful of published research focuses on the interaction of chemical inhibitors and water-based foams, Peng *et al*. (2016) used the combination of the two to evaluate the synergetic effect of the water-based foams in inhibiting the spontaneous combustion of coal and to evaluate the decay process, stability and the foamability of the water-based foam. They reported that the inhibition foams retarded the spontaneous combustion of coal efficiently since the oxygen adsorption rate decreased after the coal samples were treated.

Although chemical inhibitors are the most favoured type of inhibitor, they tend to show an unstable inhibitory effect when used to treat certain types of coal. Many researchers have committed to investigating the mechanism of spontaneous combustion and its prevention, but the topic requires more extensive research and the intelligence of scholars with abundant knowledge. Research into finding more environmentally friendly, highly effective and viable inhibitors should be continued by studying the behaviour of chemical inhibitors.

#### *2.3.3.3 Ionic liquids*

Ionic liquids are anhydrous salts that are liquid below a temperature of 100 ℃ (Seddon, 2003). They tend to behave like molten salts. However, they do not require as high a temperature to perform their function as molten salts, given that they can be used at room temperature (Chiappe & Pieraccini, 2005). They have excellent chemical and thermal stability, which means they are safe and more favourable to use than other chemical inhibitors at low temperatures. The fact that they have low vapour pressure reduces the risk of causing respiratory problems and the need for fume extraction systems when working with them. Because they possess a property of low volatility, they are deemed appropriate to be used in distillation processes to sublimate both the product and by-products and to make the separation processes easy. They can merge different combinations of reagents in one phase (Tian & Hua, 2010). They can exist steadily in a wide range of temperatures because they are thermally stable, making them suitable for the kinetic control of electrochemical and most chemical processes.

Ionic liquids can be used as solvents to assist in metal extraction, fragmentation and dispersion of materials during temperature-dependent processes such as precipitation, leaching and crystallisation because of their excellent physicochemical properties (Zhang & Kamavaram, 2006). The scope of reactions is wide when using ionic liquids in electrochemistry because they are stable in both air and water and have lower melting points than other molecular solvents, usually employed for different processes (Tian & Hua, 2010). They are featured in some electrochemical devices, such as solar batteries and cells, and metal extraction through electrodeposition. Due to the flexibility of anions and cations to form different types of ionic liquids and the possibility of adjusting their properties to suit the requirements of a specific process, they are seen as ‘designer liquids’ (Earle & Seddon, 2000). By manipulating the structure of their ions, properties such as viscosity, melting point, boiling point and density can be re-adjusted (Tian & Hua, 2010).

They can also be used as catalysts in some processes to enhance and speed up the rate of product formation (Dupont & Fonseca, 2002). By altering the number of carbons in alkyl chains of dialkyl imidazolium cations, the hydrophilicity and hydrophobicity of imidazolium-based ionic liquids can be changed (Abbott *et al*., 2011). The cations are usually bulky, asymmetrical, heteroaromatics and bonded by weak intermolecular forces (Welton, 2004). Based on the type of the cation that they carry and their functions, ionic liquids can be categorised into four groups:

I. phosphonium-
II. dialkyl imidazolium-
III. alkylammonium-
IV. alkyl pyridinium-

Zhang *et al*. (2018) reported that ionic liquids could be used as chemical inhibitors to prevent the spontaneous combustion of coal because they have a low melting point, are non-flammable and can dissolve various organic and non-organic materials. They can also be used in highly exothermic reactions, given their low vapour pressure property (Li, 2004).

#### *2.3.3.4 Application of ionic liquids in the coal industry*

Generally, there has been a fair amount of work done in line with the application of ionic liquids in the coal industry, but few studies have used ionic liquids to inhibit the spontaneous combustion of coal. Examples of ionic liquids that function on the principle of chemical inhibitors include 1-hydroxyethyl-3-methylimidazolium tetrafluoroborate ([HOEmim][$BF_4$]), 1-acetoxyetyl-methylimidazolium tetrafluoroborate ([AOEmim][$BF_4$]), 1-allyl-3-methylimidazolium chloride ([Amim][Cl]) and 1-butyl-3-methylimidazolium trifluoromethanesulfonate ([Bmim][OTf]) (Wang *et al*., 2012b).

An investigation conducted by Zhang *et al*. (2011) confirmed that ionic liquids could be used to inhibit the spontaneous combustion of coal. It was discovered that the effectiveness of ionic liquids is attributed to the reduction of hydrogen bonds in coal when Lei *et al*. (2013) investigated the effect of [Bmim] ionic liquids on a lignite sample. In another study, a lignite sample was pretreated with ionic liquids, and it was found that the pretreatment process inhibited the spontaneous combustion characteristic of lignite (Lei *et al*., 2016). The treated lignite sample was analysed to investigate the effect of the ionic liquids on its structural matrix. It was reported that the oxygen-containing functional groups of the lignite were re-modified. Cummings *et al*. (2017) reported the same in a study that aimed to investigate the effects of ionic liquids on the oxygen-containing functional groups of coal. When investigating the influence of ionic liquids on the inhibition of spontaneous combustion of coal, Wang *et al.* (2012b) found that a variety of the functional groups of coal were solvated in the ionic liquid, thus deaccelerating the oxidation of coal.

In a study conducted by Xiao *et al*. (2019), bituminous coal was treated with four imidazolium-based ionic liquids: [Emim][$BF_4$], [Bmim][$BF_4$], 1-butyl-3-methylimidazolium nitrate

[Bmim][$NO_3$] and 1-butyl-3-methylimidazolium iodide [Bmim][I] to investigate their effect on coal's spontaneous combustion characteristic. The author reported that imidazolium-based ionic liquids have an appreciable effect on the inhibition of spontaneous combustion of bituminous coal. The ionic liquids with the $[BF_4]^-$ ion were more effective than those with the $[NO_3]^-$ ion. Of the four ionic liquids, [Bmim][$BF_4$] had the best inhibitory effect. Another study on inhibiting spontaneous combustion in the goaf was conducted by Wang *et al*., (2015) using an ionic liquid. Based on the FTIR results, the author found that the ionic liquids exhibited a good performance by dissolving the active functional groups in the coal thus retarding the coal's oxidation and reducing the amounts of gases produced during the reaction.

To inhibit the spontaneous combustion of lignite coal, three imidazolium-based ionic liquids and water flushing were tested by Cui *et al*. (2018). Using TGA and FTIR, it was discovered that of the three ionic liquids, dimethyl-imidazolium iodide [Mmim][I] was the best in terms of reducing the -OH groups found in the lignite, thus inhibiting its spontaneous combustion characteristic. The effect of [Bmim][$NTf_2$], [Bmim][$BF_4$] and [HOEtmim][$NTf_2$] on the spontaneous combustion characteristic of coal was investigated by Xi *et al.* (2020). [HOEtmim][$NTf_2$] exhibited the best inhibitory effect by lowering coal's specific surface area and pore . It also enhanced the aromaticity of coal and retarded the oxidation process by limiting the reaction between the active functional groups of coal and oxygen. Likewise, Ma *et al*. (2016) revealed that ionic liquids could slow the oxidation of coal by inhibiting the release of heat during the reaction. The author found that the [Hemim][Tos]-ion from one of the ionic liquids reduced the hydrogen ions from the functional groups, thus reducing the reactivity of the peroxide radicals.

### 2.4. Spontaneous Combustion of Biomass

It is well-known that biomass has been considered an alternative to coal for power generation in centralised boilers (Schwarzer *et al*., 2017). However, substituting coal with another fuel is not simple, given that several factors should be considered. Concerning spontaneous combustion, most research has focused mainly on coal since this phenomenon is prominent in the coal mining industry. However, this phenomenon could affect other materials such as biomass, organic waste, forestry waste and coal-biomass blends (Avila, 2012).

The mechanism that controls the process of spontaneous combustion is the same in all cases, regardless of the type of material involved. Biomass burns more quickly than coal, which means there is a higher possibility of quick propagation of any ignition flame for biomass in

co-firing plants (Wang *et al*., 2012a). The different types of biomass that have been reported to undergo spontaneous combustion are composting piles, sawdust, wood chips, eucalyptus leaves, pistachio nuts, palm kernel, hay piles, rapeseed and soybean piles. More incidents of explosions have been reported while milling, conveying and storing (Krause, 2009). One major factor that has been reported to catalyse the spontaneous combustion of biomass material and coal-biomass blends is a temperature imbalance that favours the production of heat over the release of heat to the environment. Another primary cause of spontaneous combustion for these hygroscopic biological materials is bacterial activity.

Although many incidents have been reported in the literature, the mechanism associated with the oxidation reactions of these biological materials is complicated (Avila, 2012). The involvement of complex biochemistry in the reactions complicates the mechanism further. The precise details concerning the mechanism involved during the spontaneous combustion of biological materials are still unknown (Avila, 2012). However, all oxidation reactions in different types of biomass take place according to the following steps by Buggeln & Rynk (2002):

Step 1– The biological material undergoes fermentation, causing a temperature rise: The main cause of the temperature rise during fermentation is the aerobic respiration of the microbes and cells incubated into the piles of the living plant. During the interaction of the bacteria and the plant, the temperature can vary from one phase to the next. When the pile temperature ranges from 20 to 40 ℃, it is in the mesophile phase, and when it ranges from 40 to 80 ℃, it is in the facultative thermophiles phase. However, the pile temperature will only rise above 70 to 90 ℃ if the pile does not have any moisture content.

Step 2 – Loss of moisture content by evaporation: The temperature rise from the first step causes the water in the pile to evaporate, resulting in the pile temperature reaching 100 ℃. At that temperature, the microorganisms become inactive and eventually die. The pile temperature continues to increase due to the reaction between the oxygen in contact with the pile and the plant's chemicals. The heat released from the reaction accelerates the oxidation reaction of the pile.

Step 3 – The pile reaches a critical temperature, causing a thermal runaway reaction: At temperatures above 100 ℃, the pile has no moisture and is rich in carbonaceous material. The ignition point of the material is between 130 and 160 ℃ (Kayser & Boyers, 1975). As the pile reaches the ignition point, the heat produced by the oxidative chemical reaction exceeds that

lost to the environment, causing the pile to combust spontaneously as it self-ignites (Kayser & Boyers, 1975). Figure 2.5 illustrates the pile's temperature profile as a function of time and the steps leading to the self-heating of biomass.

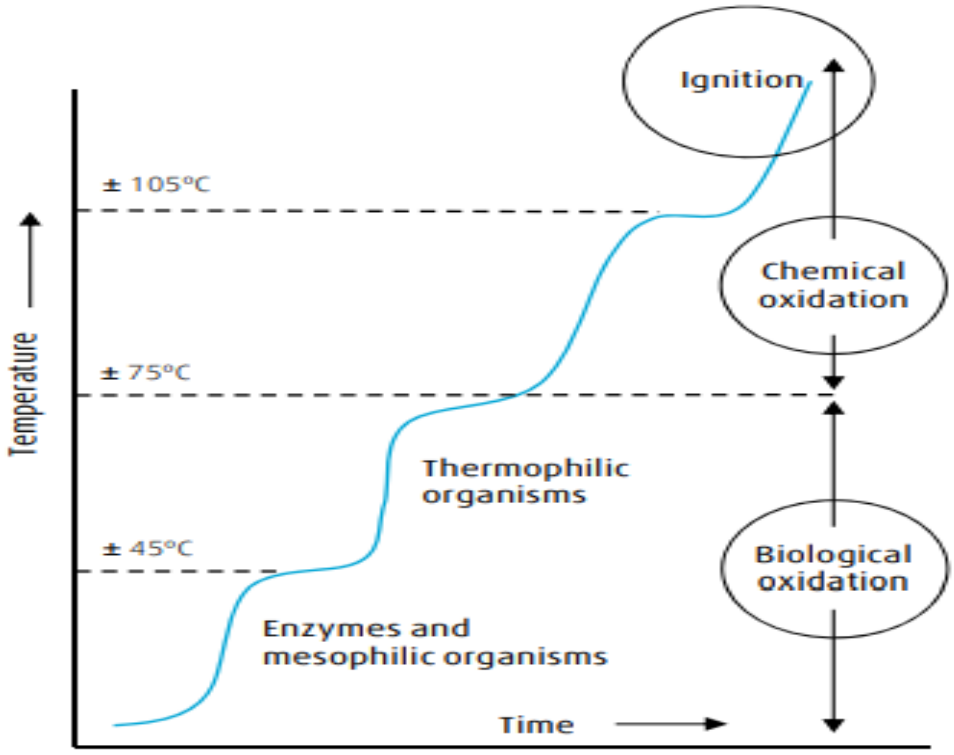



*Figure 2.5: Self-heating of biomass extracted from Meijer & Gast (2004)*

### 2.4.1 Factors affecting the spontaneous combustion characteristic of biomass

The spontaneous combustion of biological material is affected by factors that promote the growth of the microorganisms involved in the reaction. Major factors such as oxygen concentration, temperature and moisture content play a significant role in promoting the growth of the microorganism (Jirjis, 2005; Ashman & Williams, 2018). Other factors that are equally important given that they promote the self-heating of the pile include the particle size of the biomass, the porosity or compaction of the pile, the activation energy of the reaction of the microorganisms and the pile and, lastly, the bio-catalysis that is the microbe's catalytic activity (Buggeln & Rynk, 2002; Avila, 2012).

There are also minor or less studied factors that influence the propensity of biomass to undergo spontaneous combustion. Those factors include the presence of inorganic materials in the biomass piles, such as iron and aluminium since they tend to act as catalysts, the thickness of the cellular wall and the biomass's internal structure (Buggeln & Rynk, 2002; Avila *et al*., 2011). In this review, attention is given to the major factors that influence the spontaneous

combustion of biomass only and the effects of each factor will be explained in detail in the following section.

#### *2.4.1.1. Oxygen composition in the biomass*

In both abiotic and biotic reactions, oxygen is required as a primary reactant, and the presence of oxygen in the reactions results in heat generation. Luo *et al.* (2009) and Chansa *et al.* (2020) investigated the effect of oxygen concentration on the combustion characteristic of biomass. They found that as the oxygen concentration increases, the fuel's reactivity increases. Chen *et al.* (2008) also reported that the oxygen concentration greatly affects the combustibility of biomass materials such as rice straw, corn cob and corn straw. The author further reported a directly proportional relationship between the comprehensive combustion characteristic index of the materials and the oxygen concentration. Bowes (1984) concluded that the time to reach the ignition temperature doubles at lower oxygen concentrations when the effect of oxygen on the self-heating of sawdust was investigated.

#### *2.4.1.2. Temperature effect on biomass susceptibility to spontaneous combustion*

Plucking plants from the ground or cutting them at their roots does not mean they will die instantly. It is only when the plants deplete their food and water supply or when they are exposed to harsh conditions such as elevated temperature that their cells succumb to death. The cells in the wood cut from the tree trunks also continue to live for some time if the outer cambial layer of the tree is not removed. The same can be said for sapwood branches and tree chips (Kubler, 1990).

There is a relationship between oxygen and temperature as factors influencing the propensity of biomass piles to undergo spontaneous combustion. When the biomass piles are exposed to oxygen, the piles become oxidised as the inflowing oxygen behaves as an oxidant of the carbon structures of the biomass. As a result, an Arrhenius-type dependency on temperature identical to that exhibited by coal during oxidation reactions becomes evident, and a temperature rise also becomes evident (Kayser & Boyers, 1975). However, there is still some uncertainty surrounding the cause of the initial temperature rise as it is believed that bacterial activity might also affect the change. Based on casual observations, it was concluded that the respiration of the plant cells (oxygen intake) is a potential catalysing factor leading to a rapid temperature rise, if not an initial temperature rise, causing the biomass material to undergo spontaneous combustion (Buggeln & Rynk, 2002; Manic *et al*., 2021).

#### *2.4.1.3 Pile compaction*

Biomass pile compaction is one major factor influencing biomass oxygen intake and is somehow connected to the pile temperature. If the pile is tightly packed (with limited spaces in between), the amount of oxygen penetrating the pile decreases, leading to reduced heat dissipation. However, it must also be noted that in a tightly packed state, there is a possibility of heat generation by pyrolysis. Additionally, the vertical oxygen flow is obstructed, which may lead to reduced convective heat transfer and, ultimately, to an increase in pile temperature (Buggeln & Rynk, 2002). On the contrary, in a case of low compaction degree (more spaces in between), there is a high inflow of oxygen into the pile, allowing for increased heat dissipation through the pile, leading to low spontaneous combustion susceptibility of the biomass pile (Avila, 2012).

#### *2.4.1.4 The moisture content of the biomass pile*

The moisture content of the biomass can affect its tendency to self-heat in various ways, given the thermal properties of water (Luangwilai & Nelson, 2018). Moisture in the biomass pile plays a vital role in supporting the reactions that keep the microorganisms active, given that the microorganisms utilise the moisture available in the plant as a transport medium, a thermoregulator and a substrate (Buggeln & Rynk, 2002). High moisture content in the pile results in a low oxygen diffusion rate, lowering the heat production rate. Moreover, high moisture content somehow hinders the growth of microorganisms, given that the high energy required to evaporate the moisture negatively impacts the existence of the microorganisms (Yuan Kun, 2006). However, the total removal of moisture through evaporation implies a considerable reduction of the ignition temperature of the biomass, leading to a high propensity for spontaneous combustion (Jones & Puignou, 1998).

#### *2.4.1.5 Activation energy*

It is not known how many biotic and abiotic chemical reactions take place within the biomass pile, but when the biotic reactions take place, large hydrocarbon chains are broken down into compounds that can be oxidised easily (Avila, 2012). The decomposition of large hydrocarbon chains happens due to the reduction of the activation energy brought about by microbe activity (Ashman & Williams, 2018). Moreover, the decomposition of the hydrocarbons influences other subsequent chemical reactions within the pile. The chemical reactions occur due to the reduced activation barrier (Kayser & Boyers, 1975; Yuan Kun, 2006). The activation energy was regarded as the key factor leading to heat generation by Buggeln & Rynk (2002). The fundamental of chemical thermodynamics states that the type of process involved in heat

generation is independent of the total heat released when substances such as glucose are oxidised (Miao *et al*., 1994). Based on the fundamental concept, it is expected that a biomass pile with microbes will rapidly heat up when the microbes and chemical substrates are exposed to an equal amount of oxygen.

#### *2.4.1.6 Particle size of the biomass*

In terms of particle size, several studies indicate that the rules that apply to coal may also apply to biomass (Buggeln & Rynk 2002; Avila, 2012). Besides oxygen entering the active site where the reaction occurs, the surface area that is in contact with the microbe activity also affects the reactivity of the biomass materials (Avila, 2012). Smaller particle sizes imply an increased surface: ratio of the particles, leading to increased heat loss by convection. Additionally, a pile of small biomass particles tends to be highly compacted and may therefore result in less convective heat dissipation and reduced porosity (Buggeln & Rynk, 2002). The oxygen inflow into the pile also becomes difficult, given the obstruction caused by low porosity. A pile of biomass with fine particle sizes is more susceptible to spontaneous combustion due to increased microbial growth on this particle size, leading to an increased pile temperature (Rupar-Gadd, 2006). The opposite can be said about biomass piles of larger particle sizes, given that microbial growth is relatively slow because large particles tend to lose moisture faster than smaller particles (Jirjis, 2005).

### 2.4.2 The prediction of the spontaneous combustion liability of biomass

Few techniques have been explored to predict the spontaneous combustion liability of biomass (Rupar-Gadd, 2006; Avila, 2012). The problem is that those techniques only account for the last stage of oxidation, which is close to the ignition point, but the relevance of the material's biological activity is usually not accounted for. In such instances, biomass is assessed using standard thermal analysis such as the Frank-Kamenetskii, heating basket and modified XPT methods (Chen, 1999). In addition, the original XPT method and the isothermal oven test, also called the constant temperature method, are utilised (Jones & Puignou, 1998; Rynk, 2000; Van Blijderveen *et al.,* 2010).

Avila (2012) conducted an investigation focusing on understanding spontaneous combustion characteristics of biomass and biomass-coal blends, amongst other fuels, using TGA. The study concluded that the reactivity of biomass alone is different from that of coal. The oxidation reaction of biomass is influenced by the biomass' moisture and volatile matter content at low

temperatures. Additionally, the reaction rate is influenced by the components found in biomass, such as lignin, hemicellulose and cellulose. According to Avila (2012), the TGA technique provided reliable and accurate data on the spontaneous combustion liability of biomass and coal blends during low-temperature oxidation.

The combustion and co-combustion of high-ash coal, macadamia nutshell, anthracite and a blend of macadamia-coal were studied by Bada *et al*. (2015) using TGA under different atmospheric conditions. The study's results showed that at lower temperatures, all the blends of macadamia-coal at different ratios and the raw biomass were highly reactive compared to coal alone. The reactivity of material is directly proportional to its propensity to spontaneous combustion (De Korte, 2014). Jones *et al*. (2015) evaluated the spontaneous combustion characteristic of seven biomass materials using TGA, and three materials, i.e., olive cake, sunflower husk and Miscanthus, fell into the category of high risk. Overall, no novel methods exist for predicting the spontaneous combustion of biomass, leaving only the methods used for coal assessment (Avila, 2012).

### 2.4.3 Inhibition of spontaneous combustion of biomass

Before 2015, approximately 24 biomass combustion incidents were reported worldwide, and most incidents occurred in wood pellet companies (Mullerova, 2014; The Linde Group, 2015). In 2010, a fatal explosion caused by the self-ignition of wood pellet in a silo was reported in Sweden at Laxa pellets. Another incident occurred at Inferno Wood Pellets Co Rhode Island in 2013 (Pfecke & Warrenville, 2010; Mullerova, 2014). As a result, there has been a call to find preventative and control measures to minimise or eliminate the occurrence of these incidents in the future. The spontaneous combustion of biomass occurs mostly during long-term bulk storage in silos and during transportation (Guo, 2013; Persson, 2013; Larsson, 2017; Ebadat, 2019). Most methods applied in biomass power plants are based on controlling and extinguishing fires after combustion rather than treating biomass material with inhibitors to prevent or inhibit spontaneous combustion (Ennis, 2016). The recommended preventative and fire-fighting methods are discussed in detail below.

As a preventative measure, plant personnel are required to conduct a risk assessment by continuously monitoring the concentrations of $O_2$ and $CO$ in the risk areas and headspace of the silos using a calibrated measuring instrument. If the concentration of $CO$ ranges between 2-5% and that of $O_2$ is higher than 5%, there is a high risk of explosion since the levels indicate that the stored material has started to self-heat (Persson, 2013). Following the detection of

elevated $O_2$ and $CO$ concentrations, the silo openings should be sealed and the ventilation systems shut down to prevent oxygen from contacting the biomass material (Persson, 2013).

In a case where the biomass has already reached ignition point, nitrogen gas should be injected into the silo from the base of the column to serve as a fire-fighting measure. As an alternative to nitrogen gas injection, high-quality foam can be used to cover the stored biomass materials in the silo, provided that the materials have not caught fire. In doing so, the explosion can be prevented. The Compressed Air Foam System (CAFS) may also be employed to assist in managing the disaster at hand (Persson, 2013). However, it is important that in implementing the high-quality foam and the CAFS method, the silos are not overly exposed to air as that might accelerate the low-temperature oxygen of the material. Additionally, it is mandatory for the personnel responsible for implementing preventative measures to wear full personal protective gear at all times. In instances where the injection of nitrogen gas and the CAFS method are not successful in extinguishing the fire, water-based methods are usually employed as fire-fighting methods (Persson, 2013). Water is injected or sprayed directly into silos containing materials such as sawdust.

There are, however, several shortcomings associated with using water-based methods for fire extinguishing. Injecting water into silos containing wood pellets may cause the material to swell and turn into a hard cake (Persson, 2013). The pellet's swelling results in the particles of the biomass being impermeable, hindering the process of extinguishing the fire. In some instances, spraying water into the silos might accelerate the explosion by producing hydrogen gas, which is highly flammable under favourable conditions (The Linde Group, 2015). The presence of water in the silos causes damage to the walls of the column. The water discharged from the silos also causes alarming environmental pollution. Lastly, cleaning and rehabilitating the equipment and the environment requires large financial input.

While some firefighting methods are efficient, other methods tend to fail. In cases where methods are successful in controlling and extinguishing the fire, the labour and expenses associated with the damage control are always expensive. For this reason, the attention of researchers should be re-directed to exploring inhibitors to prevent the spontaneous combustion characteristic of biomass material. To date, only Tang & Zhou (2020) have investigated the suppression of the spontaneous combustion of biomass using chemical inhibitors. The authors used $MgCl_2$, $Ca(OH)_2$, $CaCl_2$, phytic acid, citric acid, ascorbic acid, $NaH_2PO_2$, $NaH_2PO_4$, $Na_3PO_4$, N-phenyl-1-naphthyl-p-phenylenediamine, N-cyclohexyl-N'-phenyl-p-

phenylenediamine and N,N'-di-2-naphthyl-p-phenylenediamine to treat pine particles. The treated samples were analysed using TGA, FTIR and DSC to observe how the spontaneous combustion characteristic of the pine particles was affected by the chemical inhibitors. Their study revealed that $CaCl_2$ exhibited the best inhibitory effect. Moreover, the FTIR results revealed that the inhibitor weakened the oxygen-containing functional groups, retarding the low-temperature oxidation reaction of the pine particles.

The quantity of previous research related to the inhibition of spontaneous biomass combustion using chemical inhibitors is insufficient to support their effectiveness. For this reason, the current study is important and necessary given that it aims to inhibit the spontaneous combustion characteristic of biomass material named *Searsia lancea* amongst other fuels, using imidazolium-based ionic liquids, which fall under the category of chemical inhibitors. The results of this research should provide more knowledge into the inhibiting potential of these inhibitors for both raw *Searsia lancea* biomass and its hydrochar/coal pellets.

### 2.5 Hydrochar Production

Hydrochar is a fuel derived from biomass material through hydrothermal carbonisation (HTC), also known as wet torrefaction (Kambo & Dutta, 2015). HTC was used to describe the coalification process by Friedrich in 1913 (cited by Bergius, 1931). The process was further investigated in the late 19$^{th}$ century for treating organic materials used in manufacturing chemicals and recovering gaseous and liquid fuels (Bobleter, 1994; Mumme *et al*., 2011). This process involves submerging biomass in water and heating it to a temperature of 180 - 350 ℃ for 5 - 240 minutes in a pressurised vessel (2-6 Mpa) (Libra *et al*., 2011; Mumme *et al*., 2011; Hoekman *et al*., 2013). Several reactions are involved in the HTC process. An overview of the process as well as the chain of reactions involved is presented in Figure 2.6.

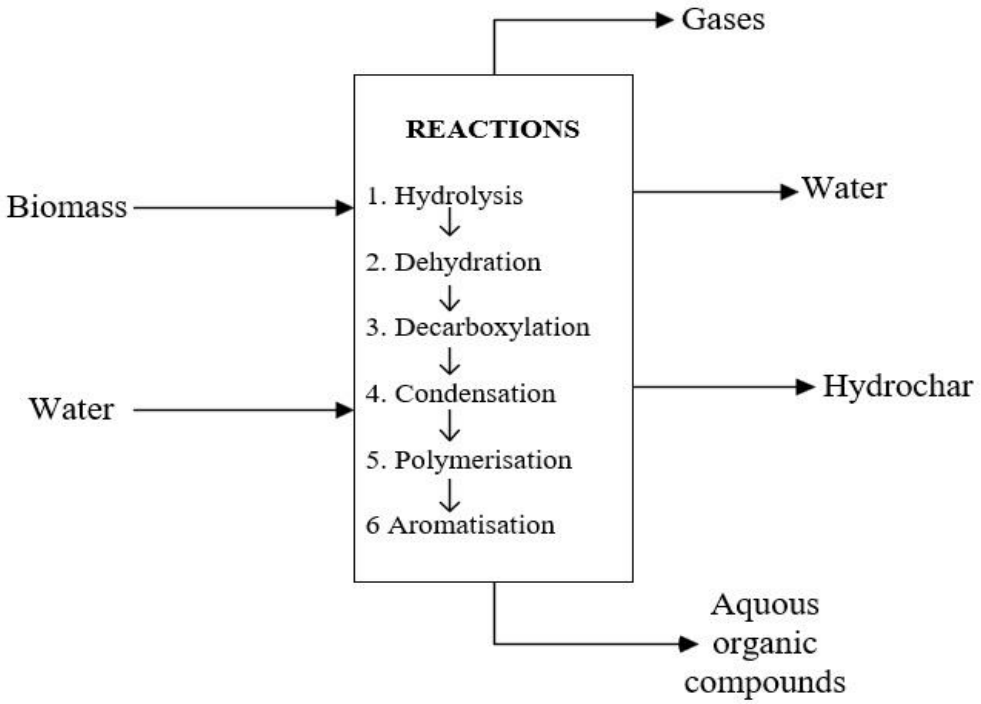



*Figure 2.6: An overview of hydrothermal carbonisation of biomass adapted from Mazumber (2019)*

Given that this process requires water, the moisture content of the biomass has no impact on the process; hence pre-drying the biomass feedstock before use is unnecessary. This process is cost-effective compared to other pretreatment processes, such as dry-torrefaction and slow-pyrolysis, which are energy-intensive given that they require pre-drying (Benavente *et al*., 2014). Kambo & Dutta (2015) conducted a comparative review of hydrochar and biochar produced through slow pyrolysis of biomass. They concluded that hydrochar produced via HTC could be used as an alternative to coal for power generation, given its favourable physicochemical properties.

## 2.6 Spontaneous Combustion of Hydrochar

Given that this study proposes hydrochar and hydrochar/discard coal blends as potential fuels to reduce the reliance on coal as a primary energy source, knowing about the susceptibility of these fuels to spontaneous combustion is of great importance. Biomass is, without question, highly reactive. Processing it to produce hydrochar does not mean the spontaneous combustion characteristic of hydrochar suddenly becomes insignificant. The hydrochar produced is a reactive and porous media like biomass and biochar; hence oxygen can easily permeate through the fuel and accelerate the low-temperature oxidation process (Dullien, 1979; Restuccia *et al*.,

2019). Therefore, hydrochar is also prone to undergo spontaneous combustion due to its porous structure. However, extensive research is required to prove this.

There is a gap in the literature concerning the factors affecting the spontaneous combustion of hydrochar because it is a relatively new fuel compared to biochar produced by other processes, such as pyrolysis and dry torrefaction. Although a study was carried out on the self-heating mechanism of biochar, the conclusion and findings from that study cannot be applied to hydrochar, given that the production processes of these two fuels are different (Restuccia *et al*., 2019). Additionally, the inhibition of spontaneous combustion of hydrochar has not been explored. Thus, a thorough investigation is required to bridge the gap identified in the literature and pave the way for future research in line with the inhibition of spontaneous combustion of hydrochar using imidazolium-based ionic liquids.

## 2.7 Summary

A thorough review of the spontaneous combustion mechanisms of coal, biomass and hydrochar was presented in this chapter. The factors influencing the spontaneous combustion characteristic of the fuels and the techniques that have been explored in various studies for predicting the spontaneous combustion liability of the fuels were also reviewed. With that in mind, this study seeks to expand on the literature and close the identified gaps by investigating the effect of three imidazolium-based ionic liquids on the spontaneous combustion characteristics of discard coal, raw biomass, specifically the *Searsia lancea* tree species, hydrochar produced using *Searsia lancea* and blends of hydrochar/discard coal.

Thermal analysis tests such as the Wits-Ehac and TGA have never been used to determine the spontaneous combustion of hydrochar produced from *Searsia lancea* and blends of hydrochar/discard coal. As a result, this study aimed to use these two techniques to measure the spontaneous combustion liability of the fuels given that the two thermal techniques have been proven to be reliable and efficient when used on other fuels in previous studies. Moreover, the fuels will be characterised before and after their treatment with imidazolium-based ionic liquids to identify any structural, morphological and physicochemical changes that might have been caused by the interaction of the fuels with the ionic liquids. The experimental techniques with be discussed in detail in Chapter 3.

## CHAPTER 3: RESEARCH METHODOLOGY

This chapter describes the nature of the material used and the experimental methods utilised to meet the objectives of this study. Procedures for sample preparation and equipment used are also provided. The chapter is divided into five sections: material preparation, hydrochar production, sample characterisation, spontaneous combustion tests and the treatment of the samples with ionic liquids.

### 3.1 Material Preparation

Samples of *Searsia lancea*, a tree species, were collected from the Vaal River Mine at the Mispah tailings facility, which has nutrient-rich soil (Joubert, 2017). The harvested tree species were 12 years old when harvested from sections S11 and S12 of the Mispah tailings facility. From each section of the tailing facility, different tree compartments (leaves, wood, twigs and roots) were sampled once as illustrated in Figure 3.1 and stored at the University of the Witwatersrand in the Genmin building.

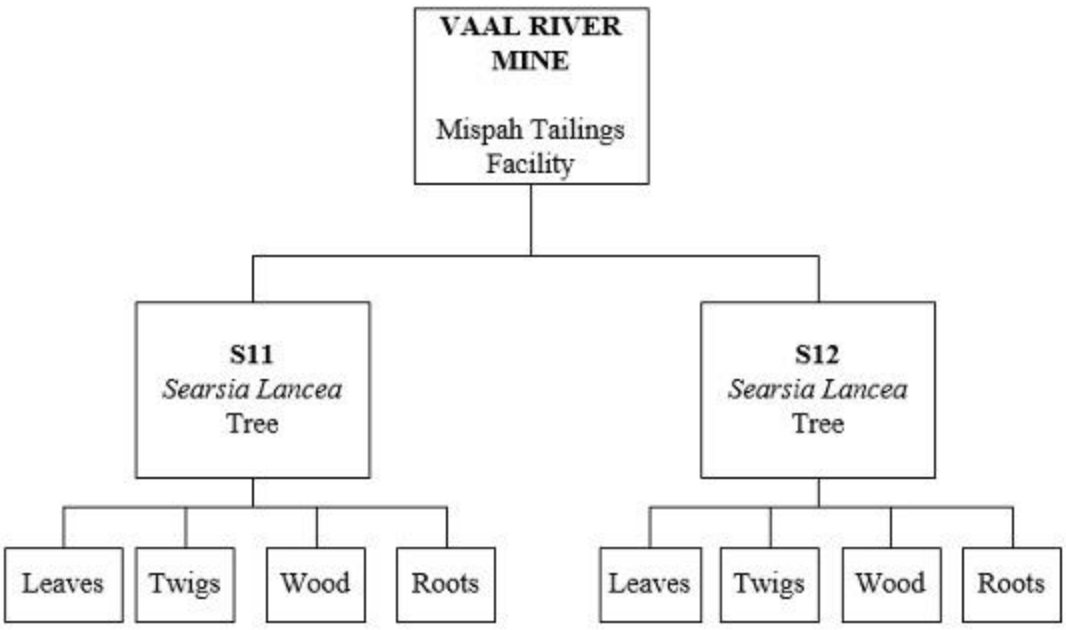



*Figure 3.1: Site for Searsia lancea samples collection*

The eight Mispah tailings facility tree compartments (Figure 3.1) were cut into smaller pieces with a table saw and a chainsaw. The samples were further milled to -212 μm using a Retsch SM 200 cutting mill for all the characterisation tests and -0.5 mm for hydrochar production. After milling, equal tree compartments from the S11 *Searsia lancea* were mixed with equal tree compartments from the S12 *Searsia lancea* to form a 50% S11 and 50% S12 raw biomass blend.

The discard coal sample used was sourced from Witbank coalfield and milled to -212 μm using a laboratory ring pulveriser for characterisation and subsequent tests. Three imidazolium-based ionic liquids, namely 1-butyl-3-methyl-imidazolium acetate [$Bmim^+OAc^-$] (IL-C), 1-ethyl-3-methyl-imidazolium hydrogen sulphate [$Emim^+HSO_4^-$] (IL-B) and 1-butyl-3-methyl-

imidazolium hydrogen sulphate [$Bmim^{+}HSO_4^{-}$] (IL-A) at 95% mass purity were purchased from Sigma-Aldrich (Pty) Ltd (Merck) South Africa.

### 3.2 Hydrochar Production

The hydrochar was produced from the raw biomass blend made from 50% S11 and 50% S12 through HTC at a particle size fraction of - 0.5 mm. The HTC process was carried out using a 1.75 L Berghof BR-1500 high-pressure reactor, illustrated in Figure 3.2. The manufacturer recommended that the solid and liquid mixture in the reactor must not exceed 80% of the reactor . For the hydrochar production, the reactor was heated to a temperature of 280 ℃, for 180 minutes (residence time), at a solid: liquid ratio of 1:8. This condition was the best test condition attained by Setepu *et al*. (2021) to produce hydrochar from the same sample.

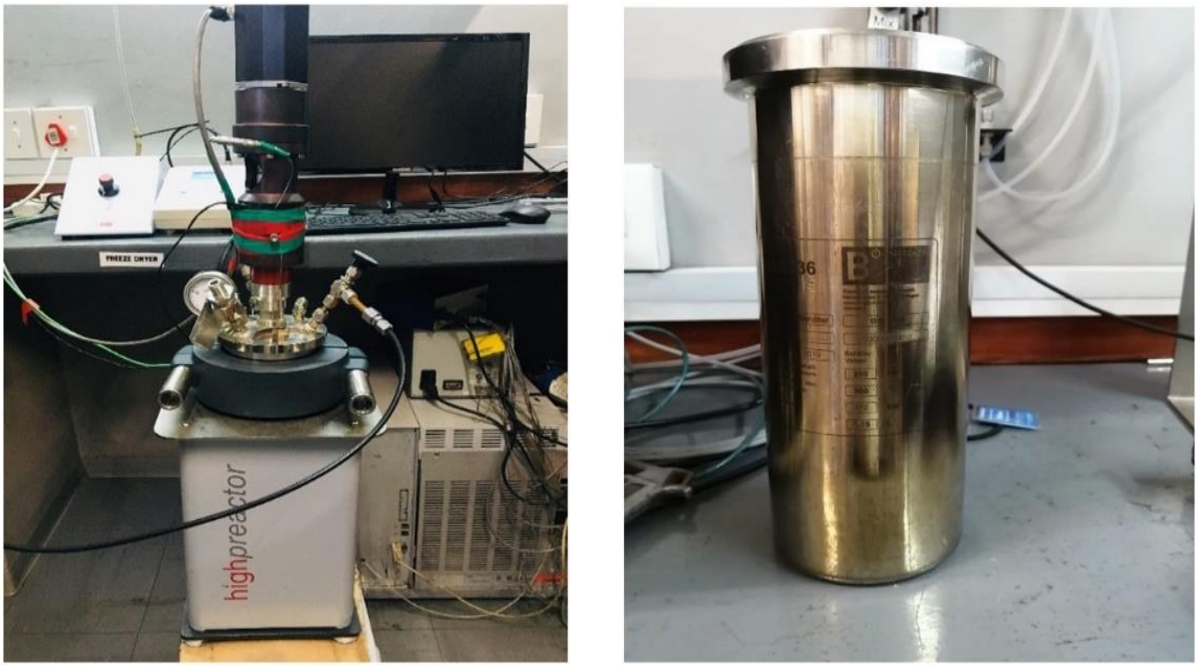
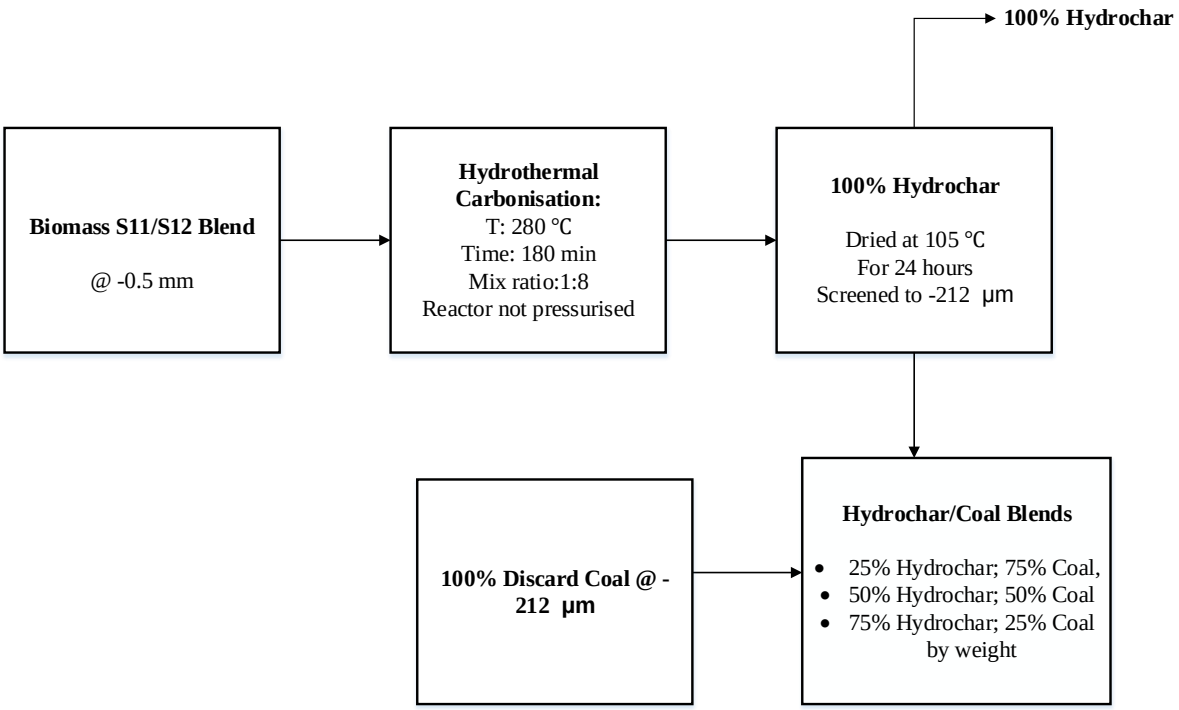



*Figure 3.2: Berghof stirring system axis and stainless-steel reactor vessel*

Three kilograms of hydrochar produced under the set conditions was dried in an oven at 105 ℃ for 24 hours to remove excess moisture and milled to a particle size of -212 μm. The sample was split into two parts, with the first part set aside for subsequent tests and analysis, while the second part was used to prepare hydrochar/coal blends at a hydrochar concentration of 25%, 50% and 75%. The overview of the hydrothermal carbonisation procedure is depicted in Figure 3.3.




## 3.3 Sample Characterisation

### 3.3.1 Proximate analysis

Proximate analysis is a characterisation test that determines the inherent moisture (%), ash content (%) and volatile matter (%) present with fixed carbon calculated by difference. The analysis was carried out on the biomass, discard coal, hydrochar and the three hydrochar/discard coal blends according to ASTM D-5142 using the TGA 701 Leco instrument. For the analysis, 1 g of each sample was loaded in ceramic crucibles that were positioned in a carousel inside the instrument. During the analysis, the samples were heated in a nitrogen atmosphere from room temperature to 107 ℃ at a heating rate of 6 ℃/min to determine their inherent moisture content by mass loss. The samples were further heated from 107 ℃ to 950 ℃ to determine their volatile matter, which was reported as a mass loss of the samples between 107 ℃ and 950 ℃. To determine the ash content, the samples were combusted in an oxygen atmosphere between 650 ℃ to 750 ℃, and the residue left after combustion was noted as the ash content of the sample.

### 3.3.2 Ultimate analysis

The ultimate analysis was carried out according to ASTM D 4239-05 and ASTM D 5373-02 to determine the sample's total sulphur content (S) and the elemental composition (total carbon (C), hydrogen (H), nitrogen (N) and oxygen (O)), respectively. Oxygen was determined by the difference according to Equation 3.1.

Oxygen (%) = 100 – (total carbon + total hydrogen+ total sulphur+ moisture content + ash content) (3.1)

### 3.3.3 Calorific value

The calorific value (the energy contained in the fuel) of the raw biomass species, discard coal, hydrochar and the three hydrochar/coal blends were determined according to ASTM D5865-04 using a Leco AC 500 bomb calorimeter. The system uses an electronic thermometer with an accuracy of 0.0001 ℃ to measure the temperature every six seconds, with the results obtained within 4.5 to 7.5 minutes.

### 3.3.4 Fourier Transforms Infrared Spectroscopy Analysis

A PerkinElmer Frontier FTIR spectrometer was used to identify the functional groups present in each sample before and after treatment with ionic liquids. The analysis was performed by placing 0.5-1.0 g of sample on the FTIR spectrometer lens. The equipment passes an infrared beam through the sample and measures the frequency at which the sample absorbs an infrared beam. The FTIR spectrometer generates an absorbance spectrum on a graph, with the peaks representing different chemical bonds and molecular structures in each sample. Each of the peaks on the graph represents a functional group such as ketones, alkanes, carbonyls, alcohols, aromatics, aliphatics and others. Figure 3.4 summarises the characterisation tests that were conducted in this study.

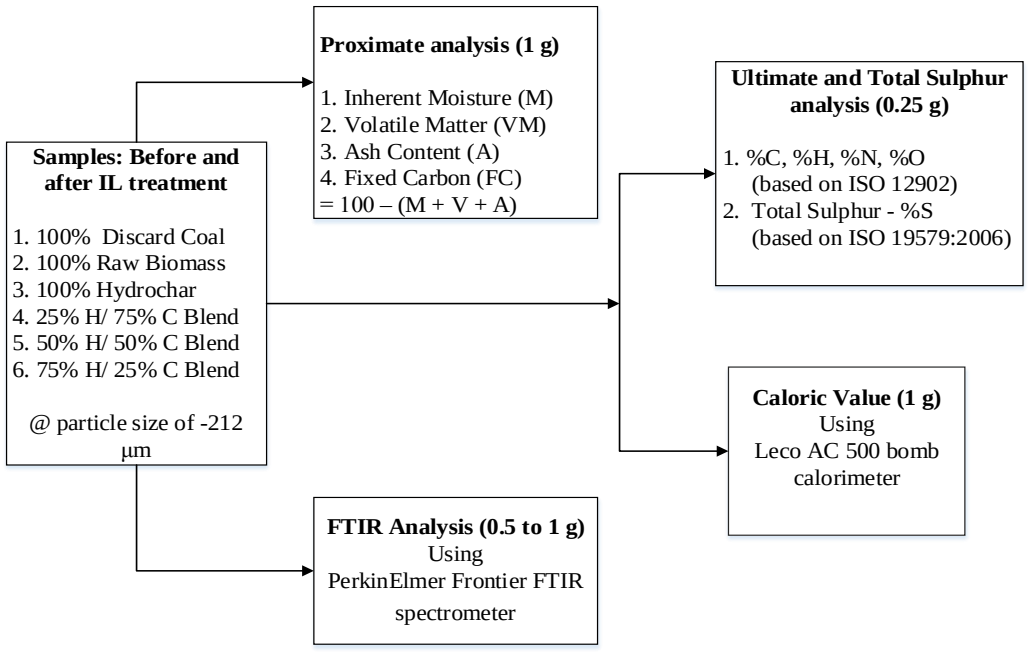


*Figure 3.4: Characterisation of the samples before and after treatment with imidazolium-based ionic liquids*

### 3.4 Spontaneous Combustion Tests

Two spontaneous combustion test methods, TGA and the Wits-Ehac tests were utilised in this study. The techniques measured the heat flow and the thermal decomposition per time to predict the tendency of discard coal, biomass, hydrochar and hydrochar/coal blend to undergo spontaneous combustion when exposed to air. Figure 3.5 depicts an outline of the two spontaneous combustion test methods. Each of the test methods has unique characteristic profiles, which are described in detail in the following section.

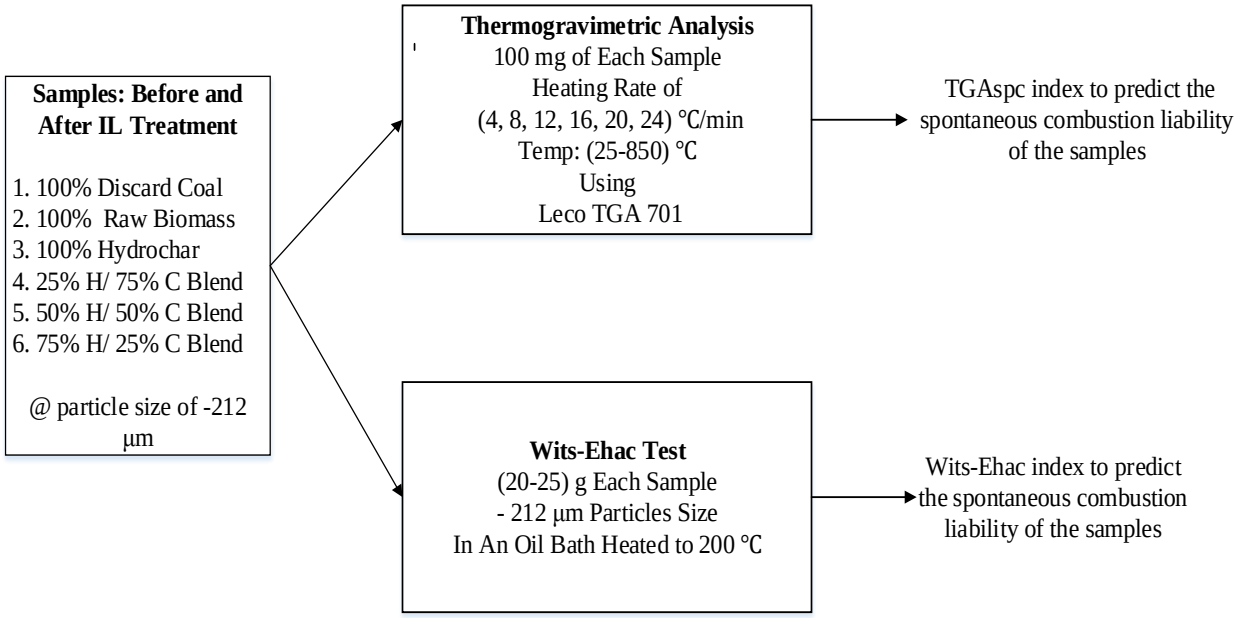



*Figure 3.5: An outline of the spontaneous combustion tests*

#### 3.4.1 Thermogravimetry analysis

All the samples (discard coal, biomass, hydrochar and hydrochar/coal blends) were subjected to TGA and DTG analyses using the TGA 701 Leco instrument. The analysis was used to predict the combustion reactivity of the samples under an oxidative medium. For each run, a 100 mg sample at a particle size of – 212 µm was heated at different heating rates (4, 8, 12, 16, 20 and 24 ℃/min) from room temperature to 850 ℃ and held at this temperature until there was no further mass loss. The data obtained from the tests were used to determine:

I) The derivatives of weight loss (%/min) as a function of time and temperature as DTG and TGA profiles.

II) The slope of the derivative plot in the linear segment of the curve at low temperatures.

A profile plot of the heating rates against the slope for each sample was generated using the data obtained. The data was also used to predict the susceptibility of discard coal, biomass, hydrochar and the hydrochar/coal blends to spontaneous combustion before and after the imidazolium-based ionic liquids treatment using $TGA_{spc}$ index, which is the thermogravimetric spontaneous combustion index. As expressed by Equation 3.2, the $TGA_{spc}$ is defined as the ratio between the rate of weight loss and the temperature change caused by an external source.

$$TGA_{spc} = \frac{\Delta\, weight\ loss}{\Delta\, Temperature} \tag{2.16}$$

### 3.4.2 Wits-Ehac test

The Wits-Ehac test method was carried out following the test procedure outlined by Onifade, (2018) and Onifade and Genc (2019). The Wits-Ehac apparatus is made up of an air circulator, oil bath, oil circulator, a flowmeter, a heater, an air supply compressor, six-cell assemblies (three cells for the discard coal sample or hydrochar/coal blends and the other three for calcined aluminium, which is the inert material) and a computer (Figure 3.6) (Wade, *et al*., 1987). The samples (100% discard coal, raw *Searsia lancea*, hydrochar and three hydrochar/coal blends) were pulverised to -212 µm, and 20 - 25 g of the pulverized samples were fed into three cells of the Wits-Ehac apparatus, while the remaining three cells fed with calcined aluminium. The sample cells and the inert material cells were placed in an oil bath heated to 200 ℃. As the oil bath was heated, the temperatures of the samples and the inert material were recorded on the system every 30 seconds using a micro-computer. The time taken for each sample test depends on the spontaneous combustion characteristic of the sample. The tests for samples with high spontaneous combustion liability take less time than samples with low spontaneous combustion liability. The Wits-Ehac apparatus incorporates the XPT and the DTA thermograph to determine the sample's spontaneous combustion index (Wits-Ehac index). The DTA thermograph provides an insight into the degradation of the sample tested in three stages, as illustrated in Figure 3.7.

The first stage denotes the temperature at which the inert material exceeds that of the tested sample. Stage II is known as the region where the exothermic reaction occurs, and information about the temperature difference between the inert material and the tested sample can be obtained from this stage. Additionally, at this stage, the heating rate of the tested sample could exceed that of the inert material due to the propensity of the tested sample to undergo self-heating and hence reach the temperature of the surroundings (oil bath temperature). The point at which the differential is zero in Stage II is the XPT. Stage III is when the tested sample burns out completely. The Wits-Ehac index was calculated according to Equation 3.3. It is expected that in Stage II, a sample with a high spontaneous combustion liability will have a very steep slope and a low XPT compared to a sample with low spontaneous combustion liability. According to Wade *et al*. (1987), a coal sample with a Wits-Ehac index below three has a low spontaneous combustion liability. Whereas, between 3 and 5 five, the likelihood of the coal undergoing spontaneous combustion is medium, and when the index is above 5, the sample spontaneous combustion liability is high.

$$\text{Wits} - \text{Ehac index} = \left(\frac{\text{Stage II slope}}{\text{XPT}}\right) \times 500 \qquad (3.3)$$

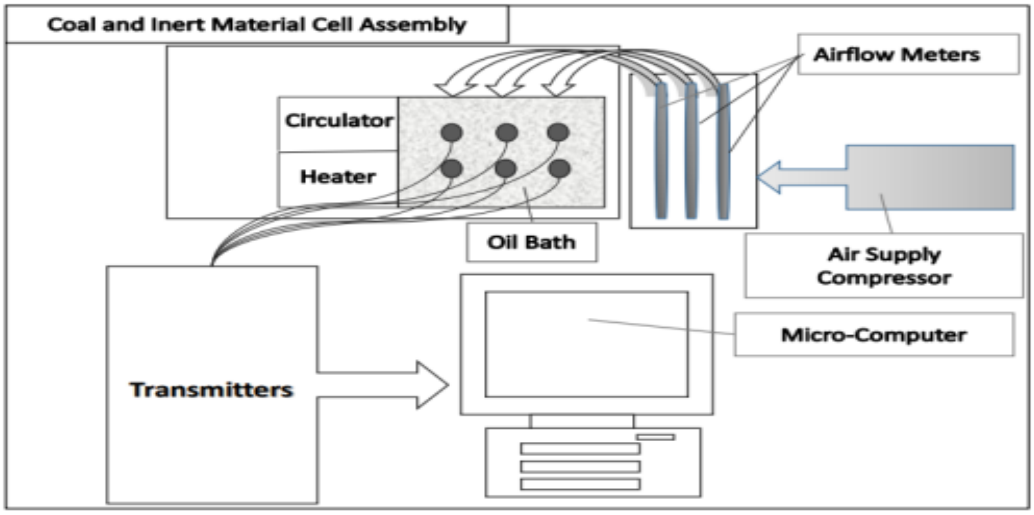



*Figure 3.6: A schematic diagram of the Wits-Ehac apparatus (Wade et al., 1987)*

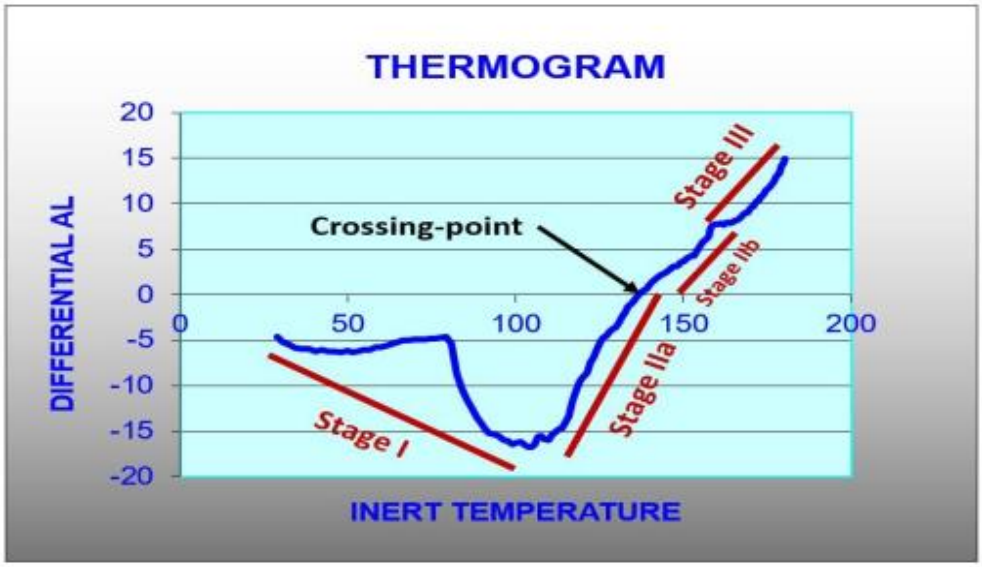



*Figure 3.7: A typical differential thermal analysis thermogram profile (Wade et al., 1987; Gouws & Eroglu, 1993)*

### 3.5 The Treatment of the Samples with Ionic Liquids

From the six samples (100% discard coal, 100% biomass, 100% hydrochar, 25% hydrochar + 75% discard coal, 50% hydrochar + 50% discard coal and 75% hydrochar + 25% discard coal), those with the highest spontaneous combustion susceptibility were treated using the following ionic liquids:

I) 1-butyl-3-methyl-imidazolium hydrogen sulphate [$Bmim^+HSO_4^-$] (IL-A)

II) 1-ethyl-3-methyl-imidazolium hydrogen sulphate [$Emim^+HSO_4^-$] (IL-B)

III) 1-butyl-3-methyl-imidazolium acetate [$Bmim^+OAc^-$] (IL-C)

Each ionic liquid was diluted with distilled water to the following concentrations: 10, 20, 30, 40 and 50%. The ionic liquids were mixed with the selected sample at a solid:liquid ratio of 1:4 (2g to 8ml) in a 50 ml Duran sample bottle. The solutions were then placed in a temperature-controlled shaker for 2 hours at 25 ℃ to alter the functional groups that make the solid samples susceptible to spontaneous combustion. After shaking, the samples were cooled, and the treated solid samples were separated from the imidazolium-based ionic liquid solutions using a vacuum filtration system. The filtered cake was then placed in a vacuum oven for 48 hours at ambient temperature to remove excess moisture. The treated samples were subjected to TGA spontaneous combustion tests at six different heating rates (4, 8, 12, 16, 20 and 24 ℃/min). The samples with the lowest $TGA_{spc}$ index were subjected to characterisation and Wits-Ehac

spontaneous combustion tests. Figure 3.8 shows the procedure for treating the samples with different imidazolium-based ionic liquids, as well as the conditions that were used for each piece of equipment.

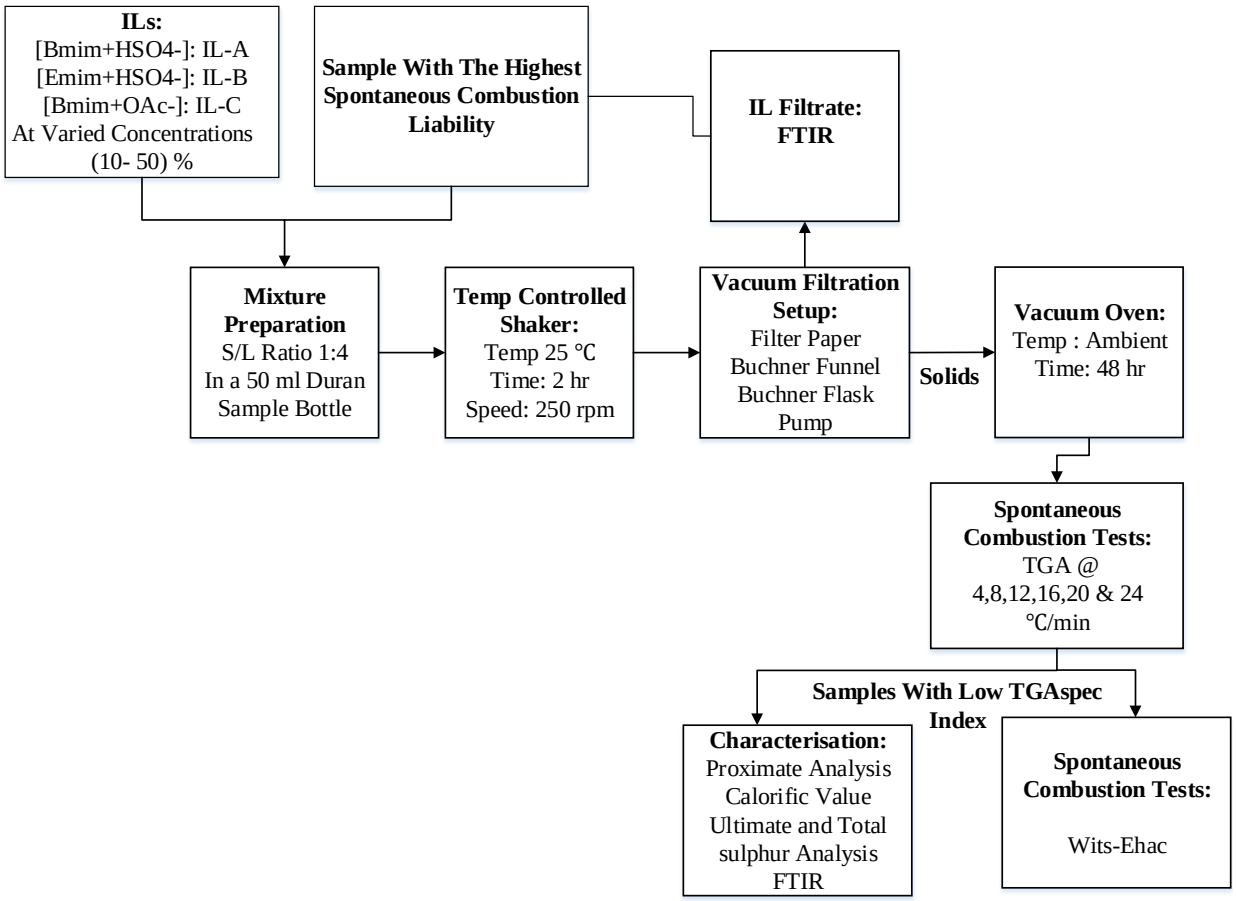



*Figure 3.8: Sample treatment with imidazolium-based ionic liquids*

## 3.6 Summary

The experimental methods required for this study and the nature of the material that was used are presented in this chapter. The chapter was divided into five sections: material preparation, hydrochar production, sample characterisation, spontaneous combustion tests and the treatment of the samples with ionic liquids. The analytical techniques used in all the section were also explained in detail. The results obtained following the analysis of the samples are presented in Chapter 4.

## CHAPTER 4: RESULTS AND DISCUSSION

This chapter discusses the results of all analyses performed in this research. The first section of this chapter presents and discusses the physicochemical properties (proximate analysis, ultimate analysis, calorific values and FTIR) of the samples and the textural properties of the biomass treated and untreated. In the second section of the chapter, the results obtained from the spontaneous combustion of the raw samples via TGA and the Wits-Ehac tests are presented. Following this, the results obtained from the samples treated with three different ionic liquids and their susceptibility to spontaneous combustion are also discussed. In general, this chapter presents the results on whether imidazolium-based ionic liquids can inhibit spontaneous combustion through various experimental studies.

### 4.1 Characterisation of Raw Biomass, Discard Coal, Hydrochar and Hydrochar/Coal Blends

#### 4.1.1 Proximate analysis, ultimate analysis and calorific value

*Table 4.1: Physicochemical analysis of biomass, discard coal, hydrochar and hydrochar/coal blends*

| Samples | Proximate Analysis (Ar) | | | | Ultimate Analysis (Db) | | | | | CV |
|---|---|---|---|---|---|---|---|---|---|---|
| | %M | %A | %FC | %VM | %S | %TC | %H | %N | %O | MJ/kg |
| 100% Biomass | 8.01 | 2.92 | 19.54 | 60.52 | 0.07 | 44.60 | 6.26 | 0.47 | 37.67 | 17.28 |
| 100% Hydrochar | 1.92 | 0.36 | 52.12 | 45.60 | 0.08 | 70.90 | 5.01 | 0.47 | 21.26 | 29.58 |
| 100% Discard coal | 3.10 | 36.23 | 40.01 | 20.65 | 1.64 | 48.20 | 2.92 | 1.11 | 6.80 | 18.55 |
| 25% H + 75% DC | 2.76 | 27.20 | 43.24 | 26.79 | 1.21 | 54.30 | 3.55 | 0.95 | 10.03 | 21.42 |
| 50% H + 50% DC | 2.45 | 18.46 | 46.06 | 33.03 | 0.87 | 60.10 | 4.03 | 0.82 | 13.27 | 25.23 |
| 75% H + 25% DC | 2.04 | 9.88 | 48.56 | 39.51 | 0.45 | 65.30 | 0.66 | 0.66 | 21.01 | 26.97 |

*M: Inherent moisture, A: Ash content, FC: Fixed carbon, VM: Volatile matter, S: Sulphur, TC: Total carbon, H: Hydrogen, N: Nitrogen, O: Oxygen, CV: Calorific value, DC: Discard coal, H: Hydrochar, Ar: Air dried, Db: Dry basis*

The proximate analysis, ultimate analysis and the calorific value of the samples are presented in Table 4.1. The inherent moisture of 100% biomass, 100% discard coal and 100% hydrochar was 8.01%, 3.10%, and 1.92%, respectively. The physicochemical results reported for the 100% biomass used in this study are similar to that reported by Setepu *et al*. (2021). The high moisture content of the 100% biomass could make it more susceptible to spontaneous combustion. According to the study by Miyawaki *et al*. (2021), biomass with high moisture content may produce accelerated microbial heat generation leading to combustion. The

moisture content of 25% hydrochar + 75% discard coal, 50% hydrochar + 50% discard coal and 75% hydrochar + 25% discard coal used in this study ranged from 2.04 - 2.76% (Table 4.1). Hao *et al*. (2014) suggest that carbonaceous materials with high moisture content act as catalysts by promoting the oxidation reaction leading to heat release and spontaneous combustion. Therefore, a hydrochar/coal blend with a higher moisture content could have a relatively high spontaneous combustion liability index compared to other blends with lower moisture content.

The ash content of 100% hydrochar, 100% biomass and 100% discard coal was 0.36%, 2.92% and 36.23%, respectively. The ash content for the hydrochar/coal blends used, i.e., 25% hydrochar + 75% discard coal, 50% hydrochar + 50% discard coal and 75% hydrochar + 25% discard coal blends, range from 9.88 - 27.20% (Table 4.1). A sample with a high ash content has a high mineral content, which act as a heat sink and blocks the pores and active sites of a fuel (Beamish & Arisoy, 2008; Onifade, 2018). Onifade & Genc (2019) reported that high ash content leads to low susceptibility to the spontaneous combustion of coal. Manic *et al*. (2021) observed the same trend during their investigation of biomass. Therefore, it is expected that 100% coal discard and the three blends of hydrochar and coal might have a lower spontaneous combustion index than 100% biomass and 100% hydrochar.

The fixed carbon content results for the samples correspond to the trend seen in their total carbon content (Table 4.1). According to Onifade *et al.* (2020), samples with high spontaneous combustion liability have high carbon content. The HTC of 100% biomass used in this study could increase its spontaneous combustion liability compared to other fuels. It is reported in the literature that coalification of coal increases carbon content leading to the densification and reduction of coal porosity (Ceballos *et al*., 2015). This is the same phenomenon that occurs when raw biomass is carbonised, leading to a hydrochar with high total carbon content. Given the high carbon content of the 100% hydrochar, this sample may have a higher spontaneous combustion liability than 100% discard coal.

The volatile matter content in fuels can be used to predict their susceptibility to spontaneous combustion. According to Manic *et al.* (2021), biomass feedstock with high volatile matter is highly susceptible to spontaneous combustion. Onifade (2018) reported that coal samples with a high average content of volatile matter have a high $TG_{spc}$ index. Given the high proportion of volatile matter in 100% biomass and 100% hydrochar, both samples are likely more reactive and easily combustible than others (Shah, 2022). Both 100% biomass and 100% hydrochar

fuels are likely more prone to spontaneous combustion as they had the highest oxygen content compared to other fuels. This is because high oxygen concentration increases the self-ignition attribute of fuels and their combustion liability (Huangfu *et al.*, 2018; Ren *et al.*, 2021).

As reported in Table 4.1, the HTC of 100% biomass to 100% hydrochar improved the calorific value of the biomass from 17.25 MJ/kg to 29.58 MJ/kg. The hydrochar produced in this study can be classified as a grade A fuel, as according to Steyn & Minnit (2010), coal or solid fuel with a calorific value $\geq 27.5$ MJ/kg is deemed as a grade A fuel. Hydrochar also has an identical characteristic to medium-rank bituminous coal with fixed carbon ranging from 45% to 86% and a calorific value in the range of 19.3 to 30.2 MJ/kg (Pang, 2016). 100% biomass had the lowest calorific value of 17.28 MJ/kg followed by 100% discard coal with a calorific value of 18.55 MJ/kg. Furthermore, the calorific value increases as the ash content decreases (Table 4.1). The blending of the discard coal with hydrochar resulted in improved calorific value among other properties. The 75% hydrochar + 25% discard coal can be classified as a grade B fuel given that it has a calorific value greater than 26.5 MJ/kg (Steyn & Minnit, 2010). Based on the physicochemical properties of the fuels, the 100% biomass may be more susceptible to spontaneous combustion than the other samples.

### 4.1.2 Fourier transform infrared spectroscopy

FTIR was used to determine the changes in the active functional groups in the samples since the functional groups significantly affect spontaneous combustion liability. The spectra obtained for each sample are presented in Figure 4.1. The tendency of carbonaceous material to undergo spontaneous combustion is associated with the composition of each functional group in the material (Geng *et al.*, 2009; Xu *et al.*, 2017). Hydroxyl, carbonyl and carboxyl are the three predominant oxygen functionalities, especially in coal (Kadioglu & Varamaz, 2003). A high concentration of the three oxygen functional groups in a sample may result in an increased contact time with air leading to increased spontaneous combustion susceptibility. The absorption peaks at 3691 $cm^{-1}$ was assigned to the hydroxyl group (-OH), which was found in 100% discard coal, 25% hydrochar + 75% discard coal, 50 % hydrochar + 50% discard coal and 75% hydrochar + 25% discard coal. The 100% discard coal had a well pronounced -OH group on its surface, indicating that this sample is highly oxidised due to weathering conditions. With -OH being dominant in this sample, it is expected to be loosely packed, leading to the likelihood of undergoing spontaneous combustion at low temperatures (Zhai *et*

*al*., 2019). Furthermore, the -OH stretch is responsible for the mass loss when spontaneous combustion takes place (Zhang *et al*., 2021).

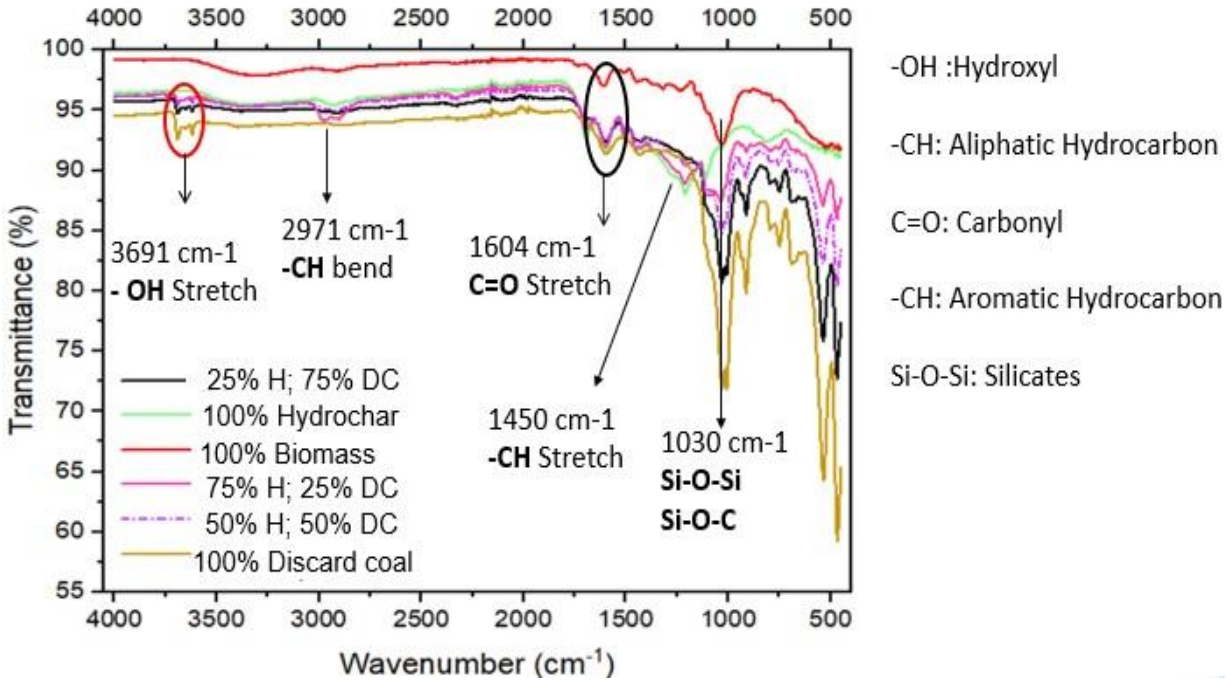



*Figure 4.7: The FTIR spectra of six samples (H: Hydrochar, DC: Discard coal)*

The aliphatic hydrocarbon group is also one of the most reactive groups that form a part of the main reactant leading to spontaneous combustion, given that it has reactive side chains (Lu & Hu, 2007). The absorption peaks at 2971 $cm^{-1}$ are ascribed to the symmetric stretching aliphatic hydrocarbon, which can be seen in the 75% hydrochar + 25% discard coal and 100% hydrochar. This shows the formation of methyl groups during HTC. Aliphatic compounds are reported to release heat energy, which is responsible for self-heating as this group oxidises readily (Moroeng, 2015). Tang (2015) and Zhong *et al*. (2019) also showed that high levels of aliphatic hydrocarbons increase coal's susceptibility to spontaneous combustion. All samples also had a carbonyl group, which is known to decompose thermally leading to spontaneous combustion at temperatures above the accepted low temperatures required for oxidation (Moroeng, 2015). The stretch on 1604 $cm^{-1}$(carbonyl group) is present in all samples (Figure 4.1) and may exist in various forms depending on the type of sample. From the ultimate analysis, all samples were rich in carbon content (Xu *et al*., 2017). The aromatic group at 1450 $cm^{-1}$ is more prominent in 100% hydrochar and 75% hydrochar + 25% discard coal (Figure 4.1). This group is formed from the upgrade made to the low proportion of lignin in raw biomass through pyrolysis, hydrothermal liquefaction and gasification (Carlson *et al.*, 2009; Mahajan *et al.*, 2020).

According to Kumar & Anand (2019), an aromatic group in biomass-derived fuels is associated with volatile matter that is composed of aromatic hydrocarbons, sulphur and different chains of hydrocarbons. It is expected that materials with high volatile matter will be more susceptible to spontaneous combustion (Onifade, 2018; Manic *et al*., 2021).

The sharp peak at 1030 $cm^{-1}$ in the fingerprint region represents the silicates associated with the inorganic minerals in the samples. This peak is more pronounced in the 100% biomass sample but was completely removed in the 100% hydrochar (Figure 4.1) because of biomass minerals that are released into the water during HTC (Setepu *et al*., 2021). The fingerprint section shows that 100% discard coal had the highest mineral content of all the fuels. It is expected that 100% coal will be the most mineral-rich with the highest ash content of all samples (Table 4.1). According to Onifade (2018), the higher the ash concentration, the lower the sensitivity to spontaneous combustion. Consequently, 100% biomass and 100% hydrochar are expected to be more susceptible to spontaneous combustion than other high-ash fuels.

## 4.2 Spontaneous Combustion Tests

The propensity of different fuels to undergo spontaneous combustion can be predicted using various techniques. Although some techniques are well established in their application, no method has been identified as a standard among the available methods, given that there has not been any validation of the reliability of all the methods (Avila *et al*., 2014; Wongthonglueang *et al*., 2022). All techniques are based on the principle that if a material is susceptible to undergoing an exothermic oxidation reaction, then the material is also liable to undergo spontaneous combustion (Onifade, 2018). For this study, TGA and Wits-Ehac tests were carried out to obtain information about the spontaneous combustion liability of the fuels.

### 4.2.1 Thermogravimetric analysis

The objective of the TGA is to quantify the weight loss of a sample as the temperature changes given that the information can provide insight into the propensity of a sample to undergo spontaneous combustion. For some fuels like coal, the weight change, which is a factor of temperature and time, can be investigated experimentally using TGA. For this study, the self-ignition potential of the fuels used was evaluated based on the approach used by Avila (2012), Garcia-Torrent *et al.* (2015) and Manic *et al.* (2021) on coal, biomass and coal-biomass blends. From the combustion profile of each fuel, the derivative weight versus time and temperature, and the slope based on the linear segment of the derivative curve at low temperatures are

derived. Equations 4.1 and 4.2 were used to derive these major variables from the TGA thermographs.

$$\dot{m} = \frac{\partial m}{\partial t} f\ (T, t) \quad (4.1)$$

$$\dot{m} = \frac{\partial m}{\partial T} f\ (T, t) \quad (4.2)$$

The derivative weight versus temperature and time profiles were obtained for 100% discard coal, 100% biomass, 100% hydrochar, 25% hydrochar + 75% discard coal, 50% hydrochar + 50% discard coal and 75% hydrochar + 25% discard coal at six different heating rates (4, 8, 12, 16, 20 and 24 ˚C/min). The linear segment that exists at the initial heating stage where the devolatilisation reaction starts was approximated using a linear trend line for every sample subjected to the six heating rates. This linear segment is associated with spontaneous combustion phenomena since it represents the oxidation reaction at the early stages (Avila, 2012).

Since each fuel has a unique linear segment at different heating rates, a graphical evaluation (Figure 4.2) was conducted to determine the ignition point, point of inflection and peak point of the fuels. Equation 4.3 was used to determine the point of inflection on the curve through linear interpolation calculation. The intersection method was used to locate the onset point or the ignition temperature (Isaac, 2019). Figure 4.2 shows the three important points that were used to calculate the slope of the linear line on the curve.

$$Y = Y1 + (X - X1)\frac{(Y2-Y1)}{(X2-X1)} \quad (4.3)$$

Where: X1, Y1 = ignition point values on the TGA profile

X, Y = point of inflection values on the TGA profile

X2, Y2 = peak point values on the TGA profile

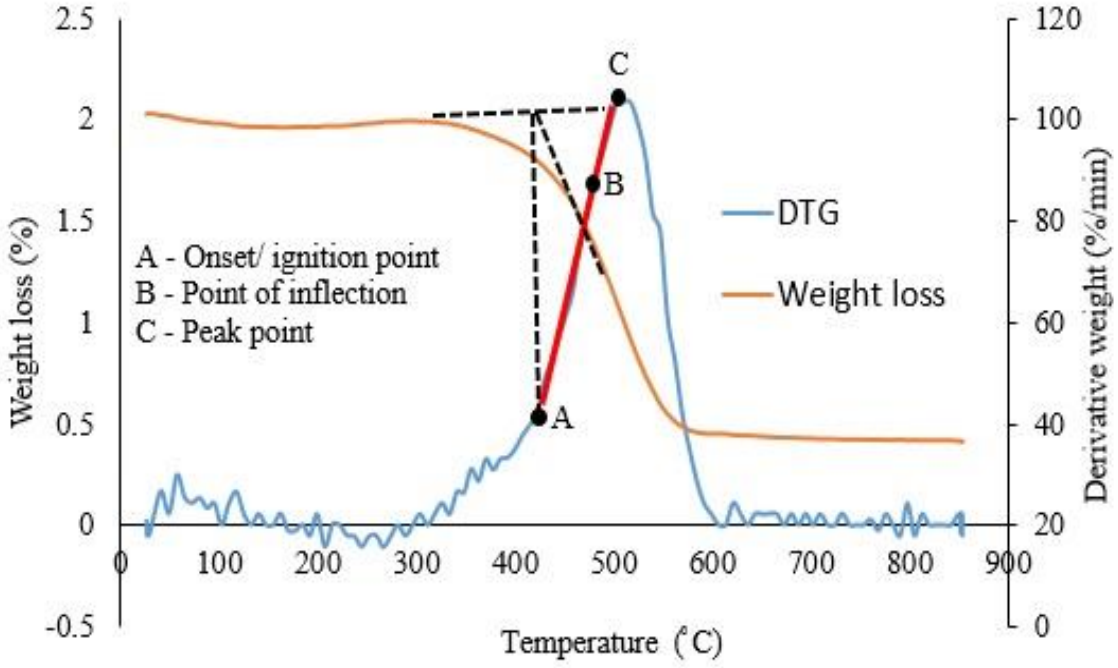



*Figure 4.2: Derivative weight versus time profile showing the intersection method and points used for gradient calculations (DTG: differential thermogravimetric)*

The TGA analysis was first carried out on 100 mg of 100% discard coal, which was the same mass used by Avila (2012) and Onifade (2018). Figure 4.3 shows the derivative profile and slopes of 100% discard coal at six heating rates. In addition, Table 4.2 shows the three points used to calculate the slope of the linear segment for every heating rate and their regression coefficients.

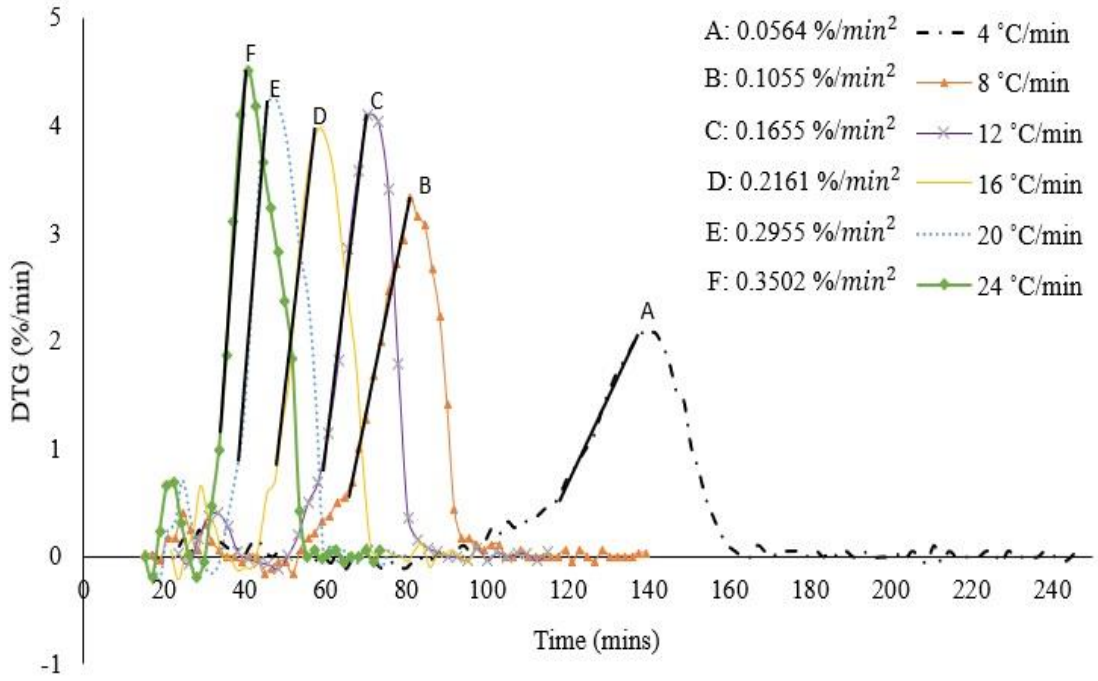



*Figure 4.3: The derivative profile and slopes obtained for 100% discard coal (DTG: differential thermogravimetric)*

Figure 4.3 shows that there is a directly proportional relationship between the heating rate and the linear segment on the derivative profile of 100% discard coal. The slope of the linear segment increases as the heating rate increases because the sample burns more rapidly, and the reactivity of the sample is improved as the heating rate increases (Avila *et al*., 2014; Bada *et al*., 2015). The discard coal sample that was tested at lower heating rates burnt out after 160 minutes whereas those that were tested at higher heating rates burnt out faster. It is also noteworthy that higher peak values are associated with highly reactive samples. It is also evident from Figure 4.3 that as the heating rate increases, the sample becomes highly reactive. The regression coefficients ($R^2$) for the approximated linear segment at different heating rates were closer to 1, which shows a strong correlation between the variables investigated.

*Table 4.2: The specific temperatures and differential thermogravimetric values used for calculating the slopes of the derivative profile of 100% discard coal at different heating rates*

| **Heating rate ˚C/min** | **Unit** | **Ignition Point** | **Inflection Point** | **Peak Point** | **Slope** | $R^2$ |
|---|---|---|---|---|---|---|
| 4 | Time (min) | 117.55 | 137.65 | 141.28 | 0.0564 | 0.9999 |
| | DTG (%/min) | 0.74 | 1.88 | 2.08 | | |
| 8 | Time (min) | 66.45 | 79.17 | 80.95 | 0.1055 | 0.9989 |
| | DTG (%/min) | 1.79 | 3.13 | 3.32 | | |
| 12 | Time (min) | 60.55 | 68.00 | 70.48 | 0.1655 | 0.9937 |
| | DTG (%/min) | 2.45 | 3.68 | 4.10 | | |
| 16 | Time (min) | 49.07 | 56.40 | 58.23 | 0.2161 | 0.9832 |
| | DTG (%/min) | 1.99 | 3.58 | 3.97 | | |
| 20 | Time (min) | 39.22 | 44.70 | 46.53 | 0.2955 | 0.9760 |
| | DTG (%/min) | 2.11 | 3.73 | 4.27 | | |
| 24 | Time (min) | 33.50 | 39.02 | 40.82 | 0.3502 | 0.9824 |
| | DTG (%/min) | 1.95 | 3.88 | 4.51 | | |

The slope values in Table 4.2 were used to calculate the spontaneous combustion index ($TG_{spc}$ index) of 100% discard coal. The $TG_{spc}$ index is the ratio between weight loss rate that happens due to the change in temperature of the surroundings caused by an external heating source (Avila, 2012; Onifade *et al*., 2020).

To determine the spontaneous combustion indices for the fuels in this study, the heating rates were grouped into three increasing sets of heating rates: lower (4, 8, 12, 16 ˚C/min), middle (4, 8, 12, 16, 20 ˚C/min), and higher (4, 8, 12, 16, 20, 24 ˚C/min). For every sample, the three sets of heating rates were plotted against the slopes of the derivative curves to determine the $TG_{spc}$ index of the samples at the lower, middle and higher heating rates. To obtain reliable results, the regression coefficient was also taken into consideration when calculating the $TG_{spc}$ index. Figure 4.4 shows the slopes of the derivative curve profile against heating rate, the $TG_{spc}$ index and the regression coefficient for 100% discard coal. Refer to Appendix A for the figures showing similar information for the other samples and their TGA profiles.

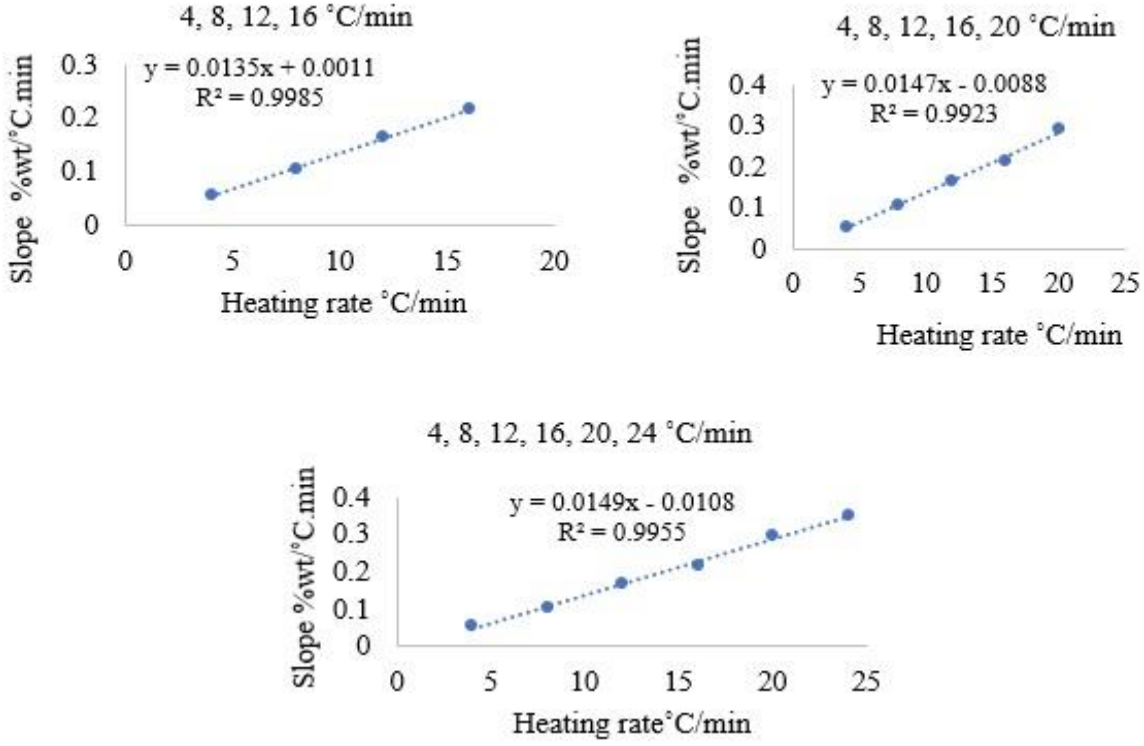



*Figure 4.4: Heating rates applied vs the slopes of the derivative curve for 100% discard coal*

The $TG_{spc}$ index of the samples was determined from the slope of the approximate linear line passing through the point of the profiles as shown in Figure 4.4. At lower heating rates (4, 8, 12, 16 ˚C/min), the $TG_{spc}$ index of 100% discard coal was 0.0135%/˚C.min. According to Onifade *et al*. (2020), the spontaneous combustion liability of a sample can be predicted based on the $TG_{spc}$ index of the sample at lower heating rates, given that the conditions of lower heating rates are much closer to the practical conditions. The $TG_{spc}$ index for 100% discard coal at the middle and the higher heating rates were 0.0147 and 0.0149%/˚C.min, respectively. The difference between the indices at the lower, middle and higher heating rates were not significant. These results also show that the spontaneous combustion susceptibility of 100% discarded coal increases as the heating rates increase because the ignition temperature is reached faster as the heating rate increases (Manic *et al*., 2021).

The procedure for calculating the $TG_{spc}$ index was applied to the other fuels, 100% biomass, 100% hydrochar, 25% hydrochar + 75% discard coal, 50% hydrochar + 50% discard coal and 75% hydrochar + 25% discard coal. Table 4.3 presents the calculated slopes for each sample at different heating rates while Table 4.4 shows the $TG_{spc}$ indices and regression coefficients

of the samples at different sets of heating rates in descending order. Lastly, Table 4.5 presents a general $TG_{spc}$ index classification values for fuel's spontaneous combustion susceptibility.

*Table 4.3: Calculated slopes for all samples at different heating rates*

| | **Heating Ramp Applied (˚C/min)** | | | | | |
|---|---|---|---|---|---|---|
| **Sample** | **4** | **8** | **12** | **16** | **20** | **24** |
| 100% biomass | 0.2545 | 0.8543 | 1.3922 | 2.0177 | 2.6788 | 3.3056 |
| 100% Hydrochar | 0.0599 | 0.1601 | 0.2533 | 0.3320 | 0.4326 | 0.5621 |
| 25% H + 75% DC | 0.0800 | 0.1584 | 0.2530 | 0.3202 | 0.4133 | 0.5007 |
| 50% H + 50% DC | 0.0330 | 0.0992 | 0.1859 | 0.2779 | 0.3573 | 0.4499 |
| 75% H + 25% DC | 0.0586 | 0.1346 | 0.2286 | 0.3093 | 0.4071 | 0.4942 |

*DC: Discard coal, H: Hydrochar*

*Table 4.4: $TG_{spc}$ and regression of fuels in descending order at the lower, middle and higher heating rates.*

| | | **4, 8, 12, 16 (˚C/min)** | | **4, 8, 12, 16, 20 (˚C/min)** | | **4, 8, 12, 16, 20, 24 (˚C/min)** | |
|---|---|---|---|---|---|---|---|
| **Order** | **Samples** | $\mathbf{TG_{spc}}$ | $\boldsymbol{R^2}$ | $\mathbf{TG_{spc}}$ | $\boldsymbol{R^2}$ | $\mathbf{TG_{spc}}$ | $\boldsymbol{R^2}$ |
| 1 | 100% Biomass | 0.1457 | 0.9992 | 0.1503 | 0.9987 | 0.1525 | 0.9990 |
| 2 | 100% Hydrochar | 0.0227 | 0.9971 | 0.0229 | 0.9985 | 0.0243 | 0.9948 |
| 3 | 75% H + 25% DC | 0.0212 | 0.9985 | 0.0218 | 0.9984 | 0.0220 | 0.9970 |
| 4 | 50% H + 50% DC | 0.0205 | 0.9948 | 0.0207 | 0.9974 | 0.0211 | 0.9981 |
| 5 | 25% H + 75% DC | 0.0204 | 0.9962 | 0.0207 | 0.9979 | 0.0210 | 0.9986 |
| 6 | 100% Discard coal | 0.0135 | 0.9985 | 0.0147 | 0.9923 | 0.0149 | 0.9955 |

*DC: Discard coal, H: Hydrochar*

*Table 4.5: Classification of spontaneous combustion susceptibility based on $TG_{spc}$ index values abducted from Manic et al. (2021)*

| **$TG_{spc}$ Index** | **Class** |
|---|---|
| <0.02 | Non-reactive |
| 0.02-0.03 | Low reactive |
| 0.03-0.05 | Reactive |
| >0.05 | High reactive |

From the results presented in Table 4.4, 100% biomass was highly reactive compared to other fuels since its $TG_{spc}$ index is 0.1457. According to Table 4.5, any samples with a $TG_{spc}$ index > 0.05 is classified as highly reactive. It is expected that 100% biomass is highly susceptible to spontaneous combustion compared to the other five fuels in Table 4.4 given that it had a high volatile matter, high moisture content and low ash content. The $TG_{spc}$ index for the samples increased with increasing sets of heating rates (Table 4.3) as expected because the rate of oxygen absorption becomes rapid as the temperature increase (Jain, 2009; Mandal *et al*., 2022).

100% discard coal and 25% hydrochar + 75% discard coal had the least spontaneous combustion liability due to their low volatile matter and high ash content (Table 4.1). These results correlate with those reported by Manic *et al.* (2021) and Garcia-Torrent *et al.* (2015). There is an indirect correlation between the fixed carbon and the $TG_{spc}$ index, which was similar to the observation made by Garcia-Torrent *et al*. (2015) on the assessment of self-ignition risks of different types of solid biofuels by thermal analysis. The correlation between the sulphur content of the samples used in this study and their spontaneous combustion liability is opposite to that reported by Onifade *et al.* (2020). For this study, the samples that exhibit high spontaneous combustion susceptibility had low sulphur content. The difference might be a result of the difference in the composition of the samples. Onifade *et al.* (2020) used coal and coal shale, whereas this study used biomass, hydrochar and hydrochar/coal blends.

### 4.2.2 Spontaneous combustion liability of the samples from the Wits-Ehac index

The sample's spontaneous combustion liability was determined from the DTA thermographs generated for the individual samples. The two important parameters used in determining the Wits-Ehac index are the XPT and Stage II slope of the DTA curve. To generate a DTA thermogram, the difference between the temperature of the sample and that of the inert material (differential temperature) is plotted against the temperature of the inert material. This approach

(Wits-Ehac index) has been used for coal several times, but not to predict the spontaneous combustion liability of biomass and hydrochar/coal blends. The results in the form of a DTA thermogram of the samples are presented in Figure 4.5.

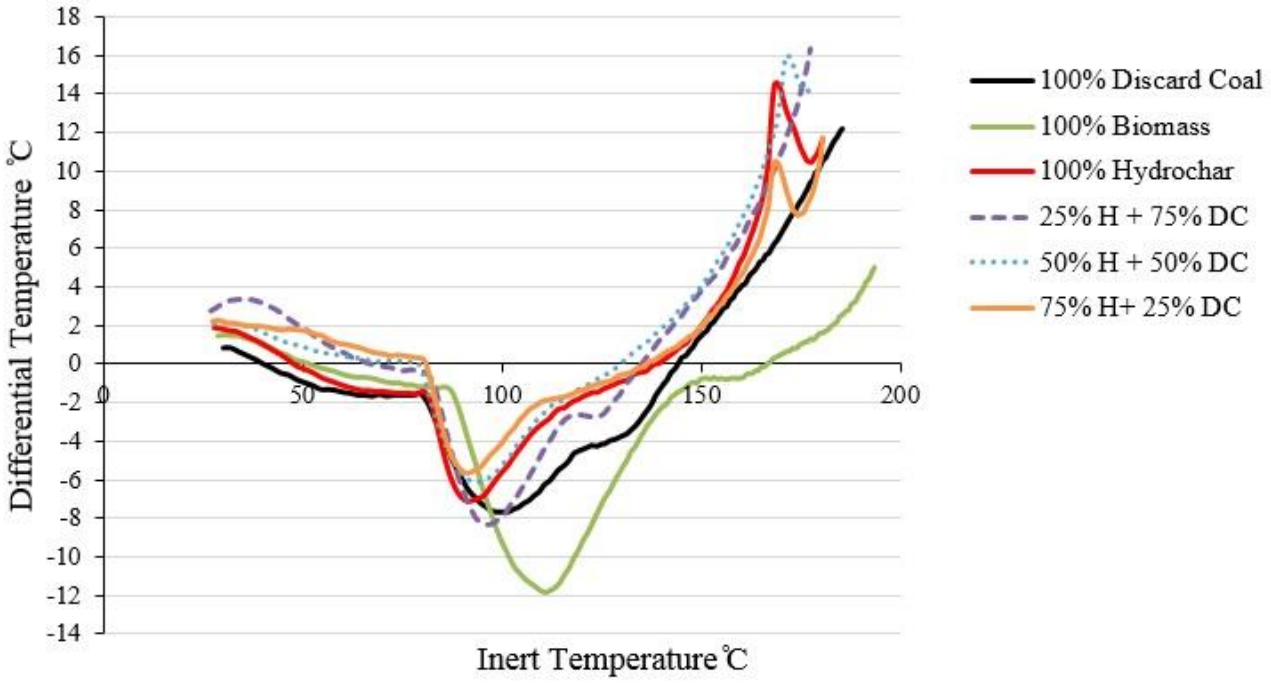



*Figure 4.5: Wits-Ehac differential thermal analysis thermograms for six samples. H: Hydrochar, DC: Discard coal*

The sample's XPT and the Stage II slopes are summarised in Table 4.6 arranged in descending order of the Wits-Ehac index. After analysing each sample, the Wits-Ehac computer system generates the DTA thermogram, giving the XPT and Wits-Ehac index values. The Stage II slope values were calculated using Equation 2.16, and the risk rating classification of the samples based on the Wits-Ehac index values are presented in Table 4.7.

*Table 4.6: A summary of crossing-point temperature, Stage II slope and the Wits-Ehac slope for six samples in Wits-Ehac index descending order*

| **Order** | **Sample** | **XPT (˚C)** | **Stage II Slope** | **Wits-Ehac Index** |
|---|---|---|---|---|
| 1 | 50% H + 50% DC | 130.80 | 1.237 | 4.73 |
| 2 | 25% H + 75% DC | 136.00 | 1.257 | 4.62 |
| 3 | 100% Hydrochar | 139.40 | 1.252 | 4.49 |
| 4 | 75% H + 25% DC | 137.00 | 1.178 | 4.30 |
| 5 | 100% Discard coa1 | 144.20 | 1.214 | 4.21 |
| 6 | 100% Biomass | 167.50 | 1.169 | 3.49 |

*DC: Discard coal, H: Hydrochar*

*Table 4.7: Classification of the spontaneous combustion potential*

| **Wits-Ehac Index** | **Risk** |
|---|---|
| <3 | Low risk |
| 3-5 | Medium risk |
| >5 | High risk |

The XPT for the six samples ranged from 130.8 ˚C to 167.5 ˚C, while their Stage II slope ranged from 1.169 to 1.257, and the Wits-Ehac index range was from 3.47 to 4.73. The results in Table 4.6 show that the higher the XPT, the lower the Wits-Ehac index. A low XPT shows that a sample ignites fast and is, therefore, highly reactive and prone to undergoing spontaneous combustion easily. The results also show that 50% hydrochar + 50% discard coal is highly susceptible to spontaneous combustion, given that it had the highest spontaneous combustion index, followed by 25% hydrochar + 75% discard coal and 100% hydrochar. Contrary to the TGA spontaneous combustion test, the Wits-Ehac results further show that 100% biomass had the lowest Wits-Ehac index.

### 4.2.3 A comparison between the thermogravimetric analysis spontaneous combustion results and the Wits-Ehac index

Given that the two spontaneous combustion tests investigated in this study were the TGA and the Wits-Ehac index, the results of the spontaneous combustion liability of the six samples from the two tests are shown in Table 4.8 for comparison. The results presented for the TGA spontaneous combustion test are those that were found at lower heating rates, given that the lower heating rates conditions are closest to the practical conditions (see section 4.2.1).

*Table 4.8: Comparison of the thermogravimetric analysis and the Wits-Ehac index spontaneous combustion tests data arranged in descending order for each test*

| Order | Samples | $TG_{spc}$ | Order | Samples | Wits-Ehac Index |
|---|---|---|---|---|---|
| 1 | 100% Biomass | 0.1457 | 1 | 50% H + 50% DC | 4.73 |
| 2 | 100% Hydrochar | 0.0227 | 2 | 25% H + 75% DC | 4.62 |
| 3 | 75% H + 25% DC | 0.0212 | 3 | 100% Hydrochar | 4.49 |
| 4 | 50% H + 50% DC | 0.0205 | 4 | 75% H + 25% DC | 4.30 |
| 5 | 25% H + 75% DC | 0.0204 | 5 | 100% Discard coa1 | 4.21 |
| 6 | 100% Discard coal | 0.0135 | 6 | 100% Biomass | 3.49 |

*DC: Discard coal, H: Hydrochar*

The results presented in Table 4.8 are arranged in descending order for each test. For the TGA spontaneous combustion test, 100% biomass was found to have the highest $TG_{spc}$ index at low heating rates. Whereas the same sample had the least spontaneous combustion susceptibility based on the Wits-Ehac index. The 100% hydrochar had the second highest $TG_{spc}$ index and the third highest Wits-Ehac index. 100% discard coal was predicted to have the least spontaneous combustion liability based on the TGA test and the second lowest based on the Wits-Ehac index. The two tests show no correlation for any sample. It is important to note that the results obtained for the TGA spontaneous combustion can be supported by the physicochemical properties of the samples, as discussed in section 4.2.1. However, the opposite may be said about the Wits-Ehac index results, as there is no direct relationship between the Wits-Ehac data, proximate and ultimate analysis results.

Since 100% biomass had the highest and lowest spontaneous combustion potential for the TGA and Wits-Ehac test, respectively, the sample was re-tested to verify the repeatability of the biomass sample using the Wits-Ehac test. The repeatability test for TGA spontaneous

combustion test was carried out using 100% discard coal and the results are presented in Appendix F1. The TGA results were reliable, reproducible and associated with the sample characterisation results. Figure 4.6 presents a Wits-Ehac DTA thermogram for a repeated 100% biomass test.

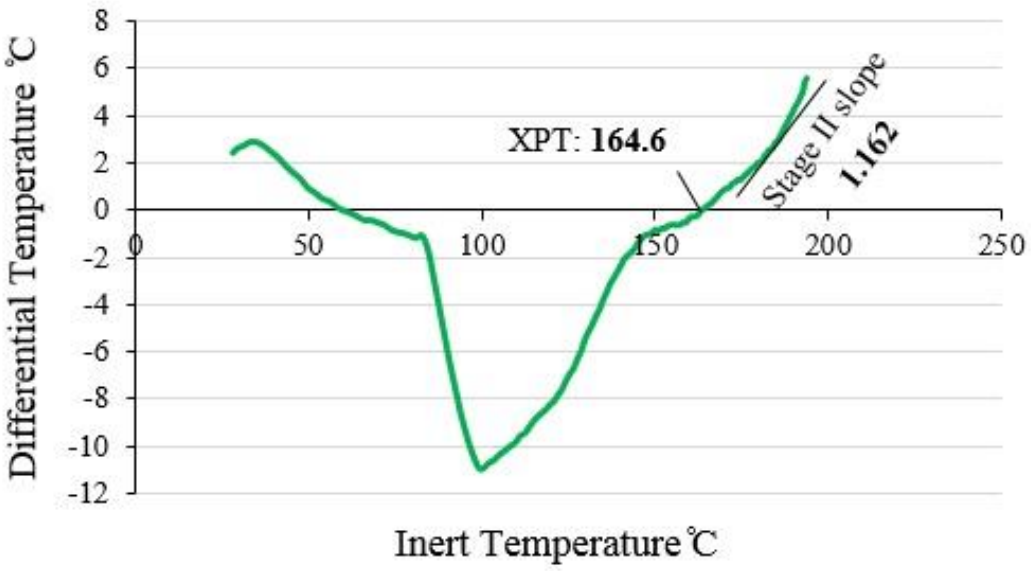



*Figure 4.6: Wits-Ehac differential thermal analysis thermogram for a repeated 100% biomass test with a Wits-Ehac index of 3.53*

The XPT for the first 100% biomass sample (Figure 4.5) was 167.5, and the repeat test was 164.6. The Wits-Ehac index for the first and the repeat tests were 3.49 and 3.53, respectively. This shows that the Wits-Ehac results are repeatable; however, the data obtained from the 100% biomass and hydrochar/coal blends are not supported by the sample's characterisation results or any data from previous studies. This method has been proven to be reliable and accurate for the analysis of coal samples Banerjee, 1985; Wade *et al.*, 1987; Gouws & Eroglu, 1993; Onifade, 2018; Onifade *et al.*, 2020), but this was not the case for biomass used in this study. The difference in the bulk density of the biomass (18 kg/$m^3$), hydrochar and hydrochar/coal blends to coal (700 kg/$m^3$) might be responsible for the discrepancy. In addition, since the sample holding cells of the Wits-Ehac apparatus are the same , less biomass sample (15 g) was used to fill the same cell, with coal at about 25 g. Given also that spontaneous combustion occurs due to a chemical reaction between the sample and oxygen, it could be that the samples are not exposed to similar airflow due to the difference in their bulk density and porosity. Given the mass difference of the samples, the spontaneous combustion results obtained from the Wits-

Ehac cannot be compared. It was thus decided to use TGA to predict the susceptibility to spontaneous combustion of samples treated with imidazolium-based ionic liquids.

### 4.3 Spontaneous Combustion Liability of Samples Treated with Imidazolium-based Ionic Liquids

The TGA spontaneous combustion results in Table 4.3 showed that 100% biomass is the only sample that is highly susceptible to undergoing spontaneous combustion, given that it had the highest $TG_{spc}$ index at low, medium and high heating rates. A decision was, therefore, made only to treat 100% biomass with imidazolium-based ionic liquids to inhibit its spontaneous combustion. The sample was treated with three ionic liquids (see section 3.5).

This section presents the TGA profiles of the 100% biomass samples treated with IL-A, showing the reactivity of each treated sample as time changes. The first peak denotes the release of moisture in the sample. The second and third peaks indicate the combustion of fixed carbon and degradation of the sample's lignin component. The samples heated at the heating rate of 24 ˚C/min had the highest reactivity and burnt out completely before the other samples (Figure 4.7). To determine the susceptibility of the samples to spontaneous combustion, the slope of the linear segment of the profiles at different heating rates was examined. Figures 4.7 to 4.11, presents the slopes of the 100% biomass sample treated with 10%, 20%, 30%, 40% and 50% IL-A. The calculated slopes for the biomass samples that were treated with the three imidazolium-based ionic liquids at different concentrations are presented in Table 4.9.

The points used to calculate the slopes of the derivative curves can be found in Table B1.1 of Appendix B. In addition, the TGA profiles of the 100% biomass samples treated with different concentrations of IL-B and IL-C can be found in Appendices C and D. The points used to calculate the slopes of the derivative curve for samples treated with both IL-B and IL-C are presented in Tables C2.1 (Appendix C) and D2.1 (Appendix D), respectively.

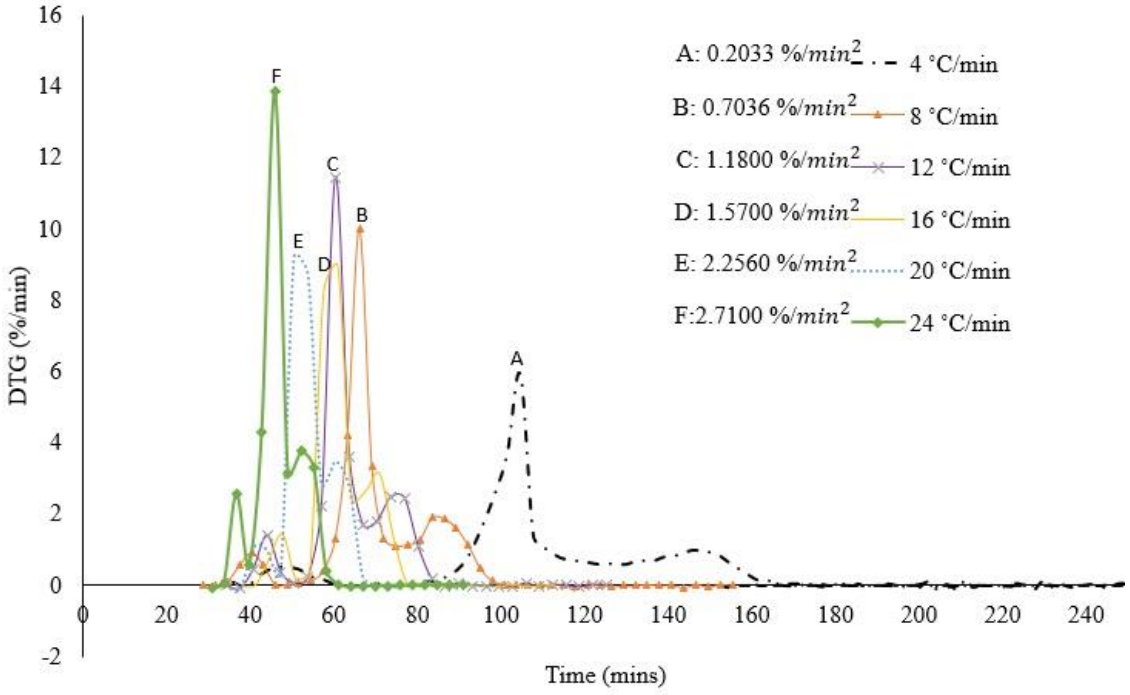



*Figure 4.7: The derivative profile of 100% biomass that was treated with 10% IL-A (DTG: differential thermogravimetric)*

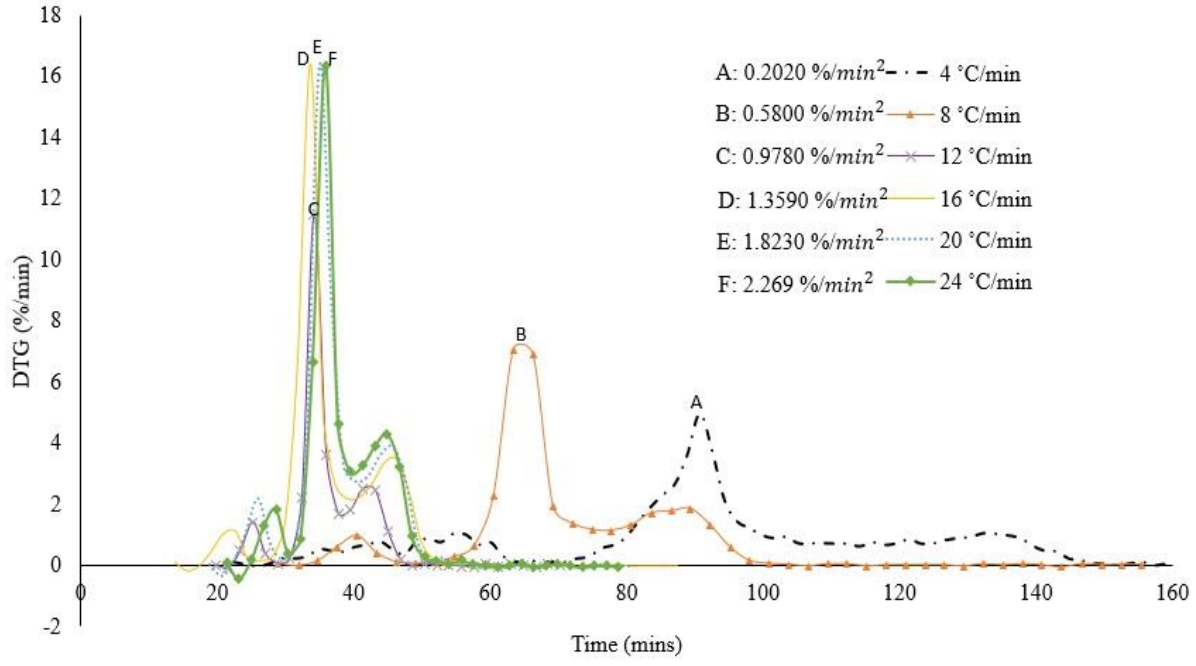



*Figure 4.8: The derivative profile of 100% biomass treated with 20% IL-A (DTG: differential thermogravimetric)*

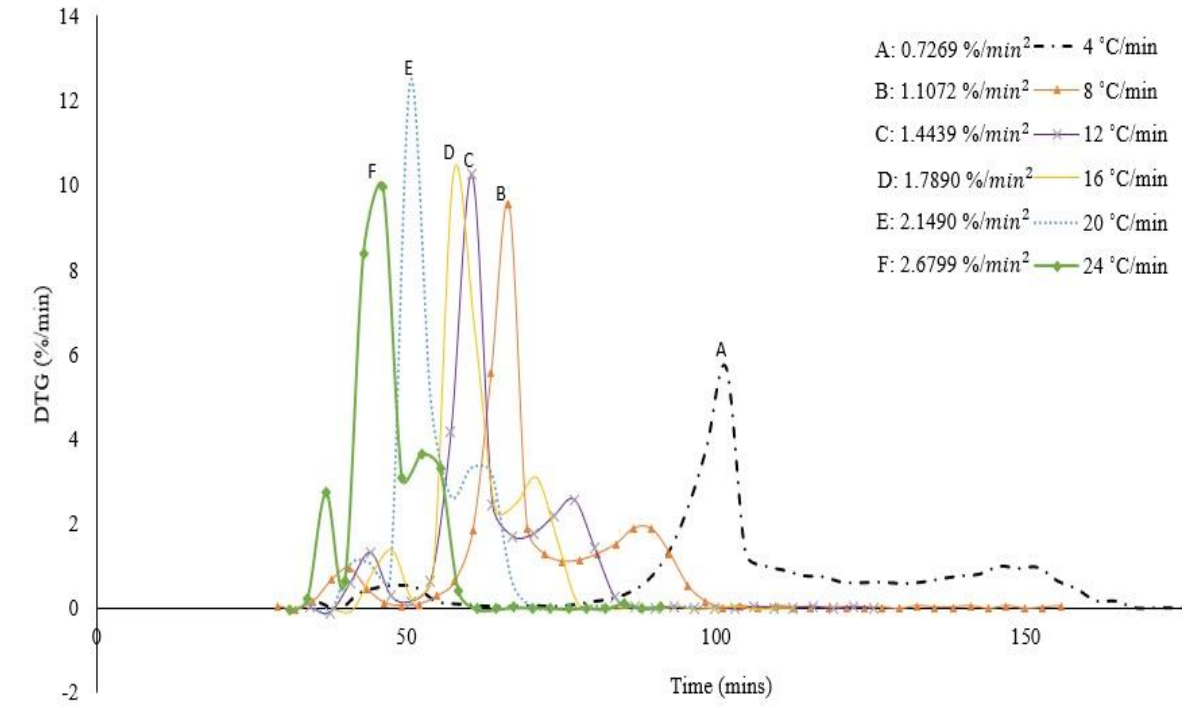



*Figure 4.9: The derivative profile of 100% biomass that was treated with 30% IL-A (DTG: differential thermogravimetric)*

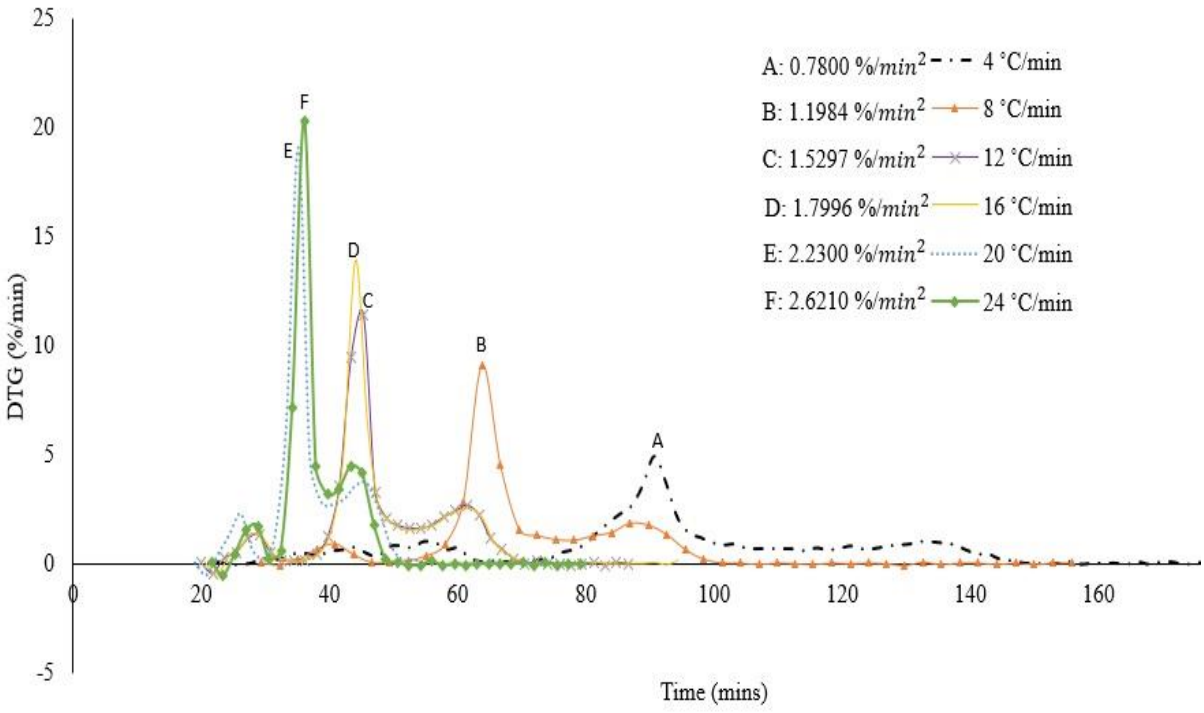



*Figure 4.10: The derivative profile of 100% biomass treated with 40% IL-A (DTG: differential thermogravimetric)*

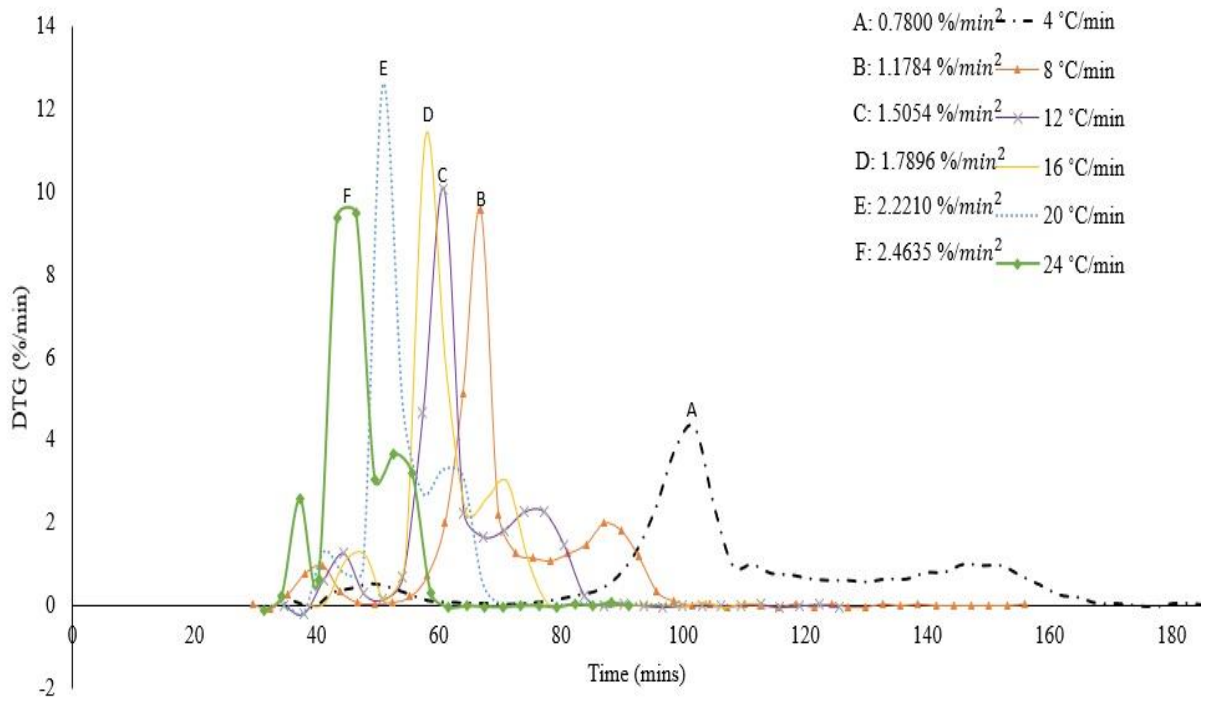



*Figure 4.11: The derivative profile of 100% biomass treated with 50% IL-A (DTG: differential thermogravimetric)*

*Table 4.9: Slopes obtained for every heating rate applied to the IL-treated 100% biomass samples.*

| Samples | Heating Rate applied (℃/$min$) | | | | | |
|---|---|---|---|---|---|---|
| | **4** | **8** | **12** | **16** | **20** | **24** |
| 10% IL-A-tb | 0.2033 | 0.7036 | 1.1800 | 1.5700 | 2.2560 | 2.7100 |
| 20% IL-A-tb | 0.2020 | 0.5800 | 0.9780 | 1.3590 | 1.8230 | 2.2690 |
| 30% IL-A-tb | 0.7269 | 1.1072 | 1.4439 | 1.7890 | 2.1490 | 2.6799 |
| 40% IL-A-tb | 0.7800 | 1.1984 | 1.5297 | 1.7996 | 2.2300 | 2.6210 |
| 50% IL-A-tb | 0.7800 | 1.1784 | 1.5054 | 1.7896 | 2.2210 | 2.4635 |
| | | | | | | |
| 10% IL-B-tb | 0.3803 | 0.7408 | 1.1061 | 1.4230 | 1.8190 | 2.3650 |
| 20% IL-B-tb | 0.4187 | 0.8071 | 1.1184 | 1.4710 | 1.8314 | 2.2924 |
| 30% IL-B-tb | 0.3753 | 0.6637 | 1.0007 | 1.2749 | 1.6789 | 2.0236 |
| 40% IL-B-tb | 0.5464 | 0.8214 | 1.1080 | 1.3946 | 1.7121 | 2.1409 |
| 50% IL-B-tb | 0.4352 | 0.6590 | 0.9250 | 1.1147 | 1.4062 | 1.6429 |
| | | | | | | |
| 10% IL-C-tb | 0.1971 | 0.4209 | 0.6995 | 0.8870 | 1.2020 | 1.4654 |
| 20% IL-C-tb | 0.2076 | 0.4214 | 0.5986 | 0.8660 | 1.0990 | 1.3560 |
| 30% IL-C-tb | 0.0709 | 0.2847 | 0.4619 | 0.6008 | 0.7997 | 0.9889 |
| 40% IL-C-tb | 0.0950 | 0.2260 | 0.3656 | 0.4931 | 0.6418 | 0.8002 |
| 50% IL-C-tb | 0.1412 | 0.2035 | 0.3000 | 0.3856 | 0.4880 | 0.5964 |

*IL-A: 1-butyl-3-methyl-imidazolium hydrogen sulphate [$Bmim^+HSO_4^-$], IL-B: 1-ethyl-3-methyl-imidazolium hydrogen sulphate [$Emim^+HSO_4^-$], IL-C: 1-Butyl-3-methyl-imidazolium acetate [$Bmim^+OAc^-$], tb: treated 100% biomass*

The results presented in Table 4.9 show that the slopes of the samples increase as the heating rate increases, horizontally in the table. This is expected because the higher the heating rates, the higher the reactivity (%/min) of the sample, which suggests an increase in combustion intensity. Also, as the heating rate increases, the linear segment used to calculate the slope on the DTG derivative profiles becomes steeper. The same trend was reported by Manic *et al.* (2021) and Onifade *et al.* (2020), although ionic liquids were not used in their studies. For IL-A treated 100% biomass samples, the calculated slope for each heating rate increases as the ionic liquid concentration increases from 10% to 50%. However, the increments to the slopes are relatively small and inconsistent, especially at high ionic liquid concentrations. The inconsistency in the combustion profiles for heating rates 12 - 24 ℃ /$min$ after increasing the

ionic concentration from 10% could be due to the influence of the ionic liquid. Hence, the DTG profile for the heating rate of 4 ℃ $/min$ has the lowest reactivity and the highest burn-out time at all concentrations.

Biomass samples treated with IL-A and IL-B exhibited greater gradients than biomass samples treated with IL-C (Table 4.9). This shows that even though the samples were treated with imidazolium-based ionic liquids, they are still highly reactive compared to those treated with IL-C. The $TG_{spc}$ index of the 100% biomass samples treated at different sets of heating rates are presented in Table 4.10. A comparative plot showing the relationship between the $TG_{spc}$ index and the imidazolium-based ionic liquids concentration at different sets of heating rates is presented in Figure 4.12. This shows the relationship between the $TG_{spc}$ indices.

*Table 4.10: The $TG_{spc}$ indices obtained at different sets of heating rates for 100% biomass treated samples.*

| | **4, 8, 12, 16 (˚C/min)** | | **4, 8, 12, 16, 20 (˚C/min)** | | **4, 8, 12, 16, 20, 24 (˚C/min)** | |
|---|---|---|---|---|---|---|
| **Samples** | $\mathbf{TG_{spc}}$ | $\boldsymbol{R^2}$ | $\mathbf{TG_{spc}}$ | $\boldsymbol{R^2}$ | $\mathbf{TG_{spc}}$ | $\boldsymbol{R^2}$ |
| 10% IL-A-tb | 0.1144 | 0.9965 | 0.1243 | 0.9924 | 0.1256 | 0.9956 |
| 20% IL-A-tb | 0.0967 | 0.9990 | 0.1005 | 0.9985 | 0.1032 | 0.9983 |
| 30% IL-A-tb | 0.0881 | 0.9993 | 0.0882 | 0.9996 | 0.0945 | 0.9938 |
| 40% IL-A-tb | 0.0848 | 0.9904 | 0.0875 | 0.9958 | 0.0845 | 0.9959 |
| 50% IL-A-tb | 0.0839 | 0.9942 | 0.0873 | 0.9958 | 0.0845 | 0.9959 |
| | | | | | | |
| 10% IL-B-tb | 0.0873 | 0.9990 | 0.0890 | 0.9992 | 0.0963 | 0.9921 |
| 20% IL-B-tb | 0.0867 | 0.9983 | 0.0872 | 0.9991 | 0.0914 | 0.9968 |
| 30% IL-B-tb | 0.0759 | 0.9985 | 0.0805 | 0.9961 | 0.0826 | 0.9970 |
| 40% IL-B-tb | 0.0708 | 0.9904 | 0.0726 | 0.9993 | 0.0781 | 0.9932 |
| 50% IL-B-tb | 0.0576 | 0.9963 | 0.0599 | 0.9968 | 0.0605 | 0.9981 |
| | | | | | | |
| 10% IL-C-tb | 0.0587 | 0.9950 | 0.0619 | 0.9951 | 0.6340 | 0.9966 |
| 20% IL-C-tb | 0.0538 | 0.9935 | 0.0557 | 0.9958 | 0.0574 | 0.9965 |
| 30% IL-C-tb | 0.0442 | 0.9911 | 0.0443 | 0.9955 | 0.0448 | 0.9974 |
| 40% IL-C-tb | 0.0333 | 0.9997 | 0.0340 | 0.9995 | 0.0350 | 0.9987 |
| 50% IL-C-tb | 0.0207 | 0.9931 | 0.0219 | 0.9942 | 0.0230 | 0.9941 |

*IL-A: 1-butyl-3-methyl-imidazolium hydrogen sulphate [$Bmim^+HSO_4^-$], IL-B: 1-ethyl-3-methyl-imidazolium hydrogen sulphate [$Emim^+HSO_4^-$], IL-C: 1-Butyl-3-methyl-imidazolium acetate [$Bmim^+OAc^-$], tb: treated 100% biomass*

According to Equation 3.2, the $TG_{spc}$ index is dependent on the heating rate applied. The $TG_{spc}$ index calculated at a lower set of heating rates is much lower than the one calculated at a higher set of heating rates. Given that spontaneous combustion takes place at lower heating rates in practical conditions, the indices obtained at a lower set of heating rates provided a clear view of how the sample would behave under practical conditions. However, higher heating rates were also considered during the experiments to obtain an optimum set of heating rates and to observe how the spontaneous combustion susceptibility of the treated samples responds to the increase in heating rate. Additionally, calculating the $TG_{spc}$ index at higher heating rates

helped in investigating the relationship between the heating rate and the reaction time. The deviation coefficients ($R^2$) for the tested samples at different sets of heating rates were close to one, showing a strong correlation between the calculated slopes of the linear segment of the TGA derivative profiles and the heating rates (Figure 4.12).

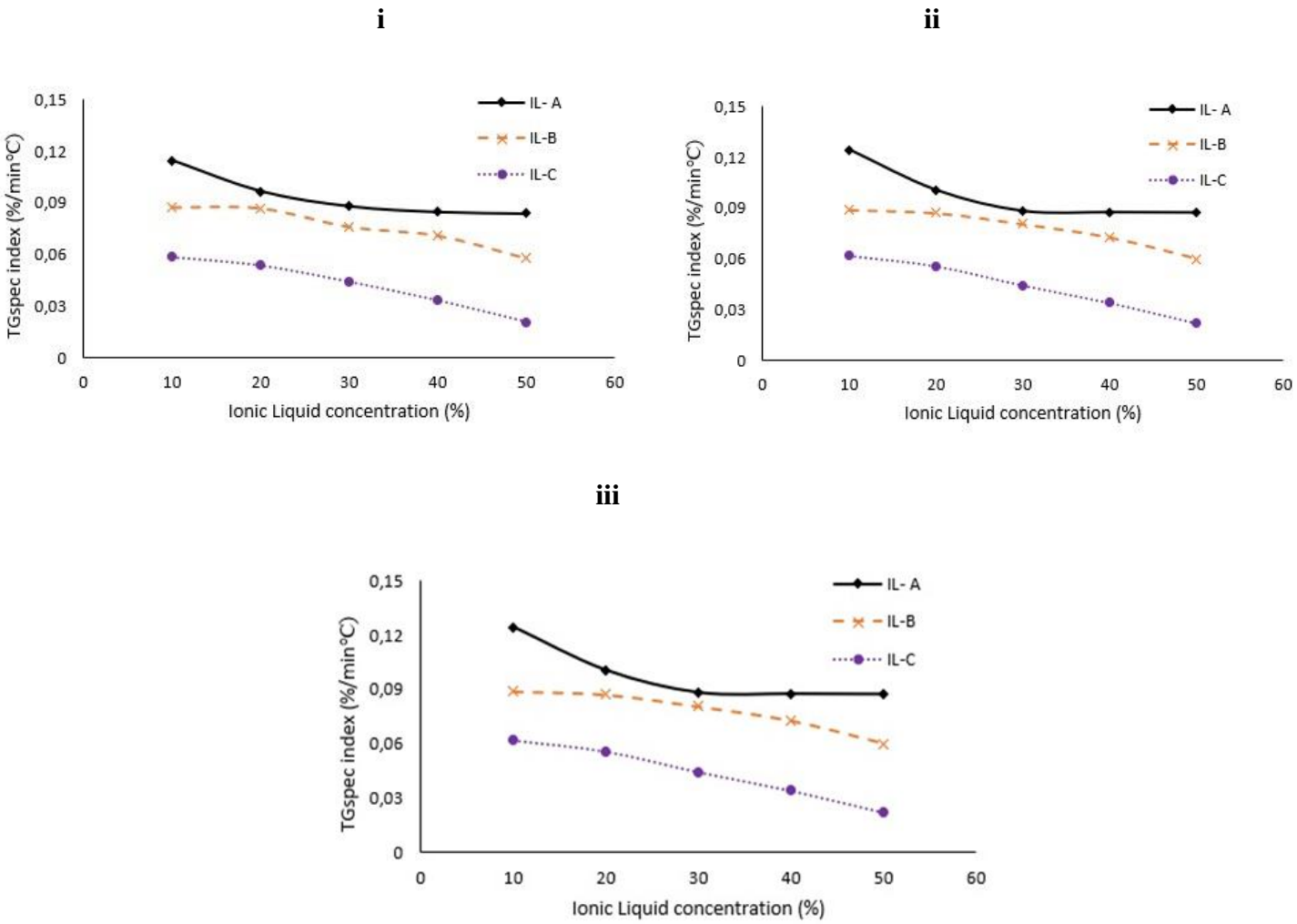



*Figure 4.12: Relationship between imidazolium-based ionic liquids concentration and $TG_{spc}$ index at (i) lower heating rates (4, 8, 12, 16 ℃/min), (ii) middle heating rates (4, 8, 12, 16, 20 ℃/min) and (iii) higher heating rates (4, 8, 12, 16, 20, 24 ℃/min)*

The comparative plot in Figure 4.12 shows that the $TG_{spc}$ index decreases as the concentration of the imidazolium-based ionic liquids increases. This shows that imidazolium-based ionic liquids can inhibit spontaneous combustion at high concentrations, particularly 50%. At lower heating rates, IL-C is the best inhibitor followed by IL-B and IL-A. The same trend is seen at middle and higher heating rates. Before treatment, 100% biomass had a $TG_{spc}$ index of 0.1457,

0.1503 and 0.1525 at the lower, middle, and higher heating rates, respectively. After the 100% biomass was treated with 50% IL-C, its $TG_{spc}$ index decreased to 0.0207, 0.0219 and 0.0230 at the lower, middle and higher heating rates respectively.

Table 4.5 provides the classification of spontaneous combustion susceptibility based on $TG_{spc}$ index. Based on Table 4.5, the treatment of the biomass sample with 50% IL-C inhibited its spontaneous combustion susceptibility by changing the combustion characteristic from highly reactive to low-reactive. For the samples treated with 50% IL-A and IL-B, the $TG_{spc}$ index decreased to a minimum of 0.0839 and 0.0576, respectively at lower heating rates. Based on Table 4.5, any sample with a $TG_{spc}$ index < 0.05 is classified as highly reactive. Therefore, the two ionic liquids are suitable for inhibiting the spontaneous combustion of 100% biomass although they were able to decrease its $TG_{spc}$ index from 0.1457, they are still not good enough.

### 4.4 Post-Treatment Characterisation

This section presents results on the physical and chemical structure of biomass, including surface morphology, textural properties and functional groups after treatment with three imidazolium-based ionic liquids. Characterisation of treated samples makes it possible to understand the mechanisms of inhibition of imidazolium-based ionic liquids on the 100% biomass utilised in this study.

#### 4.4.1 Proximate analysis, ultimate analysis and calorific value

*Table 4.11: Physicochemical analysis of 100% biomass and three biomass samples treated with IL-A, IL-B and IL-C.*

| Samples | Proximate Analysis (Ar) | | | | Ultimate Analysis (Db) | | CV |
|---|---|---|---|---|---|---|---|
| | %M | %A | %FC | %VM | %S | %TC | MJ/kg |
| 100% Biomass | 8.01 | 2.92 | 19.54 | 60.52 | 0.07 | 44.60 | 17.28 |
| 50% IL-A-tb | 7.89 | 0.24 | 15.76 | 76.11 | 0.06 | 43.10 | 18.96 |
| 50% IL-B-tb | 7.13 | 1.19 | 16.12 | 75.56 | 0.05 | 44.20 | 17.60 |
| 50% IL- C-tb | 7.02 | 1.64 | 14.40 | 74.47 | 0.02 | 42.80 | 20.55 |

*M: Inherent moisture, A: Ash content, FC: Fixed carbon, VM: Volatile matter, S: Sulphur, TC: Total carbon, H: Hydrogen, N: Nitrogen, O: Oxygen, CV: Calorific value, DC: Discard coal, H: Hydrochar, Ar: Air dried, Db: Dry basis, IL-A: 1-butyl-3-methyl-imidazolium hydrogen sulphate [$Bmim^+HSO_4^-$], IL-B: 1-ethyl-3-methyl-imidazolium hydrogen sulphate [$Emim^+HSO_4^-$], IL-C: 1-Butyl-3-methyl-imidazolium acetate [$Bmim^+OAc^-$], tb: treated 100% biomass*

The moisture content of 100% biomass decreased after treatment with imidazolium-based ionic liquids. With biomass treated with 50% IL-C had the lowest moisture content. This supports the trends seen in Figure 4.12, which shows that the sample treated with 50% IL-C is the least susceptible to spontaneous combustion, given that it has the least moisture. The ash content of 100% biomass decreased after it was treated with the three imidazolium-based ionic liquids. The 100% biomass treated with 50% IL-A had the least ash content, while the biomass treated with 50% IL-C had relatively higher ash content compared to the other treated samples. Given that high ash content results in low spontaneous combustion (Manic *et al*. 2021), it is expected that the 100% biomass treated with 50% IL-C will be less susceptible to spontaneous combustion than the 100% biomass samples treated with 50% IL-A and 50% IL-B. High fixed carbon and volatile matter content support the occurrence of spontaneous combustion (Onifade & Genc, 2019). As presented in Table 4.11 fixed carbon and volatile matter of 100% biomass decreased when it is treated with imidazolium-based ionic liquids. The biomass samples that were treated with 50% IL-C had the lowest fixed carbon and volatile matter compared to the samples treated with 50% IL-A and 50% IL-B.

The ultimate analysis results show that the total sulphur and the carbon content of 100% biomass decreased when it was treated with the three imidazolium-based ionic liquids. The 100% biomass treated with 50% IL-A had the highest total sulphur content, possibly explaining why it had the highest $TG_{spc}$ index compared to the other treated samples because high sulphur content is known to promote spontaneous combustion. The 100% biomass treated with 50% IL-C had the lowest total sulphur content amongst the three treated samples and thus the lowest $TG_{spc}$ index (Table 4.10). High total carbon content accelerates spontaneous combustion (Onifade, 2018; Manic *et al*., 2021), hence 100% biomass treated with 50% IL-C had the lowest carbon content because it is less susceptible to spontaneous combustion. Generally, ionic liquids have a positive impact on the calorific value, hence the calorific value of 100% biomass increased post-treatment for all imidazolium-based ionic liquids. The 100% biomass treated with 50% IL-C had the highest calorific value. Overall, the characterisation results support the spontaneous combustion results shown in Figure 4.12.

### 4.4.2 Fourier transform infrared spectroscopy of treated samples

For the structural characterisation, FTIR analysis was performed on the following samples: untreated 100% biomass, 50% IL-A treated 100% biomass, 50% IL-B treated 100% biomass and 50% IL-C treated 100% biomass. The FTIR spectra of the samples are presented in Figure 4.13. The characteristic peaks of 100% biomass were at 1604 $cm^{-1}$ and 1030 $cm^{-1}$, and they

were assigned to the carbonyl group and the silicate, present in the fingerprint region due to organic minerals (see section 4.1.2). The carbonyl group (C=O) promotes the spontaneous combustion of 100% biomass, given that the decomposition of the carbonyl group leads to low-temperature oxidation of the sample (Moroeng, 2015). In contrast, the silicates inhibit spontaneous combustion, given that they are associated with ash content, which has been reported to negatively impact the spontaneous combustion liability of a sample (Onifade, 2018). The hydroxyl stretch (-OH) was present at 3351 $cm^{-1}$ for 100% biomass, 50% IL-A treated 100% biomass, 50% IL-B treated 100% biomass and 50% IL-C treated 100% biomass. However, the -OH stretch is more prominent in the 50% IL-A treated 100% biomass than in any other sample, and this could be because of the reaction between 100% biomass and 50% IL-A.

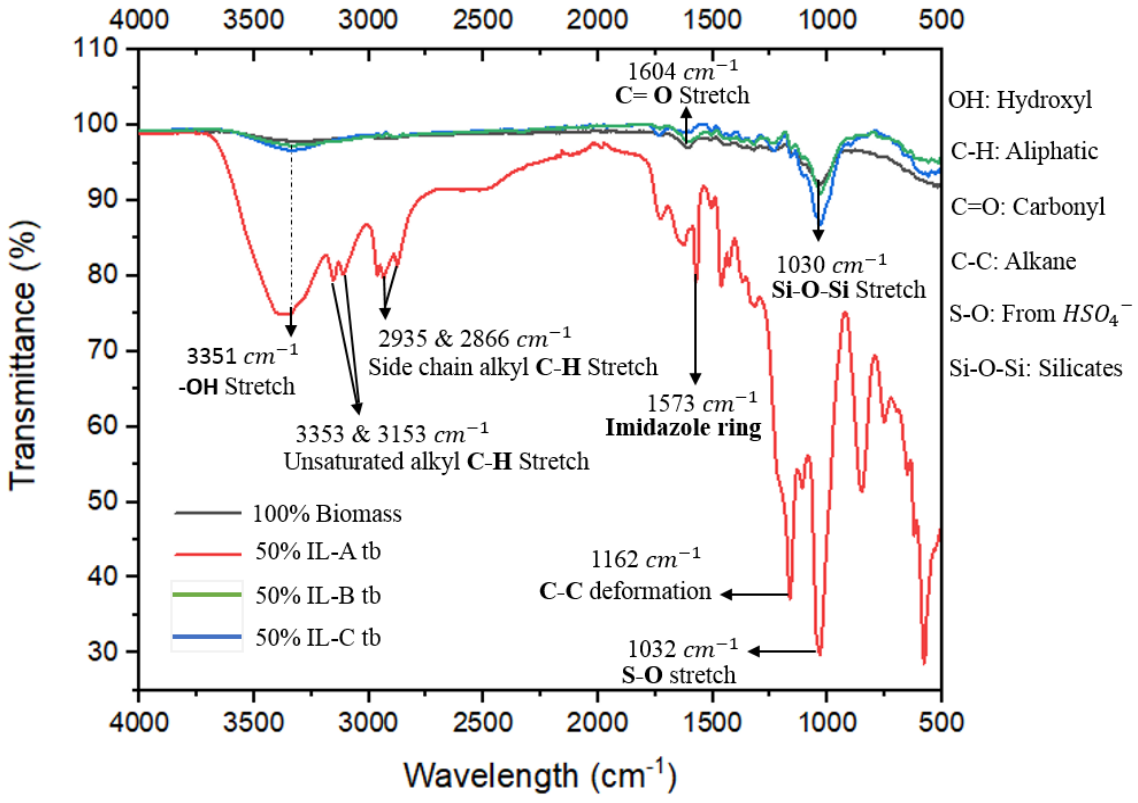



*Figure 4.13: Fourier Transform Infrared spectra of treated and untreated 100% biomass (tb: treated 100% biomass)*

Therefore, it is expected for the 100% biomass sample treated with 50% IL-A to be more susceptible to spontaneous combustion, given that the -OH stretch is known to be the most active group to promote the occurrence of spontaneous combustion. It reacts spontaneously

with the absorbed oxygen, and it was reported to be the main product of chemisorption (Zhang *et al*., 2021).

### 4.4.3 Fourier transform infrared spectroscopy of imidazolium-based ionic liquids (used and unused)

To check if the structural properties of the three imidazolium-based ionic liquids changed during their reaction with 100% biomass, FTIR analysis was used to investigate the functional groups present in the three ionic liquids before and after they were used to treat 100% biomass. The FTIR spectra of IL-A, IL-B and IL-C can be seen in Figures 4.14, 4.15 and 4.16, respectively. The characteristic functional groups of pure IL-A were the unsaturated alkyl C-H stretching vibration at 3102 $cm^{-1}$, the side chain alkyl C-H absorption peak at 2960 $cm^{-1}$, the imidazole ring skeleton vibration at 1571 $cm^{-1}$ and C-C deformation vibration at 1158 $cm^{-1}$ (Xu *et al*., 2019). The used 50% IL-A has a dominant -OH stretching vibration at 3368 $cm^{-1}$ and this is expected given that water was introduced to the ionic liquid to dilute it to 50%, given that ionic liquids are highly viscous. The spectra of 50% IL-A after treatment does not have the unsaturated alkyl C-H stretching vibration and the side chain alkyl C-H absorption peak (Figure 4.14). This shows that these two functional groups were transferred to the 100% biomass sample during treatment (see Figure 4.13).

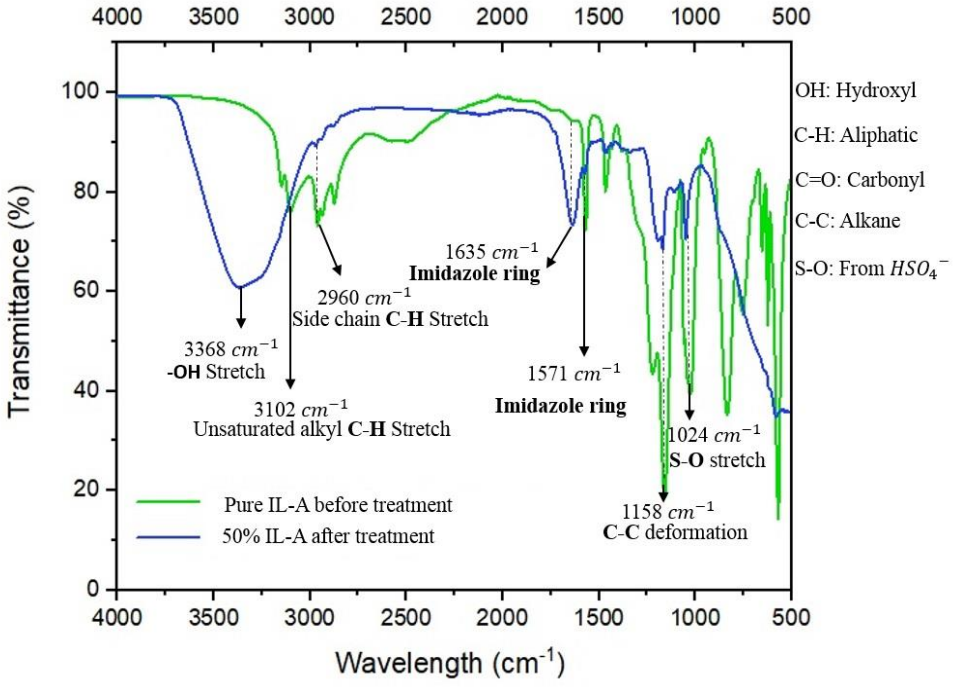



*Figure 4.14: Fourier Transform Infrared spectra of IL-A before and after it was used to treat 100% biomass*

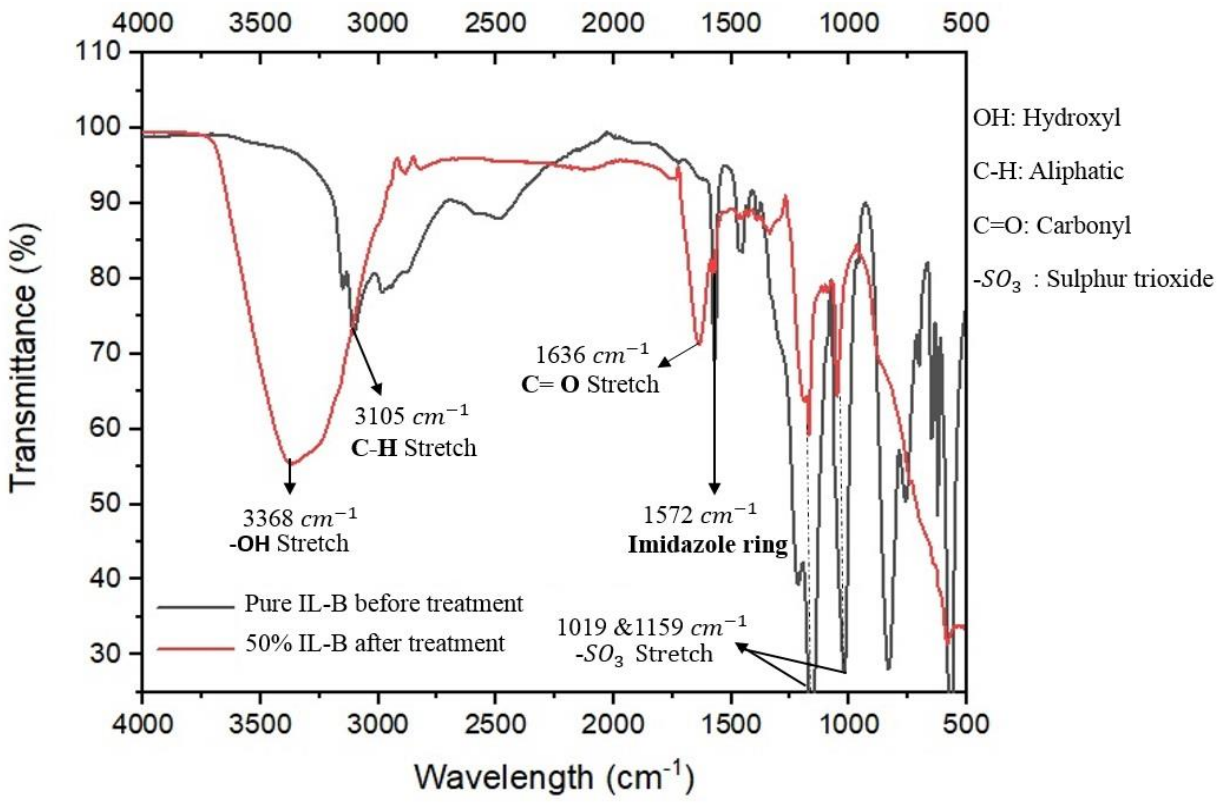



*Figure 4.15: Fourier Transform Infrared spectra of IL-B before and after it was used to treat 100% biomass*

As seen in Figure 4.15, the characteristic functional groups of pure IL-B were observed at 3105 $cm^{-1}$, 1572 $cm^{-1}$ and 1019 & 1159 $cm^{-1}$. They were attributed to the C-H stretching vibrations, the skeletal peak of the imidazole ring, and the symmetric and the asymmetric $-SO_3$ stretching vibrations, respectively (Tripathi *et al.*, 2015; Jaganathan *et al.*, 2016). The 50% IL-B after treatment had a prominent -OH stretch at 3368 $cm^{-1}$ introduced by the addition of water to dilute the ionic liquid. The used ionic liquid also had the C=O stretching vibration at 1636 $cm^{-1}$, which could have been introduced from the biomass during treatment.

Figure 4.16 shows that treating biomass with 50% IL-C changes the structural properties of the ionic liquid post-treatment. The major characteristics peaks of pure IL-C at 2960 $cm^{-1}$, 2874 $cm^{-1}$, 1573 $cm^{-1}$, 1378 $cm^{-1}$ and 1174 $cm^{-1}$ were assigned to the alkyl C-H stretch, side chain C-H stretch, the imidazole ring peak, C=C bond stretch and the C-O bond stretch (Wendler *et al.*, 2012; Mohamedali *et al.*, 2018). The fingerprint region of the used IL-C has reduced peaks, explaining why the FTIR spectra of the 50% IL-C treated 100% biomass in Figure 4.13 has a more prominent silicate peak at 1030 $cm^{-1}$ than 100% biomass and other treated biomass samples.

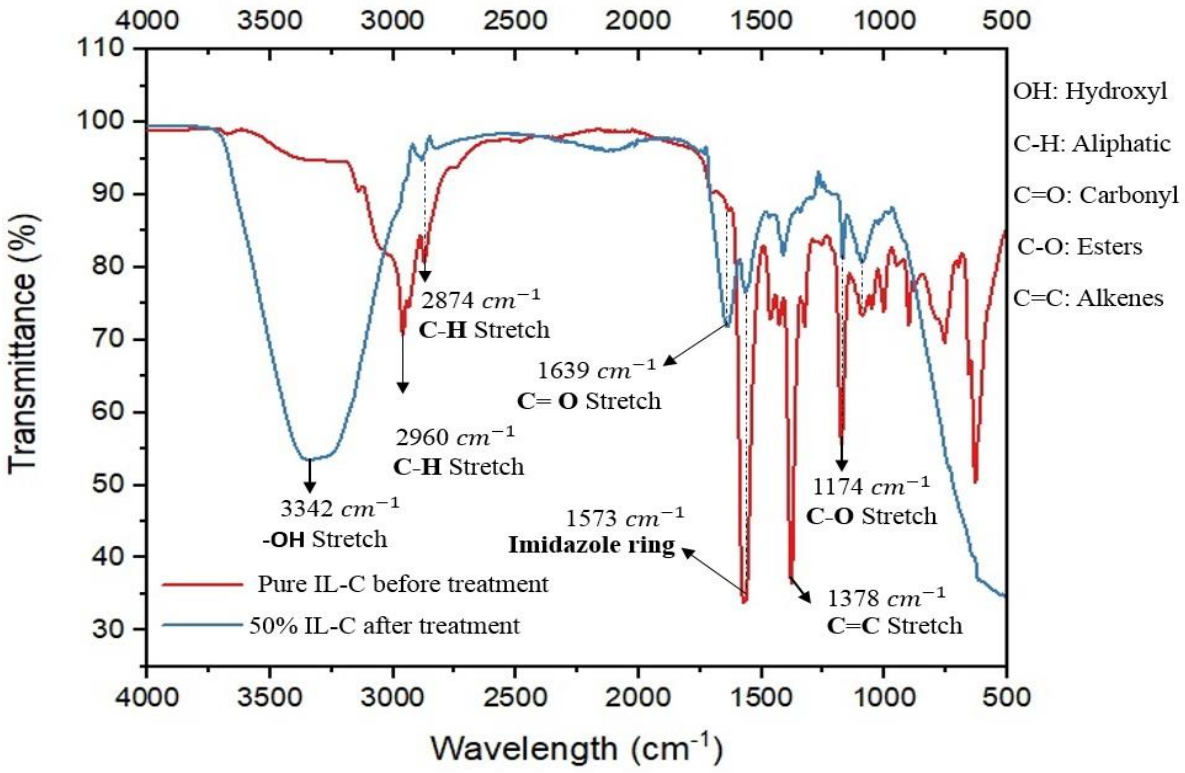



*Figure 4.16: Fourier Transform Infrared spectra of IL-C before and after it was used to treat 100% biomass*

### 4.4.4 Surface morphology and pore structure of 100% biomass untreated and treated samples

To study the micro-morphology of 100% biomass, 50% IL-A treated 100% biomass, 50% IL-B treated 100% biomass and 50% IL-C treated 100% biomass, scanning electron microscopy was used in high vacuum mode. The samples were sprayed with gold before analysis to enhance their conductivity. The BET (Brunauer-Emmett-Telle) was used to analyse the specific surface area, pore and pore diameter distribution of the same samples to identify any change in the surface area and pore following the treatment of the samples with the three imidazolium-based ionic liquids. The Density Functional Theory model was used to generate the pore diameter distribution of the untreated and treated 100% biomass samples for comparison. The surface morphology of the four samples is presented in Figure 4.17.

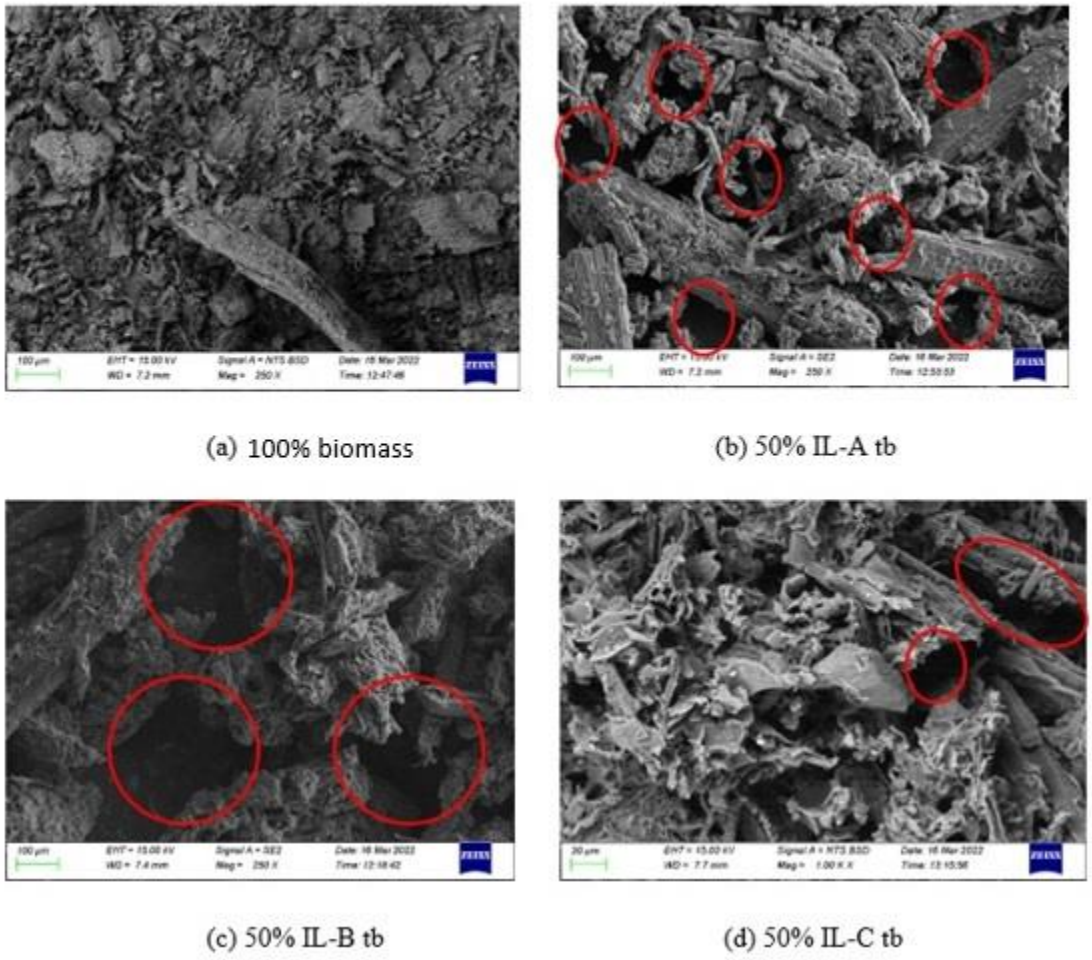



*Figure 4.17: Microscopic appearance of biomass samples (tb: treated 100% biomass)*

It can be observed from Figure 4.17 that 100% biomass had a relatively smooth and continuous surface structure with fewer cracks and pores compared to the 100% biomass samples that were treated with imidazolium-based ionic liquids. The large pores and cracks on the surfaces of the treated samples made their surfaces appear relatively rougher. The 100% biomass treated with IL-C appeared to have fewer pores and cracks compared to the 100% biomass samples treated with IL-A and IL-B. The changes in pore structure impact the oxidation process leading to spontaneous combustion (Yuan *et al*., 2016; Shi *et al*., 2018; Xi *et al*., 2020). To quantify the extent that the pores were formed on the surfaces of the treated 100% biomass samples, the nitrogen adsorption method was used on BET to test the pore structure characteristics of the samples.

*Table 4.12: Pore structure parameters of 100% biomass treated and untreated samples*

| Sample | SSA ($m^2/g$) | APD (nm) | TPV (cc/g) |
|---|---|---|---|
| 100% Biomass | 2.616 | 1.266 | 3.516 x$10^{-3}$ |
| 50% IL-A-tb | 1.208 | 1.195 | 1.609 x$10^{-3}$ |
| 50% IL-B-tb | 1.188 | 1.073 | 1.599 x$10^{-3}$ |
| 50% IL-C-tb | 1.137 | 0.961 | 1.529 x$10^{-3}$ |

*SSA: specific surface area, APD: average pore diameter, TPV: total pore , tb: treated 100% biomass, IL-A: 1-butyl-3-methyl-imidazolium hydrogen sulphate [$Bmim^+HSO_4^-$], IL-B: 1-ethyl-3-methyl-imidazolium hydrogen sulphate [$Emim^+HSO_4^-$], IL-C: 1-Butyl-3-methyl-imidazolium acetate [$Bmim^+OAc^-$]*

Treatment with imidazolium-based ionic liquids reduced the specific surface area of 100% biomass from 2.616 $m^2/g$ to 1.188 $m^2/g$, 1.137 $m^2/g$ and 1.208$m^2/g$ when treated with IL-A, IL-B and IL-C, respectively. The same trend was observed for the total pore of 100% biomass, which decreased in IL-A, IL-B, and IL-C treated samples (Table 4.12).

The changes in the pore of the samples are due to functional group degradation and the ionic liquid filling the sample's pores (see section 4.4.2). The IL-C treated 100% biomass sample had the smallest average pore diameter. This could be caused by the sample's micropores and mesopores being blocked by the ionic liquid due to the debris filling and viscosity of the ionic liquids (Liu *et al*., 2015). The pore diameter distribution of the sample's micropores generated from the Density Functional Theory model is presented in Figure 4.18. The 100% biomass appears to occupy more than the rest of the samples. The pores of the 50% IL-C treated 100% biomass sample occupy less compared to other treated samples for most of the pore diameter sizes. The 50% IL-C treated 100% biomass sample had smaller pores and reduced specific surface area. This is expected to limit the amount of oxygen absorbed by the sample during low-temperature oxidation and before spontaneous combustion. Based on these results, it can be concluded that IL-C is more efficient in inhibiting the spontaneous combustion characteristic of 100% biomass, followed by IL-B then IL-A. The BET and scanning electron microscopy results are in line with spontaneous combustion results reported for the TGA tests.

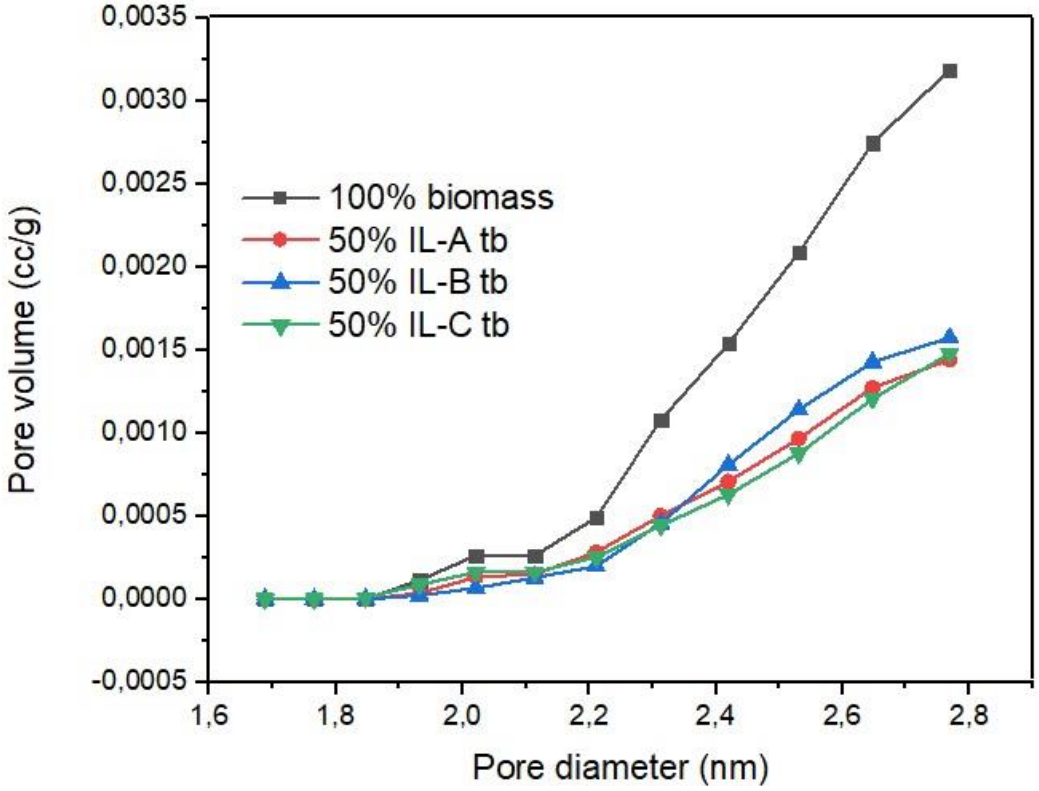



*Figure 4.18: Pore diameter distribution of treated and untreated 100% biomass samples, generated by the Density Functional Theory model (tb; treated 100% biomass)*

**4.5 Summary**

The results presented in this chapter show that 100% biomass had a higher susceptibility to spontaneous combustion than 100% discard coal, 100% hydrochar, 25% hydrochar + 75% discard coal, 50% hydrochar + 50% discard coal and 75% hydrochar + 25% discard coal. The results further proved that imidazolium-based ionic liquids impact on the spontaneous combustion characteristic of 100% biomass, with IL-C (1-Butyl-3-methyl-imidazolium acetate [$Bmim^{+}OAc^{-}$]) showing the best inhibitory effect amongst the three ionic liquids that were investigated in this study.

## CHAPTER 5: CONCLUSION AND RECOMMENDATIONS

This chapter summarises the major findings and the objectives achieved in this study. The limitations encountered in this research and the proposed recommendations for future work are also discussed.

### 5.1 Conclusion

This research aimed to determine whether the Wits-Ehac and TGA are suitable techniques for predicting the spontaneous combustion potential of coal, biomass and hydrochar/coal blends. In addition, the effect of imidazolium-base ionic liquids on the spontaneous combustion characteristic of the fuels used was also investigated. The aim and objectives of this research, identified in Chapter one, were met, and a summary of the main findings and conclusions of this research is as follows:

I. The conversion of 100% biomass into hydrochar by hydrothermal carbonisation improves the energy quality of the fuel. The hydrochar had reduced ash and volatile matter content, as well as higher fixed carbon and calorific values compared to the 100% biomass.

II. The physicochemical analysis conducted on 100% discard coal, 100% biomass, 100% hydrochar and their blends revealed that 100% biomass and 100% discard coal have the lowest energy quality. Blending 100% hydrochar with 100% coal discard at different ratios provides better quality blends. The 75% hydrochar + 25% discard coal is of the best quality, with a fixed carbon, volatile matter, moisture content and calorific value of 48.56%, 39.51%, 2.04% and 26.97 MJ/kg, respectively.

III. Wits-Ehac indices indicated that there was no direct link between the results of the Wits-Ehac spontaneous combustion test and those of the physicochemical properties of the six samples. However, the Wits-Ehac technique proved to be reproducible for all samples tested, even though it is not a reliable test for 100% biomass, 100% hydrochar, and the hydrochar/coal blends due to the difference in their bulk density from that of coal.

IV. TGA revealed that 100% biomass was highly susceptible to spontaneous combustion compared to other fuels with a $TG_{spc}$ index of 0.1457%/°C.min at lower heating rates. The results further revealed that 100% discard coal had the lowest spontaneous combustion susceptibility with a $TG_{spc}$ index of 0.0135%/°C.min at lower heating rates. The physicochemical properties of these samples correlate the findings from the TGA.

V. The 100% biomass had high inherent moisture (8.01%), high volatile matter (60.52%), low fixed carbon (19.54%) and a low calorific value (17.28%). The combination of these high physicochemical properties resulted in higher spontaneous combustion in 100% biomass compared to 100% discard coal with lower physicochemical properties.

VI. The results of the FTIR study showed that functional groups (C=O) and low silicate (mineral) transmission were responsible for the high susceptibility of 100% biomass to spontaneous combustion. Whereas the presence of a pronounced silicate peak in coal for 100% discard coal may be the reason why it is least susceptible to spontaneous combustion.

VII. Following the treatment of 100% biomass samples with the three ionic liquids, the TGA results showed that imidazolium-based ionic liquids do affect the spontaneous combustion susceptibility of 100% biomass. At lower heating rates, the $TG_{spc}$ index decreased from 0.1457%/˚C.min to 0.0839%/˚C.min for 50% IL-A, 0.0576%/˚C.min for 50% IL-B and 0.0207%/˚C.min for 50% IL-C. Given that 50% IL-C has the lowest $TG_{spc}$, it was concluded that IL-C is the preferred inhibitory liquid for the spontaneous combustion susceptibility of 100% biomass.

VIII. The ash content, fixed carbon, total sulphur and total carbon content of the 100% biomass treated with 50% IL-A, 50% IL-B or 50% IL-C were slightly reduced. However, the volatile matter content and the calorific value of the samples were significantly increased. The FTIR analysis of the treated 100% biomass samples showed that some of the functional groups in the biomass samples were enhanced (-OH stretch in 100% biomass treated with 50% IL-A and silicates in 100% biomass treated with 50% IL-C) during treatment. The susceptibility to spontaneous combustion of the 100% biomass samples treated with 50% IL-C was significantly reduced due to the presence of the silicate stretch.

IX. The surface morphology and the pore structure results reveal that the cracks and pores on the surface of the samples were reduced, especially for the sample treated with IL-C, during treatment of the 100% biomass samples with imidazolium-based ionic liquids. This allowed for minimal interaction between the oxygen and the sample, reducing the sample's susceptibility to spontaneous combustion.

### 5.2 Recommendations

This section presents recommendations for future work considering the findings and limitations of this research.

I. Further research should investigate how the spontaneous combustion characteristic is affected when treating 100% biomass samples with imidazolium-based ionic liquids at elevated temperatures.

II. The impact of different imidazolium-based ionic liquid concentrations on the susceptibility of 100% biomass to spontaneous combustion should also be examined.

III. A cost-benefit analysis of the application of this study on a large scale should be carried out to determine whether it is necessary to explore other types of imidazolium-based ionic liquids for spontaneous combustion inhibition of 100% biomass.

IV. The influence of particle size (100% biomass) on spontaneous combustion should be investigated to determine the correct particle size for safe transportation and storage.

**References**

Abbott, A., Feisch, G., Hartley, J. & Ryder, K., 2011. Dissolution of pyrite and other Fe-S-As minerals using deep eutectic solvents. *Green Chemistry,* 19(9), pp. 471-481.

Abdulsalam, J., Onifade, M., Mulopo, J. & Bada, S., 2020. Self-heating characteristics of materials for producing activated carbon. *International Journal of Coal Preparation and utilization,* 42(5), pp. 1-17.

Akgun, F. & Arisoy, A., 1994. Effect of particle size on the spontaneous heating of a coal stockpile. *Combustion and Flame,* 99(1), pp. 137-146.

Arisoy, A. & Beamish, B., 2015. Reaction kinetics of coal oxidation at low temperatures. *Fuel,* 159, pp. 412-417.

Ashman, J. M. & Williams, A., 2018. Some characteristics of the self-heating of the large storage of biomass. *Fuel Processing Technology,* 174, pp. 1-8.

Avila, C., 2010. *Study of spontaneous combustion of coals by means of Thermogravimetric analysis.* 1 ed. Berlin: Proceeding of the Second International Conference on Coal Fire Research.

Avila, C., 2012. *Predicting self-oxidation of coals and coal/biomass blends using thermal and optical methods,* United Kingdom: University of Nottingham.

Avila, C., Pang, C., Wu, T. & Lester, E., 2011. Morphology and reactivity characteristics of chars biomass particles. *Bioresource Technology,* 102(8), pp. 5237-5243.

Avila, C., Wu, T. & Lester, E., 2014. Estimating the spontaneous combustion potential of coals using Thermogravimetric analysis. *fuel,* 28(3) pp. 1765-1773.

Bada, S. O., Falcon, R. M. S., Falcon, L. M. & Makhula, M. J., 2015. Thermogravimetric investigation of macadamia nut shell, coal, and anthracite in different combustion atmosphere. *The Journal of the Southern African Institute of Mining and Metallurgy,* 115(8), pp. 741-746.

Bagchi, S., 1965. An investigation on some factors affecting the determination of crossing point of coals. *Coal Journal of Mines, Metals and Fuels,* 13(8), pp. 243-247.

Bagchi, Anujit (2010) *Assessment of Spontaneous Heating Susceptibility of Some Indian Coals using Experimental Techniques.* BTech thesis.

Banerjee, S. C., 1985. *Spontaneous combustion of coal and Mine fires.* s.l.:A. A. Balkema.

Banerjee, S. C., 2000. *Prevention and Combating Mine Fires*, Oxford: Oxford and IBH Publishing Co. Pty. Ltd.

Barve, S. D. & Mahadevan, V., 1994. Prediction of spontaneous heating liability of Indian coals based on proximate constituents. *In Proceedings 12th International Coal Preparation Congress, Cracow*, pp. 557-562.

Beamish, B. & Arisoy, A., 2008. Effect of mineral matter on coal self-heating rate. *Fuel*, 87, pp. 125-130.

Beamish, B. B. & Beamish, R., 2012. Testing and sampling requirements for input to spontaneous combustion risk assessment. Proceedings of the Australian Mine Ventilation Conference, pp. 15-21.

Beamish, B. B., Barakat, M. A. & George, J. D. S., 2000. Adiabatic testing procedures for determining the self-heating propensity of coal sample ageing effects. *Thermochimica Acta*, 362(1-2), pp. 79-87.

Beamish, B. B., Barakat, M. A. & George, J. D. S., 2001. The spontaneous-combustion propensity of New Zealand coals under adiabatic conditions. *International Journal of Coal Geology*, 45(2-3), pp. 217-224.

Beamish, B. B. & Blazak, M. A., 2005. Relationship between ash content and R70 self-heating rate of Callide coal. *International Journal of Coal Geology*, 64(1-2), pp. 7-16.

Beamish, B. B. & Hamilton, G. R., 2005. Effect of moisture content on the R70 self-heating rate of callide coal. *International Journal of Coal Geology*, 64(1-2), pp. 133-138.

Beamish, B., McLellan, P., Trunc, U. & Raab, M., 2012. Quantifying the spontaneous combustion inhibition of reactive coals. In: C. &. Nelson, ed. *Paper presented at the 14th United States/ North American Mine Ventilation Symposium.* U.S: University of Utah, pp. 145-180.

Benavente, V., Calabuig, E. & Fullana, A., 2014. *Upgrading of moist agro-industrial wastes by hydrothermal carbonization*, Press: Journal of Analytical Applied Pyrolysis.

Bergius, F., 1931. Chemical reactions under high pressure. *Nobel Foundation (Lecture Notes)*, pp. 1-33.

Bhattacharyya, K., 1971. The role of sorption of water vapour in the spontaneous heating of coal. *Fuel*, 50(4), pp. 367-380.

Bobleter, O., 1994. Hydrothermal degradation of polymers derived from plants. *Progress in Polymer Science*, 19(5), pp. 797-841.

Bo-tao, Q., Lei-lin, Z., De-ming, W. & Qin, X., 2009. The characteristic of explosion undermine gas and spontaneous combustion coupling. *Progress in Earth and Planetary Science*, 1, pp. 186-192.

Bowes, P. C., 1984. *Self-heating: evaluating and controlling the hazards. vi +500 pp.* Amsterdam: Elsevier Science Publishers.

British Standard Institute, 1995a. *Methods for analysis and testing of coal and coke. Proximate analysis of coal.* 2nd ed. London: British Standard Institute.

British Standard Institute, 1995b. *Petrographic analysis of bituminous coal and anthracite-Part 5: Method of determining microscopically the reflectance of vitrinite.* 3rd ed. London: British Standard Institute.

Buggeln, R. & Rynk, R., 2002. Self-heating in yard trimmings: Conditions leading to spontaneous combustion. *Compost Science & Utilization*, 10(2), pp. 168-182.

Cao, X. G., 2013. *Research on the prevention of coal spontaneous combustion by inhibition foam.* s.l.:Xian: Xian University of Science and Technology.

Carlson, T., Tompsett, G., Conner, W. & Huber, G., 2009. Aromatic Production from catalytic fast pyrolysis of biomass-derived feedstocks. Topics in Catalysis, 52(3), pp. 241-252.

Carpenter, D. & Giddings, D., 1964. The initial stages of oxidation of coal with molecular oxygen I - effect of time temperature + coal rank on rate of oxygen consumption. *Fuel*, 43, pp. 247-266.

Carpenter, D. & Sergeant, C., 1966. The initial stages of the oxidation of coal with molecular oxygen III- effect of particle size on rate of oxygen consumption. *Fuel*, 45, pp. 31-387.

Carras, J. N., Day, S. J., Saghafi, A. & Williams, D. J., 2009. Greenhouse gas emissions from low-temperature oxidation and spontaneous combustion at open-cut coal mines in Australia. *International Journal of Coal Geology*, pp. 161-16872.

Ceballos, D. C., Hawbolbt, K. & Helleur, R., 2015. Effect of production conditions on self-heating propensity of torrified sawmill residue. *Fuel,* 160, pp. 227-252.

Chansa, O., Luo, Z. & Yu, C., 2020. Study of the kinetic behaviour of biomass and coal during oxyfuel co-combustion. *Chinese Journal of Chemical Engineering,* 28(7), pp. 1796-1804.

Chen, G., Lu, J., X, L. & Li, B., 2015. Test and study on spontaneous ignition temperature of a Philippine coal. *Material Research Innovation,* 19(5), pp. 875-877.

Chen, P., Huang, F. & Fu, Y., 2016. Performance of water-based foams affected by chemical inhibitors to retard spontaneous combustion of coal. *Internation Journal of Mining Sciences and Technology,* 26(3), pp. 443-448.

Chen, X., 1994. The effect of drying heat and moisture condensation on the spontaneous combustibility of coal. *International Journal of Coal Preparation and Utilization,* 14, pp. 223-236.

Chen, X., 1999. On basket heating methods for obtaining exothermic reactivity of solid materials: The extent and impact of the departure of crossing-point temperature from the oven temperature. *Transactions of the Institution of Chemical Engineers*, 77, pp. 187-192.

Chen, Y., Duan, J., Lin, P. & Luo, Y. H., 2008. Effects of oxygen concentration on combustion characteristics of typical biomass materials. *Proceedings of the Chinese Society of Electrical Engineering,* 28(2), pp. 43-48.

Chiappe, C. & Pieraccini, D., 2005. Ionic liquids: Solvent properties and organic reactivity. *Journal of Physical Organic Chemistry,* 18(4), pp. 275-297.

Choudhury, N., Boral, P., Mitra, T. & Adak, A. K., 2007. Assessment of nature and distribution of inertinite in Indian coals for burning characteristics. *International Journal of Coal Geology,* 72(2), pp. 141-152.

Cimadevilla, J. L. G., Alvarez, R. & Pis, J., 2005. Influence of coal forced oxidation on technological properties of cokes produced at laboratory scale. *Fuel Process Technology,* 87(1), pp. 1-10.

Cliff, D., Rowlands, D. & Sleeman, J., 1996. *In spontaneous combustion in Australian underground coal mines,* Australia: C. Bofinder ed. Brisbane: Safety in Mines Testing and Research Station.

Colaizzi, G. J., 2004. Prevention, control and/ or extinguishment of coal seam fires using cellular grout. *International Journal of Coal Geology,* 59(1), pp. 75-81.

Cui, F.-S., Laiwang, B., Shu, C.-M. & Jiang, J.-C., 2018. Inhibiting effect of imidazolium-based ionic liquids on the spontaneous combustion characteristics of lignite. *Fuel,* 217, pp. 508-514.

Cummings, J., Tremain, P. & Shah, K., 2017. Modification of lignite via low temperature ionic liquid treatment. *Fuel Processing Technology,* 155, pp. 51-58.

De korte, J., 2014. *Tests to determine the spontaneous combustion propensity of coal.* [Online] Available at: www.fossilfuel.co.za/conferences/2014/SponCombustion130214/Teststodeterm-inethespontaneouscombustionpropensityofcoal-Jdk.pdf [Accessed 1 April 2021]

Deng, J., Ma, X., Zhang, Y. & Li, Y., 2015a. Effects of pyrite on the spontaneous combustion of coal. *International Journal of Coal Science and Technology,* 2, pp. 306-311.

Deng, J., Xiao, Y., Li, Q. & Lu, J., 2015b. Experimental studies of spontaneous combustion and anaerobic cooling of coal. *Fuel,* 157, pp. 261-269.

Deng, J., Zhao, J. Y., Zhao, Y. N. & Geng, R. L., 2014. Study on coal spontaneous combustion characteristic temperature of growth rate analysis. *Procedia Engineering,* 84, pp. 789-805.

Deng, J., Zhao, J., Zhang, Y. & Huan, A., 2016. Thermal analysis of spontaneous combustion behaviour of partially oxidized coal. *Process Safety and Environment Protection,* 104, pp. 218-224.

Dong, X. L. & Drysdale, D. D., 1997. Proc. 5th Inter. Symp. *Fire Safety Science, IAFSS,* p. 571.

Dou, G., Wang, D., Zhong, X. & Qin, B., 2014. Effectiveness of catechin and poly(ethylene glycol) at inhibiting the spontaneous combustion of coal. *Fuel Processing Technology,* 120, pp. 123-127.

Dullien, F., 1979. *Porous media: fluid transport and pore structure,* Chicago: Academic Press.

Dupont, J. & Fonseca, G., 2002. Transition-Metal Manoparticle in imidazolium Ionic Liquids: Recyclable Catalyst for Biphasic Hydrogenation Reactions. *American Chemistry Society,* 124(16), pp. 4228-4229.

Du, W., Niu, K., Wang, H. & Zhang, Y., 2020. Experiment and field application of inhibitor liquid in spontaneous combustion process of coal based on thermogravimetric analysis. *Journal of Energy, Resource and Technology,* 143(2), pp. 1-10.

Earle, M. & Seddon, K., 2000. Ionic liquid: Green solvent of the future. *Pure and Applied Chemistry,* 72(7), pp. 1391-1398.

Ebadat, V., 2019. *Self-heating hazards of biomass materials.* [Online] Available at: http://www.biomassmagazine.com/articles/16231/self-heating-hazards-of-biomass-materials [Accessed 15 March 2021].

Ejlali, A., Aminossadati, S. M., Hooman, K. & Beamish, B. B., 2009. A new criterion to design reactive coal stockpile. *International Communications in Heat and Mass transfer,* 36(7), pp. 669-673.

Elder, J., 1983. Proximate analysis by automated thermogravimetry. *Thermochimica Act,* 62(5), pp. 580-584.

Ennis, T., 2016. Fire and explosion hazards in the biomass industries. In: *Symposium Series no 161: Hazards 26.* Winsford: IChemE, pp. 1-9.

Falcon, M. S. & Snyman, C. P., 1986. *An introduction to coal petrography: atlas of petrographic constituents in bituminous coals of Southern Africa.* Johannesburg: Geological Society of South Africa.

Falcon, R. M. S., 1986. A brief review of the origin, formation and distribution of coal in Southern Africa. *In: Anhaeusser CR, Maske S (eds) Mineral deposits of Southern Africa,* I and II, pp. 1879-1898.

Fierro, V., Miranda, J., Romero, C. & Andres, J., 1999. Prevention of spontaneous combustion in coal stockpiles: Experimental results in a coal storage yard. *Fuel Processing Technology,* 59(1), pp. 23-34.

Franco, A. & Diaz, A., 2009. The future challenges for "clean coal technologies": joining efficiency increase and pollution emission control. *Energy,* 34, pp. 348-354.

Frank-Kamenetskii, 1940. Conditions for the applicability of the Bodenstein method in chemical kinetics. *Zurnal Fizicheskoy,* 14, pp. 695-700.

Fu-bao, Z., De-ming, W., Yong-jiu, Z. & Yu-liang, Z., 2007. Practice of fighting fire and suppressing explosion for a super-large and highly gassy mine. Journal of China University of Mining and Technology, 17, pp. 459-463.

Garcia, P., Hall, P. & Mondragon, F., 1999. The use of differential scanning calorimetry to identify coals susceptible to spontaneous combustion. *Thermochimica Acta,* 336, pp. 41-46.

Garcia-Torrent, J., Fernandez-Anez, N., Medic-Pejic, L. & Montenegro-Mateos, L., 2015. Assessment of self-ignition risks of solid biofuels by thermal analysis. *Fuels,* 143, pp. 484-491.

Genc, B. & Cook, A., 2015. Spontaneous combustion risk in South African Coalfields. *Journal of the South African Institute of Mining and Metallurgy,* 115, pp. 563-568.

Genc, B., Onifade, M. & Cook, A., 2018. Spontaneous combustion risk on South African Coalfields: Part 2. *Zonguldak, Turkey, Proceedings of the 21st International Coal Congress of Turkey 'ICCET',* pp. 13-25.

Geng, W., Nakajima, T., Takanashi, H. & Ohki, A., 2009. Analysis of carboxyl group in coal and coal aromaticity by Fourier transform infrared (FT-IR) spectrometry. *Fuels,* 88, pp. 139-144.

Gong, B., Pigram, P. J. & Lamb, R. N., 1998. Surface studies of low-temperature oxidation of bituminous vitrain bands using XPS and SIMS. *Fuel,* 77, pp. 1081-1087.

Gouws, M. J., 1987. *Crossing pint characteristics and thermal analysis of South Africa coals,* South Africa: MSc Dissertation, University of Witwatersrand.

Gouws, M. J. & Eroglu, H. N., 1993. A spontaneous combustion liability index. *Instanbul, The 13th MIning Congress of Turkey,* pp. 59-68.

Gouws, M. J., Gibbon, G. J., Wade, L. & Phillips, H. R., 1991. An adiabatic apparatus to establish the spontaneous combustion propensity of coal. *Mining Science and Technology,* 13, pp. 417-422.

Gouws, M. & Wade, L., 1989. The self-heating liability of coal: Prediction based on simple indices. *Mining Science and Technology,* 9(1), pp. 75-80.

Govender, S., 2015. *A critical investigation into spontaneous combustion in coal storage bunkers.* MSc Level ed. Pretoria: University of Pretoria.

Gray, B., Griffiths, J. & Hasko, S., 1984. Spontaneous ignition hazards in stockpiles of cellulosic materials: criteria for safe storage. *Journal of Chemical Technology & Biotechnology*, 34, pp. 453-463.

Guney, M., 1968. Oxidation and spontaneous combustion of coal- Review of individual factors. *Colliery Guardian,* Issue 137-143, p. 216.

Guo, W., 2013. *Self-heating and spontaneous combustion of wood pellets during storage.* Vancouver: The University of British Columbia.

Gurdal, G., Hosgormez, H., Ozcan, D. & Li, X., 2015. The properties of can basin coals (Canakkale-Turkey): Spontaneous combustion by-products. *International Journal of Coal Geology,* 138, pp. 1-15.

Hao, C. Y., Wang, J. R., Ma, N. J. & Zhao, Q. B., 2014. Thermal equilibrium study on the effect of wetting on coal spontaneous combustion. *China Safety Science Journal,* 24, pp. 54-59.

Herman, R., Simmons, G., Cole, D. & Kuzmics, V., 1984. Catalytic action of minerals in the low-temperature oxidation of coal. *Fuel,* 63, pp. 673-678.

Hoekman, S. K., Broch, A., Robbins, C. & Zielinska, B., 2013. Hydrothermal carbonization (HTC) of selected woody and herbaceous biomass feedstocks. *Biomass Convers Biorefinery,* 3, pp. 113-126.

Huangfu, W., You, F., Shao, Y. & Wang, Z., 2018. Effects of oxygen concentration and heating rate on non-isothermal combustion properties of Jet coal in east China. *Procedia Engineering,* 211, pp. 262-270.

Hull, A., Lanthier, J. & Agarwal, P., 1997. The role of the diffusion of oxygen in the ignition of a coal stockpile in confined storage. *Fuel,* 76, pp. 975-983.

Humphreys, D., 1979. *A study of the propensity of Queensland coals to spontaneous combustion,* Brisbane: ME thesis (unpublished), University of Queensland, Australia.

ICCP, 2001. The inertinite classification (ICCP system 1994). *Fuel,* 80(4), pp. 459-471.

IEA, 2017. *Clean Coal Centre (CCC TCP).* [Online] Available at: https://iea.org/tcp/fossilfuels/ccc/ [Accessed 10 July 2020].

IEA, 2018a. *Renewables.* [Online] Available at: https://www.iea.org/reports/renewables-2018 [Accessed 29 July 2020].

IEA, 2018b. *World Energy Outlook.* [Online] Available at: https://www.iea.org/data-and-statistics/charts?type=pie&energy=electricity [Accessed 25 July 2020]

Iglesias, M., De la Puente, G., Fuente, E. & Pis, J., 1998. Compositional and structural changes during aerial oxidation of coal and their relations with technological properties. *Vibrational Spectroscopy*, 17, pp. 41-52.

Isaac, K., 2019. The co-combustion performance of South African coal and refuse derived fuels. In: *Masters Thesis.* Johannesburg: University of the Witwatersrand, p. 131.

Ivanova, A. V. & Zaitseva, L. B., 2006. Influence of oxidability of carboniferous coals from Dobrudja fredeep on vitrinite reflectance. *Lithology and Mineral Resources*, 41, pp. 435-439.

Jaganathan, J. R., Sivapragasam, M. & Wilfred, C. D., 2016. Thermal characteristics of 1-butyl-3-methylimidazolium based oxidant ionic liquids. *Journal of Chemical Engineering & Process Technology.*

Jain, A., 2009. *Assessment of spontaneous heating susceptibility of coal using differential thermal analysis.* Rourkela: National Institute of Technology.

Jiang, B. Y., Lin, B., Zhu, C. & Zhai, C., 2013. Premixed methane-air deflagration in a completely adiabatic pipe and effect of the condition of the pipe wall. *Journal of Loss Prevention in the Process Industries*, 26, pp. 782-791.

Jiang, S. C., Takehiro, I. & Take, K., 1991. Simulation experiment of coal seam spontaneous combustion and the effect of fire extinguishing by nitrogen gas. *Journal of Coal Science and Engineering*, 2, pp. 2-16.

Jiao, X. M., Wang, D. M. & Zhong, X. X., 2012. Experiment study on different retarders affected to the critical temperature of coal spontaneous combustion. *Journal of Coal Science and Engineering*, 2, pp. 88-91.

Jimenez, A., Iglesias, M., Laggoun-Defarge, F. & Suarez-Ruiz, I., 1999. Effect of the increase in temperature on the evolution of the physical and chemical structure of vitrinite. *Journal of Analytical and Applied Pyrolysis*, 50, pp. 117-148.

Jirjis, R., 2005. Effect of particle size and pile height on storage and fuel quality of comminuted Salix viminalis. *Biomass and Energy,* 25, pp. 193-201.

Jones, J., 1999. Calculation of the Frank-Kamenetskii critical parameter for cubic reactant shape from experimental results on bituminous coals. *Fuel,* 78, pp. 89-91.

Jones, J. M., Saddawi, B., Dooley, B. & Mitchell, E. J. S., 2015. Low-temperature ignition of biomass. *Fuel Processing Technology,* 134, pp. 372-377.

Jones, J. & Puignou, A., 1998. On the thermal ignition of wood waste. *Transactions of the Institution of Chemical Engineers,* 76, pp. 205-210.

Jones, J. & Vais, M., 1991. Factors influencing the spontaneous heating of low-rank coals. *Journal of Hazardous Materials,* 26, pp. 203-212.

Joubert, M. K., 2017. *Contaminant Fate in Searsia lancea Woodlands on Acid Mine Drainage in the Witwatersrand Basin Goldfields.* Johannesburg, South Africa: WIts University.

Junkovic, B., Manic, N., Stojiljkovic, D. & Jovanovic, V., 2020. The assessment of spontaneous ignition potential of coal using the TGA-DTG technique. *Combustion and Flame,* 211, pp. 32-43.

Kadioglu, Y. & Varamaz, M., 2003. The effect of moisture content and air-drying on spontaneous combustion characteristic of two Turkish lignites. *Fuel,* 83, pp. 1685-1693.

Kambo, H. & Dutta, A., 2015. A comparative review of biochar and hydrochar in terms of production, physico-chemical properties, and applications. *Renewable and Sustainable Energy Reviews,* 45, pp. 359-378.

Kayser, E. & Boyers, C., 1975. *Spontaneous combustible solids- A literature study.* Maryland: Naval surface weapons center.

Kelemen, S. R., George, G. N. & Gorbaty, M. L., 1990. Direct determination and quantification of sulphur forms in heavy petroleum and coals. *The X-ray photoelectron spectroscopy (XSP) approach,* 69, pp. 939-944.

Kidena, K., Murakami, M., Murata, S. & Nomura, M., 2003. Low-temperature oxidation of coal- Suggestion of evaluation method of active methylene sites. *Energy & Fuels,* 17, pp. 1043-1047.

Kim, A. G., 1993. Fires in Abandoned Coal Mines and Waste Banks Information Circular. In: A. G. K. A. R. F. Chaiken, ed. *United States Bureau of Mines; 9352.* Washington, DC: U. S Department of Interior, Bureau of Mines, p. 93.

Kim, A. G. & Chaiken, R. F., 1990. Relative self-heating tendencies of coal, carbonaceous shales and coal refuse, West Virginia: Paper presented at the 1990 Mining and Reclamation Conference and Exhibition.

Kizgut, S. & Yilmaz, S., 2004. Characterization and non-isothermal decomposition kinetics of some Turkish bituminous coals by thermal analysis. *Fuel Processing Technology,* 85, pp. 103-111.

Kok, M., 2008. Recent developments in the application of thermal analysis techniques in fossil fuels. *Journal Thermal and Analysis Calorimetry,* 91, pp. 763-773.

Krajciova, M., Jelemensky, L., Kisa, M. & Markos, J., 2004. Model prediction on self-heating and prevention of stockpiled coals. *Journal of Loss Prevention in the Process Industries,* 17, pp. 205-216.

Krause, U., 2009. *Fires in Silos: Hazard, Prevention and Fire-Fighting.* Berlin: Wiley-VCH.

Krzesinska, M., 2002. Coal structure studied by means of molecular acoustics methods. *Fuel Processing Technology,* 77, pp. 33-43.

Kubler, H., 1990. Self-heating of lignocellulosic materials. In: G. L. Nelson, ed. *Fire and polymers- hazards identification and prevention.* Washington: American Chemical Society, pp. 429-449.

Kuchta, J. M., Rowe, V. R. & Burgress, D. S., 1980. *Spontaneous combustion susceptibility of U.S coals,* Washington: U. S Bureau of Mines.

Kucuk, A., Kadioglu, Y. & Gulaboglu, M., 2003. A study of spontaneous combustion characteristics of a Turkish lignite: particle size, moisture, humidity of air. Combustion and Flame, 133, pp. 255-261

Kumar, R. & Anand, R., 2019. Production of biofuel from biomass downdraft gasification and its application. Advanced Biofuels, pp. 29-151.

Larsson, I., 2017. *Measurement of self-heating of biomass pellets using isothermal calorimetry.* Sweden: Karlstad University.

Lei, Z., Wu, L. & Hu, Z., 2016. Pyrolysis of lignite following low temperature ionic liquid pre-treatment. *Fuel,* 166, pp. 124-129.

Lei, Z., Wu, L., Zhang, Y. Q. & Shui, H. F., 2013. The dissolution of lignite in ionic liquid. *RSC Adv,* 3(7), pp. 2385-2389.

Li, A., Chen, C., Chen, J. & Lei, P., 2021. Experimental investigation of temperature distribution and spontaneous combustion tendency of coal gangue stockpiles in storage. *Environmental Science and Pollution Research,* pp. 1-12.

Liang, X. & Wang, D., 2003. Effects of moisture on spontaneous combustion of coal. *Journal of Liaoning Technical University,* 22, pp. 472-474.

Li, B., Li, M., Gao, W. & Bi, M., 2020a. Effects of particle size on the self-ignition behaviour of a coal dust layer on a hot plate. *Fuel,* 260, pp. 116269-116278.

Libra, J. A., Ro, K. S., Kammann, C. & Funke, A., 2011. Hydrothermal carbonization of biomass residuals: a comparative review of the chemistry, processes and applications of wet and wet pyrolysis. *Biofuels,* 2, pp. 71-106.

Li, J., Li, Z., Yang, Y. & Zhang, X., 2017. Inhibitive effects of antioxidants on coal spontaneous combustion. *Energy & Fuels,* 31, pp. 14180-14190.

Liu, J., Zhu, J., Cheng, J. & Zhou, J., 2015. Pore structure and fractal analysis of Ximeng lignite under microwave irradiation. *Fuel,* pp. 41-50.

Li, X., 2004. *Green solvent synthesis and application of ionic liquids,* Beijing: Chemical Industry Engineering Press.

Li, X., Jin, Z. & Bai, G., 2020b. Experimental study on the effect of acidity on coal spontaneous combustion at different oxygen concentrations. *Energy Sources, Part A; Recovery, Utilization, and Environmental effects,* pp. 1-10.

Li, Z., 1996. Free radical reaction mechanism of coal spontaneous combustion. *Journal of China University of Mining & Technology,* 25(3), pp. 111-114.

Li, Z., Kong, B., Wei, A. & Yang, Y., 2016. Free radical reaction characteristics of coal low-temperature oxidation and its inhibition method. *Environmental Science and Pollution Research,* 23(23), pp. 23593-23605.

Lopez, D., Sanada, Y. & Mondragon, F., 1998. Effect of low-temperature oxidation of coal on hydrogen-transfer capability. *Fuel*, 77, pp. 1623-1628.

Luangwilai, T. & Nelson, M. I., 2018. One-dimensional spatial model for self-heating in compost piles: Investigating effects of moisture and airflow. *Food and Bioproducts Processing*, 108, pp. 18-26.

Luo, S. Y., Xiao, B., Hu, S. M. & Liu, Y. W., 2009. Experimental study on oxygen-enriched combustion of biomass micro fuel. *Energy*, 34, pp. 1880-1884.

Lu, W. & Hu, W., 2007. Relation between the change rules of coal structures when being oxidised and the spontaneous combustion process of coal. *Journal of the China Coal Society,* 32(9), pp. 939-944.

Lu, Y. & Qin, B., 2015a. Experimental investigation of closed porosity of inorganic solidified foam designed to prevent coal fires. *Advances in Materials Science and Engineering.*

Lu, Y. & Qin, B., 2015b. Material properties of inorganic solidified foam for mining rock fracture filling. *Materials Express*, 5, pp. 291-299.

Ma, D., Qin, B. T., Song, S. & Liang, H. J., 2017. An experimental study on the effects of air humidity on the spontaneous combustion characteristic of coal. *Journal of Combustion Science and Technology*, 189, pp. 2209-2219.

Mahajan, O. & Walker, P., 1971. Water adsorption on coals. *Fuel*, 50, pp. 308-317.

Ma, L., Wang, D., Wang, Y. & Xin, H., 2016. Experimental investigation on a sustained release type of inhibitor for retarding the spontaneous combustion of coal. *Energy Fuels,* 30(11), pp. 8904-8914.

Mandal, S., Mohalik, N., Ray, S. & Khan, A., 2022. A comparative kinetic study between TGA & DSC techniques using model-free and model-based analyses to assess the spontaneous combustion propensity of Indian coals. *Process Safety and Environmental Protection,* pp. 1113-1126.

Manic, N., Jankovic, B., Stojiljkovic, D. & Radojevic, M., 2021. Self-ignition potential assessment for different biomass feedstock based on the dynamic thermal analysis. *Cleaner Engineering and Technology*, 2, p. 100040.

Mardon, S. M. & Hower, J. C., 2004. Impact of coal properties on coal combustion, by-product quality, example from a Kentucky power plant. *International Journal of Coal Geology*, 59, pp. 153-169.

Marinov, V., 1977. Self-ignition and mechanism, of the interaction of coal with oxygen at low temperatures. 2 Changes in weight and thermal effects on gradual heating of coal in the air. *Fuel,* 56, pp. 158-164.

Marzec, A., 2002. Towards an understanding of coal structure: A review. *Fuel Processing Technology,* 25, pp. 25-32.

Mastalerz, M., Solano- Acosta, W., Schimmelmann, A. & Drobniak, A., 2009. Effects of coal storage in the air on physical and chemical properties of and on gas adsorption. *Internation Journal of Coal Geology,* 79, pp. 167-174.

Mathews, J., Hatcher, P. & Scaroni, A., 1997. Particle size dependence of coal volatile matter: is there a non-maceral-related effect? *Fuel,* 76, pp. 359-362.

Mazumber, S., 2019. Hydrothermal upgrading of coal waste with food waste. In: M. Reza Toufiq, ed. *Master of Science Thesis.* Ohio: Russ College of Engineering and Technology, p. 14.

Medek, J. & Weishauptova, Z., 1999. Effect of coal interaction with oxygen on its ignition temperature. *Energy & Fuels,* 13, pp. 77-81.

Melikoglu, M., 2018. Clean coal technologies: A global to local review for Turkey. *Energy Strategy Reviews,* 22, pp. 313-319.

Meijer, R. & Gast, C. H., 2004. Spontaneous combustion of biomass: Experimental study into guidelines to avoid and control this phenomena. *Proceedings of the 2nd World Conference on Biomass for Energy, Industry and Climate Protection,* 2, pp. 1231-1233.

Miao, Y., Amari, M. & Yoshizaki, S., 1994. Mechanism of spontaneous combustion heating of hay. Part 2- chemical changes in spontaneously heated hay. *Transaction of the American Society of Agricultural Engineering,* 37, pp. 1567-1570.

Michalski, S. R., 2004. The Jharia mine fire control technical assistance project: an analysis. International Journal of Coal Geology, 59, pp. 83-90.

Misra, B. & Singh, B., 1994. Susceptibility to spontaneous combustion of Indian coal and lignite: an organic petrographic autopsy. *Internation Journal of Coal Geology,* 25, pp. 265-286.

Miura, K., 2016. Adsorption of water vapor from the ambient atmosphere onto coal fines leading to spontaneous heating of coal stockpile. *Energy & Fuels,* 30, pp. 219-229.

Miyawaki, N., Fukushima, T. & Mizuno, T., 2021. Effect of wood biomass components on self-heating. *Bioresources and Bioprocessing,* 8(21), pp. 1-6.

Moereng, O. M., Mhuka, V., Nindi, M. M. & Roberts, R. M., 2019. Comparative study of a vitrinite-rich and an inertite-rich Witbank coal (South Africa) using pyrolysis-gas chromatography. *International Journal of Coal Science and Technology*, 6(4), pp. 621-632.

Mohalik, N. K., Lester, E. & Lowndes, 2016. Review of experimental methods to determine spontaneous combustion susceptibility of coal- Indian context. *International Journal of Mining, Reclamation and Environment,* 1, pp. 1-32.

Mohalik, N. K., Lester, E. & Lowndes, I. S., 2017. Development of a petrographic technique to assess the spontaneous combustion susceptibility of Indian coals. *International Journal of Coal Preparation and Utilization,* 40(3), pp. 186-209.

Mohalik, N. K., Singh, V. K., Pandey, J. & Singh, R. V., 2006. Proper sampling of mine gases, analysis and interpretation- a pre-requisite for assessment of sealed off fire area. *Journal of Mines, Metals and Fuels,* 54, pp. 210-27.

Mohalik, N. K., Singh, V. K. & Tripathy, D. D., 2009. Critical appraisal to assess extent of fire in old abandoned coal mine areas, Indian context. In: *Wollongong, 9th underground coal operators conference.* Australia: the University of Wollongong, pp. 271-288.

Mohamedali, M., Ibrahim, H. & Henni, A., 2018. Incorporation of acetate-based ionic liquids into a zeolitic imidazolate framework (ZiF-8) as efficient sorbents for carbon dioxide capture. *Chemical Engineering Journal,* pp. 817-828.

Moroeng, O., 2015. *Spontaneous combustion of coal- A South Africa perspective,* Pretoria: University of Pretoria.

Moxon, N. T. & Richardson, S. B., 1985. Development of a calorimeter to measure the self-heating characteristics of coal. *International Journal of Coal Preparation and Utilization,* pp. 79-90.

Mullerova, J., 2014. Heath and safety hazards of biomass storage. *Section Renewable Energy Sources and Clean Technologies,* 5000, pp. 5-10.

Mumme, J., Eckervogt, L., Pielert, J. & Rupp, F., 2011. Hydrothermal carbonization of anaerobically digested maize silage. *Bioresource Technology,* 102, pp. 9255-9260.

Nandy, D. K., Banerjee, D. D. & Chakravorty, R. N., 1972. Application of crossing point temperature for determining the spontaneous heating characteristics of coal. *Journal of Mines, Metals, Fuels,* 20(2), pp. 41-48.

Nelson, M. I. & Chen, X. D., 2007. Survey of experimental work on the self-heating and spontaneous combustion of coal. *Reviews in Engineering Geology,* 62(5), pp. 619-621.

Nishimoto, T., Morita, M. & Yajima, H., 1986. Spontaneous combustion of coal (III). Isothermal Method. *Fire Science and Technology,* 6, pp. 1-6.

Nubling, R. & Wanner, H., 1915. Spontaneous combustion of coal. *Journal of Gasbeleuchl,* 58, p. 515.

Nugroho, Y., McIntosh, A. & Gibbs, B., 2000. On the prediction of thermal runaway of coal piles of differing dimensions by using a correlation between heat release and activation energy. *Symposium on Combustion,* 28, pp. 2321-2327.

Oboirien, B. O., North, B. C., Obayopo, S. O. & Odusote, J. K., 2018. Analysis of clean coal technology in Nigeria for energy generation. *Energy Strategy. Rev,* 20, pp. 64-70.

O'Keefe, Bechtel, A., Chistanis, K. & Dai, S., 2013. On the fundamental difference between coal rank and coal type. *International Journal of Coal Geology,* 118, pp. 58-87.

Olivella, M. A., Palacious, J. M., Vairavamurthy, A. & Rio, J. C., 2002. A study of sulfur functionalities in fossil fuels using destructive- (ASTM and Py-GC-MS) and non-destructive (SEM-EDX, XANES and XPS) techniques. *Fuel,* 81(4), pp. 405-411.

Onifade, M., 2018. Spontaneous combustion liability of coal and coal-shales in the South African coalfields. In: *Ph.D. Thesis.* Johannesburg, South Africa: University of the Witwatersrand.

Onifade, M. & Genc, B., 2019. Spontaneous combustion liability of coal and coal-shale: A review of prediction methods. *International Journal of Coal Science and Technology,* pp. 1-18.

Onifade, M., Genc, B. & Bada, S., 2020. Spontaneous combustion liability between coal seams: A thermogravimetric study. *International Journal of Mining Science and Technology,* 30(5), pp. 691-698.

Pang, S., 2016. Fuel flexible gas production: biomass, coal and bio-solids waste. In: *Fuel Flexible Energy Generation: Solid, Liquid and gaseous fuels.* s.l.:Woodhead Publishing, pp. 241-266.

Parr, S. & Kressman, F., 1911. The spontaneous combustion of coal. *The Journal of Industrial and Engineering Chemistry,* 1, pp. 152-158.

Parr, S. & Wheeler, W., 1908. The deterioration of coal. *Journal of American Chemical Society,* 30, pp. 1087-1033.

Peng, C., Fujun, H. & Yue, F., 2016. Performance of water-based foams affected by chemical inhibitors to retard spontaneous combustion of coal. *Internation Journal of Mining Science and Technology,* 26(3), pp. 443-448.

Persson, H., 2013. *Silo Fires; Fire extinguishing and preventive and preparatory measures,* Sweden: Swedish Civil Contingencies Agency (MSB).

Pfecke, M. & Warrenville, R. A. O., 2010. *Explosion from smoldering silo fire,* USA: Pellet Fuel Institute.

Phillips, H., Uludag, S. & Chabedi, K., 2011. *Prevention and control of spontaneous combustion: Best practice guidelines for surface coal mines in South,* Johannesburg: Coaltech Research Association.

Pis, J. J., Puente, G. D., Fuente, E. & Moran, A., 1996. A study of the self-heating of fresh and oxidized coals by different thermal analysis. *Thermochimica Acta,* 279, pp. 93-101.

Pone, J. D. N., Hein, K. A. A., Stracher, G. B. & Annegarn, H. J., 2007. The spontaneous combustion of coal and its by-products in the Witbank and Sasolburg coalfields of South Africa. *International Journal of Coal Geology,* 72, pp. 124-140.

Qi, X., Wang, D., Zhong, X. & Gu, J., 2010. Characteristic of oxygen consumption of coal at programmed temperature. *Mining, Science and Technology,* 20, pp. 372-377.

Qi, X., Wei, C. & Li, Q., 2016. Controlled-release inhibitor for preventing the spontaneous combustion of coal. *National Hazards,* 82, pp. 891-901.

Qin, B., Wang, D., Chen, J. & Liang, X., 2005. Experimental investigation of high-performance three-foam for mine fire control. Journal of China University of Mining and Technology, 34, pp. 14-18.

Rath, D., 2012. *Application of inhibitors to prevent spontaneous heating of coal,* Odisha: National Institute of Technology Rourkela.

Raymond, C. J., 2015. Investigation of spontaneous combustion of coal fires utilizing differential scanning calorimetry and thermogravimetric analysis. *Master of Science in Chemical Science. Paper 2,* pp. 1-77.

Ren, T. X., Edwards, J. S. & Clarke, D., 1999. Adiabatic oxidation study on the propensity of pulverized coal to spontaneous combustion. *Fuel,* 78, pp. 1611-1620.

Ren, W. X. & Wang, D., 2012. A new method for reducing the prevalence of pneumoconiosis among coal miners: Foam technology for dust control. *Journal of Occupational and Environmental Hygiene,* 9(4), pp. D77-D83.

Ren, L., Li, Q. & Deng, J., 2021. Effect of oxygen concentration on the oxidative thermodynamics and spontaneous combustion of pulverized coal. ACS Omega, 6(40), pp. 26170-26179.

Restuccia, F., Masek, O. & Hadden, R. M., 2019. Quantifying self-heating ignition of biochar as a function of feedstock and pyrolysis reactor temperature. *Fuel,* 236, pp. 201-213.

Ribeiro, J., Suarez-Ruiz, I., Ward, C. R. & Flores, D., 2016. Petrography and mineralogy of self-burning coal wastes from anthracite mining in El-Bierzo coalfield (NW Spain). *International Journal of Coal Geology,* 154-155, pp. 92-106.

Rifella, A., Setyawan, D., Chun, D. H. & Yoo, J., 2019. The effects of coal particle size on spontaneous combustion. *International Journal of Coal Preparation and Utilization.*

Robert, D. L., 2008. *Chromium speciation in coal combustion by products: case study at a dry disposal power station in Mpumalanga, South Africa.* Johannesburg: Thesis for Doctor of Philosophy, University of the Witwatersrand.

Rosema, A., Guan, H. & Veld, H., 2001. Simulation of spontaneous combustion, to study the causes of the coal fire in the Rujigou Basin. *Fuel,* 80, pp. 7-16.

Rupar-Gadd, K., 2006. Biomass pre-treatment for the production of sustainable energy-Emission and Self-ignition. *Acta Wexionensia*, 88, pp. 1-71.

Saffari, A., Ataei, M. & Sereshki, F., 2019. Examination of the role of moisture content on the spontaneous combustion of coal (SCC). *The Mining-Geology-Petroleum Engineering Bulletin*, pp. 61-71.

Saffari, A., Sereshki, F. & Ataei, M., 2020. Effect of maceral content on the tendency of spontaneous coal combustion using the R70 method. *International Journal of Mining and Geo-Engineering*, pp. 93-99.

Sahu, B., Panigrahi, D. & Mishra, N., 2004. Assessment of spontaneous heating susceptibility of coals seams by differential scanning calorimetry. *Journal of Mines, Metals & Fuels*, 3, pp. 117-121.

Saleh, M. & Nugroho, Y. S., 20l3. Thermogravimetric Study of the Effect of Particle Size on the Spontaneous Combustion of Indonesian Low Rank Coal. *Applied Mechanics and Materials*, 330, pp. 101-105.

Schmal, D., 1989. Spontaneous heating of stored coal. In: C. R. Nelson, ed. *Chemistry of Coal Weathering.* Amsterdam: Elsevier, pp. 133-215.

Schwarzer, L., Jensen, P. A. & Glarborg, P., 2017. *Biomass ignition in mills and storages- it is explained by conventional thermal ignition theory.* Stockholm, Sweden: Paper presented at Nordic Flame Days.

Seddon, K., 2003. Ionic liquids: A taste of the future. *Nature Materials*, 20(2), pp. 295-300.

Serageldin, M. & Pan, W., 1984. Coal analysis using thermogravimetry. *Thermochimica Acta*, 76, pp. 145-160.

Setepu, R. L., Abdulsalam, J., Weiersbye, I. M. & Bada, S. O., 2021. Hydrothermal Carbonization of Searsia lancea Trees Grown on mine drainage: Processing variables and product composition. *ACS Omega*, 6(30), pp. 20292-20302.

Shah, K. P., 2022. *Spontaneous combustion of coal.* [Online] Available at: Ahttps://practicalmaintenance.net/wp-content/uploads/Spontaneous-Combustion-of-Coal.pdf

Shen, L. & Zheng, Q., 2021. Investigation of the kinetics of spontaneous combustion of the major coal seam in Dahuangshan mining area of the Southern Junggar, Xinjiang, China. *Scientific Reports*, 11, pp. 876-888.

Shi, Q., Qin, B., Bi, Q. & Qu, B., 2018. Effect of igneous intrusions on chemical structure and combustion characteristic of coal in Daxing Mine, China. *Fuel*, pp. 181-189.

Shi, X., Zhang, Y., Chen, X. & Zhang, Y., 2021. Effects of thermal boundary conditions on spontaneous combustion of coal under temperature-programmed conditions. *Fuel*, 295, pp. 120591-120603.

Schonardt, J. A., 1984. Calorimeter design and the assessment of self-heating in coal. Coal Journal, 1, pp. 79-85.

Shui-jun, Y., Feng-cheng, X., Bo-yu, J. & Peng-Fei, Z., 2012. Influenced study of organic and inorganic additive to coal combustion characteristic. Procedia Environmental Sciences, 12, pp. 459-467.

Sima-Ella, E., Yuan, G. & Mays, T., 2005. A simple kinetic analysis to determine the intrinsic reactivity of coal chars. *Fuel*, 84, pp. 1920-1925.

Singh, A., Singh, R. V. K., Singh, M. P. & Chandra, H., 2007. Mine fire gas indices and their application to Indian underground coal mine fires. *International Journal of Coal Geology*, 69(3), pp. 192-204.

Singh, R. & Demirbilek, S., 1987. Statistical appraisal of intrinsic factors affecting spontaneous combustion of coal. *Mining Science and Technology*, 4, pp. 155-165.

Singh, R. N., 1984. *A practical system of classifying coal seams liable to spontaneous combustion*, Australia: Lecture, Department of Civil and Mining Engineering, University of Wollongong.

Sinha, A. & Singh, V. K., 2005. Spontaneous coal seam fires: a global phenomenon. ERSEC Ecological Book Series 4. *International Conference on Spontaneous coal seam fires: Mitigating a global disaster at Beijing PR China*, 1, pp. 42-65.

Slabbert, A., 2017. *Experts warns SA on too much renewable energy.* [Online] Available at: https://www.techcentral.co.za/expert-warns-on-too-much-renewableenergy/72586/[Accessed 10 July 2020].

Sloss, L. L., 2015. *Assessing and managing spontaneous combustion of coal,* London: IEA Clean Coal Centre.

Slovak, V. & Taraba, B., 2012. Urea and calcium chloride as inhibitors of coal low-temperature oxidation. *Journal of Thermal Analysis and Calorimetry,* 110, pp. 363-367.

Smith, A. C. & Lazzara, C. P., 1987. *Spontaneous combustion studies of U. S coals,* Washington: U. S Bureau of Mines.

Smith, A. & Glasser, D., 2005. Spontaneous combustion of carbonaceous stockpiles. Part II: Factors affecting the rate of the low-temperature oxidation reaction. *Fuel,* 84(9), pp. 1161-1170.

Song, Z. & Kuenzer, C., 2014. Coal fires in China over the last decade; a comprehensive review. *International Journal of Coal Geology,* 133, pp. 72-99.

Steyn, M. & Minnit, R. C. A., 2010. Thermal coal products in South Africa. *Journal of the Southern African Institute of Mining and Metallurgy,* 110, pp. 593-559.

Stracher, G. B. & Taylor, T. P., 2004. Coal fires burning out of control around the world: thermodynamic recipe of environmental catastrophe. *International Journal of Coal Geology,* 59, pp. 7-17.

Suarez-Ruiz, I. & Crelling, J., 2007. *Applied coal petrology, the role of petrology in coal utilization,* England: Oxford.

Sunjanti, W. S. & Zhang, D., 2000. Investigation into the role of inherent inorganic matter and additives in low-temperature oxidation of a Victorian brown coal. *Combustion Sciences and Technology,* 152, pp. 99-114.

Sunjanti, W. & Zhang, D., 1999. A laboratory study of spontaneous combustion of coal: the influence of inorganic matter and reactor size. *Fuel,* 78, pp. 549-556.

Sun, T. & Duan, Y., 2011. Geochemical characteristics of steranes of coal generated hydrocarbons: A case of high temperature and fined simulated experiment. *Journal of Natural Gas Geoscience,* 22, pp. 1082-1087.

Tang, Y., 2015. Analysis of coals with different spontaneous combustion characteristics using Infrared spectrometry. *Journal of Application Spectroscopy,* 82, pp. 316-321.

Tang, Y., 2017a. Experimental investigation of a novel Zn foam for preventing the spontaneous combustion of coal. *Journal of Chemical Engineering of Japan,* 50(7), pp. 527-534.

Tang, Y., 2017b. Inhibition effect of phosphorus flame retardants on the fire disasters induced by spontaneous combustion of coal. *Journal of Spectroscopy,* pp. 1-10.

Tang, Y. B. & Xue, S., 2017. Influence of long-term water immersion on spontaneous combustion characteristics of Bulianta bituminous coal. *International Journal of Oil, Gas, and Coal Technology,* 14, pp. 398-411.

Tang, Y. & Zhou, J., 2020. Laboratory investigation on the spontaneous combustion of lignocellulosic biomass and its suppression by chemical inhibitors. *Energy & Fuels,* 30, pp. 4693-4702.

Tang, Z., Xu, G., Yang, S. & Deng, J., 2021. Fire-retardant foam design to control the spontaneous combustion and the fire of coal: Flame retardant and extinguishing properties. *Powder Technology,* 384, pp. 258-266.

The Linde Group, 2015. *Biomass fire suppression,* Unterschleibheim: Linde-gas.

Tian, G. & Hua, Y., 2010. Application of ionic liquids in hydrometallurgy of nonferrous metals. Transaction of Nonferrous Metals Society of China, 20, pp. 513-520.

Tian, G. & Hua, Y., 2010. Application of ionic liquids in hydrometallurgy of nonferrous metals. *Transaction of Nonferrous Metals Society of China,* 20, pp. 513-520.

Tripathi, A. K., Verma, Y. L. & Singh, R. K., 2015. Thermal, electrical and structural studies on the ionic liquid in ordered mesoporous. *Journal of Materials Chemistry,* pp. 23809-23820.

Tsai, Y. T., Yang, Y., Wang, C. & Shu, C. M., 2017. Comparison of the inhibition mechanisms of five types of inhibitors on spontaneous coal combustion. *Journal of International Energy Research,* 42, pp. 1158-1171.

Uludag, S., 2007. A visit to the research on Wits-EHAC Index and its relationship to inherent coal properties for Witbank coalfield. *The South African Institute of Mining and Metallurgy,* 107, pp. 671-679.

Vaan Graan, M. & Blunt, J. R., 2016. Evaluation of TGA method to predict the ignition temperature and spontaneous combustion propensity of coals of different ranks. *International*

*Conference on Advanced in Science, Engineering, Technology and Natural Resources,* 16, pp. 24-25.

Vamvuka, D., Kastanaki, E. & Lasithiotakis, M., 2003. Devolatilization and combustion kinetics of low-rank coal blends from dynamic measurements. *Industrial and Engineering Chemistry Research,* 42, pp. 4732-4740.

Van der Plaats, G., Soons, H. & Chermin, H., 1984. Low-temperature oxidation of coal. *Thermochimica Acta,* 82, pp. 131-136.

Van Krevelen, D., 1993. *Coal.* 3rd ed. New York: Elsevier scientific publishing.

Wade, L., Gouws, M. J. & Phillips, H. R., 1987. An apparatus to establish the spontaneous combustion propensity of South African coal. *In. Proceedings of the symposium on safety in coal mines, Pretoria; CSIR,* pp. 71-72.

Wagner, N. J. & Hlatshwayo, B., 2005. The occurrence of potentially hazardous trace elements in five Highveld coals, South Africa. *International Journal of Coal Geology,* 63, pp. 228-246.

Wang, C. P., Yang, N., Xiao, Y. & Bai, Z. J., 2020a. Effects of moisture and associated pyrite on the microstructure of Anthracite coal for spontaneous combustion. *ACS Omega,* 5, pp. 27607-27617.

Wang, C. P., Zhao, X. Y., Bai, Z. J. & Deng, J., 2021a. Comprehensive index evaluation of the spontaneous combustion capability of different ranks of coal. *Fuel,* 201, pp. 1-12.

Wang, C., Yang, Y., Tsai, Y. & Deng, J., 2016. Spontaneous combustion in six types of coal by using the simultaneous thermal analysis-Fourier transforms infrared spectroscopy technique. *Journal of Thermal Analysis and Calorimetry,* 126(3), pp. 1591-1602.

Wang, D., Dou, G., Zhong, X. & Xin, H., 2014. An experimental approach of selecting chemical inhibitors to retard the spontaneous combustion of coal. *Fuel,* 117, pp. 218-223.

Wang, H., Dlugogorski, B. Z. & Kennedy, E. M., 2002. Examination of Carbon dioxide, Carbon monoxide and water formation during low-temperature oxidation of bituminous coal. *Energy Fuel,* 17, pp. 586-592.

Wang, H. H., Dlugogorski, E. M. & Kennedy, E. M., 2003. Coal oxidation at low temperature; oxygen consumption oxidation products, reaction mechanism and kinetic modeling. *Progress in Energy and Combustion Science,* 29, pp. 487-513.

Wang, H., Tan, B., Shap, Z. & Guo, Y., 2021b. Influence of different content of FeS2 on spontaneous combustion characteristics of coal. *Fuel,* 288, pp. 119582-119590.

Wang, Y., Zhang, X., Sugai, Y. & Sasaki, K., 2015. A study on preventing spontaneous combustion of residual coal in a coal mine goafs. Journal pf Geological Research, pp. 1-8.

Wang, J., 2011. *Inhibiting mechanism for preventing spontaneous combustion of coal.* Beijing: China Coal Industry Publishing.

Wang, J., Zhang, S., Guo, X. & Dong, A., 2012a. Thermal behaviours and kinetics of Pingshuo coal/biomass blends during co-pyrolysis and co-combustion. *Energy & Fuels,* 26(12), pp. 7120-7126.

Wang, K., Fan, H., Gao, P. & He, Y., 2020b. Influence of water content on the coal spontaneous combustion behaviour during low-temperature pre-pyrolysis processes. *Combustion Science and Technology.*

Wang, K., Liu, X., D. J. & Zhang, Y., 2019. Effect of pre-oxidation temperature on coal secondary spontaneous combustion. *Journal of Thermal Analysis and Calorimeter,* 138, pp. 1363-1370.

Wang, L. Y., Xu, X. L., Jiang, S. G. & Yu, M. G., 2012b. Imidazolium-based ionic liquid affecting functional groups and oxidation properties of bituminous coal. *Safety Science,* 50, pp. 1528-1534.

Wang, X., Wang, J., Deng, C. & Deng, H., 2012c. Research on Ca ion as an inhibitor for nitrogen-containing active groups in coal. *China Safety Science Journal,* 22, pp. 50-55.

Watanable, W. S. & Zhang, D., 2001. The effect of the inherent and added inorganic matter on low-temperature oxidation of coal. *Fuel Processing Technology,* 74, pp. 145-160.

WEC, 2018. World Energy Council report confirms global abundance of energy resources and exposes myth of peak oil. [Online] Available at: https://www.worldenergy.org [Accessed 25th June 2020].

Welton, T., 2004. Ionic liquids in catalysis. *Coordination Chemistry Reviews,* 248(21-24), pp. 2459-2477.

Wendler, F., Todi, L. N. & Meister, F., 2012. Thermostability of imidazolium ionic liquid as direct solvent for cellulose. *Themochimica Acta,* pp. 76-84.

Wen, H. J., Guo, Y., Jin, K. & Wang, Y., 2017. Experimental study on the influence of different oxygen concentrations on coal spontaneous combustion characteristic parameters. *International Journal of Oil Gas and Coal Technology*, 16(2), pp. 187-202.

Whitehead, W. L. & Breger, I. A., 1950. Vacuum differential thermal analysis. *Science,* 111, pp. 279-281.

Williams, B., 2013. *Challenges facing the solar energy industry*. [Online] Available at: https://www.saveonenergy.com/green-energy/3-challenges-facing-the-solar energy-industry/ [Accessed 15 July 2020].

William, W., 1986. *Thermal methods of analysis.* 1 ed. New York: Wiley Interscience.

Winmill, T. F., 1914. The adsorption of oxygen by coal Part 1. *Transaction Institution of Mining Engineers,* 48.

Wongthonglueang, T., Rousset, P. & Commandre, J. M., 2022. Spontaneous combustion of wheat straw residue at different cooling temperatures: Combined effect of water sorption and air oxidation. *Thermochimica Acta,* p. 179216.

World Nuclear Association, 2020. *'Clean Coal' Technologies, Carbon Capture & Sequestration.* [Online] Available at: https://www.world-nuclear.org/information-library /energy-and-the-environment/clean-coal-technologies.aspx [Accessed 1 July 2020].

Xi, X., Shi, Q., S, J. & Zhang, W., 2020. Study on the effects of ionic liquids on coal spontaneous combustion characteristic by microstructure and thermodynamics. *Process Safety and Environmental Protection,* 40, pp. 190-198.

Xiao, Y., Lu, H., Yi, X. & Deng, J., 2019. Treating bituminous coal with ionic liquids to inhibit coal spontaneous combustion. *Journal of Thermal Analysis and Calorimetry*, 135, pp. 2711-2721.

Xue, D., Hu, X., Cheng, W. & Wu, M., 2020. Carbon dioxide sealing-based inhibition of coal spontaneous combustion: A temperature-sensitive micro-encapsulated fire-retardant foamed gel. *Fuel,* 266, pp. 1-14.

Xue, S., Wang, J., Xie, J. & Wu, J., 2010. A laboratory study on the temperature dependence of the radon concentration in coal. *International Journal of Coal Geology,* 83, pp. 82-84.

Xu, J., Feng, Z., Zhang, J. & Wang, Y., 2019. The study on fuel-cell performance by using alkyl imidazole ionic liquid as electrolytes for fuel cells. *Earth and Environmental Science*, pp. 1-8.

Xu, T., Wang, D. & He, Q., 2013. The study of the critical moisture content at which coal has the most high tendency to spontaneous combustion. *International Journal of Coal Preparation and Utilization,* 33, pp. 117-127.

Xu, T., Xie, Q. & Y, K., 2017. Heat effect of the oxygen-containing functional groups in coal during spontaneous combustion processes. *Advanced Powder Technology*, 28(8), pp. 1841-1848.

Yang, Y., Li, Z., Si, L. & Li, J., 2017. SOM's effect on coal spontaneous combustion and its inhibition efficiency. *Combustion Science and Technology,* 189(12), pp. 2266-2283.

Yang, Y. & Yu, S., 1999. Study on a new type of inhibitor for preventing spontaneous combustion of coal. *Journal of Coal Industry,* 2, pp. 53-56.

Yin, W. & Song, Z., 2019. An innovative method to calculate oxygen consumption rate. *Journal of Central South University,* 26, pp. 873-880.

Yuan Kun, L., 2006. *Microbial biotechnology: principles and applications.* Singapore: World Scientific Publishing Co.

Yuan, L. & Smith, A., 2011. Carbon monoxide and Carbon dioxide emissions from spontaneous heating of coal under different ventilation rates. *International Journal of Coal Geology,* 88, pp. 24-30.

Yuan, L. & Smith, A. C., 2012. The effect of ventilation on spontaneous heating of coal. *Journal of Loss Prevention in the Process Industries*, 25(1), pp. 131-137.

Yuan, S., Liu, J. & Zhu, J., 2016. Effect of microwave irradiation on the propensity for spontaneous combustion of inner Mongolia lignite. *Journal of Loss Prevention in the Process Industries*, pp. 390-396.

Yu, M., Meng, D., Lu, C. & Xie, F., 2010. Experimental study of effects of inhibitors on coal oxidation based on cone calorimeter. *Journal of Thermal Science and Technology,* 9, pp. 343-347.

Yu, S., Xie, F., Jia, B. & Zhang, P., 2011. Influence study of the organic and inorganic additive soal combustion characteristic. *International Conference on Environmental Science and Engineering,* 12, pp. 459-467.

Zaman, R., Brudermann, T., Kumar, S. & Islam, N., 2018. A multi-criteria analysis of coal-based power generation in Bangladesh. *Energy Pol,* 116, pp. 182-192.

Zeng, F. & Xie, K., 2004. Theoretical system and methodology of coal structural chemistry. *Journal of China Coal Society,* 29, pp. 443-447.

Zeng, L. F., 2010. Test and analysis of salty retardants performance to restrain in coal oxidized spontaneous combustion. *International Journal of Coal Science & Technology,* 38(5), pp. 70-73.

Zhai, X. W., Wang, B., Wang, K. & Obracaj, D., 2019. Study on the influence of water immersion on the characteristic parameters of spontaneous combustion oxidation of low-rank bituminous coal. *Journal of Combustion Science and Technology,* 191(7), pp 1101-1122

Zhang, J., 2004. Detecting coal fires using remote sensing techniques. *International Journal of Remote Sensing,* 25(16), pp. 3193-3220.

Zhang, L. & Qin, B., 2014. Development of a new material for mine fire control. *Combustion Science and Technology,* 186(7), pp. 928-942.

Zhang, M. & Kamavaram, V., 2006. *Ionic liquids from fundamental study of industrial application.* 344-344 ed. Beijing: Science Press.

Zhang, S., Wen, L. Y., Wang, K. & Zou, C., 2015a. Effects of additives on sulfur transformation, Crystallite structure and properties of coke during coking of high-sulfur coal. *Journal of Iron and Steel Research International,* 22, pp. 897-904.

Zhang, W., Jiang, S., Wu, Z. & Wang, K., 2018. Influence of imidazolium-base ionic liquids on coal oxidation. *Fuel,* 217, pp. 529-535.

Zhang, W. Q., Wang, H. H. & Song, S. N., 2011. Study on coal spontaneous combustion characteristic structures affected by ionic liquids. *Procedia Engineer,* 26, pp. 480-485.

Zhang, X., Yang, J., Xie, P. & Liu, H., 2020. Experimental study on controlled-release inhibitor foam for restraining spontaneous combustion of coal. *Energy Exploration & Exploitation,* 38(4), pp. 1159-1177.

Zhang, Y. T., Zhang, Y. B., Li, Y. P. & Zhang, J., 2020. Study on the characteristics of coal spontaneous combustion during the development and decaying processes. *Process Safety and Environmental Protection,* 138, pp. 9-17.

Zhang, Y., Wang, J., Wu, J. & Xue, S., 2015b. Modes and kinetics of carbon dioxide and carbon monoxide production from low-temperature oxidation of coal. *International Journal of Coal Geology,* 140, pp. 1-8.

Zhang, Y., Wang, J., Xue, S. & Wu, J., 2016. Kinetic study on changes in methyl and methylene groups during low-temperature oxidation of coal via in-situ FTIR. *International Journal of Coal Geology,* 154-155, pp. 155-164.

Zhang, Y., Wu, J., Chang, L. & Wang, J., 2013. Kinetic and thermodynamic studies on the mechanism of low-temperature oxidation of coal: a case study of Shandong coal (China). *International Journal of Coal Geology,* 120(1), pp. 41-47.

Zhang, Y., Zhang, J., Li, Y. & Gao, S., 2021. Oxidation Characteristics of Functional Groups in Relation to Spontaneous combustion. *ACS Omega,* 6(11), pp. 7669-7679.

Zhao, Y., Zhang, J., Chou, C. & Li, Y., 2008. Trace element emissions from spontaneous combustion of gob piles in coal mines, Shanxi, China. *International Journal of Coal Geology,* 73(1), pp. 52-62.

Zheng, H., Li, Y., Zhang, L. & He, W., 2021. Study on the effect of organic sulfur on coal spontaneous combustion based on model compounds. *Fuel,* 289, pp. 119846-1198455.

Zheng, X. Z., Lu, J. H., Xiao, Y. & Zhao, Y. H., 2014. Experimental study over the effect of high moisture on coal spontaneous combustion characteristic parameters. *Journal of Environment and Safety,* 38, pp. 325-354.

Zhong, X. X., Kan, L., Xin, H. H. & Dou, G. L., 2019. Thermal effects and active group differentiation of low-rank coal during low-temperature oxidation under vacuum drying after water immersion. *Fuel,* 236, pp. 1204-1212.

Zhou, F. B., Ren, W., Wang, D. & Song, T., 2006. Application of three-phase foam to fight an extraordinarily serious coal mine fire. *Internal Journal of Coal Geology,* 67(1), pp. 95-100.

## APPENDIX A

### A1. Thermogravimetric analysis derivative profiles of untreated samples

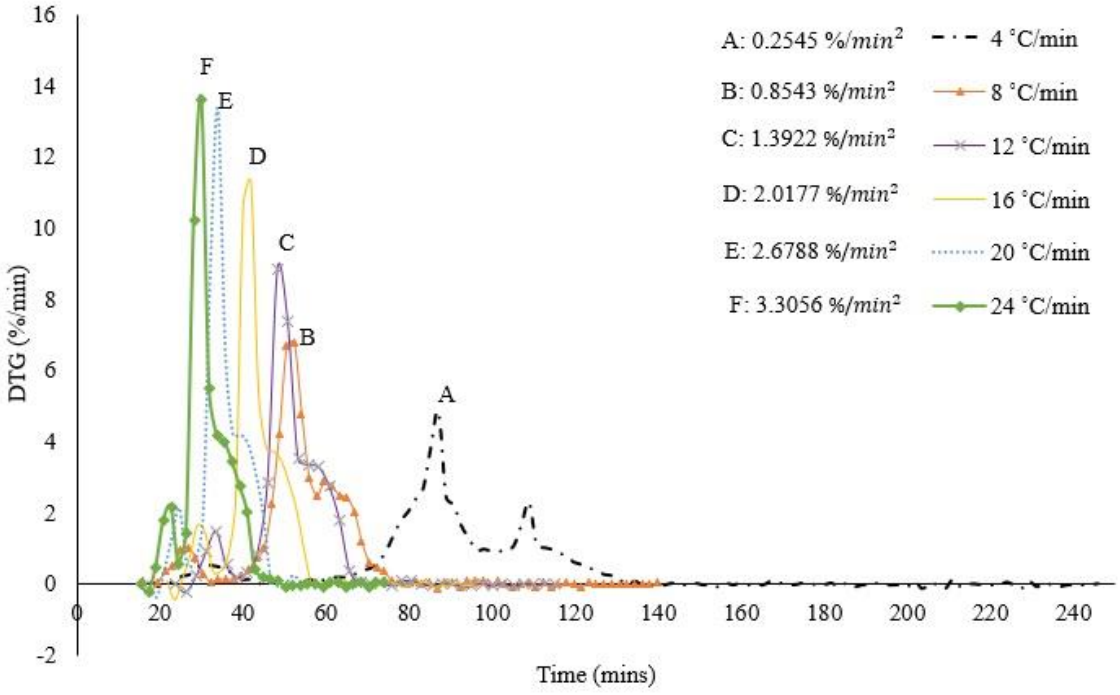



*Figure A1.1: The derivative profile of 100% biomass*

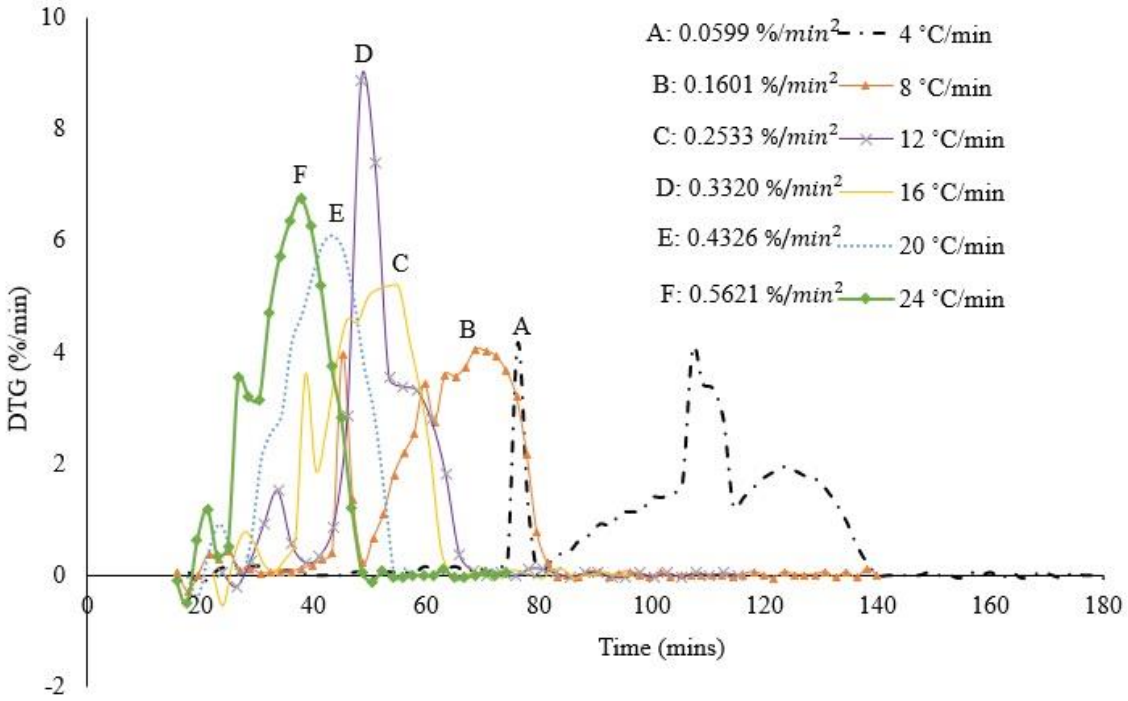



*Figure A1.2: The derivative profile of 100% hydrochar*

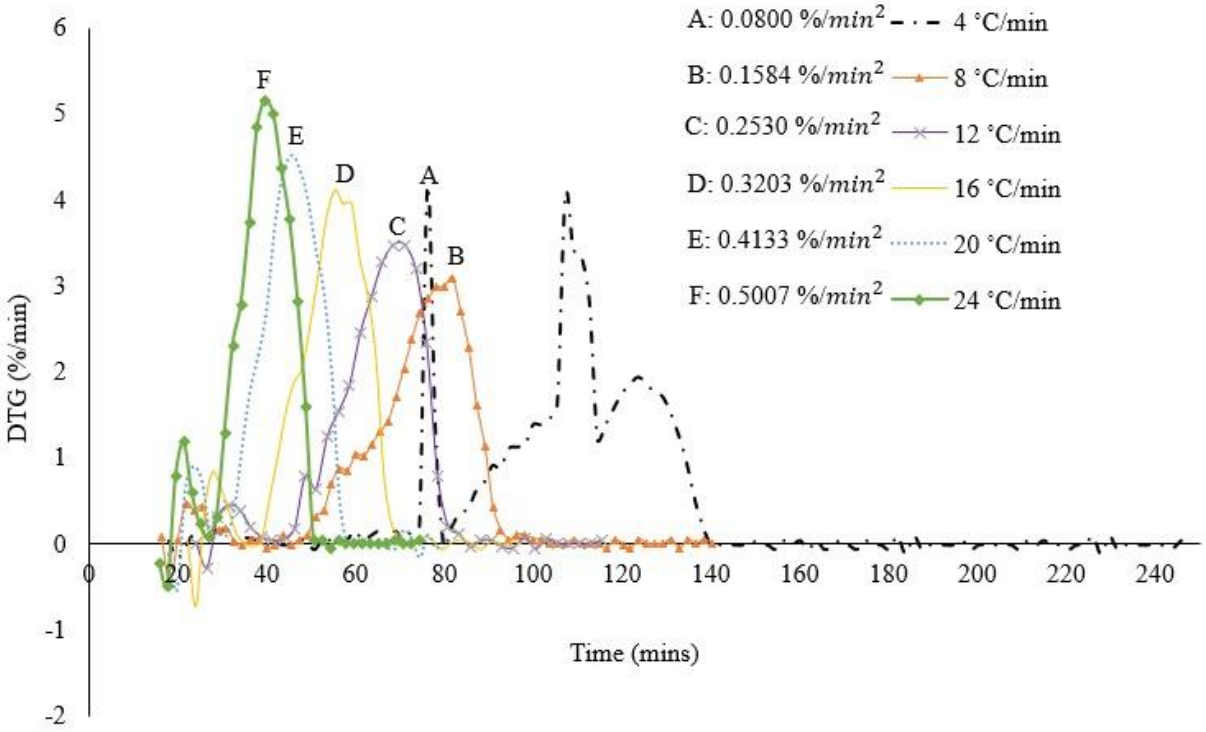



*Figure A1.3: The derivative profile of 25% hydrochar + 75% discard coal*

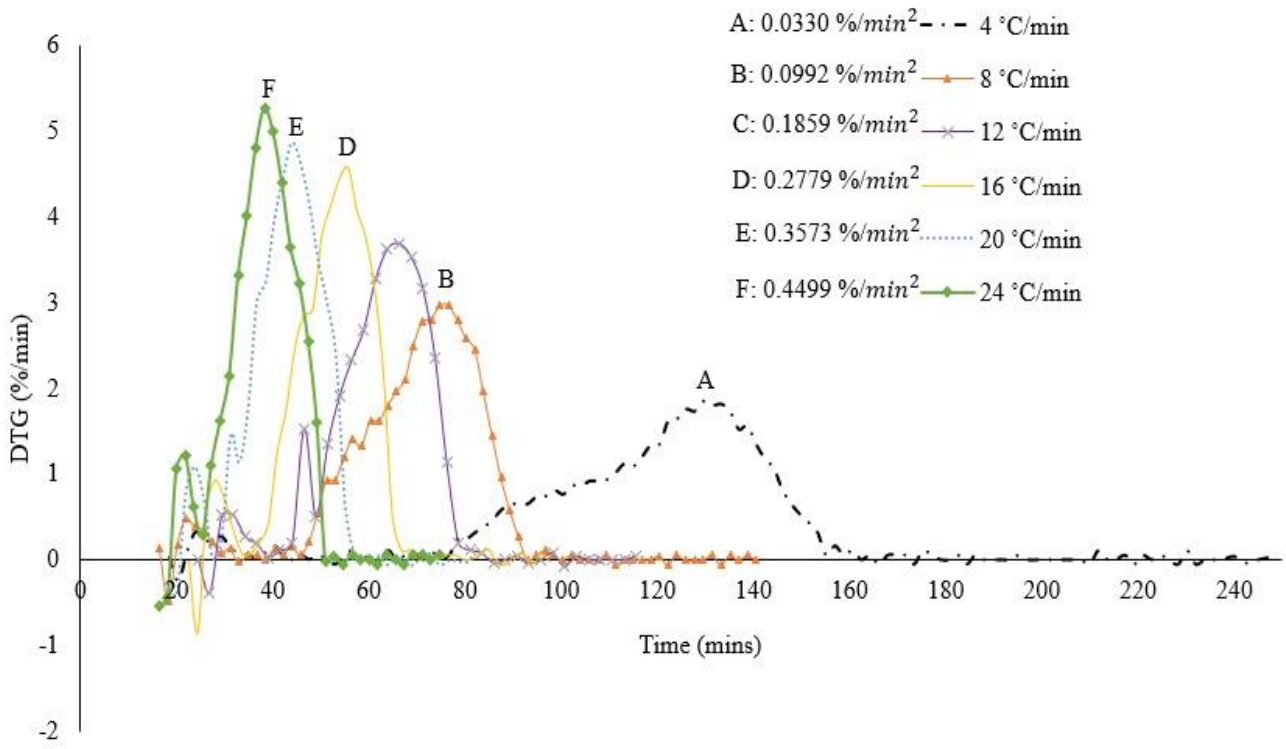



*Figure A1.4: The derivative profile of 50% hydrochar + 50% discard coal*

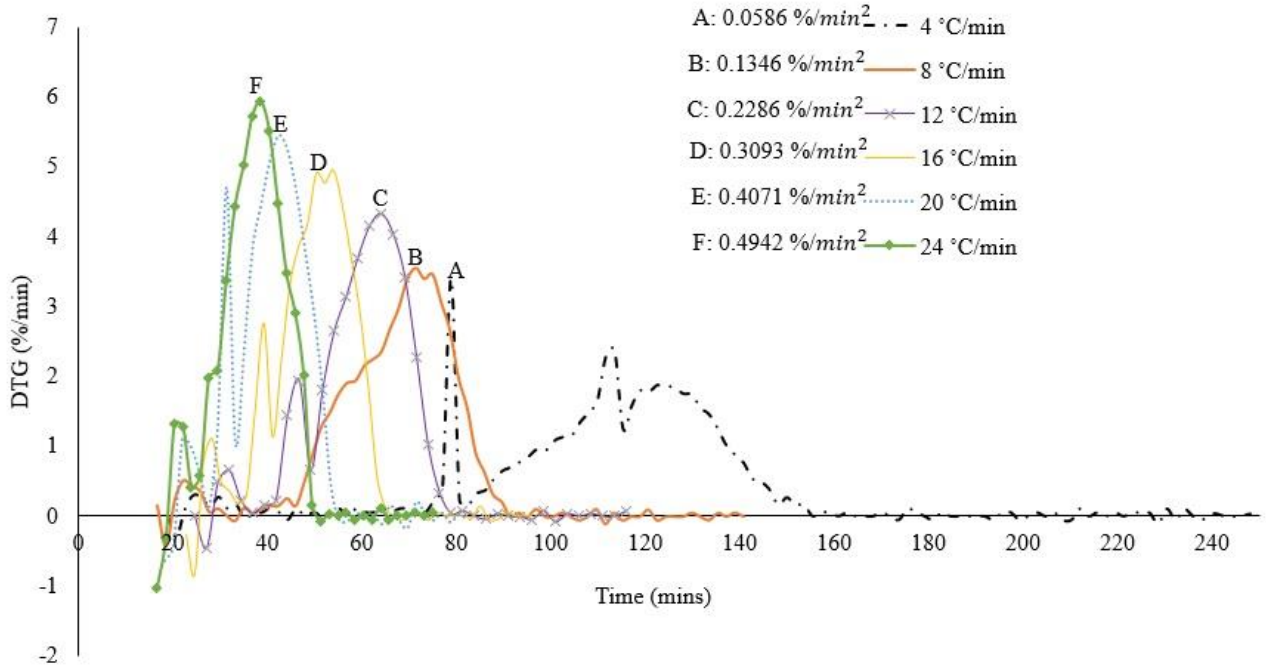



*Figure A1.5: The derivative profile of 75% hydrochar + 25% discard coal*

**A2. Three points that were used for calculating the slopes of the sample's derivative profile at different heating rates**

*Table A2.1: The specific temperatures and differential thermogravimetric analysis values used for calculating the slopes of the sample's derivative profile at different heating rates (H; Hydrochar, DC: Discard coal)*

| Heating Rate ˚C/min | Points | 100% Biomass | | 100% Hydrochar | | 25% H + 75% DC | | 50% H + 50% DC | | 75% H + 25% DC | |
|---|---|---|---|---|---|---|---|---|---|---|---|
| 4 | Ignition Point | 79.78 | 0.90 | 92.22 | 1.27 | 80.05 | 1.46 | 92.38 | 1.34 | 92.38 | 1.34 |
| | Inflection Point | 87.05 | 2.66 | 98.47 | 3.77 | 85.50 | 3.59 | 98.63 | 3.79 | 98.63 | 3.79 |
| | Peak Point | 90.70 | 4.98 | 101.65 | 5.67 | 87.32 | 4.81 | 101.82 | 4.31 | 101.82 | 4.31 |
| 8 | Ignition Point | 57.68 | 0.63 | 60.70 | 1.85 | 57.98 | 0.88 | 58.18 | 0.73 | 58.18 | 0.73 |
| | Inflection Point | 60.53 | 2.26 | 63.62 | 5.54 | 60.87 | 2.83 | 63.97 | 5.13 | 63.97 | 5.13 |
| | Peak Point | 63.43 | 7.06 | 66.50 | 9.54 | 63.80 | 9.10 | 66.85 | 9.58 | 66.85 | 9.58 |
| 12 | Ignition Point | 41.30 | 1.97 | 53.88 | 0.61 | 41.57 | 3.59 | 54.05 | 0.68 | 54.05 | 0.68 |
| | Inflection Point | 43.12 | 5.65 | 57.17 | 4.14 | 43.40 | 9.47 | 57.37 | 4.65 | 57.37 | 4.65 |
| | Peak Point | 45.05 | 13.55 | 60.57 | 10.24 | 45.32 | 11.43 | 60.77 | 10.08 | 60.77 | 10.08 |
| 16 | Ignition Point | 29.87 | 1.36 | 51.10 | 0.20 | 40.35 | 1.67 | 54.55 | 1.01 | 54.55 | 1.01 |
| | Inflection Point | 31.70 | 6.53 | 54.37 | 0.78 | 42.08 | 4.98 | 54.55 | 1.01 | 54.55 | 1.01 |
| | Peak Point | 33.65 | 16.40 | 57.70 | 10.32 | 44.00 | 13.96 | 57.92 | 11.38 | 57.92 | 11.38 |
| 20 | Ignition Point | 31.17 | 0.56 | 47.30 | 0.66 | 31.43 | 1.14 | 47.48 | 0.81 | 47.48 | 0.81 |
| | Inflection Point | 32.95 | 3.63 | 47.30 | 0.66 | 33.27 | 6.39 | 47.48 | 0.81 | 47.48 | 0.81 |
| | Peak Point | 34.88 | 16.36 | 50.58 | 12.46 | 35.15 | 19.09 | 50.75 | 12.58 | 50.75 | 12.58 |
| 24 | Ignition Point | 35.92 | 18.24 | 40.08 | 0.62 | 32.43 | 0.57 | 40.25 | 0.61 | 40.25 | 0.61 |
| | Inflection Point | 34.00 | 6.68 | 43.12 | 8.37 | 34.22 | 7.16 | 43.32 | 9.39 | 43.32 | 9.39 |
| | Peak Point | 34.88 | 16.36 | 43.12 | 8.37 | 36.13 | 20.34 | 43.32 | 9.39 | 43.32 | 9.39 |

**A3. Heating rates applied vs the slopes of the derivative curve for the untreated samples**

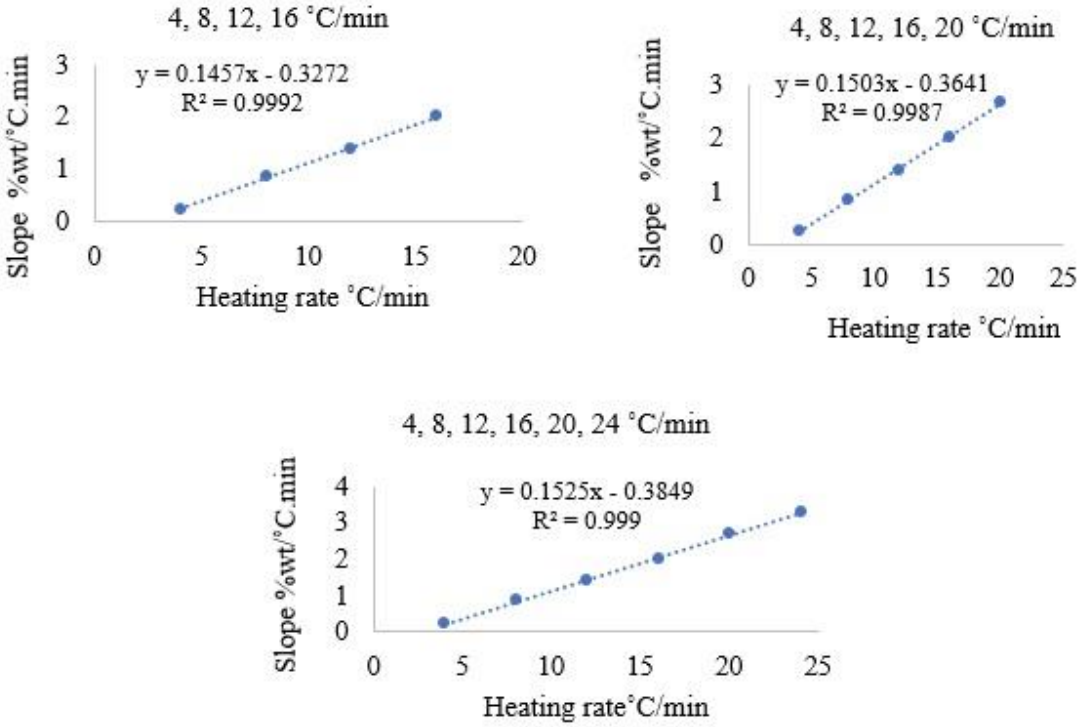



*Figure A3.1: Heating rates applied vs the slopes of the derivative curve for 100% biomass*

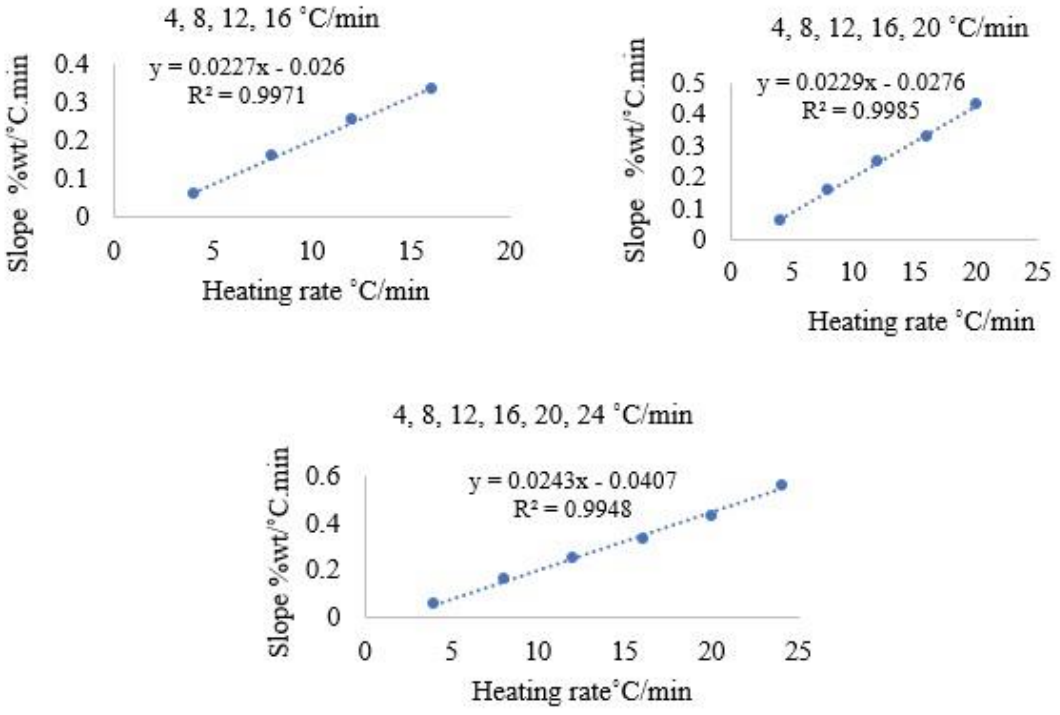



*Figure A3.2: Heating rates applied vs the slopes of the derivative curve for 100% hydrochar*

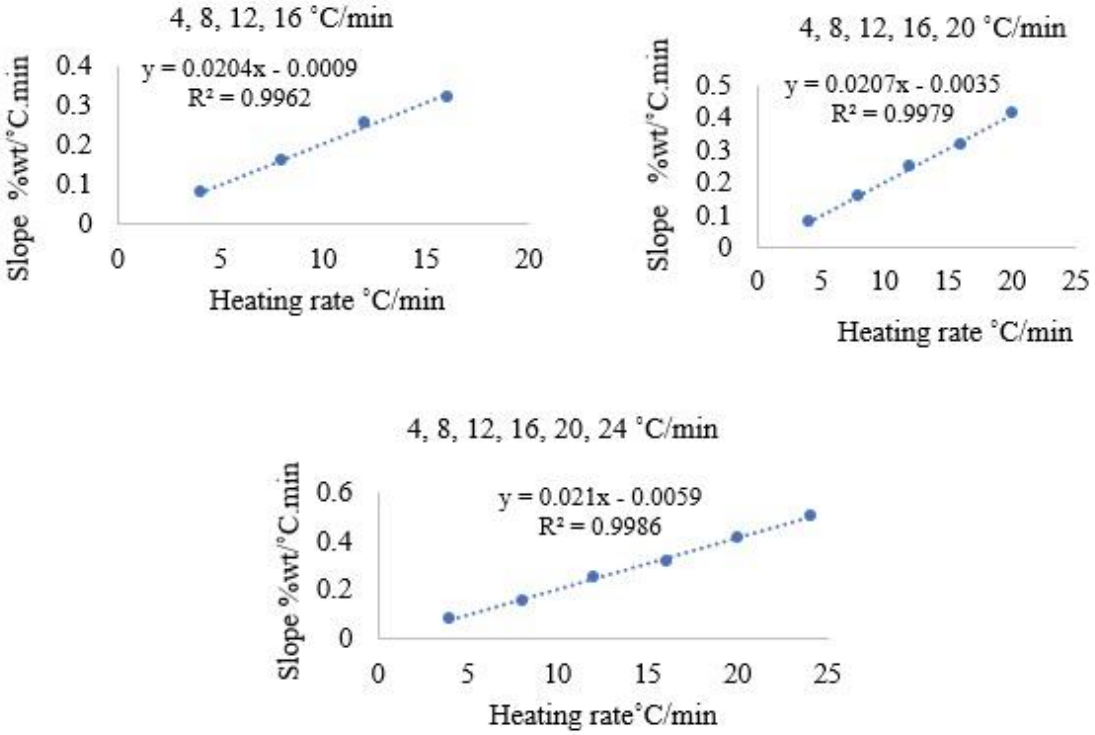



*Figure A3.3: Heating rates applied vs the slopes of the derivative curve for 25% hydrochar + 75% discard coal*

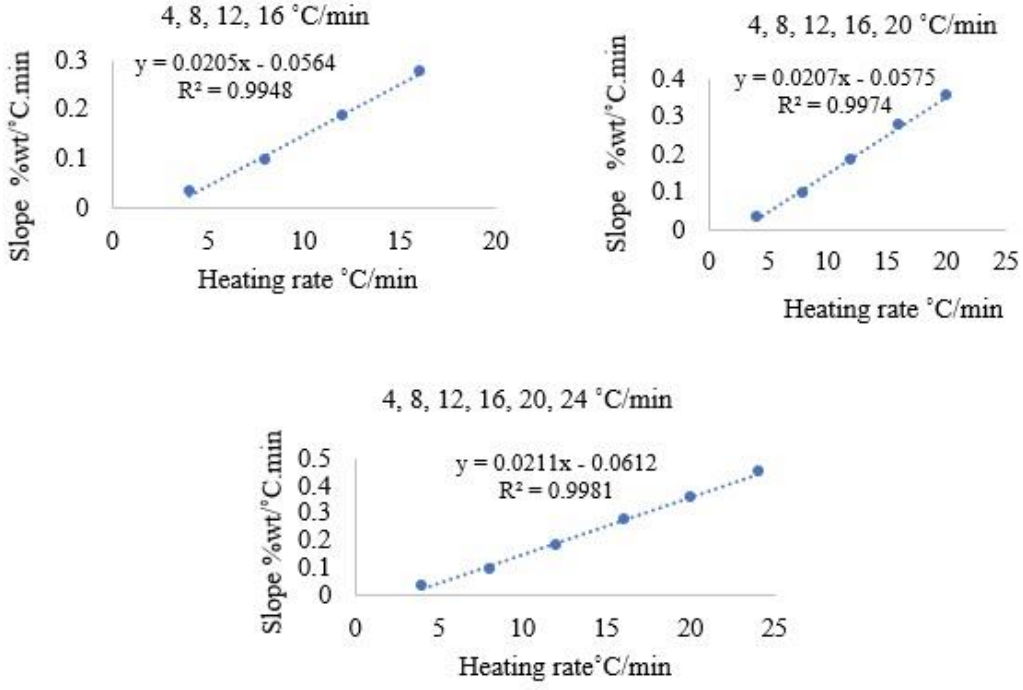



*Figure A3.4: Heating rates applied vs the slopes of the derivative curve for 50% hydrochar + 50% discard coal*

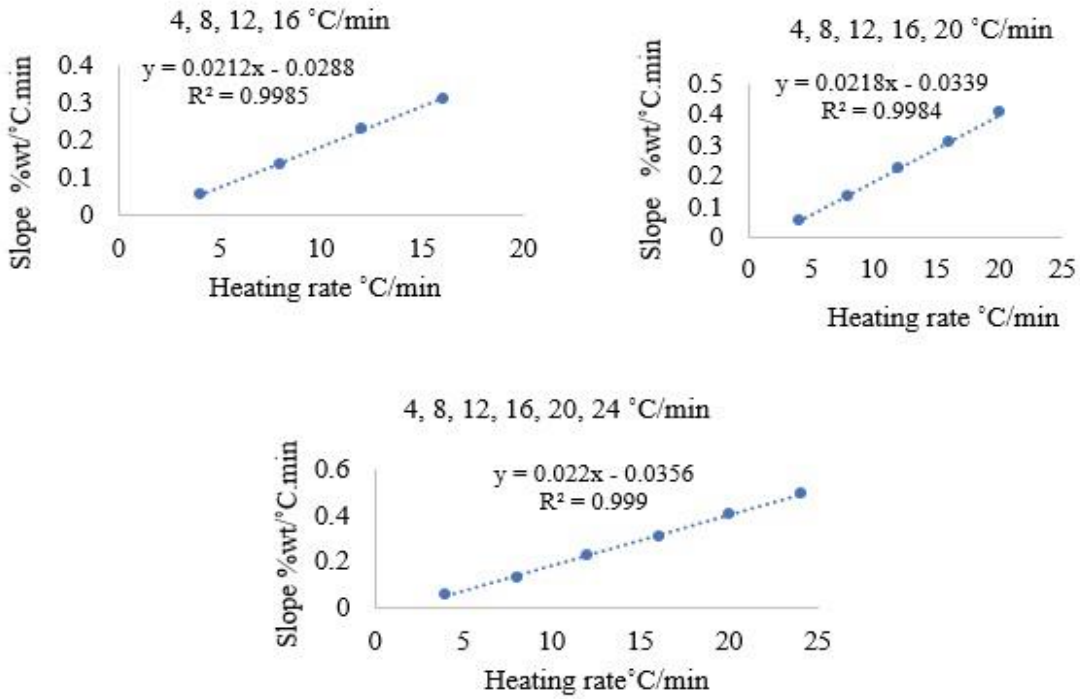



*Figure A3.5: Heating rates applied vs the slopes of the derivative curve for 75% hydrochar + 25%discardcoal.*

## APPENDIX B

### B1. Three points used for calculating the slopes of the derivative profile of the biomass samples treated with IL-A at different concentrations and heating rates

*Table B1.1: The specific temperatures and differential thermogravimetric analysis values used for calculating the slopes of the derivative profile of the samples treated with IL-A*

| Heating Rate ˚C/min | Points | 10% IL-A-tb | | 20% IL-A-tb | | 30% IL-A-tb | | 40% IL-A-tb | | 50% IL-A-tb | |
|---|---|---|---|---|---|---|---|---|---|---|---|
| 4 | Ignition Point | 95.15 | 1.57 | 79.78 | 0.90 | 92.22 | 1.27 | 80.05 | 1.46 | 92.38 | 1.34 |
| | Inflection Point | 95.15 | 1.57 | 87.05 | 2.66 | 98.47 | 3.77 | 85.50 | 3.59 | 98.63 | 3.79 |
| | Peak Point | 104.58 | 5.91 | 90.70 | 4.98 | 101.65 | 5.67 | 87.32 | 4.81 | 101.82 | 4.31 |
| 8 | Ignition Point | 60.38 | 1.33 | 57.68 | 0.63 | 60.70 | 1.85 | 57.98 | 0.88 | 58.18 | 0.73 |
| | Inflection Point | 63.27 | 4.21 | 60.53 | 2.26 | 63.62 | 5.54 | 60.87 | 2.83 | 63.97 | 5.13 |
| | Peak Point | 66.17 | 10.01 | 63.43 | 7.06 | 66.50 | 9.54 | 63.80 | 9.10 | 66.85 | 9.58 |
| 12 | Ignition Point | 57.00 | 2.21 | 41.30 | 1.97 | 53.88 | 0.61 | 41.57 | 3.59 | 54.05 | 0.68 |
| | Inflection Point | 57.00 | 2.21 | 43.12 | 5.65 | 57.17 | 4.14 | 43.40 | 9.47 | 57.37 | 4.65 |
| | Peak Point | 60.40 | 11.46 | 45.05 | 13.55 | 60.57 | 10.24 | 45.32 | 11.43 | 60.77 | 10.08 |
| 16 | Ignition Point | 54.20 | 0.44 | 29.87 | 1.36 | 51.10 | 0.20 | 40.35 | 1.67 | 54.55 | 1.01 |
| | Inflection Point | 57.50 | 8.24 | 31.70 | 6.53 | 54.37 | 0.78 | 42.08 | 4.98 | 54.55 | 1.01 |
| | Peak Point | 60.90 | 8.96 | 33.65 | 16.40 | 57.70 | 10.32 | 44.00 | 13.96 | 57.92 | 11.38 |
| 20 | Ignition Point | 47.13 | 0.30 | 31.17 | 0.56 | 47.30 | 0.66 | 31.43 | 1.14 | 47.48 | 0.81 |
| | Inflection Point | 47.13 | 0.30 | 32.95 | 3.63 | 47.30 | 0.66 | 33.27 | 6.39 | 47.48 | 0.81 |
| | Peak Point | 50.38 | 9.23 | 34.88 | 16.36 | 50.58 | 12.46 | 35.15 | 19.09 | 50.75 | 12.58 |
| 24 | Ignition Point | 42.87 | 4.30 | 35.92 | 18.24 | 40.08 | 0.62 | 32.43 | 0.57 | 40.25 | 0.61 |
| | Inflection Point | 42.87 | 4.30 | 34.00 | 6.68 | 43.12 | 8.37 | 34.22 | 7.16 | 43.32 | 9.39 |
| | Peak Point | 46.90 | 13.87 | 34.88 | 16.36 | 43.12 | 8.37 | 36.13 | 20.34 | 43.32 | 9.39 |

*tb: treated 100% biomass*

**B2. Heating rates applied vs the slopes of the derivative curve for the samples treated with IL-A at different concentrations**

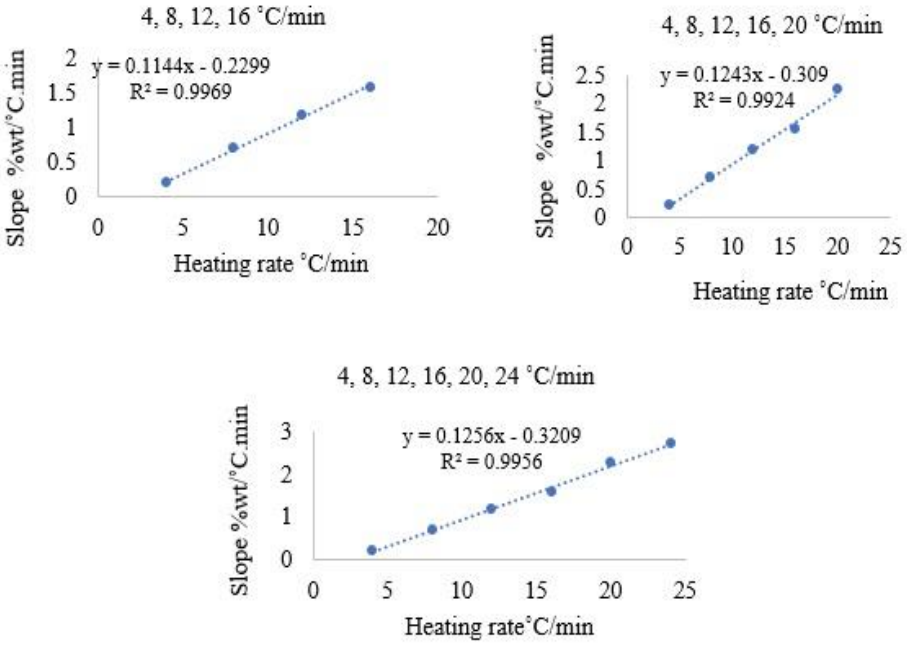



*Figure B2.1: Heating rates applied vs the slopes of the derivative curve for 100% biomass treated with 10% IL-A*

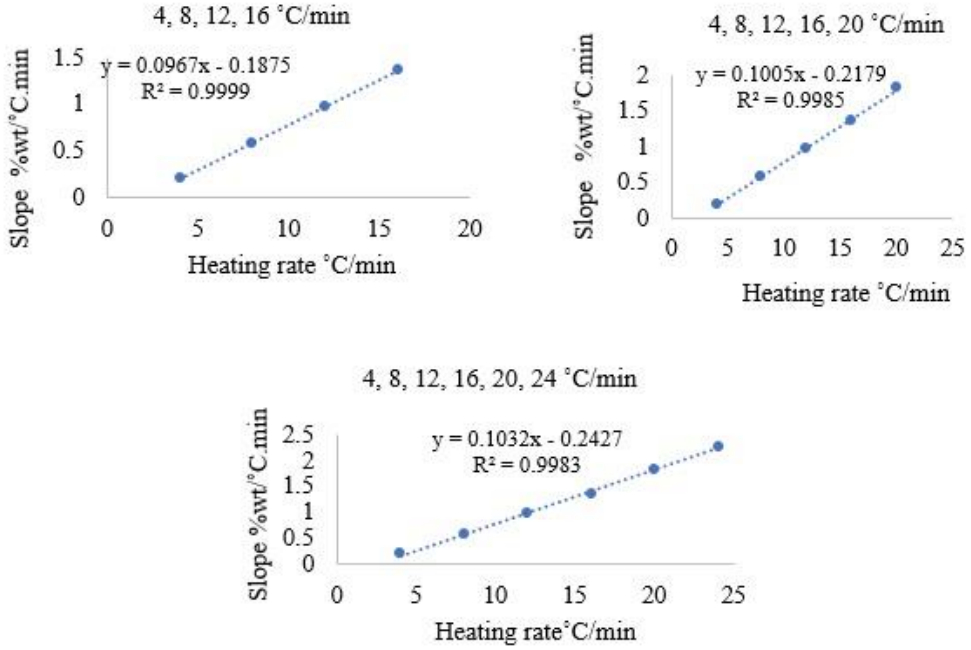



*Figure B2.2: Heating rates applied vs the slopes of the derivative curve for 100% biomass treated with 20% IL-A*

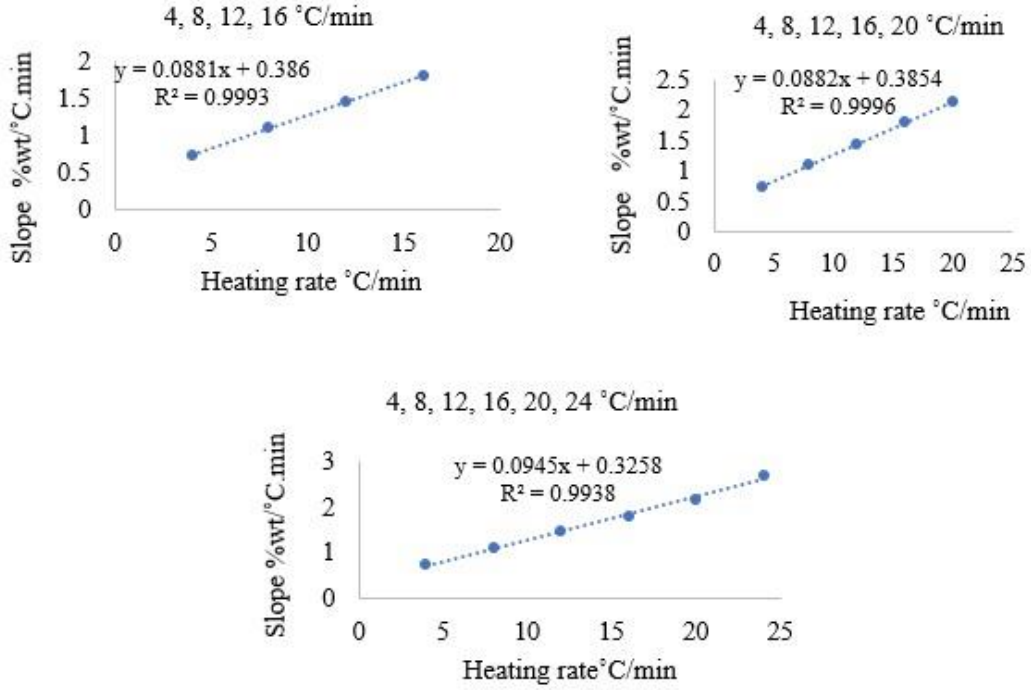



*Figure B2.3: Heating rates applied vs the slopes of the derivative curve for 100% biomass treated with 30% IL-A*

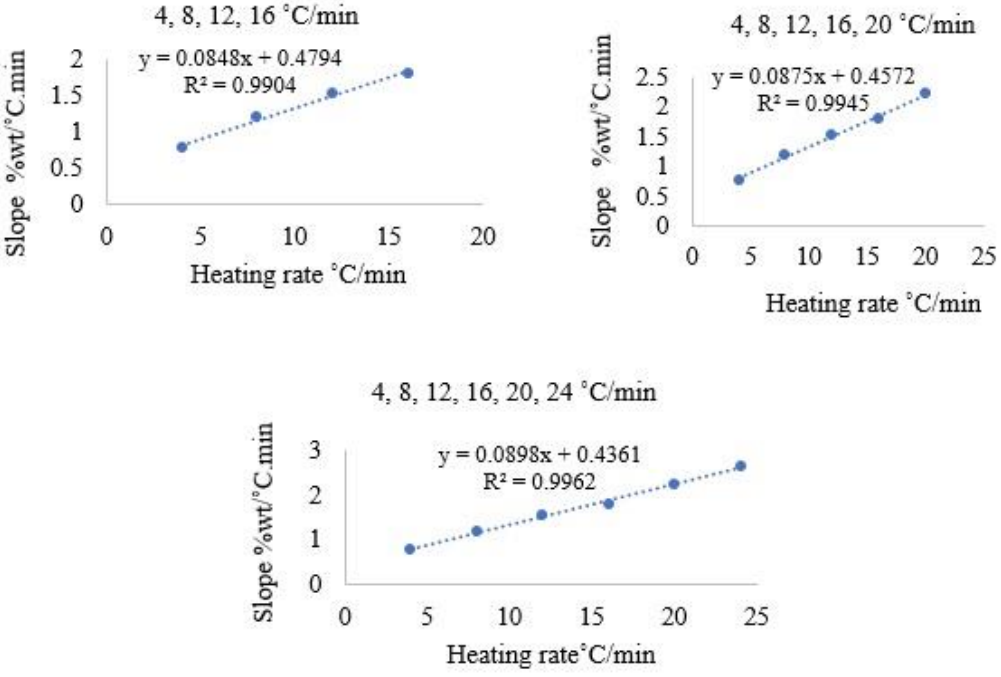



*Figure B2.4: Heating rates applied vs the slopes of the derivative curve for 100% biomass treated with 40% IL-A*

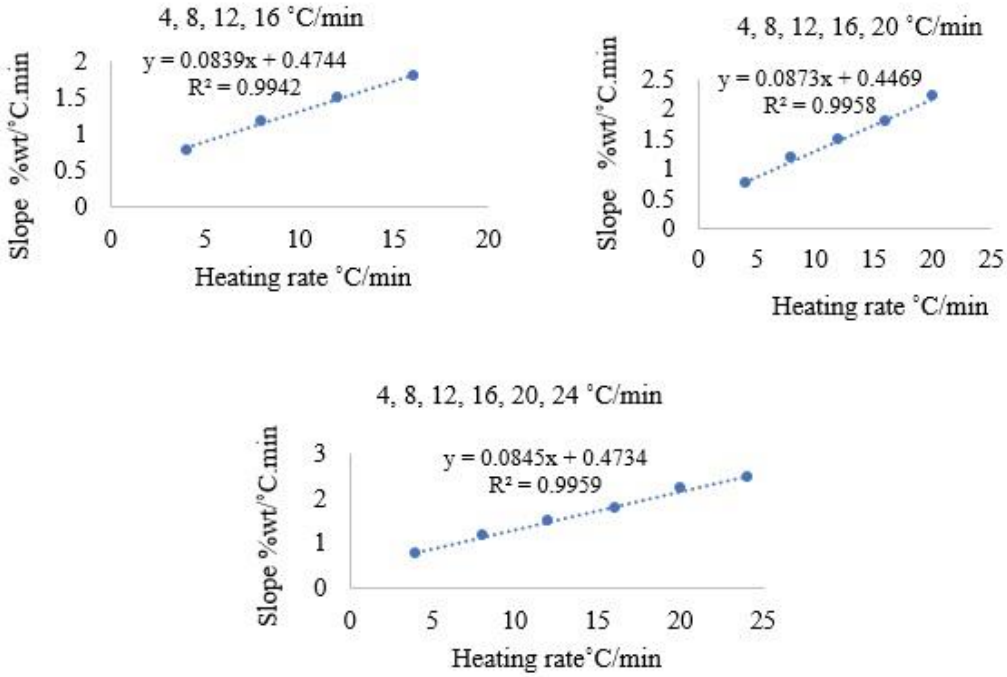



*Figure B2.5: Heating rates applied vs the slopes of the derivative curve for 100% biomass treated with 50% IL-A*

**APPENDIX C**

**C1. Thermogravimetric analysis derivative profile of 100% biomass treated with IL-B at different concentrations**

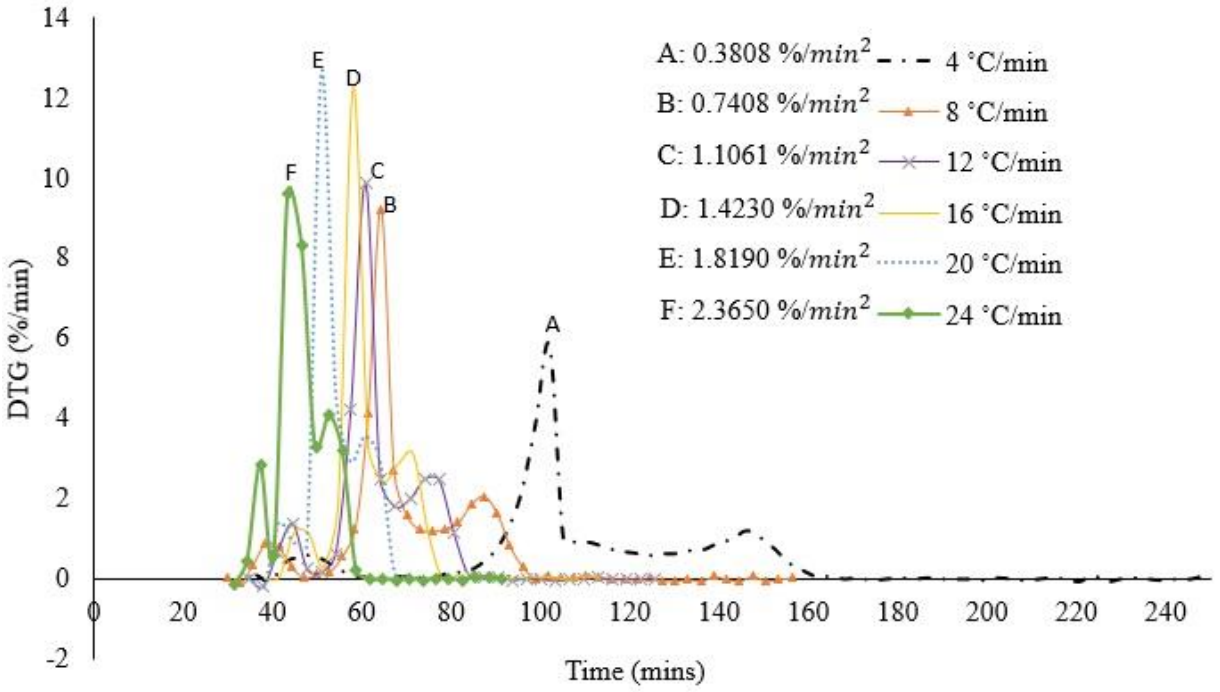



*Figure C1.1: The derivative profile of 100% biomass treated with 10% IL-B*

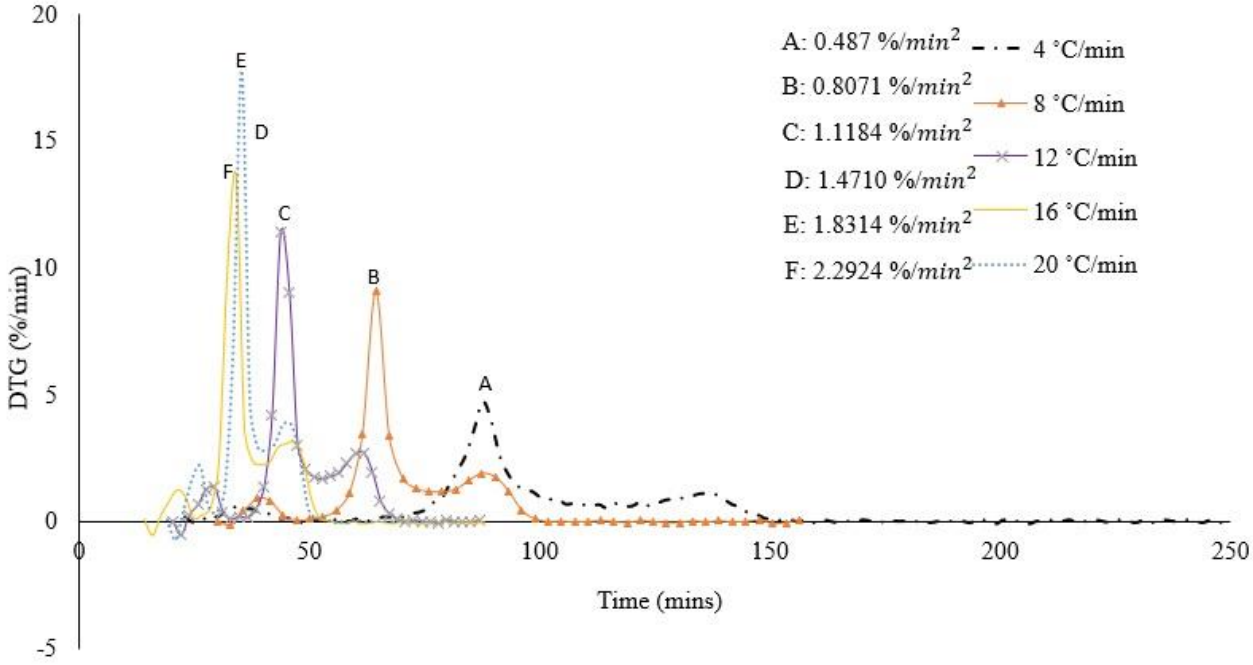



*Figure C1.2: The derivative profile of 100% biomass treated with 20% IL-B*

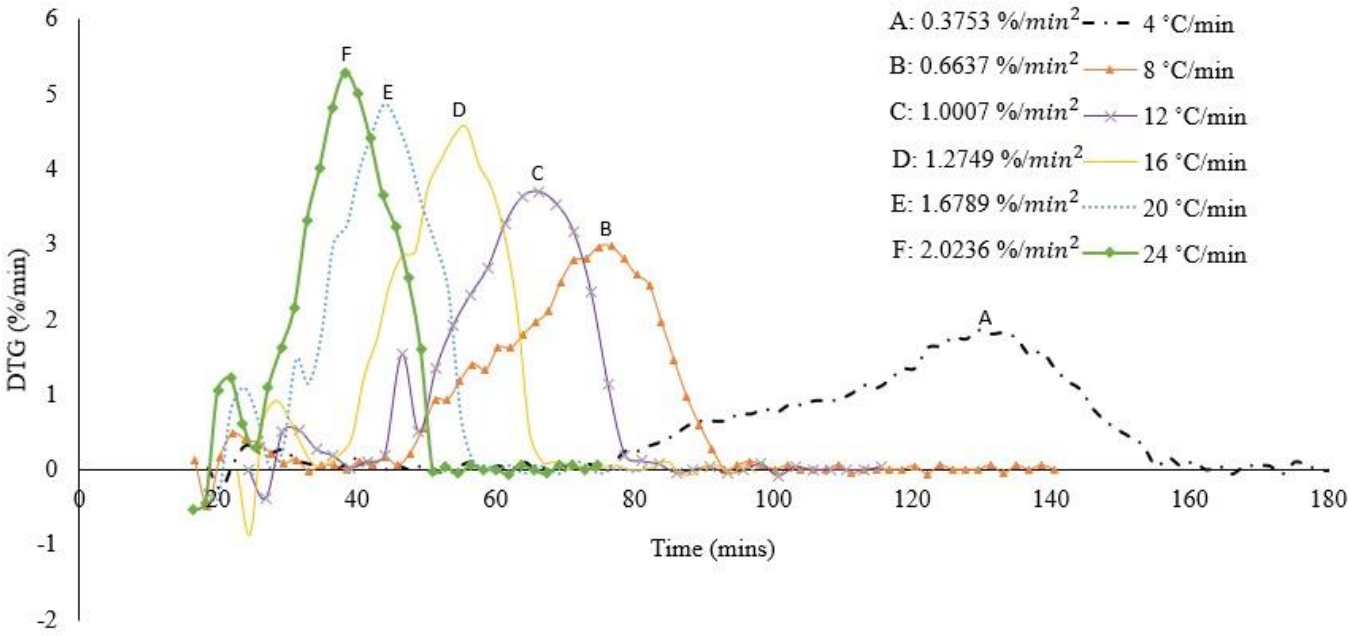



*Figure C1.8: The derivative profile of 100% biomass that was treated with 30% IL-B*

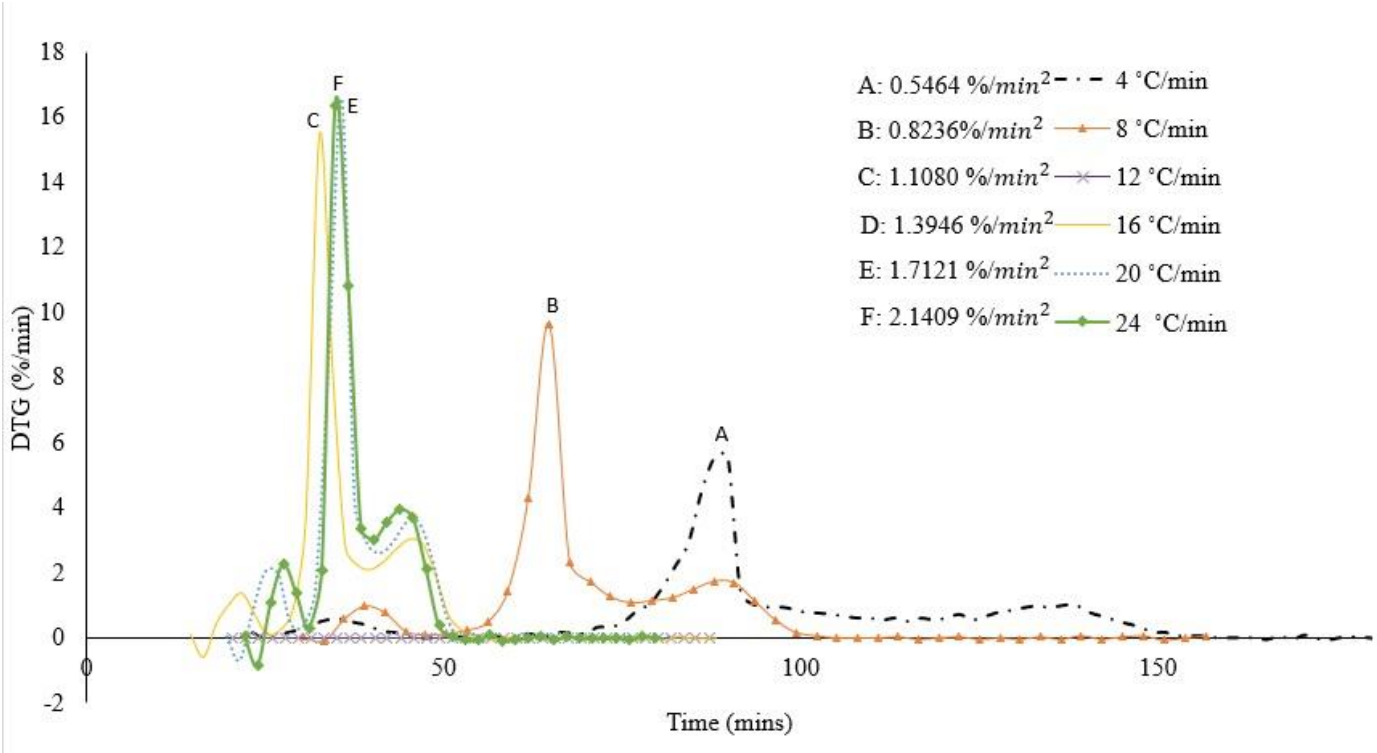



*Figure C1.9: The derivative profile of 100% biomass that was treated with 40% IL-B*

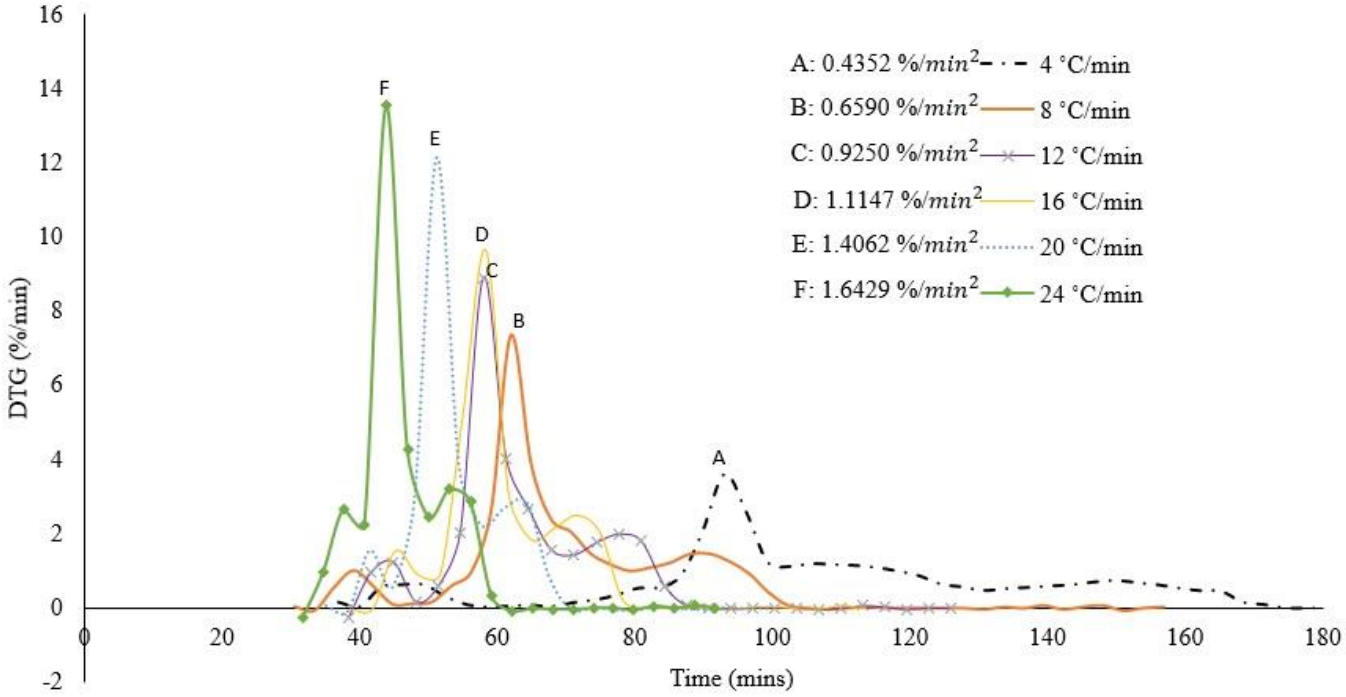



*Figure C1.10: The derivative profile of 100% biomass that was treated with 50% IL-B*

**C2. Three points were used for calculating the slopes of the derivative profile of the samples treated with IL-B at different concentrations and heating rates**

*Table C2.1: The specific temperatures and differential thermogravimetric analysis values used for calculating the slopes of the derivative profile of the samples treated with IL-B*

| Heating Rate ˚C/min | Points | 10% IL-B-tb | | 20% IL-B-tb | | 30% IL-B-tb | | 40% IL-B-tb | | 50% IL-B-tb | |
|---|---|---|---|---|---|---|---|---|---|---|---|
| 4 | Ignition Point | 89.42 | 0.66 | 78.53 | 0.88 | 92.73 | 1.23 | 80.60 | 1.55 | 86.65 | 0.89 |
| | Inflection Point | 98.82 | 3.88 | 83.95 | 2.64 | 98.33 | 3.40 | 86.05 | 4.49 | 89.78 | 2.08 |
| | Peak Point | 101.98 | 5.83 | 87.58 | 4.74 | 102.15 | 4.76 | 87.85 | 5.52 | 92.93 | 3.63 |
| 8 | Ignition Point | 58.43 | 1.26 | 58.60 | 1.12 | 58.77 | 1.26 | 58.93 | 1.43 | 56.25 | 0.99 |
| | Inflection Point | 61.30 | 4.13 | 61.47 | 3.43 | 61.65 | 3.88 | 61.82 | 4.28 | 59.12 | 2.67 |
| | Peak Point | 64.22 | 9.23 | 64.40 | 9.11 | 64.57 | 8.52 | 64.73 | 9.63 | 61.98 | 7.37 |
| 12 | Ignition Point | 54.23 | 0.64 | 40.07 | 1.37 | 54.40 | 0.79 | 40.50 | 1.67 | 51.32 | 0.58 |
| | Inflection Point | 57.57 | 4.21 | 41.82 | 4.22 | 57.77 | 5.61 | 42.08 | 4.98 | 54.57 | 2.03 |
| | Peak Point | 60.99 | 9.87 | 43.70 | 11.46 | 61.10 | 9.26 | 44.00 | 13.96 | 57.95 | 8.89 |
| 16 | Ignition Point | 51.45 | 0.28 | 30.38 | 2.24 | 51.62 | 0.22 | 28.85 | 0.85 | 51.78 | 0.88 |
| | Inflection Point | 54.72 | 1.84 | 32.30 | 9.98 | 54.88 | 1.82 | 30.65 | 3.56 | 55.05 | 5.15 |
| | Peak Point | 58.10 | 12.28 | 34.18 | 13.60 | 58.27 | 12.99 | 32.62 | 15.46 | 58.43 | 9.63 |
| 20 | Ignition Point | 47.65 | 0.80 | 31.70 | 1.20 | 47.80 | 0.77 | 31.95 | 1.46 | 47.98 | 2.87 |
| | Inflection Point | 47.65 | 0.80 | 33.55 | 6.75 | 47.80 | 0.77 | 33.85 | 8.65 | 47.98 | 2.87 |
| | Peak Point | 50.95 | 12.66 | 35.42 | 17.78 | 51.12 | 13.63 | 35.68 | 16.54 | 51.28 | 12.14 |
| 24 | Ignition Point | 40.43 | 0.59 | 32.68 | 1.41 | 40.58 | 0.57 | 31.20 | 0.30 | 40.73 | 2.23 |
| | Inflection Point | 40.43 | 0.59 | 34.53 | 12.30 | 40.58 | 0.57 | 32.98 | 2.07 | 40.73 | 2.23 |
| | Peak Point | 43.52 | 9.60 | 36.40 | 14.92 | 43.72 | 10.96 | 34.87 | 16.36 | 43.88 | 13.55 |

*tb: treated 100% biomass*

**C3. Heating rates applied vs the slopes of the derivative curve for the samples treated with IL-B at different concentrations**

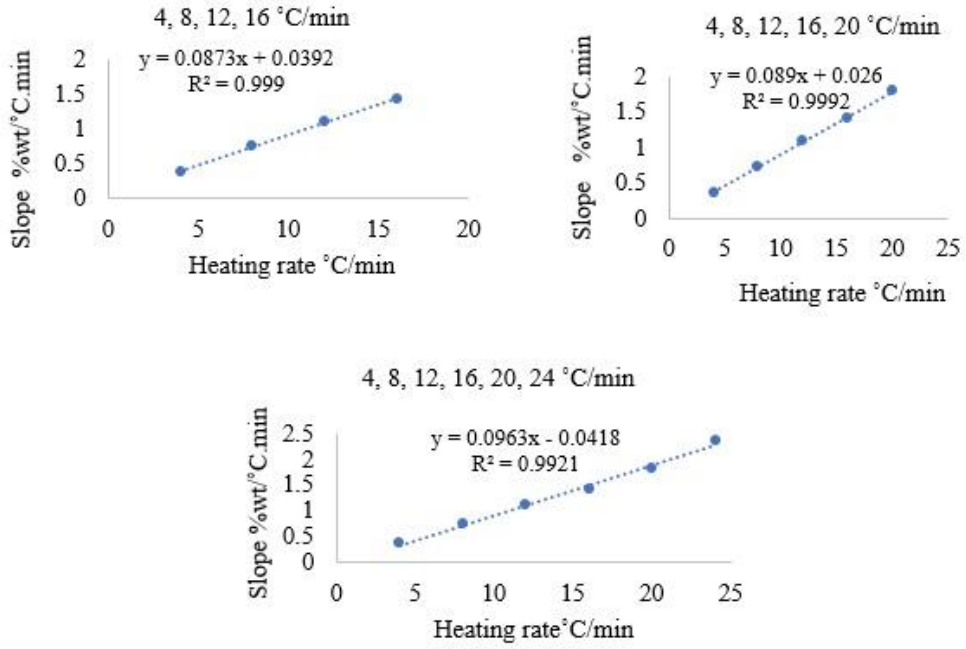



*Figure C3.1: Heating rates applied vs the slopes of the derivative curve for biomass treated with 10% IL-B*

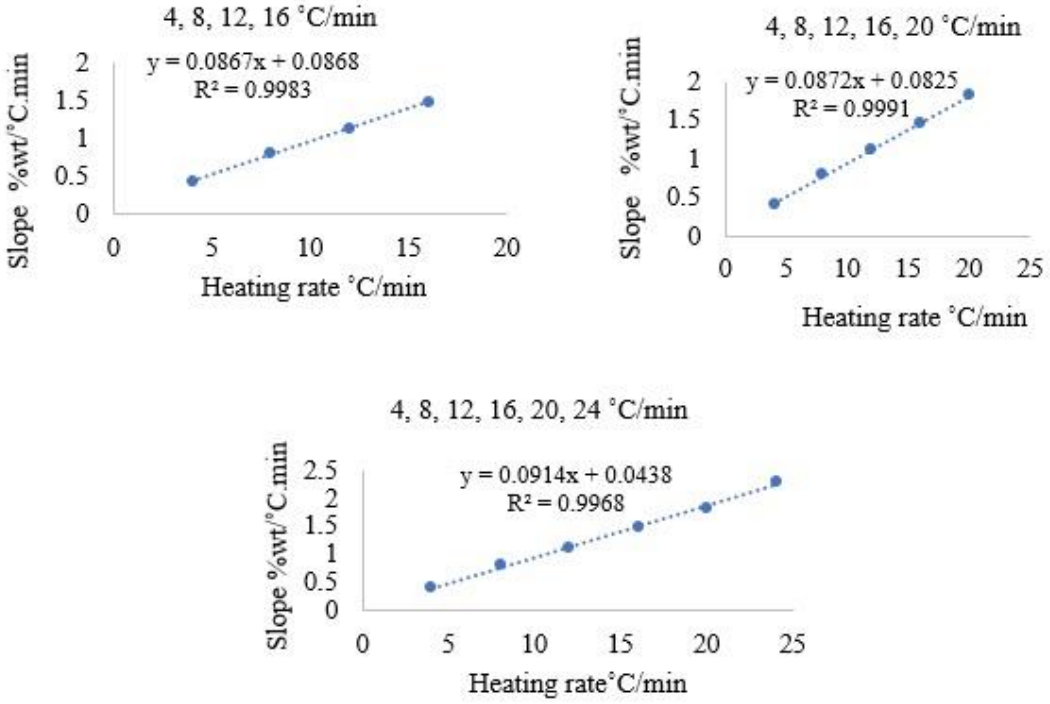



*Figure C3.2: Heating rates applied vs the slopes of the derivative curve for biomass treated with 20% IL-B*

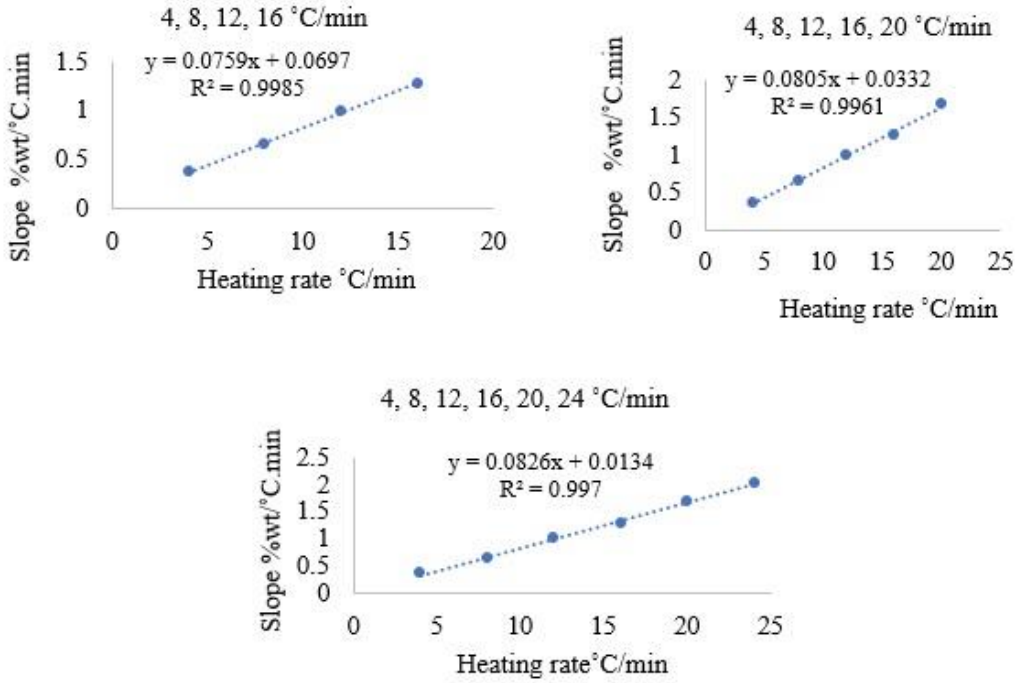



*Figure C3.3: Heating rates applied vs the slopes of the derivative curve for biomass treated with 30% IL-B*

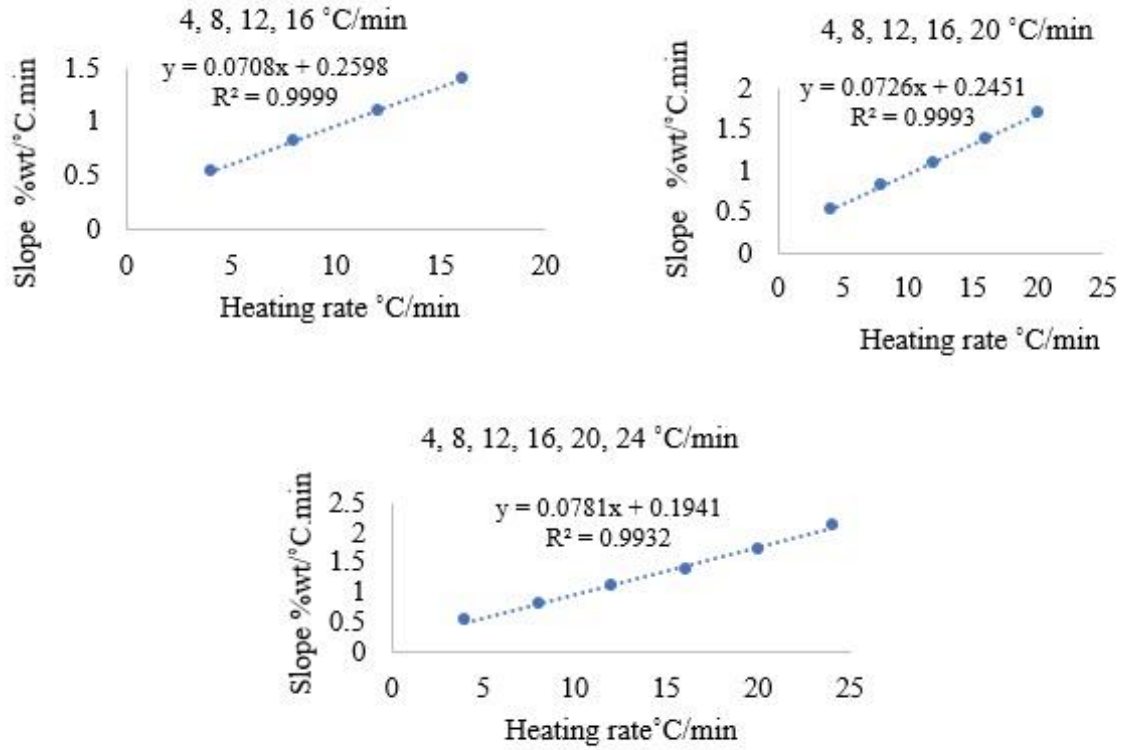



*Figure C3.4: Heating rates applied vs the slopes of the derivative curve for biomass treated with 40% IL-B*

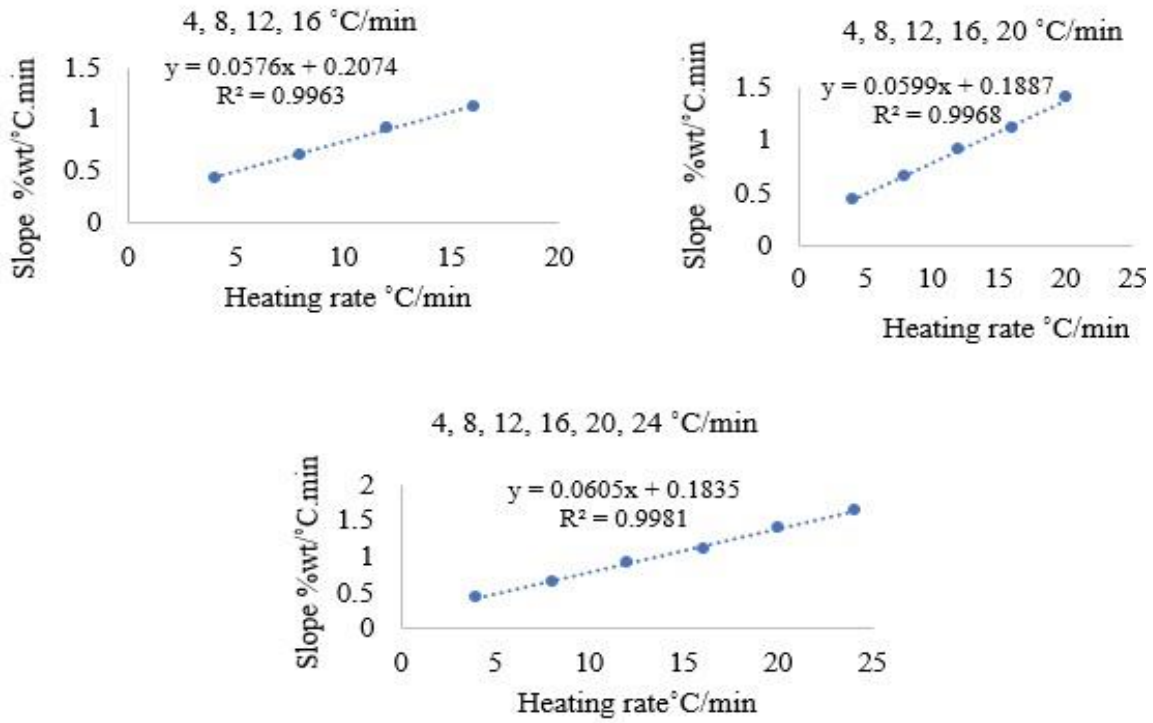



*Figure C3.5: Heating rates applied vs the slopes of the derivative curve for biomass treated with 50% IL-B*

**APPENDIX D**

**D1. Thermogravimetric analysis derivative profile of 100% biomass that was treated with IL-C at different concentrations**

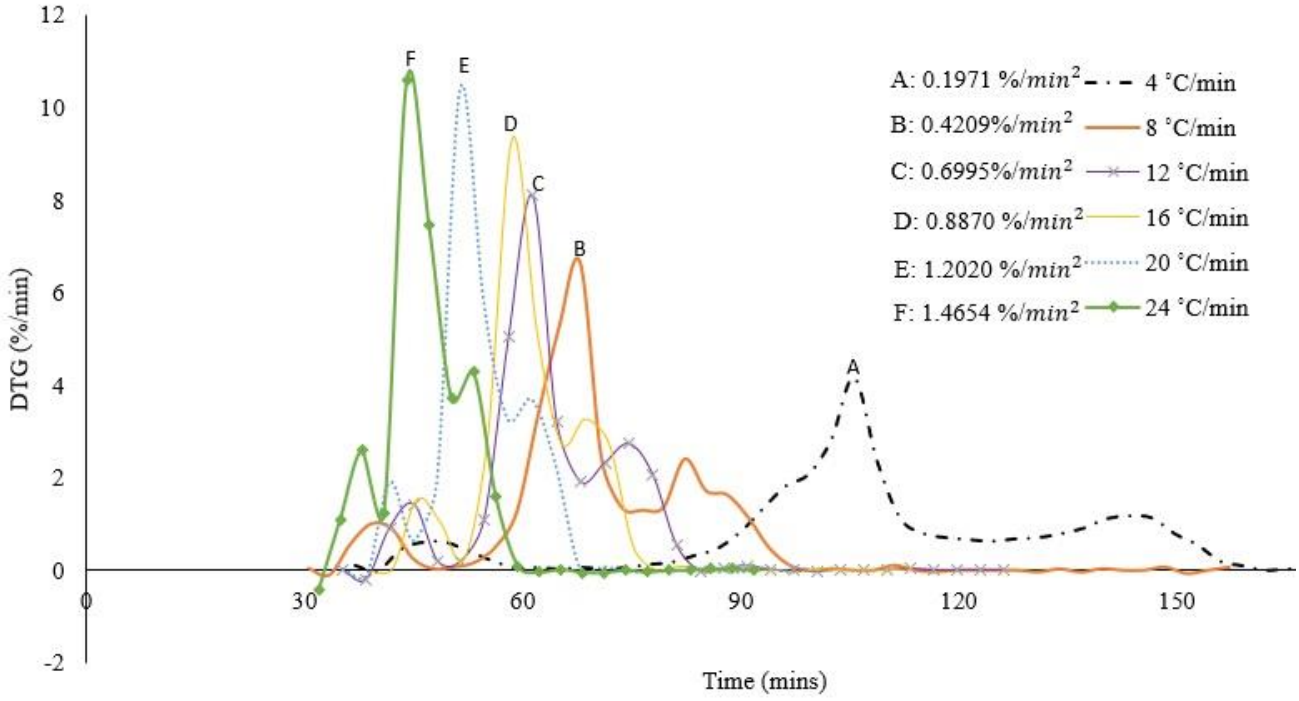



*Figure D1.1: The derivative profile of 100% biomass that was treated with 10% IL-C*

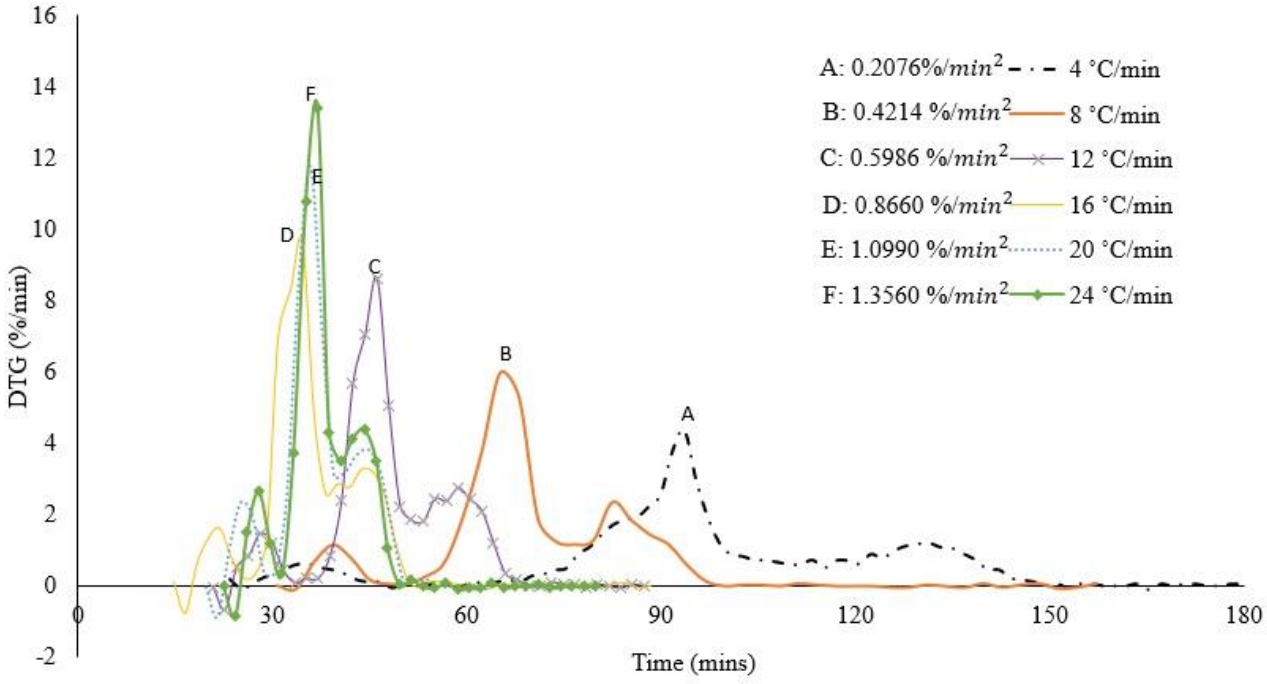



*Figure D1.2: The derivative profile of 100% biomass that was treated with 20% IL-C*

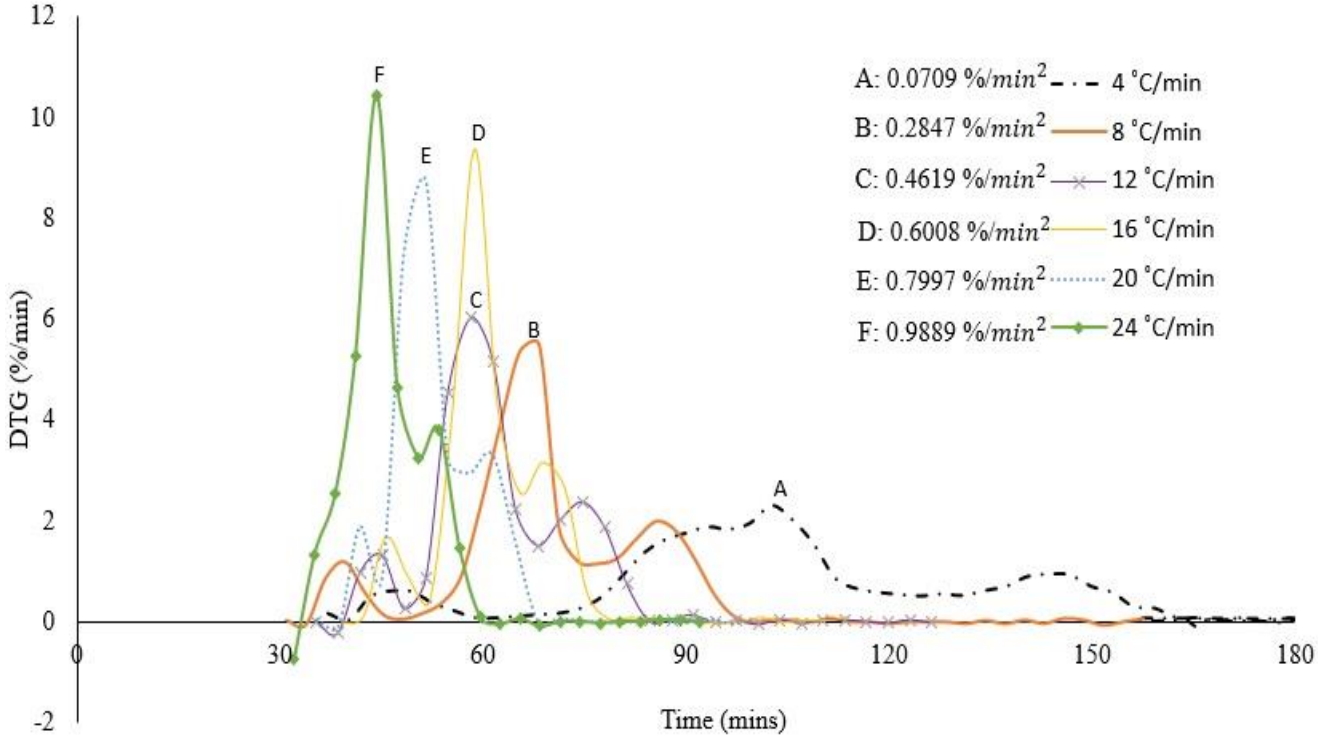



*Figure D1.3: The derivative profile of 100% biomass that was treated with 30% IL-C*

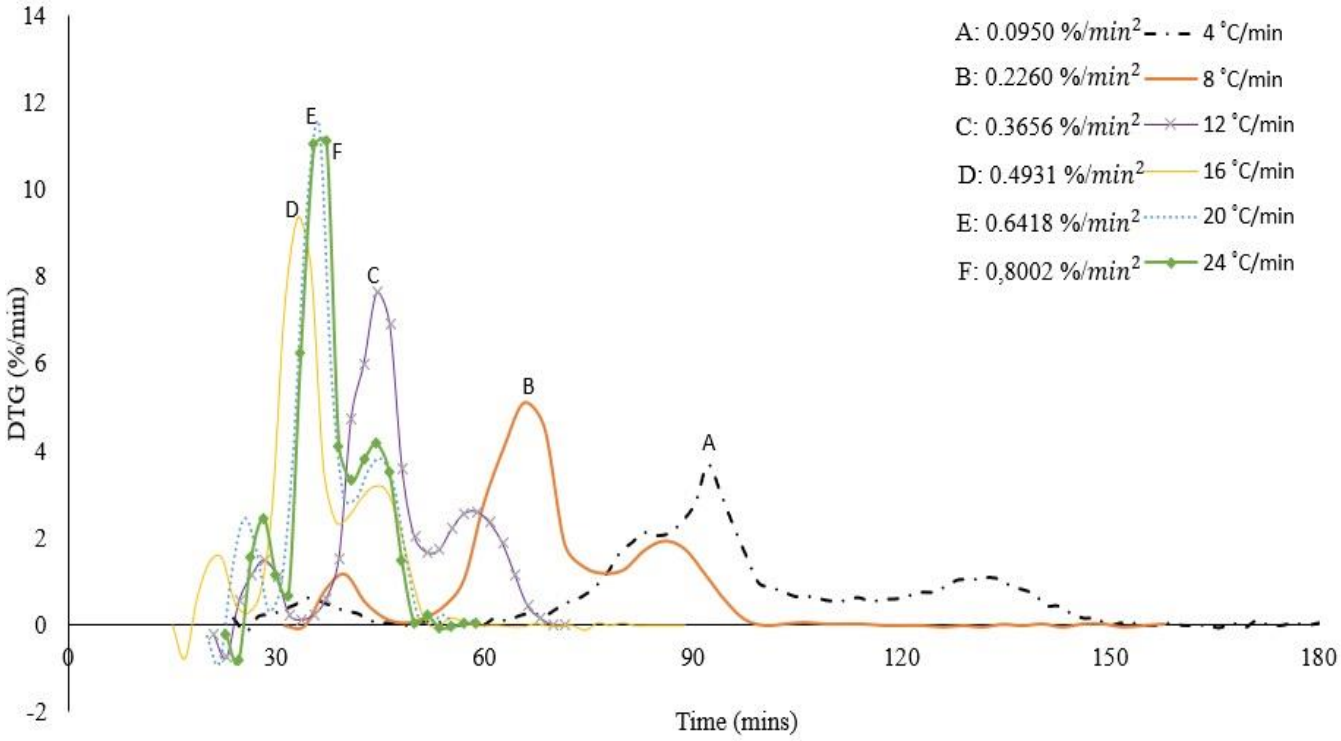



*Figure D1.4: The derivative profile of 100% biomass that was treated with 40% IL-C*

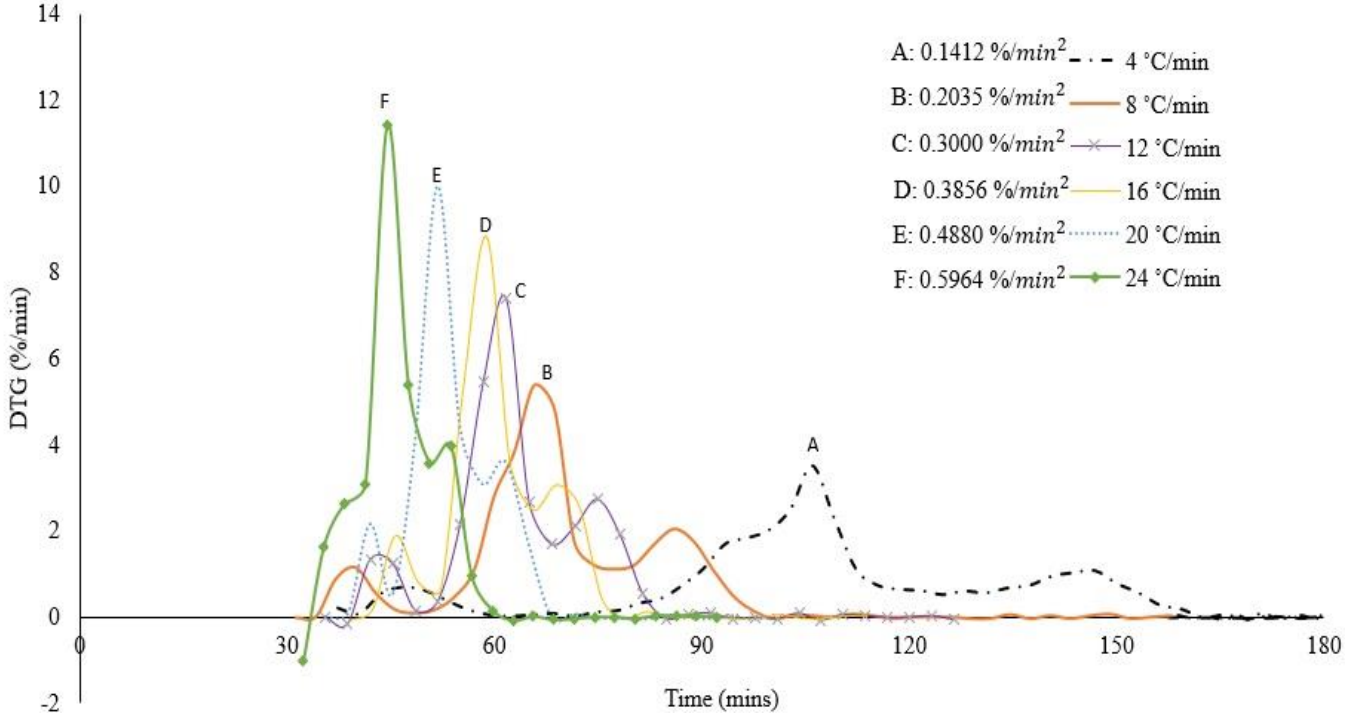



*Figure D1.5: The derivative profile of 100% biomass that was treated with 50% IL-C*

**D2. Three points were used for calculating the slopes of the derivative profile of the samples treated with IL-C at different concentrations and heating rates**

*Table D2.1: The specific temperatures and differential thermogravimetric analysis values used for calculating the slopes of the derivative profile of the samples treated with IL-C*

| Heating Rate ˚C/min | Points | 10% IL-C-tb | | 10% IL-C-tb | | 10% IL-C-tb | | 10% IL-C-tb | | 10% IL-C-tb | |
|---|---|---|---|---|---|---|---|---|---|---|---|
| 4 | Ignition Point | 89.97 | 0.82 | 75.47 | 0.50 | 77.62 | 0.48 | 75.73 | 0.88 | 87.15 | 0.74 |
| | Inflection Point | 102.52 | 2.82 | 91.77 | 3.75 | 99.55 | 1.96 | 90.23 | 2.83 | 99.73 | 2.03 |
| | Peak Point | 105.63 | 4.15 | 93.62 | 4.36 | 102.70 | 2.31 | 92.05 | 3.70 | 105.98 | 3.52 |
| 8 | Ignition Point | 59.27 | 1.26 | 59.42 | 1.92 | 59.68 | 2.27 | 57.03 | 1.06 | 54.30 | 0.47 |
| | Inflection Point | 65.07 | 5.24 | 62.33 | 3.75 | 65.50 | 5.35 | 62.77 | 4.09 | 62.93 | 3.84 |
| | Peak Point | 67.97 | 6.63 | 65.23 | 6.00 | 68.40 | 5.48 | 65.67 | 5.11 | 65.82 | 5.40 |
| 12 | Ignition Point | 54.75 | 1.09 | 40.60 | 2.39 | 51.67 | 0.85 | 39.07 | 1.53 | 51.83 | 0.35 |
| | Inflection Point | 58.12 | 5.05 | 44.27 | 7.06 | 54.92 | 4.54 | 42.63 | 5.99 | 58.47 | 5.46 |
| | Peak Point | 61.43 | 8.09 | 46.10 | 8.63 | 58.32 | 6.01 | 44.53 | 7.64 | 61.78 | 7.39 |
| 16 | Ignition Point | 51.95 | 0.24 | 29.13 | 1.24 | 52.12 | 0.39 | 29.38 | 2.67 | 52.28 | 0.64 |
| | Inflection Point | 55.20 | 2.85 | 32.88 | 8.32 | 55.37 | 4.00 | 31.22 | 7.33 | 55.53 | 5.31 |
| | Peak Point | 58.62 | 9.33 | 34.68 | 9.65 | 58.78 | 9.38 | 33.15 | 9.36 | 58.95 | 8.83 |
| 20 | Ignition Point | 48.17 | 1.88 | 32.22 | 2.44 | 45.08 | 0.82 | 32.43 | 3.97 | 45.23 | 0.53 |
| | Inflection Point | 48.17 | 1.88 | 34.12 | 8.61 | 48.33 | 7.31 | 34.33 | 9.46 | 48.50 | 4.09 |
| | Peak Point | 51.43 | 10.41 | 35.95 | 11.78 | 51.62 | 8.73 | 36.15 | 11.51 | 51.78 | 10.02 |
| 24 | Ignition Point | 40.95 | 1.22 | 33.25 | 3.75 | 38.13 | 2.52 | 31.68 | 0.67 | 41.30 | 3.09 |
| | Inflection Point | 40.95 | 1.22 | 35.15 | 10.77 | 41.13 | 5.28 | 33.47 | 6.24 | 41.30 | 3.09 |
| | Peak Point | 44.10 | 10.59 | 36.97 | 13.41 | 44.28 | 10.43 | 35.38 | 11.05 | 44.48 | 11.43 |

*tb: treated 100% biomass*

**D3. Heating rates applied vs the slopes of the derivative curve for the samples treated with IL-C at different concentrations**

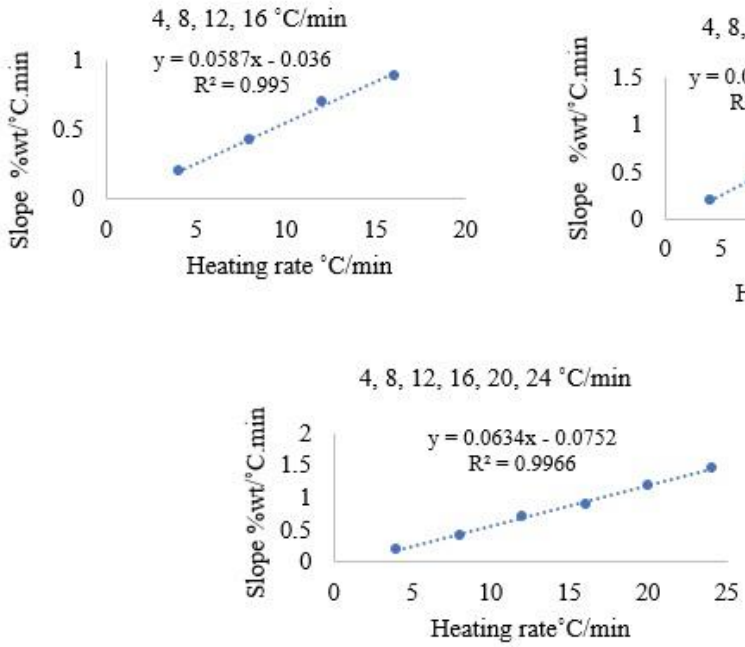



*Figure D3.1: Heating rates applied vs the slopes of the derivative curve for biomass treated with 10% IL-C*

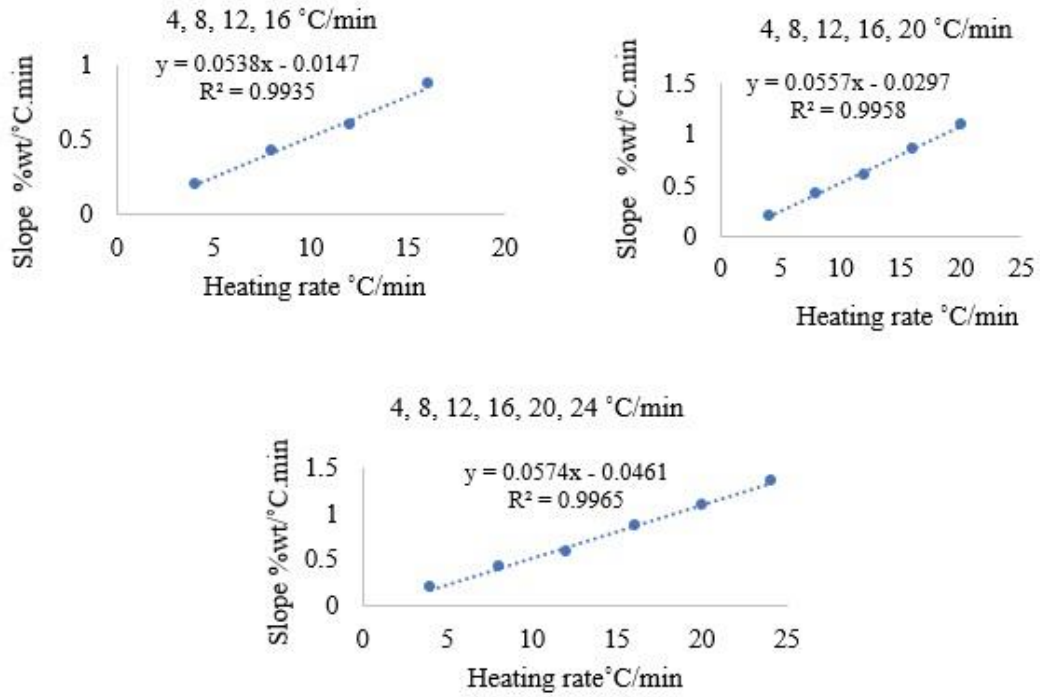



*Figure D3.2: Heating rates applied vs the slopes of the derivative curve for biomass treated with 20% IL-C*

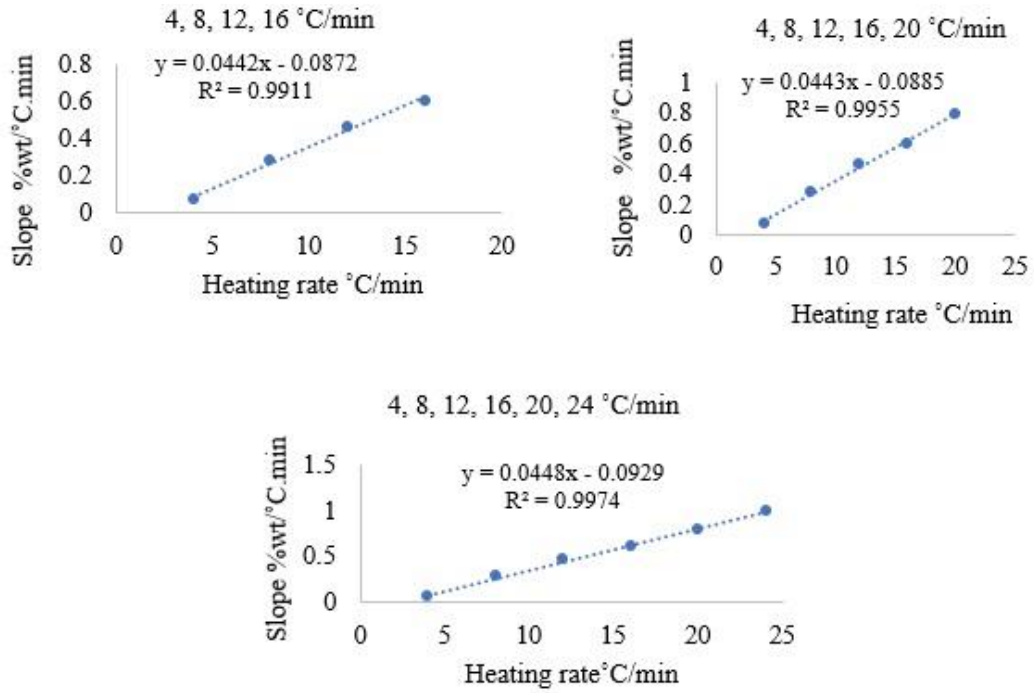



*Figure D3.3:Heating rates applied vs the slopes of the derivative curve for biomass treated with 30% IL-C*

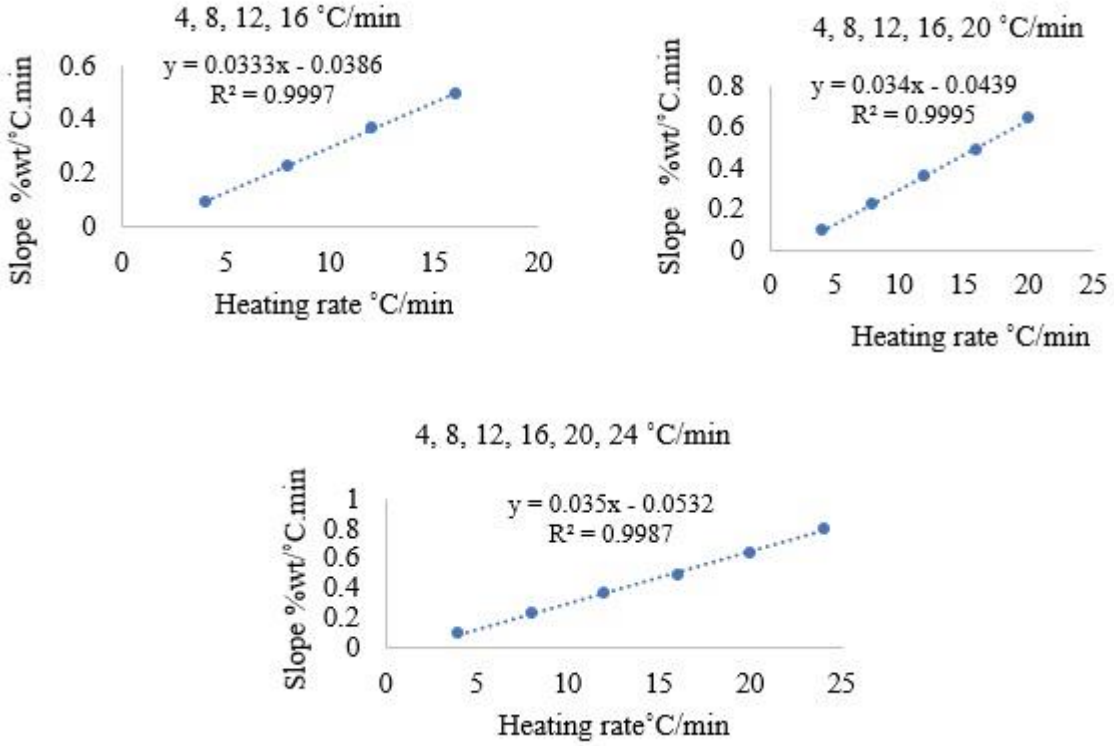



*Figure D3.4: Heating rates applied vs the slopes of the derivative curve for biomass treated with 40% IL-C*

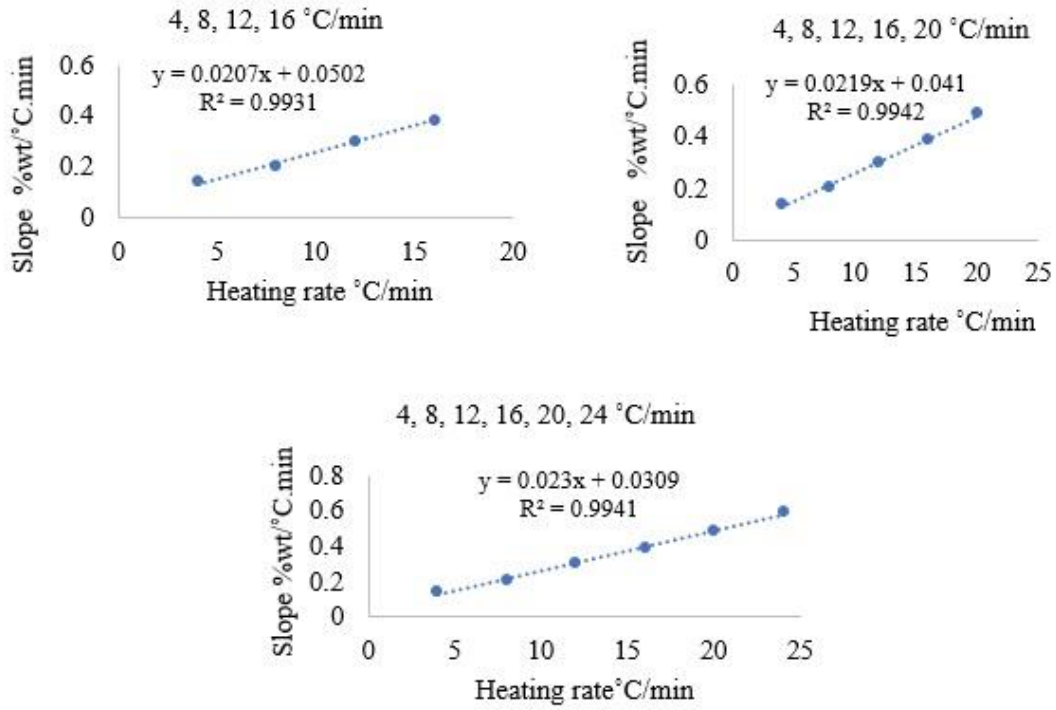



*Figure D3.5: Heating rates applied vs the slopes of the derivative curve for biomass treated with 40% IL-C*

## APPENDIX E

### E1: Pore diameter distribution data for 100% biomass and the treated biomass samples generated by the Density Functional Theory method

*Table E1.1: The pore diameter distribution data*

| 100% Biomass | | 50% IL-A-tb | | 50% IL-B-tb | | 50% IL-C-tb | |
|---|---|---|---|---|---|---|---|
| Pore diameter (nm) | Pore (cc/g) | Pore diameter (nm) | Pore (cc/g) | Pore diameter (nm) | Pore (cc/g) | Pore diameter (nm) | Pore (cc/g) |
| 1.6879 | 0 | 1.6879 | 0 | 1.6879 | 0 | 1.6879 | 0 |
| 1.7656 | 0 | 1.7656 | 0 | 1.7656 | 0 | 1.7656 | 0 |
| 1.8469 | 0 | 1.8469 | 0 | 1.8469 | 0 | 1.8469 | 9.69E-06 |
| 1.9319 | 1.15E-04 | 1.9319 | 3.63E-05 | 1.9319 | 2.26E-05 | 1.9319 | 8.69E-05 |
| 2.0208 | 2.62E-04 | 2.0208 | 1.34E-04 | 2.0208 | 6.69E-05 | 2.0208 | 1.63E-04 |
| 2.1138 | 2.62E-04 | 2.1138 | 1.52E-04 | 2.1138 | 1.30E-04 | 2.1138 | 1.63E-04 |
| 2.2111 | 4.92E-04 | 2.2111 | 2.83E-04 | 2.2111 | 1.99E-04 | 2.2111 | 2.54E-04 |
| 2.3129 | 0.00108 | 2.3129 | 5.04E-04 | 2.3129 | 4.58E-04 | 2.3129 | 4.44E-04 |
| 2.4194 | 0.00154 | 2.4194 | 7.08E-04 | 2.4194 | 8.10E-04 | 2.4194 | 6.31E-04 |
| 2.5307 | 0.00209 | 2.5307 | 9.68E-04 | 2.5307 | 1.14E-03 | 2.5307 | 8.78E-04 |
| 2.6472 | 0.00275 | 2.6472 | 1.27E-03 | 2.6472 | 1.43E-03 | 2.6472 | 1.21E-03 |
| 2.7691 | 0.00319 | 2.7691 | 1.44E-03 | 2.7691 | 1.58E-03 | 2.7691 | 1.48E-03 |

*tb: treated 100% biomass*

**APPENDIX F**

**F1: Thermogravimetric analysis repeatability test of 100% discard coal**

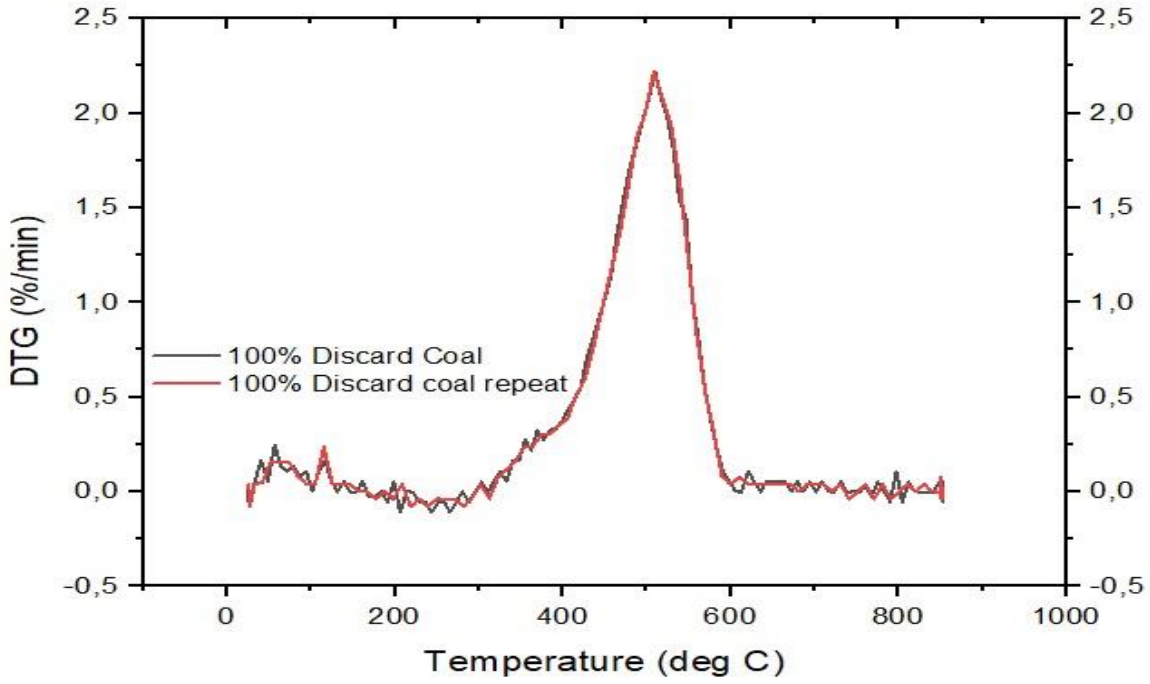



*Figure F1.1: Repeatability test of 100% discard coal at a heating rate of 4 ℃/min*